Electronic Supplementary Material (ESI) for Chemical Science.

Supporting Information

Catalytic Asymmetric Defluorinative Allylation of Silyl Enol Ethers

Jordi Duran, Javier Mateos, Albert Moyano and Xavier Companyó*

Section of Organic Chemistry – Department of Inorganic and Organic Chemistry
University of Barcelona
carrer Martí i Franquès 1, 08028 Barcelona, Spain

E-mail: x.companyo@ub.edu

Table of Contents

A. General Information

NMR experiments: NMR spectra (^{1}H, ^{13}C and ^{19}F) were recorded on a Bruker Avance III HD 400 (400 MHz) spectrometer equipped with a CryoProbe™ Prodigy or a Bruker Avance Neo 500 (500 MHz) equipped with a broadband *i*Prob. The chemical shifts (δ) for ^{1}H and ^{13}C are given in ppm relative to residual signals of the solvents ($CHCl_3$, 7.26 ppm, ^{1}H NMR, 77.16 ppm ^{13}C NMR). Coupling constants are given in Hz. The following abbreviations are used to indicate the multiplicity: s, singlet; d, doublet; t, triplet; q, quartet; m, multiplet; bs, broad signal. NMR yields were calculated by using 1,3,5-trimethoxybenzene or mesitylene as internal standards.

High-Resolution Mass Spectra (HRMS): were obtained with an Agilent LC/MSD-TOC 2006 instrument.

Chiral High-Performance Liquid Chromatography (HPLC): analyses were performed on a Shimadzu LC-20AD instrument with DGU-20A5 and a SPD-20A UV/VIS detector using Phenomenex Lux® 5 µm Cellulose-1, Cellulose-2, Cellulose-5 or Amylose-2 LC Columns 254 x 4.6 mm in *n*-hexane/2-propanol mixtures.

Chiral Gas Chromatography (GC): analyses were performed on a Shimadzu GC-2010 instrument using an Agilent CP-Chirasil Dex CB GC Column 25 m x 0.32 mm x 0.25 µm – 20 to 200/225 C.

Gas Chromatography (GC): analyses were performed on a Shimadzu GC-2010 Pro instrument using an Agilent DB-5 GC column 30 m x 0.250 mm x 0.25 µm – 60 to 325/350 C.

Chromatographic purification of products was accomplished by flash chromatography in Sigma Aldrich silica gel 60 N (spherical, particle size 63−210 mm). Thin-layer chromatography (TLC) was carried out with Silicycle TLC plates with silica gel 60 F254. Visualization of the developed chromatography was performed by checking UV absorbance (254nm) as well as with aqueous ceric ammonium molybdate and potassium permanganate solutions. Organic solutions were concentrated under reduced pressure on Büchi rotary evaporators.

Electrochemical characterizations: were carried out in acetonitrile (MeCN)/0.1 M tetrabutylammonium perchlorate/lithium perchlorate ($TBAClO_4$/$LiClO_4$) at room temperature, on a BASi Epsilon EClipse™ instrument (Metrohm, The Netherlands) in a glass cell. A typical three-electrode cell was employed, which was composed of glassy carbon (GC) working electrode (3 mm diameter), a platinum wire as counter electrode and a Ag/AgCl as reference electrode (RE). Oxygen was removed by purging the solution with high-purity Nitrogen. The potential of ferrocenium/ferrocene (Fc/Fc^{+}) couple was measured and found to be 0.49 V vs Ag/AgCl, in agreement with the value reported in literature in MeCN.[1] The GC electrode was polished before any measurement with diamond paste and ultrasonically rinsed with deionized water for 15 minutes. The electrode was electrochemically activated in the background solution by means of several voltammetric cycles at 100 mV/s between the anodic and cathodic solvent/electrolyte discharges.

Materials: Commercial grade reagents and solvents were purchased at the highest commercial quality from Sigma Aldrich, Apollo Scientific, TCI and Fluorochem and used as received, unless otherwise stated.

B. Synthesis of Starting Materials

B.1. General Procedure A – Synthesis of Morita-Baylis-Hillman alcohols

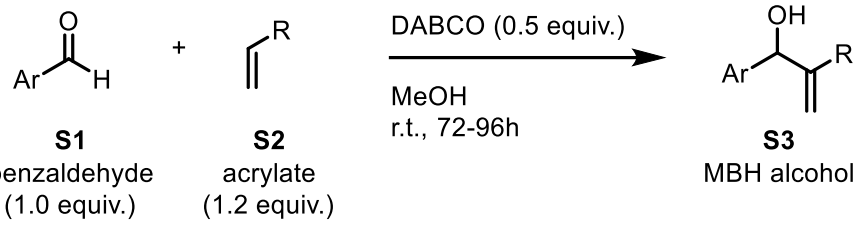

S1 benzaldehyde (1.0 equiv.) | **S2** acrylate (1.2 equiv.) | **S3** MBH alcohol

The reaction was carried out following the previously described procedure[2]

To a round bottom flask containing MeOH (0.75 equiv., 37.5 mmol) benzaldehyde **S1** (1.0 equiv., 50 mmol) and the corresponding acrylate **S2** (1.2 equiv., 60 mmol) were added at room temperature. Then, DABCO **5a** (0.5 equiv., 25 mmol) was added, and the solution was stirred for 72-96 h until full consumption of the aldehyde starting material was observed by TLC analysis. The crude reaction mixture was purified by column chromatography using a mixture of hexane/ethyl acetate as eluent, obtaining **S3** derivatives as oils/solids.

methyl 2-(hydroxy(phenyl)methyl)acrylate (S3b)

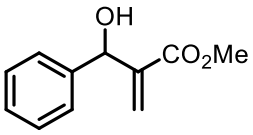

85% yield. Spectroscopic data match with those previously reported.[3a]

^{1}H NMR (400 MHz, $CDCl_3$) δ 7.33-7.29 (5H, m), 6.33 (1H, s), 5.84 (1H, s), 5.56 (1H, d, *J* = 5.5 Hz), 3.71 (3H, s), 3.14 (1H, d, *J* = 5.5 Hz) ppm.

methyl 2-((4-fluorophenyl)(hydroxy)methyl)acrylate (S3c)

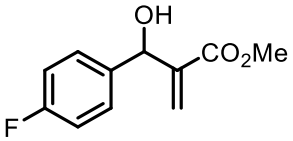

88% yield. Spectroscopic data match with those previously reported..[3b]

^{1}H NMR (400 MHz, $CDCl_3$) δ 7.30-7.36 (2H, m), 6.98–7.05 (2H, m), 6.32 (1H, s), 5.80 (1H, s), 5.53 (1H, s), 3.71 (3H, s), 2.57 (1H, bs) ppm.

methyl 2-(hydroxy(4-(trifluoromethyl)phenyl)methyl)acrylate (S3d)

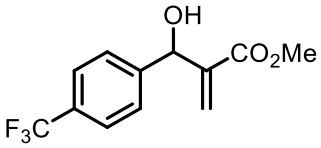

80% yield. Spectroscopic data match with those previously reported.[3c]

^{1}H NMR (400 MHz, $CDCl_3$) δ 7.60 (2H, m), 7.50 (2H, m), 6.37 (1H, s), 5.84 (1H, s), 5.60 (1H, d, *J* = 5.9 Hz), 3.74 (3H, s), 3.25 (1H, d, *J* = 5.2 Hz) ppm.

methyl 2-((4-cyanophenyl)(hydroxy)methyl)acrylate (S3e)

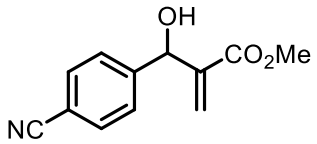

78% yield. Spectroscopic data match with those previously reported.[3c]

^{1}H NMR (400 MHz, $CDCl_3$) δ 7.46 (2H, d, *J* = 7.8 Hz), 7.33 (2H, d, *J* = 7.8 Hz), 6.20 (1H, s), 5.69 (1H, s), 5.41 (1H, bs), 3.55 (3H, s), 1.98 (1H, bs) ppm.

methyl 4-(1-hydroxy-2-(methoxycarbonyl)allyl)benzoate (S3f)

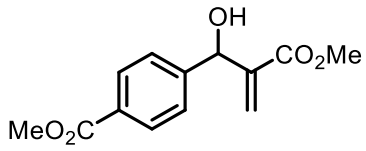

85% yield. Spectroscopic data match with those previously reported.[3b]

^{1}H NMR (400 MHz, $CDCl_3$) δ 8.04 (2H, d, *J* = 8.5 Hz), 7.46 (2H, d, *J* = 8.5 Hz), 6.35 (1H, s), 5.84 (1H, s), 5.60 (1H, s), 3.89 (3H, s), 3.75 (3H, s), 3.70 (1H, bs) ppm.

methyl 2-((4-chlorophenyl)(hydroxy)methyl)acrylate (S3g)

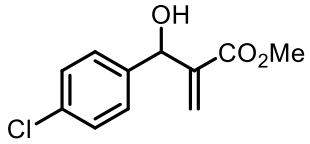

93% yield. Spectroscopic data match with those previously reported.[3b]

^{1}H NMR (400 MHz, $CDCl_3$) δ 7.33 (2H, d, *J* = 7.6 Hz), 7.20 (2H, d, *J* = 7.6 Hz), 6.32 (1H, s), 5.80 (1H, s), 5.49 (1H, s), 3.74 (3H, s) 2.59 (1H, bs) ppm.

methyl 2-(hydroxy(4-methoxyphenyl)methyl)acrylate (S3h)

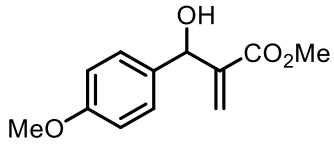

71% yield. Spectroscopic data match with those previously reported.[3a]

^{1}H NMR (400 MHz, $CDCl_3$) δ 7.28 (2H, *J* = 8.6 Hz d), 6.87 (2H, *J* = 8.7 Hz, d), 6.32 (1H, s), 5.85 (1H, s), 5.52 (1H, d, *J* = 4.8 Hz), 3.71 (3H, s), 2.93 (1H, bs) ppm.

methyl 2-(hydroxy(p-tolyl)methyl)acrylate (S3i)

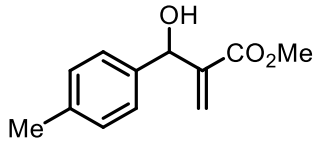

91% yield. Spectroscopic data match with those previously reported.[3b]

^{1}H NMR (400 MHz, $CDCl_3$) δ 7.28 (2H, d, *J* = 8.8 Hz), 6.70 (2H, d, *J* = 8.8 Hz), 6.34 (1H, s), 6.30 (1H, s), 5.10 (1H, s), 3.78 (3H, s), 3.74 (3H, s), 2.85 (1H, bs) ppm.

methyl 2-((4-bromophenyl)(hydroxy)methyl)acrylate (S3j)

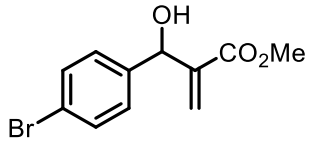

75% yield. Spectroscopic data match with those previously reported.[3a]

^{1}H NMR (400 MHz, $CDCl_3$) δ 7.46 (2H, *J* = 8.4 Hz d), 7.24 (2H, *J* = 8.4 Hz, d), 6.33 (1H, s), 5.83 (1H, s), 5.49 (1H, d, *J* = 5.6 Hz), 3.71 (3H, s), 3.22 (1H, d, *J* = 5.7 Hz) ppm.

methyl 2-(hydroxy(m-tolyl)methyl)acrylate (S3k)

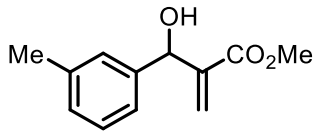

86% yield. Spectroscopic data match with those previously reported.[3d]

^{1}H NMR (400 MHz, $CDCl_3$) δ 7.25-7.06 (4H, m), 6.36 (1H, s), 5.84 (1H, s), 5.54 (1H, s), 3.73 (3H, s), 2.35 (3H, s) ppm.

methyl 2-(hydroxy(o-tolyl)methyl)acrylate (S3l)

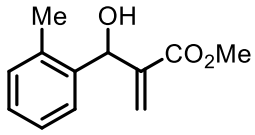

69% yield. Spectroscopic data match with those previously reported.[3d]

^{1}H NMR (400 MHz, $CDCl_3$) δ 7.47-7.39 (1H, m), 7.26-7.12 (3H, m), 6.33 (1H, s), 5.81 (1H, s), 5.60 (1H, t, *J* = 1.2 Hz), 3.77 (3H, s), 2.33 (3H, s) ppm.

methyl 2-(hydroxy(naphthalen-2-yl)methyl)acrylate (S3m)

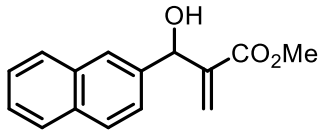

88% yield. Spectroscopic data match with those previously reported.[3b]

^{1}H NMR (400 MHz, $CDCl_3$) δ 7.9-7.3 (7H, m), 6.36 (1H, s), 6.31 (1H, s), 5.19 (1H, s), 3.75 (3H, s), 2.58 (1H, bs) ppm.

methyl 2-(hydroxy(naphthalen-1-yl)methyl)acrylate (S3n)

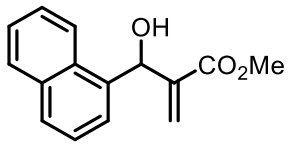

74% yield. Spectroscopic data match with those previously reported.[3e]

^{1}H NMR (400 MHz, $CDCl_3$) δ 8.02-8.05 (1H, m), 7.89-7.91 (1H, m), 7.85 (1H, d, *J* = 8.3 Hz), 7.67 (1H, d, *J* = 7.1 Hz), 7.52 (3H, m), 6.42 (1H, d, *J* = 4.0 Hz) 6.39 (1H, s) 5.6 (1H, s), 3.82 (3H, s), 3.08 (1H, d, *J* = 4.6 Hz) ppm.

methyl 2-(hydroxy(pyridin-2-yl)methyl)acrylate (S3o)

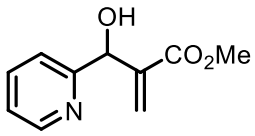

50% yield. Spectroscopic data match with those previously reported.[3f]

^{1}H NMR (400 MHz, $CDCl_3$) δ 8.55 (1H, dt, J = 4.8, 1.7 Hz), 7.68 (1H, td, J = 7.7, 1.7 Hz), 7.43 (1H, dq, J = 7.9, 1.0 Hz), 7.22 (1H, ddd, J = 7.5, 4.9, 1.3 Hz), 6.37 (1H, s), 5.98 (1H, s), 5.64 (1H, s), 4.89 (1H, s), 3.74 (3H, s) ppm.

ethyl 2-(hydroxy(phenyl)methyl)acrylate (S3p)

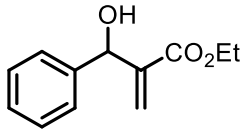

83% yield. Spectroscopic data match with those previously reported.[3a]

^{1}H NMR (400 MHz, $CDCl_3$) δ 7.38-7.26 (5H, m), 6.32 (1H, s), 5.83 (1H, s), 5.53 (1H, d, *J* = 5.2 Hz), 4.14 (2H, q, *J* = 7.1 Hz), 3.34 (1H, d, *J* = 5.3 Hz), 1.22 (3H, t, *J* = 7.1 Hz) ppm.

hexyl 2-(hydroxy(phenyl)methyl)acrylate (S3q)

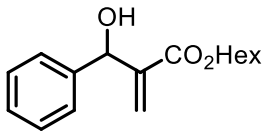

78% yield. Spectroscopic data match with those previously reported.[3g]

^{1}H NMR (400 MHz, $CDCl_3$) δ 7.41-7.26 (5H, m), 6.34 (1H, s), 5.82 (1H, t, *J* = 1.25 Hz), 5.56 (1H, bs), 4.11 (2H, td, *J* = 6.7, 1.2 Hz), 3.04 (1H, bs), 1.67-1.54 (2H, m), 1.34-1.20 (6H, m), 0.94-0.81 (3H, m) ppm.

***tert*-butyl 2-(hydroxy(phenyl)methyl)acrylate (S3r)**

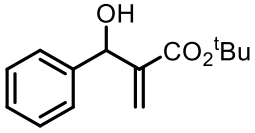

72% yield. Spectroscopic data match with those previously reported.[3c]

^{1}H NMR (400 MHz, $CDCl_3$) δ 7.06-7.16 (5H, m), 6.05 (1H, s), 5.58 (1H, s), 5.28 (1H, bs), 3.30 (1H, bs), 1.19 (9H, s) ppm.

methyl 2-(cyclohexyl(hydroxy)methyl)acrylate (S3s)

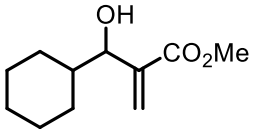

50% yield. Spectroscopic data match with those previously reported.[3c]

^{1}H NMR (400 MHz, $CDCl_3$) δ 6.25 (1H, d, *J* = 1.2 Hz), 5.72 (1H, d, *J* = 0.8 Hz,), 4.06 (1H, d, *J* = 5.9 Hz), 3.78 (3H, s), 2.52 (1H, s), 1.97 (1H, d, *J* = 12.8 Hz), 1.82-1.42 (5H, m), 1.3-1.07 (3H, m), 1.06-0.83 (2H, m).

methyl 3-hydroxy-2-methylene-4-phenylbutanoate (S3t)

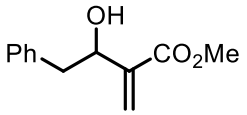

17% yield. Spectroscopic data match with those previously reported.[3h]

^{1}H NMR (400 MHz, $CDCl_3$) δ 7.21 (5H, m), 6.22 (1H, s), 5.76 (1H, t, *J* = 1.2 Hz), 4.64 (1H, m), 3.77 (3H, s), 2.89 (2H, m), 2.48 (1H, d, *J* = 6.0 Hz).

***B.2. General Procedure B** – Synthesis of allyl fluorides*

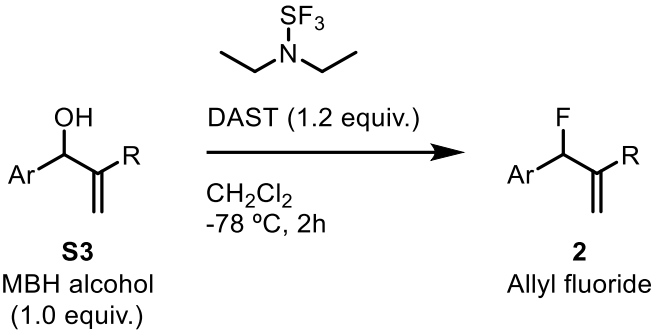

S3
MBH alcohol
(1.0 equiv.)

2
Allyl fluoride

The reaction was carried out following the previously described procedure.[4]

Into a two-necked round-bottom flask equipped with a magnetic stirring bar the corresponding MBH alcohol **S3** (1.0 equiv., 15 mmol) was dissolved in dry CH_2Cl_2 (0.33 M) at -78 °C under nitrogen atmosphere. To this solution, DAST (1.2 equiv., 18 mmol) was added dropwise. The reaction mixture was stirred for 2 h at -78 °C and then quenched with a saturated $NaHCO_3$ aqueous solution. The aqueous layer was extracted with CH_2Cl_2 (3x50 mL). The combined organic layers were dried over $MgSO_4$ and concentrated under reduced pressure. The crude product **2** was purified by column chromatography using a mixture of hexane and CH_2Cl_2 obtaining **2** derivatives as oils.

methyl 2-(fluoro(phenyl)methyl)acrylate (2b)

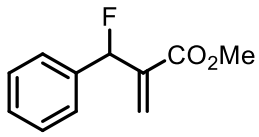

44% yield. Spectroscopic data match with those previously reported.[4]

^{1}H NMR (400 MHz, $CDCl_3$) δ 7.41-7.34 (m, 5H), 6.45 (s, 1H), 6.29 (d, J_{H-F} = 45.9 Hz, 1H), 6.02 (s, 1H), 3.72 (s, 3H) ppm.

methyl 2-((4-fluorophenyl)(hydroxy)methyl)acrylate (2c)

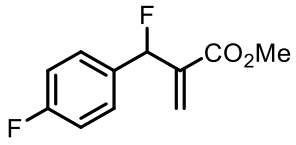

***2c** was prepared following the abovementioned procedure.*

S3c (1.00 g, 1.0 equiv., 4.8 mmol) was dissolved in 30 mL of CH_2Cl_2 and the solution was cooled to -78 °C. Then, DAST (0.92 g, 1.2 equiv., 5.7 mmol) was added dropwise. After 2h, the reaction was quenched and purified. **2c** was obtained in *52% yield* (534 mg, 2.5 mmol) as a transparent oil.

^{1}H NMR (400 MHz, $CDCl_3$) δ 7.41-7.34 (2H, m), 7.10-7.02 (2H, m), 6.46 (1H, dt, *J* = 3.05, 0.99 Hz), 6.25 (1H, d, *J* = 45.84 Hz), 6.04 (1H, dd, *J* = 1.56, 0.90 Hz), 3.72 (3H, s) ppm. **^{13}C NMR** (126 MHz, $CDCl_3$) δ 165.2 (d, J_{C-F} = 6.8 Hz), 163.2 (dd, J_{C-F} = 245, 3.0 Hz), 139.2 (d, J_{C-F} = 23.1 Hz), 135.5 (dd, J_{C-F} = 17.9, 3.1 Hz), 129.3 (dd, J_{C-F} = 8.5, 5.5 Hz), 125.9 (d, J_{C-F} = 23.1 Hz), 115.7 (dd, J_{C-F} = 22, 1.31 Hz), 90.3 (d, J_{C-F} = 174.2 Hz), 52.2 ppm. **^{19}F NMR** (471 MHz, $CDCl_3$) δ -112.55, -169.73 ppm. **HRMS (ESI)** Calculated for $C_{11}H_{11}F_2O_2^+$ ($[M+H]^+$) 212.1958. Found 212.1956.

methyl 2-(fluoro(p-tolyl)methyl)acrylate (2d)

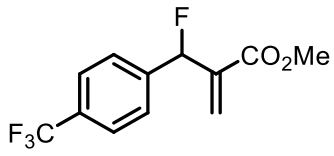

48% yield. Spectroscopic data match with those previously reported.[4]

^{1}H NMR (400 MHz, $CDCl_3$) δ 7.64 (d, *J* = 7.9 Hz, 2H), 7.52 (d, *J* = 7.9 Hz, 2H), 6.49 (s, 1H), 6.33 (d, $J_{H\text{-}F}$ = 45.9 Hz, 1H), 6.06 (s, 1H), 3.74 (s, 3H) ppm.

methyl 2-((4-cyanophenyl)fluoromethyl)acrylate (2e)

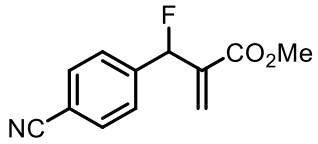

30% yield. Spectroscopic data match with those previously reported.[5a]

^{1}H NMR (400 MHz, $CDCl_3$) δ 7.70 (d, *J* = 8.0 Hz, 2H), 7.54 (d, *J* = 8.0 Hz, 2H), 6.52 (d, J =2.8 Hz, 1H), 6.33 (d, $J_{H\text{-}F}$ = 45.6 Hz, 1H), 6.09 (s, 1H), 3.76 (s, 3H) ppm.

methyl 4-(1-fluoro-2-(methoxycarbonyl)allyl)benzoate (2f)

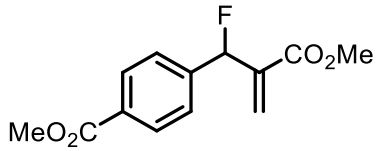

40% yield. Spectroscopic data match with those previously reported.[5a]

^{1}H NMR (400 MHz, $CDCl_3$) δ 8.07 (d, *J* = 8.1 Hz, 2H), 7.49 (d, *J* = 7.6 Hz, 2H), 6.50 (d, *J* = 2.3 Hz, 1H), 6.35 (d, $J_{H\text{-}F}$ = 45.8 Hz, 1H), 6.05 (s, 1H), 3.94 (s, 3H), 3.75 (s, 3H) ppm.

methyl 2-((4-chlorophenyl)fluoromethyl)acrylate (2g)

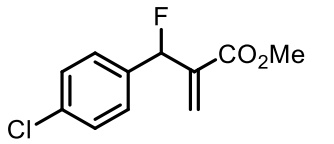

32% yield. Spectroscopic data match with those previously reported.[4]

^{1}H NMR (400 MHz, $CDCl_3$) δ 7.51 (d, *J* = 7.9 Hz, 2H), 7.27 (dd, *J* = 7.6, 1.8 Hz, 2H), 6.46 (d, *J* = 2.9 Hz, 1H), 6.23 (d, $J_{H\text{-}F}$ = 45.9 Hz, 1H), 6.04 (s, 1H), 3.72 (s, 3H) ppm.

methyl 2-(fluoro(4-methoxyphenyl)methyl)acrylate (2h)

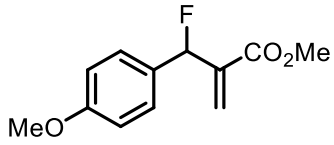

10% yield. Spectroscopic data match with those previously reported.[5a]

^{1}H NMR (400 MHz, $CDCl_3$) δ 7.34 (d, *J* = 8.6, 2H), 6.92 (d, *J* = 8.3 Hz, 2H), 6.46 (d, *J* = 3.0 Hz, 1H), 6.25 (d, $J_{H\text{-}F}$ = 46.2 Hz, 1H), 6.06 (s, 1H), 3.83 (s, 3H), 3.73 (s, 3H) ppm.

methyl 2-(fluoro(p-tolyl)methyl)acrylate (2i)

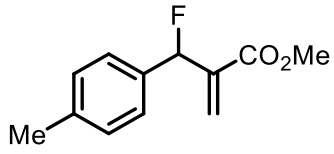

36% yield. Spectroscopic data match with those previously reported.[4]

^{1}H NMR (400 MHz, $CDCl_3$) δ 7.28 (d, *J* = 9.1 Hz, 2H), 7.18 (d, *J* = 7.6 Hz, 2H), 6.45-6.44 (m, 1H), 6.25 (d, $J_{H\text{-}F}$ = 46.2 Hz, 1H), 6.03 (d, *J* = 1.0 Hz, 1H), 3.71 (s, 3H), 2.36 (s, 3H) ppm.

methyl 2-((4-bromophenyl)(fluoro)methyl)acrylate (2j)

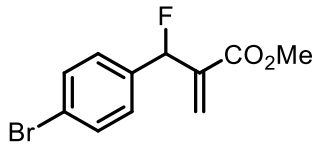

43% yield. Spectroscopic data match with those previously reported.[4]

^{1}H NMR (400 MHz, $CDCl_3$) δ 7.51 (d, *J* = 7.9 Hz, 2H), 7.27 (dd, *J* = 7.6, 1.8 Hz, 2H), 6.46 (d, *J* = 2.9 Hz, 1H), 6.23 (d, $J_{H\text{-}F}$ = 45.9 Hz, 1H), 6.04 (s, 1H), 3.72 (s, 3H) ppm.

methyl 2-(fluoro(m-tolyl)methyl)acrylate (2k)

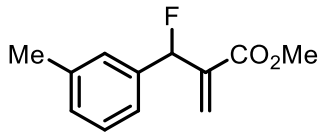

39% yield. Spectroscopic data match with those previously reported.[4]

^{1}H NMR (400 MHz, $CDCl_3$) δ 7.28-7.17 (m, 4H), 6.45 (s, 1H), 6.25 (d, $J_{H\text{-}F}$ = 45.9 Hz, 1H), 6.02 (s, 1H), 3.72 (s, 3H), 2.36 (s, 3H) ppm.

methyl 2-(fluoro(o-tolyl)methyl)acrylate (2l)

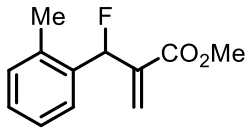

40% yield. Spectroscopic data match with those previously reported.[4]

^{1}H NMR (400 MHz, $CDCl_3$): δ 7.33 (d, *J* = 7.9 Hz, 1H), 7.29-7.18 (m, 3H), 6.55 (d, $J_{H\text{-}F}$ = 45.9 Hz, 1H), 6.49 (s, 1H), 5.88 (d, *J* = 0.9 Hz, 1H), 3.75 (s, 3H), 2.40 (s, 3H) ppm.

methyl 2-(fluoro(naphthalen-2-yl)methyl)acrylate (2m)

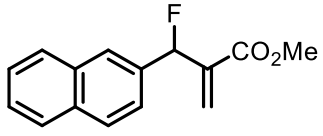

26% yield. Spectroscopic data match with those previously reported.[4]

^{1}H NMR (400 MHz, $CDCl_3$) δ 7.88-7.85 (m, 4H), 7.53-7.48 (m, 3H), 6.47 (d, $J_{H\text{-}F}$ = 45.9 Hz, 1H), 6.51 (d, *J* = 2.4 Hz, 1H), 6.10 (s, 1H), 3.72 (s, 3H) ppm.

methyl 2-(fluoro(naphthalen-1-yl)methyl)acrylate (2n)

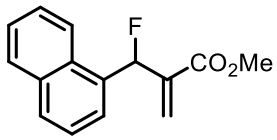

***2n** was prepared following the abovementioned procedure.*

S3n (2.00 g, 1.0 equiv., 8.2 mmol) was dissolved in 25 mL of CH_2Cl_2 and the solution was cooled down to -78 °C. Then, DAST (1.59 g, 1.2 equiv., 9.8 mmol) was added dropwise. After 2h, the reaction was quenched and purified. **2n** was obtained in *35% yield* (701 mg, 2.9 mmol) as a white solid.

^{1}H NMR (500 MHz, $CDCl_3$) δ 8.01 (1H, d, J = 8.19 Hz), 7.88 (2H, t, J = 7.8 Hz), 7.59-7.45 (4H, m), (1H, d, J_{H-F} = 45.7 Hz), 6.54 (1H, s), 5.88 (1H, s), 3.77 (3H, s) ppm. **^{13}C NMR** (126 MHz, $CDCl_3$) δ 165.8 (d, J_{C-F} = 4.6 Hz), 139.0 (d, J_{C-F} = 21.4 Hz), 138.9, 133.0 (d, J_{C-F} = 19.0 Hz), 129.8 (d, J_{C-F} = 2.6 Hz), 128.9, 128.6 (d, J_{C-F} = 7.8 Hz), 129.8 (d, J = 2.6 Hz), 126.8, 126.1, 125.3, 125.1 (d, J_{C-F} = 8.6 Hz), 123.6, 87.9 (d, J_{C-F} = 172.3 Hz), 52.3 ppm. **^{19}F NMR** (471 MHz, $CDCl_3$) δ -171.93 (1F, d, J_{H-F} = 45.7 Hz) ppm. **HRMS (ESI)** Calculated for $C_{15}H_{13}FNaO_2^+$ ($[M+Na]^+$) 267.0792. Found 267.08.

methyl 2-(fluoro(pyridin-2-yl)methyl)acrylate (2o)

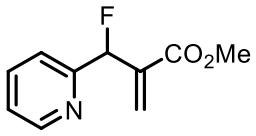

***2o** was prepared following the abovementioned procedure.*

S3o (1.00 g, 1.0 equiv., 5.1 mmol) was dissolved in 16 mL of CH_2Cl_2 and the solution was cooled down to -78 °C. Then, DAST (0.99 g, 1.2 equiv., 6.1 mmol) was added dropwise. After 2h, the reaction was quenched and purified. **2o** was obtained in *26% yield* (259 mg, 1.3 mmol) as a purple viscous oil.

^{1}H NMR (500 MHz, $CDCl_3$) δ 8.59 (1H, d, J = 4.8 Hz), 7.75 (1H, td, J = 7.7, 1.74 Hz), 7.52 (1H, d, J = 7.8 Hz), 7.29-7.23 (1H, m), 6.53 (1H, s), 6.34 (1H, d, J_{H-F} = 46.2 Hz), 6.01 (1H, s), 3.73 (3H, s) ppm. **^{13}C NMR** (126 MHz, $CDCl_3$) δ 165.4 (d, J_{C-F} = 5.1 Hz), 157.0 (d, J_{C-F} = 23.1 Hz), 149.5, 138.2 (d, J_{C-F} = 20.5 Hz), 137.0, 128.3 (d, J_{C-F} = 8.8 Hz), 123.6 (d, J_{C-F} = 1.9 Hz), 121.8 (d, J_{C-F} = 5.0 Hz), 91.4 (d, J_{C-F} = 175.1 Hz), 52.2 ppm. **^{19}F NMR** (471 MHz, $CDCl_3$) δ -183.39 (1F, d, J_{H-F} = 46.2 Hz) ppm. **HRMS (ESI)** Calculated for $C_{10}H_{11}FO_2^+$ ($[M+H]^+$) 196.0768. Found 196.077.

ethyl 2-(fluoro(phenyl)methyl)acrylate (2p)

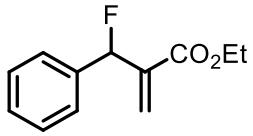

36% yield. Spectroscopic data match with those previously reported.[5b]

^{1}H NMR (400 MHz, $CDCl_3$): δ 7.44-7.30 (5H, m), 6.45 (1H, s), 6.29 (1H, d, J_{H-F} = 46.2 Hz), 6.01 (1H, s), 4.23-4.10 (2H, m) 1.22 (1H, t, J = 7.12 Hz) ppm.

hexyl 2-(fluoro(phenyl)methyl)acrylate (2q)

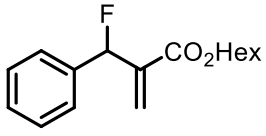

***2q** was prepared following the abovementioned procedure.*

S3q (2.00 g, 1.0 equiv.,7.6 mmol) was dissolved in 23 mL of CH_2Cl_2 and the solution was cooled down to -78 °C. Then, DAST (1.5 g, 1.2 equiv., 9.1 mmol) was added dropwise. After 2h, the reaction was quenched and purified. **2q** was obtained in *37% yield* (687 mg, 2.8 mmol) as a yellowish oil.

^{1}H NMR (500 MHz, $CDCl_3$) δ 7.42-7.31 (5H, m), 6.46 (1H, dt, *J* = 2.9, 1.01 Hz), 6.27 (1H, d, J_{H-F} = 46.1 Hz), 6.02 (1H, t, *J* = 1.2 Hz), 4.17-4.02 (2H, m), 1.62-1.53 (2H, m), 1.32-1.19 (6H, m), 0.92-0.82 (3H, m) ppm. **^{13}C NMR** (126 MHz, $CDCl_3$) δ 165.0 (d, J_{C-F} = 6.4 Hz), 139.7 (d, J_{C-F} = 22.5 Hz), 137.6 (d, J_{C-F} = 20.0 Hz), 129.1 (d, J_{C-F} = 2.9 Hz), 128.6 (d, J_{C-F} = 1.1 Hz), 127.3 (d, J_{C-F} = 5.52 Hz), 125.8 (d, J_{C-F} = 9.0 Hz), 91.1 (d, J_{C-F} = 174.0 Hz), 65.3, 31.5, 28.6, 25.6, 22.6, 14.1 ppm. **^{19}F NMR** (471 MHz, $CDCl_3$) δ -175.60 (1F, d, J_{H-F} = 46.1 Hz) ppm. **HRMS (ESI)** Calculated for $C_{16}H_{22}FO_2^+$ ($[M+H]^+$) 265.1598. Found 265.1599.

tert-butyl 2-(fluoro(phenyl)methyl)acrylate (2r)

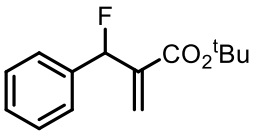

20% yield. Spectroscopic data match with those previously reported.[4]

^{1}H NMR (400 MHz, $CDCl_3$) δ 7.37–7.39 (5H, m), 6.37 (1H, d, *J* = 3.3 Hz) 6.21 (1H, d, J_{H-F} = 46.5 Hz), 5.94 (1H, s), 1.37 (9H, s) ppm.

methyl 2-(cyclohexylfluoromethyl)acrylate (2s)

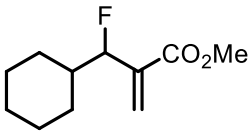

38% yield. Spectroscopic data match with those previously reported.[4]

^{1}H NMR (400 MHz, $CDCl_3$) δ 6.38 (1H, d, *J* = 2.1 Hz), 5.87 (1H, s), 5.12 (1H, dd, *J* = 46.5, 4.2 Hz), 3.78, (3H, s), 1.63-1.76 (6H, m), 1.02-1.26 (5H, m) ppm.

methyl 3-fluoro-2-methylene-4-phenylbutanoate (2t)

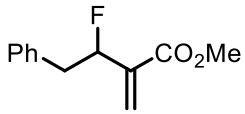

***2t** was prepared following the abovementioned procedure.*

S3t (300 mg, 1.0 equiv., 1.46 mmol) was dissolved in 4.5 mL of CH_2Cl_2 and the solution was cooled down to -78 °C. Then, DAST (282 mg, 1.2 equiv., 1.75 mmol) was added dropwise. After 2h, the reaction was quenched and purified. **2t** was obtained in *35% yield* (106 mg, 0.51 mmol) as a colourless oil.

^{1}H NMR (400 MHz, $CDCl_3$) δ 7.35 – 7.19 (5H, m), 6.33 (1H, dt, *J* = 3.30, 0.93 Hz), 5.86 (1H, dd, *J* = 1.46, 0.98 Hz), 5.51 (1H, ddddd, *J* = 46.63, 7.79, 3.53, 1.47, 0.85 Hz), 3.78 (3H, s), 3.27-3.10 (1H, m), 3.04-2.88 (1H, m). **^{13}C NMR** (100 MHz, $CDCl_3$) δ 165.5 (d, J_{C-F} = 7.43 Hz), 139.1 (d, J_{C-F} = 20.06 Hz), 136.7, 129.7, 128.5, 126.9, 126.1 (d, J_{C-F} = 9.79 Hz), 91.1 (d, J_{C-F} = 176.86 Hz), 52.1, 41.7 (d, J_{C-F} = 22.55 Hz). **^{19}F NMR** (471 MHz, $CDCl_3$) δ -183.60 (1F, dddd, *J* = 46.63, 31.52, 22.89, 3.22 Hz).

***B.3. General Procedure C** – Synthesis of TBS-, TES-, and TIPS-protected silyl enol ethers*

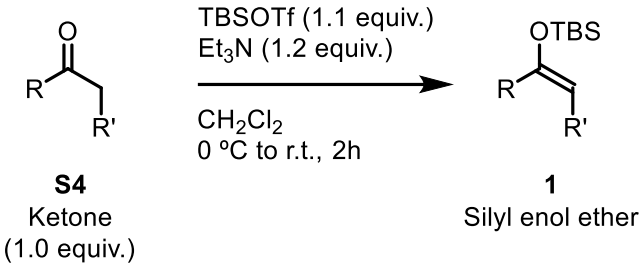

S4
Ketone
(1.0 equiv.)

1
Silyl enol ether

The reaction was carried out following the previously described procedure.[6]

To a flame-dried two necked round bottom flask ketone **S4** (1 equiv., 20 mmol) was added under nitrogen atmosphere and dissolved with freshly distilled CH_2Cl_2 (0.5 M). Subsequently, triethylamine (1.2 equiv., 24 mmol) was added at room temperature. The mixture was stirred for 5 minutes at room temperature. Then, the reaction mixture was cooled to 0 °C and TBSOTf (1.1 equiv., 22 mmol) was added dropwise. The reaction was stirred for 2 h at room temperature and then quenched with a saturated NH_4Cl aqueous solution. The aqueous layer was extracted with hexane (3x25 mL). The combined organic layers were dried over $MgSO_4$ and concentrated under reduced pressure. The crude product **1** was purified by column chromatography on silica gel using hexane as eluent, to afford **1** as an oil.

tert-butyl(cyclohex-1-en-1-yloxy)dimethylsilane (1b)

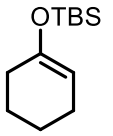

90% yield. Spectroscopic data match with those previously reported.[7a]

^{1}H NMR (400 MHz, $CDCl_3$) δ 4.89-4.84 (1H, bm), 2.03-1.96 (4H, m), 1.69-1.61 (2H, m), 1.53-1.47 (2H, m), 0.91 (9H, s), 0.12 (6H, s) ppm.

(cyclohex-1-en-1-yloxy)triethylsilane (1c)

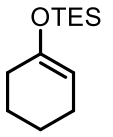

78% yield. Spectroscopic data match with those previously reported.[7a]

^{1}H NMR (400 MHz, $CDCl_3$) δ 4.89-4.83 (1H, m), 2.04-1.96 (4H, m), 1.68-1.60 (2H, m), 1.54-1.46 (2H, m), 0.97 (9H, t, *J* = 8.0 Hz), 0.64 (6H, q, *J* = 8.0 Hz) ppm.

(cyclohex-1-en-1-yloxy)triisopropylsilane (1d)

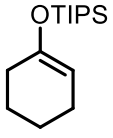

65% yield. Spectroscopic data match with those previously reported.[7b]

^{1}H NMR (400 MHz, $CDCl_3$) δ 4.87 (m, 1H), 2.04 (m, 2H), 1.99 (m, 2H), 1.65 (m, 2H), 1.50 (m, 2H), 1.14 (m, 3H), 1.07 (d, *J* = 5 Hz, 18H) ppm.

***tert*-butyl(cyclopent-1-en-1-yloxy)dimethylsilane (1e)**

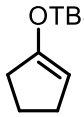

79% yield. Spectroscopic data match with those previously reported.[7c]

^{1}H NMR (400 MHz, $CDCl_3$) δ 4.64-4.60 (m, 1H), 2.29-2.21 (m, 4H), 1.89-1.81 (m, 2H), 0.92 (s, 9H), 0.15 (s, 6H) ppm.

***tert*-butyl(cyclohept-1-en-1-yloxy)dimethylsilane (1f)**

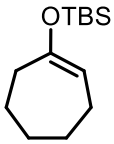

66% yield. Spectroscopic data match with those previously reported.[7a]

^{1}H NMR (400 MHz, $CDCl_3$) δ 5.01 (1H, t, *J* = 6.4 Hz), 2.26-2.19 (2H, m), 1.98 (2H, dd, *J* = 11.6, 6.4 Hz), 1.71-1.63 (2H, m), 1.61-1.48 (4H, m), 0.91 (9H, s), 0.11 (6H, s) ppm.

(*E*)-*tert*-butyl(cyclooct-1-en-1-yloxy)dimethylsilane (1g)

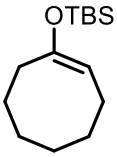

35% yield. Spectroscopic data match with those previously reported.[7a]

^{1}H NMR (400 MHz, $CDCl_3$) δ 4.74-4.66 (1H, m), 2.20-2.14 (2H, m), 2.04-1.96 (2H, m), 1.61-1.45 (8H, m), 0.91 (9H, s), 0.14 (6H, s) ppm.

***tert*-butyl((3,6-dihydro-2H-pyran-4-yl)oxy)dimethylsilane (1h)**

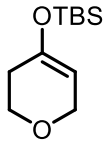

***1h** was prepared following the abovementioned procedure.*

To a flame-dried two necked round bottom flask, ketone **S4h** (500 mg, 1 equiv., 5.0 mmol) was added under nitrogen atmosphere and dissolved with freshly distilled CH_2Cl_2 (0.5 M). Subsequently, triethylamine (836 µL 1.2 equiv., 6.0 mmol) was added at room temperature. The mixture was stirred for 5 minutes at room temperature. Then, the reaction mixture was cooled to 0 °C and TBSOTf (1.26 mL, 1.1 equiv., 5.5 mmol) was added dropwise. The reaction was stirred for 2 h at room temperature and then quenched and purified. **1h** was obtained in *70% yield* (750 mg, 3.5 mmol) as an oil.

^{1}H NMR (400 MHz, $CDCl_3$) δ 4.85-4.80 (m, 1H), 4.14 (q, *J* = 2.58 Hz, 2H), 3.81 (t, *J* = 5.58 Hz, 2H), 2.16-2.10 (m, 2H), 0.93 (s, 9H), 0.15 (s, 6H) ppm. **^{13}C NMR** (100 MHz, $CDCl_3$) *δ* 148.1, 102.5, 64.9, 64.9, 30.6, 25.8, 18.1, 0.1 ppm. **HRMS (ESI)** Calculated for $C_{22}H_{44}NaO_4Si_2^+$ ($[2M+Na]^+$) 451.2670. Found 451.2698.

***tert*-butyl((4,4-dimethylcyclohex-1-en-1-yl)oxy)dimethylsilane (1i)**

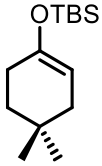

79% yield. Spectroscopic data match with those previously reported.[7c]

^{1}H NMR (400 MHz, $CDCl_3$) δ 4.78 (t, *J* = 4.0 Hz, 1H), 2.01-1.99 (m, 2H), 1.83-1.81 (m, 2H), 1.42 (t, *J* = 1.5Hz, 2H), 0.93 (s, 15H), 0.14 (s, 6H) ppm.

***tert*-butyl((3,4-dihydronaphthalen-1-yl)oxy)dimethylsilane (1j)**

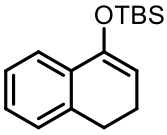

41% yield. Spectroscopic data match with those previously reported.[7a]

^{1}H NMR (400 MHz, $CDCl_3$) δ 7.46 (1H, d, *J* = 7.2 Hz), 7.22-7.08 (3H, m), 5.17 (1H, t, *J* = 4.6 Hz), 2.76 (2H, t, *J* = 8.0 Hz), 2.35-2.27 (2H, m), 1.01 (9H, s), 0.20 (6H, s) **ppm.**

((1,4-dioxaspiro[4.5]dec-7-en-8-yl)oxy)(*tert*-butyl)dimethylsilane (1k)

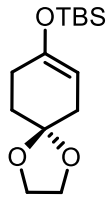

78% yield. Spectroscopic data match with those previously reported.[7a]

^{1}H NMR (500 MHz, $CDCl_3$) δ 4.72 (1H, t, *J* = 4.0 Hz), 3.98-3.95 (4H, m), 2.60 (2H, dd, *J* = 16.5, 1.5 Hz), 2.21 (2H, dd, *J* = 6.5 Hz, 1.0 Hz), 1.80 (2H, t, *J* = 6.5 Hz), 0.91 (9H, s), 0.13 (6H, s) ppm.

***tert*-butyldimethyl((1-phenylvinyl)oxy)silane (1l)**

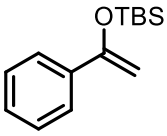

81% yield. Spectroscopic data match with those previously reported.[7d]

^{1}H NMR (500 MHz, $CDCl_3$) δ 7.62-7.60 (2H, m), 7.34-7.28 (3H, m), 4.89 (1H, d, *J* = 1.7 Hz), 4.42 (1H, d, *J* = 1.7 Hz), 1.01 (9H, s), 0.21 (6H, s) ppm.

***tert*-butyl((1-(4-methoxyphenyl)vinyl)oxy)dimethylsilane (1m)**

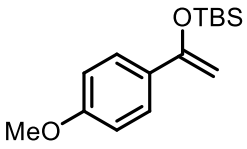

82% yield. Spectroscopic data match with those previously reported.[7d]

^{1}H NMR (500 MHz, $CDCl_3$) δ 7.55-7.58 (2H, m), 6.85-6.88 (2H, m), 4.79 (1H, d, *J* = 1.6 Hz), 4.35 (1H, d, *J* = 1.6 Hz), 3.82 (3H, s), 1.02 (9H, s), 0.23 (6H, s) ppm.

((1-([1,1'-biphenyl]-4-yl)vinyl)oxy)(tert-butyl)dimethylsilane (1n)

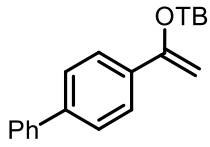

76% yield. Spectroscopic data match with those previously reported.[7d]

^{1}H NMR (500 MHz, $CDCl_3$) δ 7.70-7.72 (2H, m), 7.62-7.64 (2H, m), 7.58-7.60 (2H, m), 7.44-7.48 (2H, m), 7.36 (1H, t, *J* = 7.4 Hz), 4.97 (1H, d, *J* = 1.8 Hz), 4.48 (1H, d, *J* = 1.8 Hz), 1.06 (9H, s), 0.27 (6H, s) ppm.

((1H-inden-3-yl)oxy)(*tert*-butyl)dimethylsilane (1o)

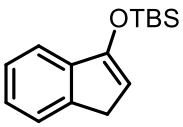

69% yield. Spectroscopic data match with those previously reported.[7e]

^{1}H NMR (400 MHz, $CDCl_3$) δ 7.28 (2H, dd, *J* = 11.2, 7.6 Hz), 7.19 (1H, t, *J* = 7.6 Hz), 7.10 (1H, t, *J* = 7.6 Hz), 5.30 (1H, s), 3.15 (2H, d, *J* = 2.0 Hz), 0.93 (9H, s), 0.15 (6H, s) ppm.

***tert*-butyl((3,4-dihydronaphthalen-2-yl)oxy)dimethylsilane (1p)**

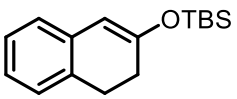

68% yield. Spectroscopic data match with those previously reported.[7f]

^{1}H NMR (400MHz, $CDCl_3$) δ 7.16-6.86 (4H, m), 5.7 (1H, s), 2.90 (2H, t, *J* = 7.0 Hz), 2.36 (3H, t, *J* = 7.0 Hz), 0.97 (9H, s), 0.22 (6H, s) ppm.

(*Z*)-*tert*-butyl((1,2-diphenylvinyl)oxy)dimethylsilane (1q)

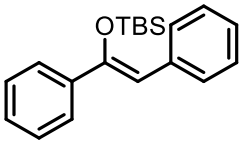

76% yield. Spectroscopic data match with those previously reported.[7g]

^{1}H NMR (400MHz, $CDCl_3$) δ 7.71-7.63 (4H, m), 7.43-7.26 (5H, m), 7.21-7.16 (1H, m), 6.24 (1H, s), 0.97 (9H, s), -0.22 (6H, s) ppm.

1-benzyl-4-((*tert*-butyldimethylsilyl)oxy)-1,2,3,6-tetrahydropyridine (1r)

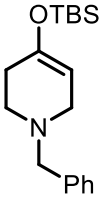

***1r** was prepared following the abovementioned procedure.*

To a flame-dried two necked round bottom flask ketone **S4r** (473 mg, 1 equiv., 2.5 mmol) was added under nitrogen atmosphere and dissolved with freshly distilled CH_2Cl_2 (0.5 M). Subsequently, triethylamine (418 µL, 1.2 equiv., 3.0 mmol) was added at room temperature. The mixture was stirred for 5 minutes at room temperature. Subsequently, it was cooled to 0 °C and TBSOTf (631 µL, 1.1 equiv., 2.75 mmol) was added dropwise. The reaction mixture was stirred for 2 h at room temperature and then quenched and purified. **1r** was obtained in *80% yield* (603 mg, 2 mmol) as an oil.

^{1}H NMR (500 MHz, Acetone-d_6) δ 7.36-7.28 (4H, m), 7.26-7.21 (1H, m), 4.79 (1H, m), 3.55 (2H, s), 2.95-2.90 (2H, m) 2.58 (2H, t, *J* = 5.8 Hz), 2.13-2.08 (2H, m), 0.92 (9H, s), 0.15 (6H, s) ppm. **^{13}C NMR** (126 MHz, Acetone-d_6) δ 149.9, 140.1, 129.6, 129.0, 127.7, 102.5, 62.7, 52.1, 50.8, 31.4, 26.1, 26.0, 18.6 ppm. **HRMS (ESI)** Calculated for $C_{18}H_{30}NOSi^+$ ($[M+H]^+$) 304.2091. Found 304.2094.

(*Z*)-tert-butyldimethyl((1-phenylbut-1-en-1-yl)oxy)silane (1s)

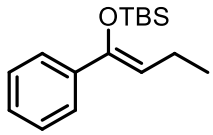

79% yield. Spectroscopic data match with those previously reported.[7a]

^{1}H NMR (400 MHz, $CDCl_3$) δ 7.43 (2H, d, J = 6.8 Hz), 7.31-7.25 (3H, m), 5.09 (1H, t, J = 7.6 Hz), 2.22 (2H, quin, J = 7.6 Hz), 1.03 (3H, t, J = 7.6 Hz), 0.98 (9H, s), –0.05 (6H, s) ppm.

B.4. General Procedure D – *Synthesis of TMS-protected silyl enol ethers*

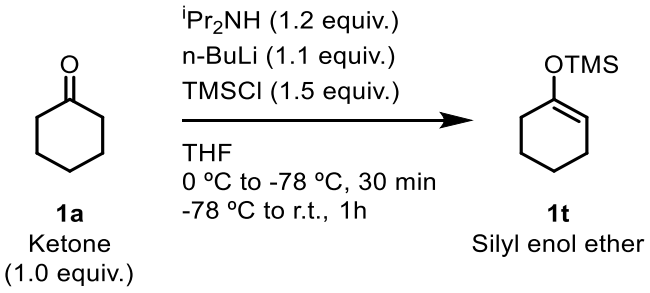

The reaction was carried out following the previously described procedure.[8a]

A flame-dried round bottom flask was charged with *N*,*N*-diisopropylamine (2.0 mL, 1.2 equiv., 14 mmol) and with dry tetrahydrofuran (20 mL, 0.5 M) under Ar atmosphere. The ~~round bottom~~ flask was cooled down to 0 °C and n-BuLi (5.1 mL of a 2.5 M THF solution, 1.1 equiv., 13 mmol) was added dropwise. The reaction mixture was stirred at 0 °C for additional 30 min. After cooling down to –78 °C and cyclohexanone (**1a**) (1.2 mL, 1.0 equiv., 12 mmol) followed by trimethylsilyl chloride (2.2 mL, 1.5 equiv., 17 mmol) were added dropwise under Ar. The resulting mixture was stirred for additional 15 min at –78 °C, then it was allowed to warm at room temperature and further stirred for 1 h. Next, the reaction was quenched with 10 mL of aqueous saturated $NaHCO_3$ and the resultant mixture was extracted with hexane (2x15 mL). The organic layer was washed with brine (15 mL), dried over $MgSO_4$ and concentrated under vacuum. The residue was purified through flash chromatography with silica gel deactivated with triethylamine (SiO_2/Et_3N 5% v/v) using hexane as eluent to give the silyl enol ether **1t** (colourless oil, 72% yield).

(cyclohex-1-en-1-yloxy)trimethylsilane (1t)

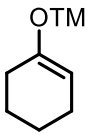

Spectroscopic data match with those previously reported.[7a]

^{1}H NMR (400 MHz, Acetone-d_6) δ 4.88-4.85 (1H, m), 2.03-1.96 (4H, m), 1.68-1.62 (2H, m), 1.53-1.48 (2H, m), 0.18 (9H, s).

B.5. Synthesis of TBS-protected silyl enol ethers from natural products

Acetylation of estrone

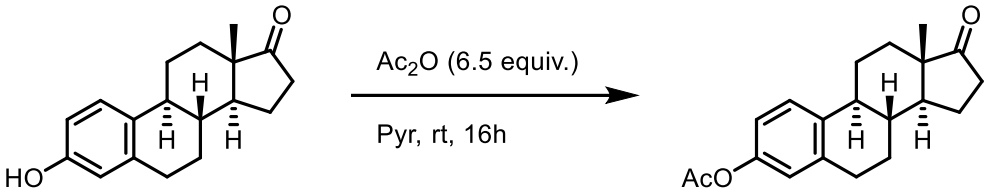

S5
(1.0 equiv.)

S4u

The reaction was carried out following the previously described procedure.[9]

A solution of estrone (**S5**) (1.35 g, 1.0 equiv., 5.0 mmol) in pyridine (7 mL) was cooled to 0 ºC. Then, acetic anhydride (3.31 g, 6.5 equiv., 32.5 mmol) was added dropwise and, after 20 min at the same temperature, the reaction was stirred at room temperature for 16 h. The reaction mixture was then poured into ice water (70 mL) and the resulting solid was filtered, washed with water and dried at 60 ºC under high vacuum to afford estrone acetate (**S4u**) in quantitative yield.

Spectroscopic data match with those previously reported.[9]

Silylation of estrone acetate

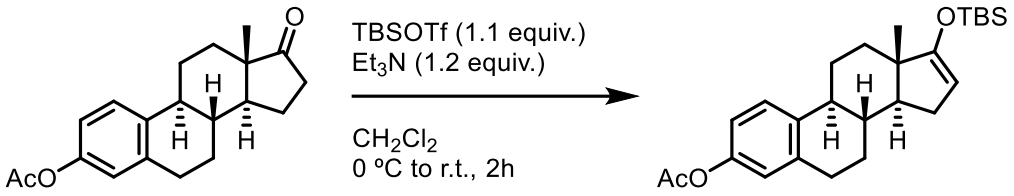

S4u
(1.0 equiv.)

1u

The reaction was carried out following the previously described procedure.[7e]

To a flame-dried two necked round bottom flask ketone **S4u** (780 mg, 1 equiv., 2.5 mmol) was added under nitrogen atmosphere and dissolved with freshly distilled CH_2Cl_2 (0.5 M). Subsequently, triethylamine (418 µL, 1.2 equiv., 3 mmol) was added at room temperature. The mixture was stirred for 5 minutes at room temperature. Then, the reaction mixture was cooled to 0 °C and TBSOTf (631 µL, 1.1 equiv., 2.75 mmol) was added dropwise. The reaction was stirred for 2 h at room temperature and then quenched with a saturated NH_4Cl aqueous solution. The aqueous layer was extracted with hexane. The combined organic layers were dried over $MgSO_4$ and concentrated under reduced pressure. The crude product **1u** was purified by column chromatography on silica gel using hexane as eluent to afford **1u** (940 mg, 88% yield) as a colourless solid.

Spectroscopic data match with those previously reported.[7e]

Silylation of pregnenolone acetate

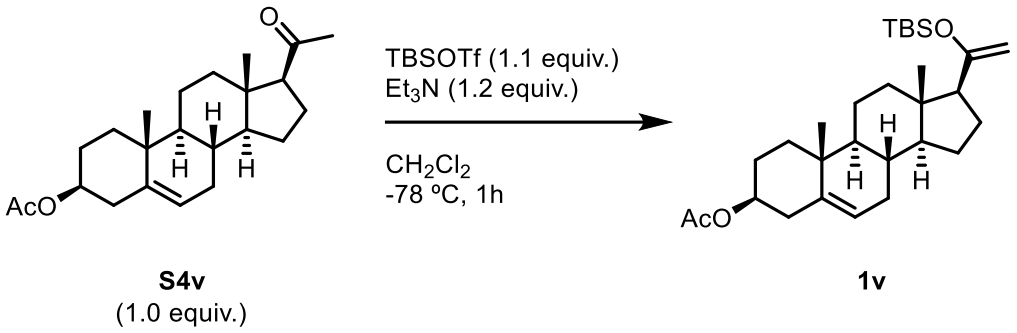

S4v
(1.0 equiv.)

1v

The reaction was carried out following the previously described procedure.[10a]

To a flame-dried two necked round bottom flask ketone **S4v** (896 mg, 1 equiv., 2.5 mmol) was added under nitrogen atmosphere and dissolved with freshly distilled CH_2Cl_2 (0.5 M). The reaction mixture was cooled to -78 °C. Then, triethylamine (418 µL, 1.2 equiv., 3 mmol) and TBSOTf (631 µL, 1.1 equiv., 2.75 mmol) were added dropwise. The reaction was stirred for 1 h and then quenched with a saturated NH_4Cl aqueous solution at room temperature. The aqueous layer was extracted with CH_2Cl_2. The combined organic layers were dried over $MgSO_4$ and concentrated under reduced pressure. The crude product was purified by column chromatography on silica gel using hexane as eluent to afford **1v** (1 g, 85% yield) as a colourless solid.

Spectroscopic data match with those previously reported.[10a]

Silylation of (+)-camphor

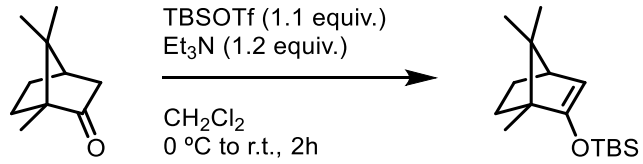

S4w
(1.0 equiv.)

1w

The reaction was carried out following the previously described procedure.[10b]

To a flame-dried two necked round bottom flask ketone **S4w** (380 mg, 1 equiv., 2.5 mmol) was added under nitrogen atmosphere and dissolved with freshly distilled CH_2Cl_2 (0.5 M). Subsequently, triethylamine (418 µL, 1.2 equiv., 3 mmol) was added at room temperature. The mixture was stirred for 5 minutes at room temperature. Then, the reaction mixture was cooled to 0 °C with and TBSOTf (631 µL, 1.1 equiv., 2.75 mmol) was added dropwise. The reaction was stirred for 2 h at room temperature and then quenched with a saturated NH_4Cl aqueous solution. The aqueous layer was extracted with hexane. The combined organic layers were dried over $MgSO_4$ and concentrated under reduced pressure. The crude product was purified by column chromatography chromatography on silica gel using hexane as eluent to afford **1w** (505 mg, 78% yield) as an oil.

Spectroscopic data match with those previously reported.[10b]

B.6. Synthesis of tert-butyldimethyl((2-methylcyclohex-1-en-1-yl)oxy)silane

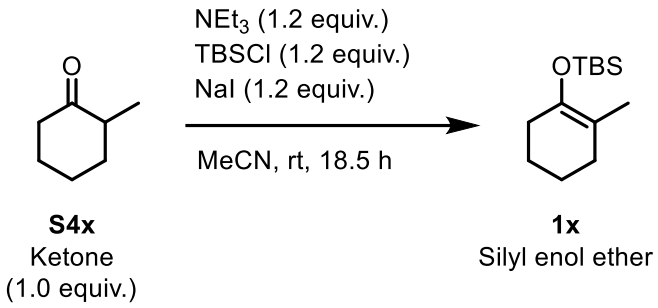

The reaction was carried out following the previously described procedure.[8b]

A nitrogen-purged, 250-mL round-bottomed flask is equipped with a magnetic stirring bar. The flask is charged with 2-methylcyclohexanone (10.0 mL, 1 equiv., 82.6 mmol), triethylamine (13.9 mL, 1.2 equiv., 100 mmol), and t-butyldimethylsilyl chloride (TBSCl) (15.1 g, 1.2 equiv., 100 mmol). To the flask is added a solution of sodium iodide (15.0 g, 1.2 equiv., 100 mmol) in acetonitrile (100 mL) via syringe over 30 min at ambient temperature. The reaction solution is stirred at ambient temperature for 18 h. The resulting mixture is quenched by addition of saturated sodium bicarbonate solution (100 mL). The mixture is extracted with hexane twice (2 × 200 mL). The combined organic phases are washed with brine (40 mL) and dried over $MgSO_4$, filtered and concentrated at reduced pressure the crude product as a pale yellow oil. This crude product is purified by filtration through a silica gel pad with *n*-hexanes to provide 17.8 g **1x**. (colourless oil, 95% yield.)

tert-butyldimethyl((2-methylcyclohex-1-en-1-yl)oxy)silane (1x)

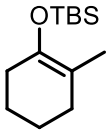

Spectroscopic data match with those previously reported.[8b]

^{1}H NMR (400 MHz, $CDCl_3$) δ 1.98-2.02 (2H, m), 1.92-1.95 (2H, m), 1.60-1.66 (2H, m), 1.56 (3H, s), 1.51-1.55 (2H, m), 0.94 (9H, s), 0.10 (6H, s).

B.7. Synthesis of Starting Materials for the control experiments

General procedure for synthesis of allyl carbonate and acetate

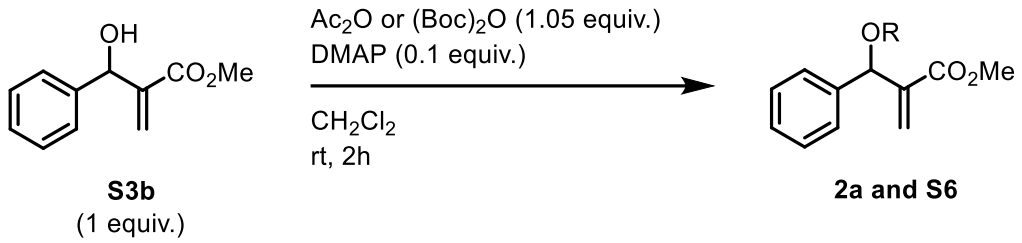

S3b (1 equiv.)

2a and S6

The reaction was carried out following the previously described procedure.[2]

To a solution of 1.0 equiv. of the Morita-Baylis-Hillman alcohol **S3b** in CH_2Cl_2 (0.5 M), 1.05 equiv. of the corresponding anhydride and 0.1 equiv. of 4-dimethylaminopyridine (DMAP) were added. The solution was stirred until consumption of starting material (monitored by TLC). Then, the solvent was removed by rotary evaporation and the reaction mixture was purified by flash column chromatography on silica gel (hexane/EtOAc mixtures).

methyl 2-(((tert-butoxycarbonyl)oxy)(phenyl)methyl)acrylate (2a)

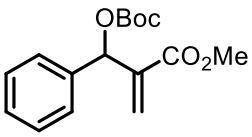

91% yield. Spectroscopic data match with those previously reported.[2]

^{1}H NMR (400MHz, $CDCl_3$) δ 7.34 (5H, m), 6.48 (1H, s), 6.40 (1H, s), 5.91 (1H, s), 3.71 (3H, s), 1.46 (9H, s) ppm.

methyl 2-(acetoxy(phenyl)methyl)acrylate (S6)

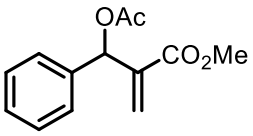

86% yield. Spectroscopic data match with those previously reported.[11]

^{1}H NMR (400MHz, $CDCl_3$) δ 7.40-7.25 (5H, m), 6.67 (1H, s), 6.41 (1H, s), 5.80 (1H, s), 3.62 (3H, s), 2.11 (3H, s) ppm.

General procedure for synthesis of Enol Adducts

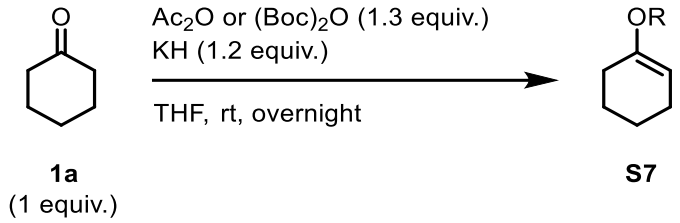

The reaction was carried out following the previously described procedure.[12]

Into a 100 mL round-bottom flask under argon was added KH (0.94 g, 1.2 equiv., 23.4 mmol). Then, dry THF (55 mL) and cyclohexanone **1a** (2.0 g, 1.0 equiv., 20.4 mmol) were consecutively added dropwise via syringe over a 10 min period. After 15 min, the resulting mixture was treated by the dropwise addition of the corresponding anhydride (1.3 equiv., 26.5 mmol). After the addition, the mixture was stirred at room temperature overnight. The reaction mixture was quenched with 35 mL of Na_2CO_3 (sat.) and then extracted three times with 25 mL of Et_2O. The combined ether layers were washed twice with 25 mL of Na_2CO_3 (sat.) and once with brine, dried with $MgSO_4$ and concentrated under vacuum pressure. The crude product was purified by flash column chromatography obtaining a colourless oil.

Spectroscopic data for all compounds matched with those previously reported in literature.[12]

***tert*-butyl cyclohex-1-en-1-yl carbonate (S7a)**

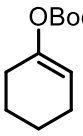

***S7a** was prepared following the abovementioned procedure.*

90% yield.[1]**H NMR** (500 MHz, Acetone-d_6) δ 5.38-5.34 (1H, m), 2.16-2.10 (2H, m), 2.10-2.06 (2H, m), 1.74-1.67 (2H, m), 1.60-1.53 (2H, m), 1.46 (9H, s) ppm. **^{13}C NMR** (126 MHz, Acetone-d_6) δ 152.5, 149.5, 114.1, 82.6, 27.9, 27.3, 24.3, 23.5, 22.6 ppm. **HRMS (ESI)** Calculated for $C_{11}H_{19}O_3^+$ ($[M+H]^+$) 199.1329. Found 199.1332.

cyclohex-1-en-1-yl acetate (S7b)

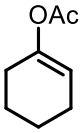

***S7b** was prepared following the abovementioned procedure.*

81% yield. **^{1}H NMR** (400MHz, $CDCl_3$) δ 5.33 (1H, t, *J* = 3.8 Hz), 2.13-2.04 (7H, m), 1.76-1.66 (2H, m), 1.61-1.52 (2H, m) ppm.

C. Defluorinative Allylation of Silyl Enol Ethers – Racemic reaction

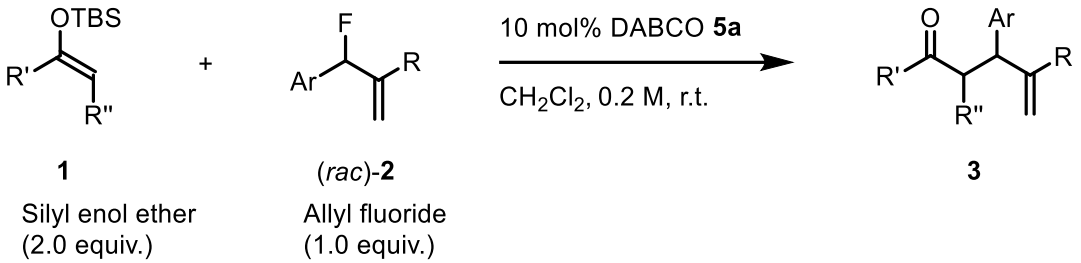

1 Silyl enol ether (2.0 equiv.)

(*rac*)-**2** Allyl fluoride (1.0 equiv.)

3

The corresponding allyl fluoride **2** (1 equiv., 0.2 mmol) was weighted into a 5 mL vial equipped with a magnetic stirring bar and dissolved with 1 mL of distilled CH_2Cl_2 (0.2 M). Subsequently, the corresponding silyl enol ether **1** (2 equiv., 0.4 mmol) and a 10 mol% of DABCO **5a** were added. The reaction mixture was stirred at room temperature until full conversion of the starting material was detected either by ^{1}H NMR or by TLC analysis. The crude product **3** was directly purified by flash column chromatography on silica gel using hexane and ethyl acetate mixtures as eluents.

D. Optimization of the Asymmetric Reaction

D.1. Optimization – Catalyst screening

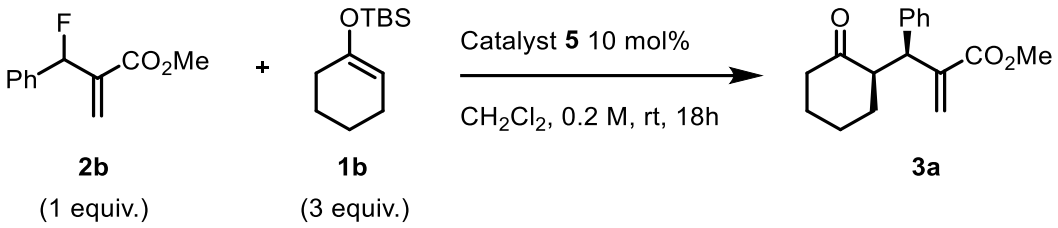

2b (1 equiv.) **1b** (3 equiv.) **3a**

Entry	Catalyst[c]	NMR yield (%)[a]	r.r.	d.r.	e.r.[b]
1	(-)-Cinchonidine **5c**	48	4:1	>20:1	38:62
2	Quinine **5d**	9	6:1	>20:1	42:58
3	Quinidine benzoate **5e**	<5	10:1	>20:1	61:39
4	Cinchonidine benzoate **5f**	<5	10:1	>20:1	36:64
5	β-isocupreidine **5g**	47	5:1	>20:1	31:69
6	Thiourea quinine **5h**	-	-	-	-
7	Squaramide cinchonidine **5i**	-	-	-	-
8	$(DHQ)_2PYR$ **5j**	64	3:1	>20:1	39:61
9	$(DHQD)_2AQN$ **5k**	26	1:1f	5:1	21:79
10	$(DHQD)_2PHAL$ **5b**	**61**	**>20:1**	**>20:1**	**82:17**

Table S1. Optimisation of the chiral Lewis base catalyst used in this study. [a] The yield was determined by ^1H NMR spectroscopy using 1,3,5-trimethoxybenzene as the internal standard, [b] Determined by HPLC analysis using a chiral column.

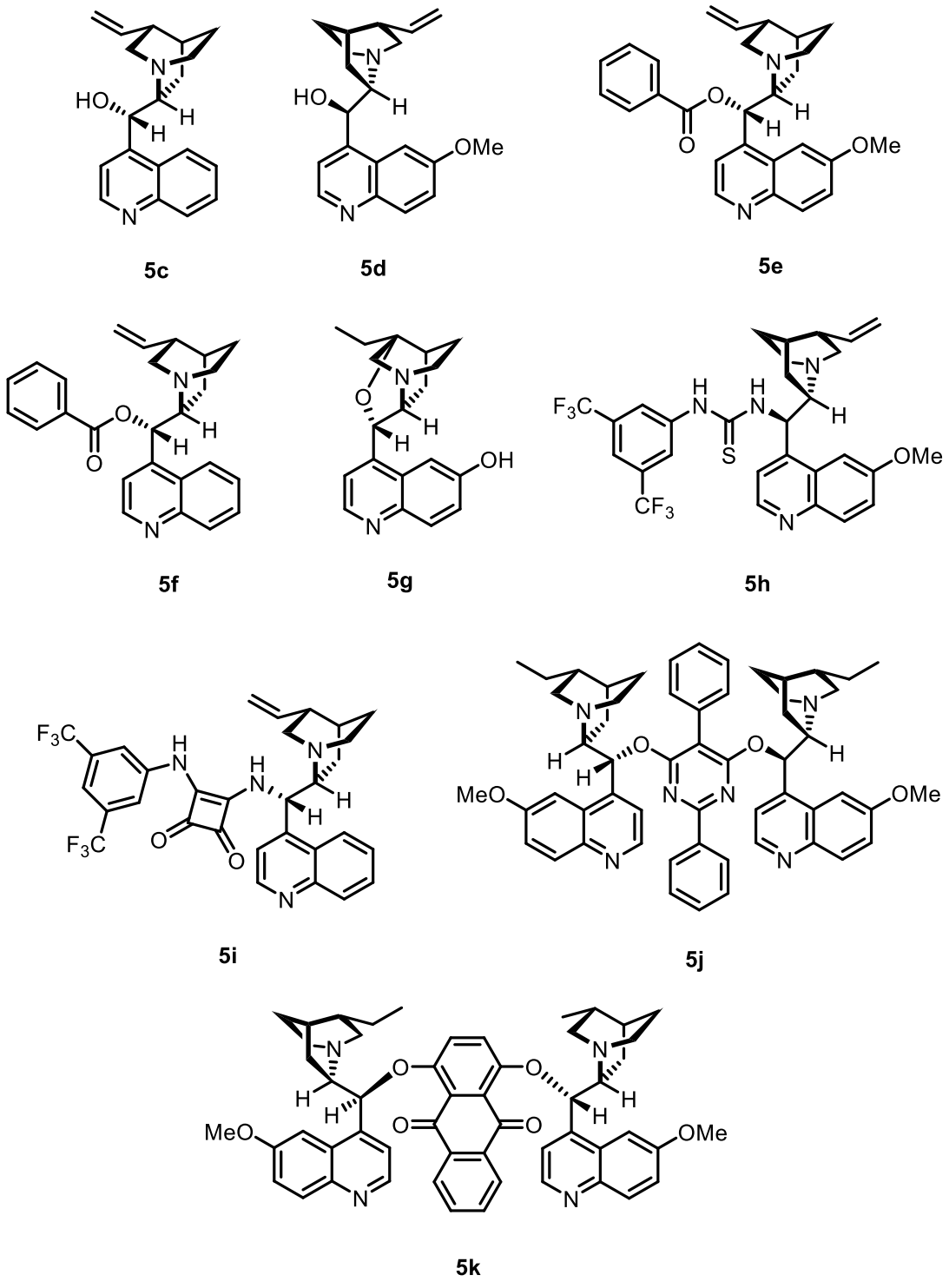

Figure S1. Catalysts **5c-k**.

D.2. Optimization – Solvent screening

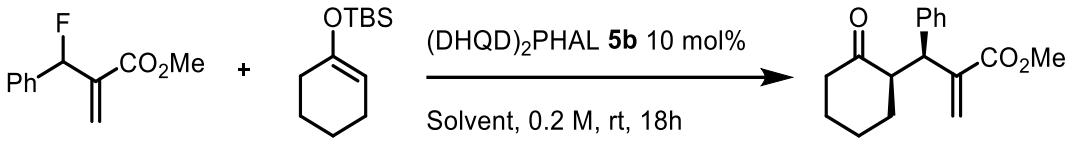

2b (1 equiv.) **1b** (3 equiv.) **3a**

Entry	Solvent	NMR yield (%)[a]	r.r.	d.r.	e.r.[b]
1	CH_2Cl_2	**61**	>20:1	>20:1	82:17
2	DCE	40	>20:1	>20:1	68:32
3	$CHCl_3$	7	5:1	>20:1	92:8
4	Toluene	nr	-	-	-
5	$PhCF_3$	nr	-	-	-
6	1,2-DCB	25	6:1	>20:1	73:27
7	Acetone	30	1.5:1	>20:1	88:12
8	THF	9	10:1	>20:1	95:5
9	Dioxane	nr	-	-	-
10	THP	22	10:1	>20:1	81:19
11	2-MeTHF	5	8:1	>20:1	92:8
12	THF 1:1 CH_2Cl_2	55	18:1	>20:1	88:12
13	THF 9:1 CH_2Cl_2	**20**	**14:1**	**>20:1**	**95:5**
14	THF 1:9 CH_2Cl_2	65	19:1	>20:1	79:21
15	THF 8:2 CH_2Cl_2	47	14:1	>20:1	93:7
16	THF 6:4 CH_2Cl_2	25	15:1	>20:1	89:11

Table S2. Solvent optimisation. [a] The yield was determined by ^{1}H NMR spectroscopy using 1,3,5-trimethoxybenzene as the internal standard, [b] Determined by HPLC analysis using a chiral column. DCE: dichloroethane, 1,2-DCB: 1,2-dichlorobenzene, THF: tetrahydrofuran, THP: tetrahydropyran.

***D.3. Optimization** – Substituent at the silyl group screening*

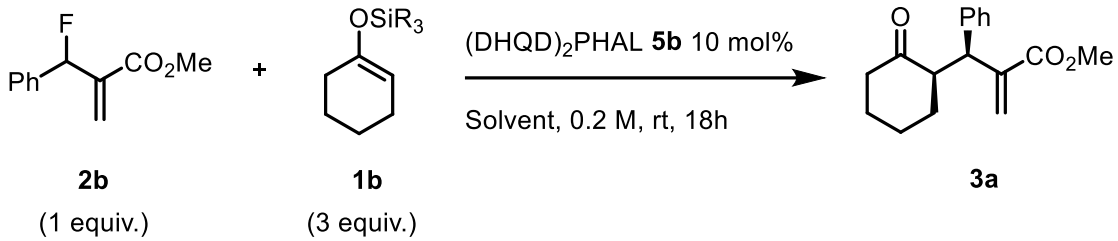

2b (1 equiv.) **1b** (3 equiv.) **3a**

Entry	Silyl group	Solvent	NMR yield (%)[a]	r.r.	d.r.	e.r.[b]
1	TMS	CH_2Cl_2	80	17:1	>20:1	85:15
2	TES	CH_2Cl_2	71	>20:1	>20:1	85:15
3	TIPS	CH_2Cl_2	18	12:1	>20:1	85:15
4	TMS	THF	20	7:1	>20:1	93:7
5	TES	THF	11	6:1f	>20:1	94:6
6	TIPS	THF	<5	10:1	>20:1	76:24
7	TMS	THF 9:1 CH_2Cl_2	31	11:1	>20:1	89:11
8	TES	THF 9:1 CH_2Cl_2	31	9:1	>20:1	88:12
9	**TBS**	**THF 9:1 CH_2Cl_2**	**20**	**14:1**	**>20:1**	**95:5**

Table S3. Screening of the substituent at the silyl group of the silyl enol ether. [a] The yield was determined by ^{1}H NMR spectroscopy using 1,3,5-trimethoxybenzene as the internal standard, [b] Determined by HPLC analysis using a chiral column.

***D.4. Optimization** – Temperature, concentration, catalyst loading and time screening*

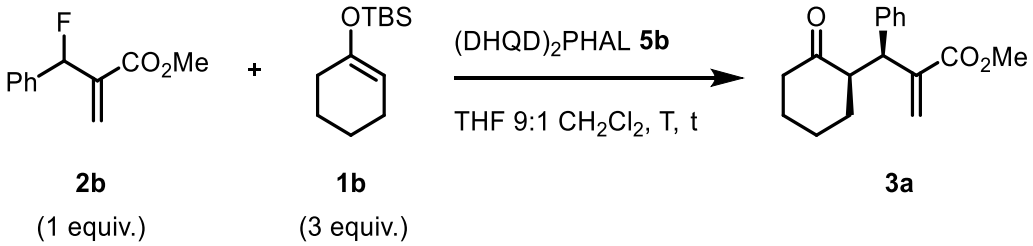

2b (1 equiv.) **1b** (3 equiv.) **3a**

Entry	Temp. (°C)	Conc. (M)	Cat. loading (mol%)	Time (h)	NMR yield (%)[a]	r.r.	d.r.	e.r.[b]
1	25	0.2	10	18	20	14:1	>20:1	95:5
2	-20	0.2	10	18	20	>20:1	>20:1	95:5
3	40	0.2	10	18	30	4:1	>20:1	93:7
4	25	0.4	10	72	71[c]	13:1	>20:1	91:9
5	25	0.4	20	72	76[c]	12:1	>20:1	89:11
6	25	**0.2**	**20**	**72**	**75[c]**	**14:1**	**>20:1**	**95:5**

Table S4. Optimisation of the temperature, concentration, catalyst loading and time. [a] The yield was determined by ^{1}H NMR spectroscopy using 1,3,5-trimethoxybenzene as the internal standard, [b] Determined by HPLC analysis using a chiral column. [c] Isolated yield.

E. Asymmetric Defluorinative Allylation of Silyl Enol Ethers – General procedure

E.1. Generality of the asymmetric transformation

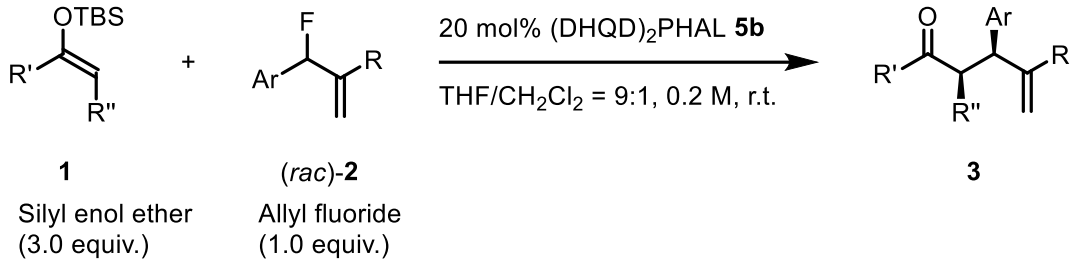

The corresponding allyl fluoride **2** (1 equiv., 0.2 mmol) was weighted into a 5 mL vial equipped with a magnetic stirring bar and dissolved with 1 mL of a 9:1 = THF/CH_2Cl_2 mixture (0.2 M). Subsequently, the corresponding silyl enol ether **1** (3 equiv., 0.6 mmol) and a 20 mol% of $(DHQD)_2PHAL$ **5b** were added. The reaction mixture was stirred at room temperature until full conversion of the starting material was detected either by ^1H NMR or TLC analysis. The crude product **3** was directly purified by flash column chromatography on silica gel using hexane and ethyl acetate mixtures as eluents.

methyl 2-((*S*)-((*R*)-2-oxocyclohexyl)(phenyl)methyl)acrylate (3a)

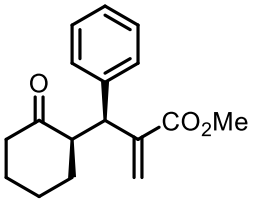

***3a** was prepared following the abovementioned procedure.*

75% yield (41 mg, 0.15 mmol), colourless solid. **^{1}H NMR** (500 MHz, $CDCl_3$) δ 7.34-7.21 (5H, m), 6.26 (1H, s), 5.65 (1H, s), 4.26 (1H, d, J = 11.41 Hz), 3.72 (3H, s), 3.12 (1H, td, J = 11.10, 4.98 Hz), 2.51-2.45 (1H, m), 2.43-2.36 (1H, m), 2.12-2.02 (1H, m), 1.89-1.68 (3H, m), 1.67-1.56 (1H, m), 1.40-1.24 (1H, m); **^{13}C NMR** (100 MHz, $CDCl_3$) δ 212.2, 167.3, 143.3, 140.8, 128.7, 128.6, 126.8, 122.9, 54.9, 52.1, 45.8, 42.6, 33.4, 29.2, 24.8; **HRMS (ESI)** Calculated for $C_{17}H_{21}O_3^+$ ($[M+H]^+$) 273.1485. Found 273.1473; **$[\alpha]_D^{25}$** = +103.4 (c = 1.78, $CHCl_3$); **HPLC** Phenomenex Lux Cellulose-5 (80:20 *n*-Hexane: 2-Propanol, 1 mL/min, 218 nm); tr (major) = 17.4, tr (minor) = 29.4 (95:5 e.r.).

methyl 2-((*S*)-((*R*)-5,5-dimethyl-2-oxocyclohexyl)(phenyl)methyl)acrylate (3b)

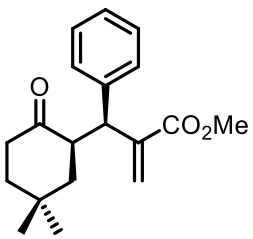

***3b** was prepared following the abovementioned procedure.*

55% yield (33 mg, 0.11 mmol), orange solid. **^{1}H NMR** (400 MHz, $CDCl_3$) δ 7.39-7.18 (5H, m), 6.21 (1H, s), 5.60 (1H, s), 4.18 (1H, d, J = 10.78 Hz), 3.75 (3H, s), 3.45-3.28 (1H, m), 2.61 (1H, td, J = 13.46, 6.15 Hz), 2.39-2.23 (1H, m), 1.87-1.76 (1H, m), 1.75-1.63 (1H, m), 1.49-1.39 (1H, m), 1.34-1.29 (1H, m), 1.23 (3H, s), 0.93 (3H, s); **^{13}C NMR** (100 MHz, $CDCl_3$) δ 212.4, 167.4, 144.2, 141.0, 128.6, 128.6, 126.7, 121.9, 52.0, 50.1, 46.4, 45.7, 41.3, 39.3, 31.3, 31.2, 24.6. **HRMS (ESI)** Calculated for $C_{19}H_{25}O_3^+$ ($[M+H]^+$) 301.1798. Found 301.1802. **$[\alpha]_D^{25}$** = +167.6 (c = 2.05, $CHCl_3$). **HPLC** Phenomenex Lux Cellulose-5 (95:5 *n*-hexane: 2-propanol, 1 mL/min, 218 nm); tr (major) = 54.2, tr (minor) = 61.1 (93:7 e.r.).

methyl 2-((*S*)-((*R*)-8-oxo-1,4-dioxaspiro[4.5]decan-7-yl)(phenyl)methyl)acrylate (3c)

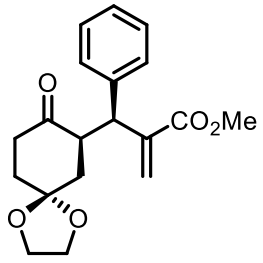

***3c** was prepared following the abovementioned procedure.*

73% yield (50 mg, 0.15 mmol), orange solid. **^{1}H NMR** (400 MHz, $CDCl_3$) δ 7.35-7.19 (5H, m), 6.24 (1H, s), 5.64 (1H, s), 4.30 (1H, d, *J* = 10.98 Hz), 4.06-3.83 (4H, m), 3.73 (3H, s), 3.52 (1H, td, *J* = 11.70, 5.43 Hz), 2.72 (1H, td, *J* = 13.38, 6.39 Hz), 2.56 (1H, t, *J* = 7.06 Hz), 2.50-2.41 (1H, m), 2.15-2.08 (1H, m), 2.04-1.94 (1H, m), 1.77-1.69 (1H, m); **^{13}C NMR** (100 MHz, $CDCl_3$) δ 210.3, 167.2, 143.5, 140.3, 128.6, 128.6, 126.8, 122.3, 107.5, 64.8, 64.6, 52.0, 50.3, 45.1, 39.9, 38.7, 38.3, 35.7, 34.0. **HRMS (ESI)** Calculated for $C_{19}H_{23}O_5^+$ ([M+H]$^+$) 331.154. Found 331.1546. **$[\alpha]_D^{25}$** = +113.6 (c = 2.34, $CHCl_3$). **HPLC** Phenomenex Lux Cellulose-5 (90:10 *n*-hexane: 2-propanol, 1 mL/min, 218 nm); tr (major) = 31.0, tr (minor) = 54.0 (95:5 e.r.)

methyl 2-((*S*)-((*S*)-4-oxotetrahydro-2H-pyran-3-yl)(phenyl)methyl)acrylate (3d)

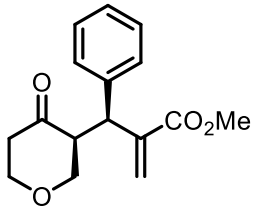

***3d** was prepared following the abovementioned procedure.*

68% yield (37 mg, 0.14 mmol), yellow solid. **^{1}H NMR** (500 MHz, $CDCl_3$) δ 7.41-7.15 (5H, m), 6.31 (1H, s), 5.77 (1H, s), 4.43 (1H, d, *J* = 11.78 Hz), 4.09-3.87 (2H, m), 3.69 (3H, s), 3.65 (1H, dd, *J* = 11.52, 4.37 Hz), 3.47 (1H, dd, *J* = 11.60, 6.59 Hz), 3.23-3.14 (1H, m), 2.69-2.58 (1H, m), 2.55-2.44 (1H, m); **^{13}C NMR** (126 MHz, $CDCl_3$) δ 207.8, 167.0, 141.6, 139.3, 128.9, 128.6, 127.3, 124.8, 72.0, 69.6, 56.2, 52.1, 43.8, 42.7. **HRMS (ESI)** Calculated for $C_{16}H_{19}O_4^+$ ([M+H]$^+$) 275.1278. Found 275.1286. **$[\alpha]_D^{25}$** = +135.7 (c = 2.56, $CHCl_3$). **HPLC** Phenomenex Lux Cellulose-5 (90:10 *n*-hexane: 2-propanol, 1 mL/min, 218 nm); tr (major) = 19.2, tr (minor) = 29.4 (95:5 e.r.)

methyl 2-((*S*)-((*S*)-1-benzyl-4-oxopiperidin-3-yl)(phenyl)methyl)acrylate (3e)

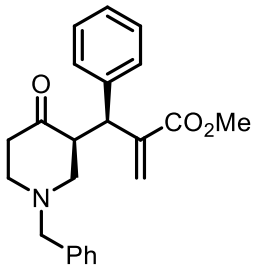

***3e** was prepared following the abovementioned procedure.*

72% yield (52 mg, 0.14 mmol), yellow solid. **^{1}H NMR** (500 MHz, $CDCl_3$) δ 7.43-7.30 (5H, m), 7.28-7.18 (5H, m) 6.35 (1H, s), 5.83 (1H, s), 4.63 (1H, d, *J* = 11.70 Hz), 3.74 (3H, s), 3.50 (2H, dd, *J* = 24.67, 13.02 Hz), 3.25-3.17 (1H, m), 2.84-2.76 (1H, m), 2.76-2.69 (1H, m), 2.66-2.59 (2H, m), 2.49-2.40 (2H, m); **^{13}C NMR** (126 MHz, $CDCl_3$) δ 210.6, 167.2, 141.9, 140.0, 138.0, 129.1, 128.6, 128.6, 128.4, 127.4, 127.0, 124.8, 61.8, 58.0, 54.8, 54.1, 52.1, 44.8, 40.8. **HRMS (ESI)** Calculated for $C_{23}H_{26}NO_3^+$ ([M+H]$^+$) 364.1907. Found 364.1913. **$[\alpha]_D^{25}$** = +124.4 (c = 2.13, $CHCl_3$). **HPLC** Phenomenex Lux Amylose-2 (95:5 *n*-hexane: 2-propanol, 1 mL/min, 218 nm); tr (minor) = 20.0, tr (major) = 22.8 (90:10 e.r.)

methyl 2-((*S*)-((*R*)-2-oxocyclopentyl)(phenyl)methyl)acrylate (3f)

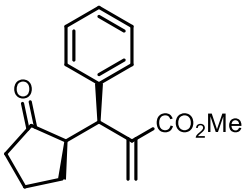

3f *was prepared following the abovementioned procedure.*

70% yield (36 mg, 0.14 mmol), yellow oil. **^{1}H NMR** (400 MHz, $CDCl_3$) δ 7.31-7.13 (5H, m), 6.36 (1H, s), 5.70 (1H, s), 4.33 (1H, d, J = 7.16 Hz), 3.65 (3H, s), 2.84-2.73 (1H, m), 2.33-2.21 (1H, m), 2.08-1.96 (2H, m), 1.82-1.68 (2H, m), 1.50-1.45 (1H, m); **^{13}C NMR** (100 MHz, $CDCl_3$) δ 218.9, 167.3, 142.6, 140.5, 128.7, 128.5, 126.9, 124.7, 52.1, 46.4, 38.4, 28.1, 20.5. **HRMS (ESI)** Calculated for $C_{16}H_{19}O_3^+$ ([M+H]$^+$) 259.1329. Found 259.1324. **$[\alpha]_D^{25}$** = +163.5 (c = 2.07, $CHCl_3$). **HPLC** (for major diastereomer) Phenomenex Lux Cellulose-5 (80:20 *n*-hexane: 2-propanol, 1 mL/min, 218 nm); tr (major) = 13.0, tr (minor) = 20.5 (93:7 e.r.)

methyl 2-((*S*)-((*R*)-2-oxocycloheptyl)(phenyl)methyl)acrylate (3g)

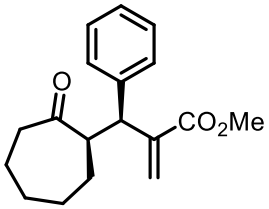

3g *was prepared following the abovementioned procedure.*

75% yield (43 mg, 0.15 mmol), orange solid. **^{1}H NMR** (400 MHz, $CDCl_3$) δ 7.32-7.17 (5H, m), 6.18 (1H, s), 5.64 (1H, s), 4.22 (1H, d, J = 11.60 Hz), 3.66 (3H, s), 3.37 (1H, td, J = 11.07, 3.27 Hz), 2.59-2.40 (2H, m), 2.43-2.36 (2H, m), 1.96-1.78 (2H, m), 1.24-1.19 (2H, m), 1.18-1.06 (2H, m); **^{13}C NMR** (100 MHz, $CDCl_3$) δ 214.5, 167.1, 143.3, 140.9, 128.9, 128.6, 126.9, 123.5, 55.0, 52.0, 47.8, 43.7, 30.3, 28.8, 28.3, 23.8. **HRMS (ESI)** Calculated for $C_{18}H_{23}O_3^+$ ([M+H]$^+$) 287.1642. Found 287.1644. **$[\alpha]_D^{25}$** = +90.4 (c = 1.95, $CHCl_3$). **HPLC** Phenomenex Lux Cellulose-5 (80:20 *n*-hexane: 2-propanol, 1 mL/min, 218 nm); tr (major) = 11.1, tr (minor) = 27.5 (95:5 e.r.)

methyl 2-((*S*)-((*R*)-2-oxocyclooctyl)(phenyl)methyl)acrylate (3h)

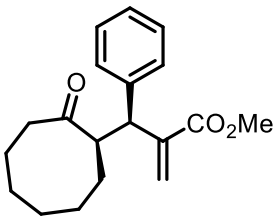

3h *was prepared following the abovementioned procedure.*

88% yield (53 mg, 0.18 mmol), orange solid. **^{1}H NMR** (500 MHz, $CDCl_3$) δ 7.30-7.23 (4H, m), 7.23-7.14 (1H, m), 6.18 (1H, s), 5.72 (1H, s), 4.17 (1H, d, J = 11.60 Hz), 3.64 (3H, s), 3.53 (1H, td, J = 11.23, 3.86 Hz), 2.46-2.30 (2H, m), 2.23-2.08 (1H, m), 1.92-1.79 (1H, m), 1.68-1.57 (1H, m), 1.57-1.49 (2H, m), 1.49-1.42 (2H, m), 1.41-1.28 (2H, m), 0.92-0.78 (1H, m); **^{13}C NMR** (126 MHz, $CDCl_3$) δ 218.7, 166.9, 143.0, 140.8, 128.8, 128.6, 126.9, 124.1, 52.3, 52.0, 49.4, 44.7, 33.7, 28.7, 25.1, 23.5. **HRMS (ESI)** Calculated for $C_{19}H_{25}O_3^+$ ([M+H]$^+$) 301.1798. Found 301.1804. **$[\alpha]_D^{25}$** = +38.9 (c = 2.15, $CHCl_3$). **HPLC** Phenomenex Lux Cellulose-1 (95:5 *n*-hexane: 2-propanol, 1 mL/min, 218 nm); tr (major) = 7.4, tr (minor) = 9.3 (93:7 e.r.)

methyl 2-((*S*)-((*R*)-1-oxo-1,2,3,4-tetrahydronaphthalen-2-yl)(phenyl)methyl)acrylate (3i)

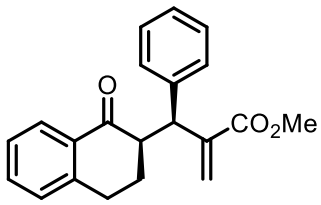

***3i** was prepared following the abovementioned procedure.*

63% yield (40 mg, 0.13 mmol), yellow oil. **^{1}H NMR** (400 MHz, $CDCl_3$) δ 7.93 (1H, dd, *J* = 7.87, 1.19 Hz), 7.41 (1H, td, *J* = 7.52, 1.48 Hz) 7.31-7.24 (5H, m), 7.21-7.13 (2H, m) 6.29 (1H, s), 5.71 (1H, s), 4.44 (1H, d, *J* = 9.66 Hz), 3.64 (3H, s), 3.28 (1H, td, *J* = 10.23, 4.04 Hz), 2.98-2.87 (2H, m), 2.02-1.89 (1H, m), 1.74-1.60 (1H, m**); ^{13}C NMR** (100 MHz, $CDCl_3$) δ 199.0, 167.4, 143.4, 143.0, 140.8, 133.3, 133.0, 128.9, 128.7, 128.6, 127.7, 126.9, 126.7, 123.8, 52.0, 50.8, 45.6, 28.3, 27.4. **HRMS (ESI)** Calculated for $C_{21}H_{21}O_3^+$ ($[M+H]^+$) 321.1485. Found 321.1493. **$[\alpha]_D^{25}$** = +51.3 (c = 0.65, $CHCl_3$). **HPLC** Phenomenex Lux Cellulose-5 (90:10 *n*-hexane: 2-propanol, 1 mL/min, 218 nm); tr (major) = 24.1, tr (minor) = 29.1 (89:11 e.r.)

methyl 2-((1-oxo-2,3-dihydro-1H-inden-2-yl)(phenyl)methyl)acrylate (3j)

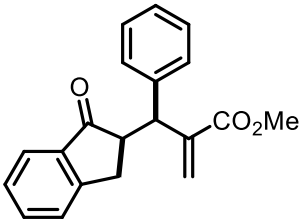

***3j** was prepared following the abovementioned procedure. This product has been characterized as a mixture of diastereoisomers* (dr = 4:1).

38% yield (23 mg, 0.076 mmol), yellow oil. **^{1}H NMR** (500 MHz, $CDCl_3$) (for major diastereomer) δ 7.71 (1H, d, *J* = 7.83 Hz), 7.50 (1H, td, *J* = 7.51, 1.20 Hz), 7.34-7.29 (2H, m), 7.26-7.20 (4H, m), 7.19-7.11 (1H, m), 6.42 (1H, s), 5.76 (1H, dd, *J* = 1.24, 0.69 Hz), 4.48 (1H, dd, *J* = 7.41, 1.22 Hz), 3.69 (3H, s), 3.47 (1H, td, *J* = 7.74, 4.21 Hz), 3.24 (1H, dd, *J* = 17.23, 8.39 Hz), 2.83 (1H, dd, *J* = 17.29, 4.19 Hz), (for minor diastereomer) δ 7.72 (1H, d, *J* = 8.04 Hz), 7.56 (1H, dd, *J* = 7.44, 1.29 Hz), 7.42- 7.38 (1H, m), 7.37-7.34 (1H, m) 7.29-7.20 (5H, m), 6.32 (1H, t, *J* = 0.71 Hz), 5.48 (1H, dd, *J* = 1.45, 0.55 Hz), 4.45 (1H, d, *J* = 7.03 Hz), 3.61 (3H, s), 3.39 (1H, ddd, *J* = 8.04, 6.97, 4.34 Hz), 3.26 (1H, dd, *J* = 17.23, 8.39 Hz), 3.03 (1H, dd, *J* = 17.28, 4.38 Hz); **^{13}C NMR** (100 MHz, $CDCl_3$) (for major diastereomer) δ 206.7, 167.2, 153.4, 142.7, 140.1, 136.9, 134.8, 128.7, 128.5, 127.5, 127.0, 126.5, 124.1, 52.1, 50.1, 48.0, 31.6, (for minor diastereomer) δ 206.0, 167.3, 152.8, 141.5, 140.7, 137.3, 134.8, 128.6, 128.6, 127.6, 126.6, 126.1, 125.6, 52.1, 50.5, 48.0, 31.6. **HRMS (ESI)** Calculated for $C_{20}H_{19}O_3^+$ ($[M+H]^+$) 307.1329. Found 307.1332. **$[\alpha]_D^{25}$** = +85.0 (c = 0.010, $CHCl_3$). **HPLC** (for major diastereomer) Phenomenex Lux Amylose-2 (80:20 *n*-hexane: 2-propanol, 1 mL/min, 218 nm); tr (minor) = 32.1, tr (major) = 37.0 (93:7 e.r.).

methyl 2-((*S*)-((*S*)-2-oxo-1,2,3,4-tetrahydronaphthalen-1-yl)(phenyl)methyl)acrylate (3k)

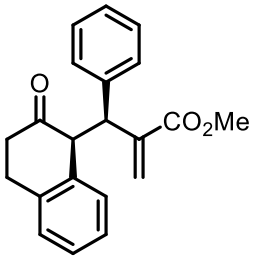

***3k** was prepared following the abovementioned procedure.*

48% global yield (31 mg, 0.10 mmol) of 5:1 diastereomer mixture. Pure samples of each diastereomer were obtained upon careful chromatographic purification.

major diastereomer, yellow oil. **^{1}H NMR** (400 MHz, $CDCl_3$) δ 7.18-7.12 (4H, m), 7.12-7.07 (1H, m), 6.98-6.91 (2H, m), 6.90-6.83 (1H, m), 6.48 (1H, s), 6.45-6.41 (1H, d, J = 7.58 Hz) 5.99 (1H, d, J = 1.1 Hz), 4.57 (1H, d, J = 10.78 Hz), 4.17 (1H, d, J = 10.78 Hz), 3.73 (3H, s), 3.44-3.30 (1H, m), 3.01-2.90 (1H, m), 2.75-2.66 (1H, m), 2.51-2.40 (1H, m); **^{13}C NMR** (100 MHz, $CDCl_3$) δ 211.1, 167.5, 140.2, 138.9, 136.9, 135.4, 130.2, 129.1, 128.3, 127.8, 127.3, 127.2, 126.3, 59.9, 52.3, 48.0, 37.0, 29.8, 27.8. **HRMS (ESI)** Calculated for $C_{21}H_{21}O_3^+$ ($[M+H]^+$) 321.1485. Found 321.1486. **HPLC** Phenomenex Lux Cellulose-1 (90:10 *n*-hexane: 2-propanol, 1 mL/min, 218 nm); tr (major) = 10.8, tr (minor) = 17.4 (91:9 e.r.).

methyl 2-((*S*)-((*R*)-2-oxo-1,2,3,4-tetrahydronaphthalen-1-yl)(phenyl)methyl)acrylate (3k')

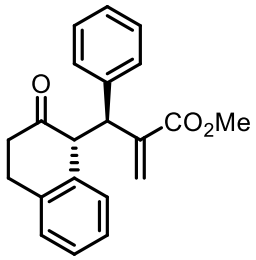

***3k'** was prepared following the abovementioned procedure.*

48% global yield (31 mg, 0.10 mmol) of 5:1 diastereomerr mixture. Pure samples of each diastereomer were obtained upon careful chromatographic purification.

minor diastereomer, yellow oil. **^{1}H NMR** (400 MHz, $CDCl_3$) δ 7.31-7.27 (1H, m), 7.26-7.22 (3H, m), 7.21-7.17 (2H, m), 7.17-7.12 (2H, m), 7.11-7.07 (1H, m) 6.32 (1H, s), 5.83 (1H, s), 4.62 (1H, d, J = 9.37 Hz), 4.17 (1H, d, J = 9.37 Hz), 3.55 (3H, s), 3.22-3.10 (1H, m), 2.91-2.82 (1H, m), 2.55-2.46 (1H, m), 2.44-2.33 (1H, m); **^{13}C NMR** (100 MHz, $CDCl_3$) δ 210.6, 167.2, 141.6, 139.2, 137.3, 136.0, 130.0, 129.0, 128.6, 128.1, 127.5, 126.8, 126.7, 58.8, 52.0, 48.9, 37.0, 27.6. **HRMS (ESI)** Calculated for $C_{21}H_{21}O_3^+$ ($[M+H]^+$) 321.1485. Found 321.1486. **HPLC** Phenomenex Lux Cellulose-1 (90:10 *n*-hexane: 2-propanol, 1 mL/min, 218 nm); tr (major) = 9.2, tr (minor) = 13.4 (92:8 e.r.)

methyl 4-benzoyl-2-methylene-3-phenylhexanoate (3l)

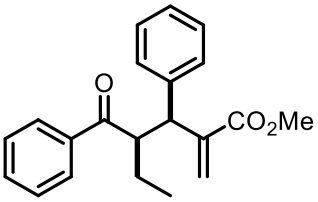

3l *was prepared following the abovementioned procedure. This product has been characterized as a mixture of diastereoisomers* (dr = 2:1).

66% yield (43 mg, 0.13 mmol) (dr = 2:1), yellow oil. **^{1}H NMR** (500 MHz, $CDCl_3$) (for major diastereomer) δ 7.82-7.77 (2H, m), 7.52-7.48 (1H, m), 7.38-7.34 (3H, m), 7.25-7.21 (2H, m), 7.10-7.04 (2H, m), 6.36 (1H, d, J = 0.88 Hz), 5.89 (1H, s), 4.50-4.41 (1H, m), 4.35 (1H, d, J = 11.30 Hz), 3.71 (3H, s), 1.83-1.75 (2H, m), 0.83 (3H, t, J = 7.50 Hz), (for minor diastereomer) δ 8.07-8.02 (2H, m), 7.60-7.56 (1H, m), 7.48-7.44 (2H, m), 7.34-7.29 (3H, m), 7.02-6.96 (2H, m), 6.06 (1H, s), 5.62 (1H, s), 4.44 (1H, d, J = 11.74 Hz), 4.27-4.20 (1H, m), 3.60 (3H, s), 1.56-1.49 (2H, m), 0.71 (3H, t, J = 7.55 Hz); **^{13}C NMR** (126 MHz, $CDCl_3$) (for major diastereomer) δ 203.6, 167.2, 141.7, 140.9, 138.6, 132.8, 128.6, 128.5, 128.2, 128.1, 126.6, 126.2, 52.0, 50.0, 49.3, 25.0, 11.3, (for minor diastereomer) δ 203.0, 166.9, 142.9, 140.7, 138.0, 133.2, 129.0, 128.9, 128.6, 128.4, 127.0, 124.0, 51.9, 49.8, 48.2, 24.7, 10.9. **HRMS (ESI)** Calculated for $C_{21}H_{23}O_3^+$ ($[M+H]^+$) 323.1642. Found 323.1642. **HPLC** Phenomenex Lux Cellulose-1 (99:1 *n*-hexane: 2-propanol, 1 mL/min, 218 nm); (for major diastereomer) tr (major) = 11.4, tr (minor) = 17.5, (63:37 e.r.); (for minor diastereomer) tr = 9.1, 16.6, (50:50 e.r.).

methyl 2-methylene-5-oxo-3,4,5-triphenylpentanoate (3m)

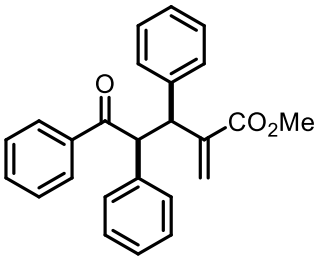

3m *was prepared following the abovementioned procedure. This product has been characterized as a mixture of diastereoisomers* (dr = 1.3:1).

78% yield (58 mg, 0.16 mmol) (dr = 2:1), colourless solid. **^{1}H NMR** (400 MHz, $CDCl_3$) (for major diastereomer) δ 8.04-7.98 (2H, m), 7.44-7.38 (5H, m), 7.23-7.16 (3H, m), 7.10-7.08 (5H, m), 6.26 (1H, s), 5.69 (1H, s), 5.20 (1H, d, J = 11.80 Hz), 4.84 (1H, d, J = 11.75 Hz) 3.65 (3H, s), (for minor diastereomer) δ 7.96-7.90 (2H, m), 7.52-7.44 (2H, m), 7.38-7.32 (2H, m), 7.30-7.24 (3H, m), 7.15-7.10 (3H, m), 7.04-6.99 (3H, m), 6.02 (1H, s), 5.77 (1H, d, J = 11.68 Hz) 5.59 (1H, s), 4.95 (1H, d, J = 11.76 Hz), 3.58 (3H, s); **^{13}C NMR** (100 MHz, $CDCl_3$) (for major diastereomer) δ 198.4, 166.9, 142.9, 139.8, 137.0, 136.7, 133.2, 129.0, 128.8, 128.8, 128.6, 128.6, 128.0, 127.3, 126.6, 123.4, 58.0, 52.1, 50.5, (for minor diastereomer) δ 198.5, 166.9, 141.4, 141.0, 137.1, 137.1, 133.0, 129.2, 128.9, 128.6, 128.6, 128.5, 128.3, 127.4, 127.4, 126.7, 55.5, 51.8, 51.5. **HRMS (ESI)** Calculated for $C_{25}H_{23}O_3^+$ ($[M+H]^+$) 371.1642. Found 371.1643. **HPLC** Phenomenex Lux Cellulose-5 (98:2 *n*-hexane: 2-propanol, 1 mL/min, 218 nm); (for minor diastereomer) tr (minor) = 19.5, tr (major) = 55.3, (86:14 e.r.); (for major diastereomer) tr (major) = 22.9, tr (minor) = 29.7 (68:32 e.r.).

methyl (*S*)-2-methylene-5-oxo-3,5-diphenylpentanoate (3n)

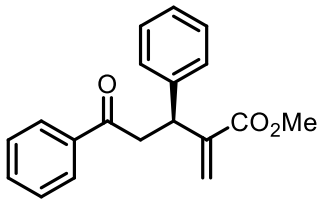

***3n** was prepared following the abovementioned procedure.*

76% yield (44 mg, 0.15 mmol), colourless solid. **^{1}H NMR** (400 MHz, $CDCl_3$) δ 8.00-7.88 (2H, m), 7.60-7.51 (1H, m), 7.50-7.40 (2H, m), 7.33-7.25 (4H, m), 7.24-7.15 (1H, m), 6.31 (1H, s), 5.62 (1H, s), 4.69 (1H, t, *J* = 7.37 Hz), 3.69 (3H, s), 3.56 (2H, qd, *J* = 17.17, 7.56 Hz); **^{13}C NMR** (100 MHz, $CDCl_3$) δ 197.7, 167.1, 142.9, 141.9, 137.0, 133.3, 128.7, 128.6, 128.2, 128.0, 126.8, 124.9, 52.1, 43.5, 42.2. **HRMS (ESI)** Calculated for $C_{19}H_{19}O_3^+$ ($[M+H]^+$) 295.1329. Found 295.1328. **$[\alpha]_D^{25}$** = +50.7 (c = 1.82, $CHCl_3$). **HPLC** Phenomenex Lux Cellulose-1 (99:1 *n*-hexane: 2-propanol, 1 mL/min, 218 nm); tr (major) = 30.1, tr (minor) = 43.0 (91:9 e.r.).

methyl (*S*)-5-(4-methoxyphenyl)-2-methylene-5-oxo-3-phenylpentanoate (3o)

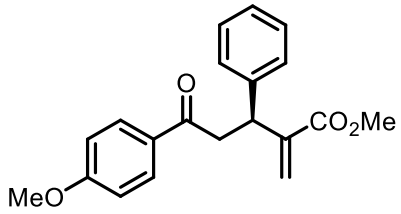

***3o** was prepared following the abovementioned procedure.*

70% yield (46 mg, 0.14 mmol), colourless solid. **^{1}H NMR** (400 MHz, $CDCl_3$) δ 7.92 (2H, d, *J* = 8.95 Hz), 7.30-7.24 (4H, m), 7.21-7.15 (1H, m), 6.90 (2H, d, *J* = 8.95 Hz), 6.29 (1H, s), 5.60 (1H, s), 4.66 (1H, t, *J* = 7.38 Hz), 3.85 (3H, s), 3.68 (3H, s), 3.49 (2H, qd, *J* = 16.98, 7.09 Hz); **^{13}C NMR** (100 MHz, $CDCl_3$) δ 196.3, 167.2, 163.7, 143.0, 142.1, 130.5, 130.1, 128.6, 128.1, 126.8, 124.8, 113.9, 55.6, 52.1, 43.2, 42.3. **HRMS (ESI)** Calculated for $C_{20}H_{21}O_4^+$ ($[M+H]^+$) 325.1434. Found 325.1446. **$[\alpha]_D^{25}$** = +42.9 (c = 2.07, $CHCl_3$). **HPLC** Phenomenex Lux Amylose-2 (80:20 *n*-hexane: 2-propanol, 1 mL/min, 218 nm); tr (minor) = 41.1, tr (major) = 45.0 (93:7 e.r.).

methyl (*S*)-5-([1,1'-biphenyl]-4-yl)-2-methylene-5-oxo-3-phenylpentanoate (3p)

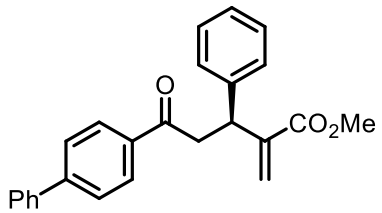

***3p** was prepared following the abovementioned procedure.*

62% yield (46 mg, 0.12 mmol), colourless solid. **^{1}H NMR** (400 MHz, $CDCl_3$) δ 8.02 (2H, d, *J* = 8.00 Hz), 7.67 (2H, d, *J* = 8.00 Hz), 7.64-7.59 (2H, m), 7.50-7.44 (2H, m), 7.43-7.37 (1H, m), 7.33-7.27 (4H, m), 7.24-7.16 (1H, m), 6.33 (1H, s), 5.64 (1H, s), 4.71 (1H, t, *J* = 7.39 Hz), 3.70 (3H, s) 3.59 (2H, qd, *J* = 17.01, 7.10 Hz); **^{13}C NMR** (100 MHz, $CDCl_3$) δ 197.3, 167.1, 146.0, 142.9, 141.9, 140.0, 135.7, 129.1, 128.8, 128.7, 128.4, 128.1, 127.4, 126.9, 124.9, 52.1, 43.6, 42.3. **HRMS (ESI)** Calculated for $C_{25}H_{23}O_3^+$ ($[M+H]^+$) 371.1642. Found 371.1649. **$[\alpha]_D^{25}$** = +38.6 (c = 1.85, $CHCl_3$). **HPLC** Phenomenex Lux Amylose-2 (80:20 *n*-hexane: 2-propanol, 1 mL/min, 218 nm); tr (minor) = 44.0, tr (major) = 47.6 (92:8 e.r.).

methyl 2-((*S*)-(4-fluorophenyl)((*R*)-2-oxocyclohexyl)methyl)acrylate (3q)

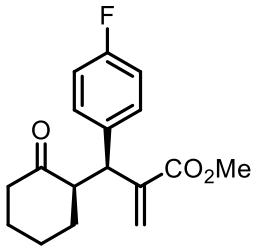

***3q** was prepared following the abovementioned procedure.*

70% yield (41 mg, 0.14 mmol), colourless solid. **^{1}H NMR** (500 MHz, $CDCl_3$) δ 7.17 (2H, dd, J_{HH} = 8.73 Hz, $^4J_{HF}$ = 5.37 Hz), 6.96 (2H, t, $^3J_{HF}$ = 8.72 Hz, J_{HH} = 8.69 Hz), 6.22 (1H, s), 5.58 (1H, s), 4.21 (1H, d, J = 11.20 Hz), 3.68 (3H, s), 3.03 (1H, td, J = 11.10, 4.95 Hz), 2.49-2.40 (1H, m), 2.39-2.30 (1H, m), 2.09-1.99 (1H, m), 1.86-1.77 (2H, m), 1.77-1.64 (1H, m), 1.63-1.59 (1H, m), 0.93-0.78 (1H, m); **^{13}C NMR** (126 MHz, $CDCl_3$) δ 211.9, 167.2, 161.8 (d, $^1J_{CF}$ = 245.43 Hz), 143.2, 136.4 (d, $^4J_{CF}$ = 3.24 Hz), 130.1 (d, $^3J_{CF}$ = 7.93 Hz), 122.9, 115.4 (d, $^2J_{CF}$ = 21.21 Hz), 54.8, 52.1, 45.0, 42.6, 33.4, 29.1, 24.8; **^{19}F NMR** (471 MHz, $CDCl_3$) δ -116.24 (s). **HRMS (ESI)** Calculated for $C_{17}H_{20}FO_3^+$ ($[M+H]^+$) 291.1391. Found 291.1388. **$[\alpha]_D^{25}$** = +139.9 (c = 1.03, $CHCl_3$). **HPLC** Phenomenex Lux Cellulose-5 (95:5 *n*-hexane: 2-propanol, 1 mL/min, 218 nm); tr (minor) = 37.8, tr (major) = 42.6 (93:7 e.r.).

methyl 2-((*S*)-(4-chlorophenyl)((*R*)-2-oxocyclohexyl)methyl)acrylate (3r)

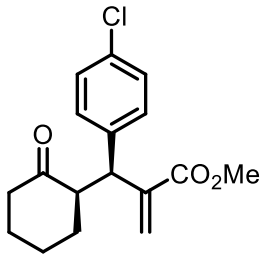

***3r** was prepared following the abovementioned procedure.*

56% yield (34 mg, 0.11 mmol), orange solid. **^{1}H NMR** (400 MHz, $CDCl_3$) δ 7.24 (2H, d, J = 8.50 Hz), 7.14 (2H, d, J = 8.49 Hz), 6.22 (1H, s), 5.58 (1H, s), 4.20 (1H, d, J = 11.12 Hz), 3.68 (3H, s), 3.04 (1H, td, J = 11.13, 4.94 Hz), 2.49-2.39 (1H, m), 2.39-2.30 (1H, m), 2.11-1.97 (1H, m), 1.85-1.64 (3H, m), 1.62-1.51 (1H, m), 0.95-0.76 (1H, m); **^{13}C NMR** (100 MHz, $CDCl_3$) δ 211.7, 167.1, 142.9, 139.3, 132.6, 130.1, 128.8, 123.1, 54.6, 52.1, 45.2, 42.6, 33.4, 29.1, 24.9. **HRMS (ESI)** Calculated for $C_{17}H_{20}ClO_3^+$ ($[M+H]^+$) 307.1095. Found 307.1099. **$[\alpha]_D^{25}$** = +153.6 (c = 0.72, $CHCl_3$). **HPLC** Phenomenex Lux Cellulose-5 (90:10 *n*-Hexane: 2-Propanol, 1 mL/min, 218 nm); tr (minor) = 21.1, tr (major) = 24.8 (93:7 e.r.).

methyl 2-((*S*)-((*R*)-2-oxocyclohexyl)(4-(trifluoromethyl)phenyl)methyl)acrylate (3s)

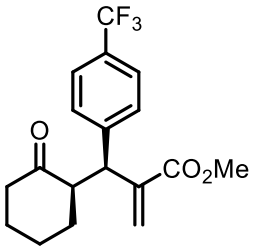

***3s** was prepared following the abovementioned procedure.*

50% yield (34 mg, 0.10 mmol), pale red solid. **^{1}H NMR** (500 MHz, $CDCl_3$) δ 7.53 (2H, d, J = 8.12 Hz), 7.34 (2H, d, J = 8.12 Hz), 6.26 (1H, s), 5.63 (1H, s), 4.29 (1H, d, J = 11.10 Hz), 3.68 (3H, s), 3.10 (1H, td, J = 11.16, 4.93 Hz), 2.48-2.41 (1H, m), 2.40-2.32 (1H, m), 2.10-2.01 (1H, m), 1.85-1.77 (1H, m), 1.76-1.68 (1H, m), 1.68-1.62 (2H, m), 1.62-1.54 (1H, m); **^{13}C NMR** (126 MHz, $CDCl_3$) δ 211.4, 167.0, 145.1, 142.6, 129.2 (q, $^2J_{CF}$ = 32.41 Hz), 129.1, 125.6 (q, $^3J_{CF}$ = 3.69 Hz), 124.3 (q, $^1J_{CF}$ = 272.14 Hz), 123.4, 54.5, 52.2, 45.7, 42.7, 33.4, 29.1, 24.9; **^{19}F NMR (471 MHz, $CDCl_3$)** δ -62.46 (s). **HRMS (ESI)** Calculated for $C_{18}H_{20}F_3O_3^+$ ($[M+H]^+$) 341.1359. Found 341.1358. **$[\alpha]_D^{25}$** = +112.3 (c = 0.97, $CHCl_3$). **HPLC** Phenomenex Lux Cellulose-5 (98:2 *n*-hexane: 2-propanol, 1 mL/min, 218 nm); tr (minor) = 29.1, tr (major) = 49.7 (86:14 e.r.).

methyl 2-((*S*)-(4-cyanophenyl)((*R*)-2-oxocyclohexyl)methyl)acrylate (3t)

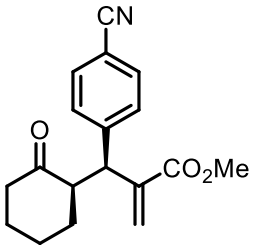

***3t** was prepared following the abovementioned procedure.*

52% yield (30 mg, 0.10 mmol), orange oil. **^{1}H NMR** (400 MHz, $CDCl_3$) δ 7.57 (2H, d, *J* = 8.43 Hz), 7.34 (2H, d, *J* = 8.32 Hz), 6.28 (1H, s), 5.62 (1H, s), 4.28 (1H, d, *J* = 10.97 Hz), 3.68 (3H, s), 3.08 (1H, td, *J* = 11.15, 4.1 Hz), 2.48-2.31 (2H, m), 2.13-2.01 (1H, m), 1.86-1.76 (1H, m), 1.76-1.60 (3H, m), 0.9-0.8 (1H, m); **^{13}C NMR** (100 MHz, $CDCl_3$) δ 211.0, 166.9, 146.6, 142.2, 132.4, 129.6, 123.7, 118.9, 110.8, 54.2, 52.2, 46.0, 42.7, 33.4, 29.0, 25.0. **HRMS (ESI)** Calculated for $C_{18}H_{20}NO_3^+$ ($[M+H]^+$) 298.1438. Found 298.1430. **$[\alpha]_D^{25}$** = +190.9 (c = 1.20, $CHCl_3$). **HPLC** Phenomenex Lux Cellulose-5 (80:20 *n*-hexane: 2-propanol, 1 mL/min, 218 nm); tr (minor) = 29.1, tr (major) = 36.8 (91:9 e.r.)

methyl 4-((*S*)-2-(methoxycarbonyl)-1-((*R*)-2-oxocyclohexyl)allyl)benzoate (3u)

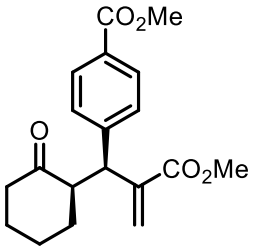

***3u** was prepared following the abovementioned procedure.*

73% yield (48 mg, 0.15 mmol), orange oil. **^{1}H NMR** (400 MHz, $CDCl_3$) δ 7.94 (2H, d, *J* = 8.39 Hz), 7.28 (2H, d, *J* = 8.35 Hz), 6.25 (1H, s), 5.62 (1H, s), 4.28 (1H, d, *J* = 11.11 Hz), 3.88 (3H, s), 3.67 (3H, s), 3.09 (1H, td, *J* = 11.16, 4.80 Hz), 2.48-2.40 (1H, m), 2.40-2.30 (1H, m), 2.09-1.98 (1H, m), 1.83-1.74 (1H, m), 1.74-1.64 (2H, m), 1.63-1.51 (2H, m); **^{13}C NMR** (100 MHz, $CDCl_3$) δ 211.5, 167.1, 167.0, 146.3, 142.6, 129.9, 128.8, 128.8, 123.4, 54.5, 52.2, 52.1, 45.8, 42.7, 33.4, 29.1, 24.9. **HRMS (ESI)** Calculated for $C_{19}H_{23}O_5^+$ ($[M+H]^+$) 331.154. Found 331.1538. **$[\alpha]_D^{25}$** = +112.3 (c = 1.71, $CHCl_3$). **HPLC** Phenomenex Lux Cellulose-1 (90:10 *n*-hexane: 2-propanol, 1 mL/min, 218 nm); tr (minor) = 11.6, tr (major) = 17.6 (91:9 e.r.).

methyl 2-((*S*)-(4-methoxyphenyl)((*R*)-2-oxocyclohexyl)methyl)acrylate (3v)

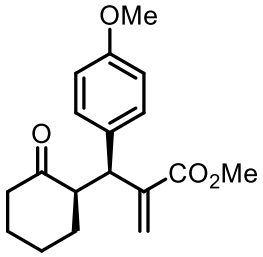

***3v** was prepared following the abovementioned procedure.*

34% yield (21 mg, 0.07 mmol), yellow solid. **^{1}H NMR** (500 MHz, $CDCl_3$) δ 7.12 (2H, d, *J* = 8.69 Hz), 6.81 (2H, d, *J* = 8.69 Hz), 6.19 (1H, s), 5.58 (1H, s), 4.17 (1H, d, *J* = 11.28 Hz), 3.77 (3H, s), 3.68 (3H, s), 3.03 (1H, td, *J* = 11.02, 4.95 Hz), 2.47-2.39 (1H, m), 2.68-2.30 (1H, m), 2.06-1.97 (1H, m), 1.85-1.76 (1H, m), 1.76-1.66 (2H, m), 1.59-1.52 (1H, m), 0.91-0.80 (1H, m); **^{13}C NMR** (126 MHz, $CDCl_3$) δ 212.4, 167.4, 158.5, 143.5, 132.7, 129.6, 122.6, 114.0, 55.3, 55.0, 52.0, 44.9, 42.5, 33.4, 29.2, 24.7. **HRMS (ESI)** Calculated for $C_{18}H_{23}O_4^+$ ($[M+H]^+$) 303.1591. Found 303.159. **$[\alpha]_D^{25}$** = +125.0 (c = 1.15, $CHCl_3$). **HPLC** Phenomenex Lux Cellulose-5 (90:10 *n*-hexane: 2-propanol, 1 mL/min, 218 nm); tr (major) = 54.1, tr (minor) = 70.4 (92:8 e.r.).

methyl 2-((*S*)-(4-bromophenyl)((*R*)-2-oxocyclohexyl)methyl)acrylate (3w)

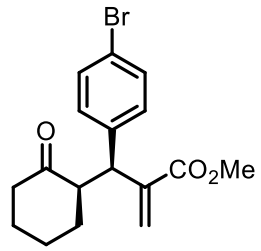

***3w** was prepared following the abovementioned procedure.*

68% yield (48 mg, 0.14 mmol), orange solid. **^{1}H NMR** (400 MHz, $CDCl_3$) δ 7.39 (2H, d, *J* = 8.41 Hz), 7.09 (2H, d, *J* = 8.41 Hz), 6.22 (1H, s), 5.58 (1H, s), 4.18 (1H, d, *J* = 11.10 Hz), 3.68 (3H, s), 3.03 (1H, td, *J* = 11.13, 4.94 Hz), 2.47-2.39 (1H, m), 2.39-2.29 (1H, m), 2.08-1.99 (1H, m), 1.85-1.74 (1H, m), 1.74-1.64 (2H, m), 1.62-1.52 (1H, m), 0.91-0.81 (1H, m); **^{13}C NMR** (100 MHz, $CDCl_3$) δ 211.7, 167.1, 142.8, 139.9, 131.7, 130.4, 123.1, 120.7, 54.5, 52.1, 45.3, 42.6, 33.4, 29.1, 24.9**. HRMS (ESI)** Calculated for $C_{17}H_{20}BrO_3^+$ ($[M+H]^+$) 351.059. Found 351.059. **$[\alpha]_D^{25}$** = +119.1 (c = 1.34, $CHCl_3$). **HPLC** Phenomenex Lux Cellulose-5 (90:10 *n*-hexane: 2-propanol, 1 mL/min, 218 nm); tr (minor) = 19.9, tr (major) = 24.2 (93:7 e.r.)

methyl 2-((*S*)-((*R*)-2-oxocyclohexyl)(p-tolyl)methyl)acrylate (3x)

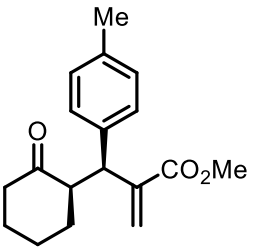

***3x** was prepared following the abovementioned procedure.*

75% yield (43 mg, 0.15 mmol), pale red solid. **^{1}H NMR** (400 MHz, $CDCl_3$) δ 7.13-7.05 (4H, m), 6.20 (1H, s), 5.59 (1H, s), 4.18 (1H, d, *J* = 11.36 Hz), 3.68 (3H, s), 3.06 (1H, td, *J* = 11.03, 4.93 Hz), 2.48-2.39 (1H, m), 2.39-2.31 (1H, m), 2.30 (3H, s), 2.07-1.97 (1H, m), 1.85-1.76 (1H, m), 1.76-1.65 (3H, m), 1.63-1.53 (1H, m); **^{13}C NMR** (100 MHz, $CDCl_3$) δ 212.4, 167.4, 143.4, 137.7, 136.4, 129.3, 128.5, 122.8, 54.9, 52.0, 45.3, 42.6, 33.4, 29.2, 24.7, 21.2. **HRMS (ESI)** Calculated for $C_{18}H_{23}O_3^+$ ($[M+H]^+$) 287.1642. Found 287.1643. **$[\alpha]_D^{25}$** = +118.1 (c = 0.98, $CHCl_3$). **HPLC** Phenomenex Lux Amylose-2 (90:10 *n*-hexane: 2-propanol, 1 mL/min, 218 nm); tr (minor) = 15.4, tr (major) = 23.7 (88:12 e.r.)

methyl 2-((*S*)-((*R*)-2-oxocyclohexyl)(m-tolyl)methyl)acrylate (3y)

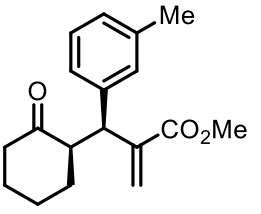

***3y** was prepared following the abovementioned procedure.*

43% yield (17 mg, 0.06 mmol), yellow solid. **^{1}H NMR** (500 MHz, $CDCl_3$) δ 7.18-7.13 (1H, m), 7.06-6.96 (3H, m), 6.21 (1H, s), 5.60 (1H, s), 4.18 (1H, d, *J* = 11.35 Hz), 3.68 (3H, s), 3.07 (1H, td, *J* = 11.05, 4.99 Hz), 2.47-2.40 (1H, m), 2.39-2.32 (1H, m), 2.31 (3H, s), 2.07-1.98 (1H, m), 1.85-1.76 (1H, m), 1.75-1.64 (2H, m), 1.63-1.53 (1H, m), 1.34-1.27 (1H, m); **^{13}C NMR** (100 MHz, $CDCl_3$) δ 212.3, 167.3, 143.3, 140.6, 138.1, 129.4, 128.4, 127.6, 125.7, 122.8, 55.0, 52.0, 45.6, 42.6, 33.4, 29.2, 24.7, 21.6. **HRMS (ESI)** Calculated for $C_{18}H_{23}O_3^+$ ($[M+H]^+$) 287.1642. Found 287.1644. **$[\alpha]_D^{25}$** = +144.0 (c = 1.28, $CHCl_3$). **HPLC** Phenomenex Lux Cellulose-5 (80:20 *n*-hexane: 2-propanol, 1 mL/min, 218 nm); tr (major) = 15.7, tr (minor) = 27.4 (94:6 e.r.)

methyl 2-((*S*)-((*R*)-2-oxocyclohexyl)(o-tolyl)methyl)acrylate (3z)

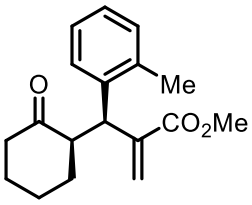

3z *was prepared following the abovementioned procedure.*

60% yield (34 mg, 0.12 mmol), orange solid. **^{1}H NMR** (500 MHz, $CDCl_3$) δ 7.15-7.05 (4H, m), 6.24 (1H, s), 5.53 (1H, s), 4.52 (1H, d, J = 11.33 Hz), 3.66 (3H, s), 3.03 (1H, td, J = 11.45, 4.82 Hz), 2.46 (3H, s), 2.45-2.41 (1H, m), 2.41-2.33 (1H, m), 2.10-2.02 (1H, m), 1.80-1.73 (1H, m), 1.73-1.66 (1H, m), 1.66-1.58 (1H, m), 1.58-1.50 (1H, m), 1.37-1.27 (1H, m); **^{13}C NMR** (126 MHz, $CDCl_3$) δ 212.2, 167.4, 143.5, 139.1, 137.5, 130.6, 127.1, 126.4, 126.2, 122.9, 56.0, 52.0, 43.0, 40.3, 32.8, 29.4, 25.5, 20.3. **HRMS (ESI)** Calculated for $C_{18}H_{23}O_3^+$ ($[M+H]^+$) 287.1642. Found 287.164. **$[\alpha]_D^{25}$** = +114.8 (c = 1.50, $CHCl_3$). **HPLC** Phenomenex Lux Cellulose-1 (99:1 *n*-hexane: 2-propanol, 1 mL/min, 218 nm); tr (minor) = 21.9, tr (major) = 31.2 (96:4 e.r.)

methyl 2-((*S*)-naphthalen-2-yl((*R*)-2-oxocyclohexyl)methyl)acrylate (3aa)

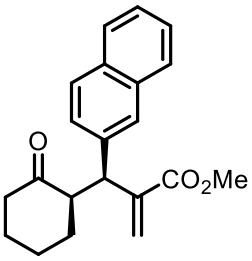

3aa *was prepared following the abovementioned procedure.*

40% yield (26 mg, 0.08 mmol), yellow solid. **^{1}H NMR** (500 MHz, $CDCl_3$) δ 7.82-7.74 (3H, m), 7.67 (1H, s), 7.48-7.40 (2H, m), 5.48 (1H, dd, J = 8.46, 1.80 Hz), 6.27 (1H, s), 5.69 (1H, s), 4.41 (1H, d, J = 11.25 Hz), 3.67 (3H, s), 3.18 (1H, td, J = 11.07, 5.00 Hz), 2.51-2.44 (1H, m), 2.42-2.34 (1H, m), 2.09-1.99 (1H, m), 1.84-1.65 (3H, m), 1.63-1.56 (1H, m), 1.38-1.28 (1H, m); **^{13}C NMR** (126 MHz, $CDCl_3$) δ 212.2, 167.3, 143.1, 138.2, 133.6, 132.6, 128.3, 127.9, 127.7, 127.7, 126.6, 126.2, 125.8, 123.0, 54.8, 52.1, 45.9, 42.7, 33.5, 29.2, 24.8. **HRMS (ESI)** Calculated for $C_{21}H_{23}O_3^+$ ($[M+H]^+$) 323.1642. Found 323.1642. **$[\alpha]_D^{25}$** = +158.4 (c = 1.48, $CHCl_3$). **HPLC** Phenomenex Lux Cellulose-1 (95:5 *n*-hexane: 2-propanol, 1 mL/min, 218 nm); tr (minor) = 13.7, tr (major) = 23.0 (91:9 e.r.)

methyl 2-((*S*)-naphthalen-1-yl((*R*)-2-oxocyclohexyl)methyl)acrylate (3ab)

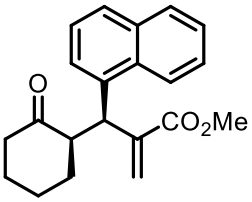

3ab *was prepared following the abovementioned procedure.*

44% yield (28 mg, 0.09 mmol), yellow solid. **^{1}H NMR** (500 MHz, $CDCl_3$) δ 8.42 (1H, d, J = 8.51 Hz), 7.84 (1H, d, J = 8.09 Hz), 7.72 (1H, d, J = 8.16 Hz), 7.55 (1H, t, J = 7.80 Hz), 7.47 (1H, t, J = 7.45 Hz), 7.42 (1H, t, J = 7.69 Hz), 7.35-7.31 (1H, m), 6.3 (1H, s), 5.63 (1H, s), 5.20 (1H, d, J = 10.96 Hz), 3.59 (3H, s), 3.24-3.11 (1H, m), 2.54-2.48 (1H, m), 2.42 (1H, td, J = 12.33, 5.80 Hz), 1.76-1.66 (2H, m), 1.52-1.44 (2H, m), 1.35-1.28 (2H, m); **^{13}C NMR** (126 MHz, $CDCl_3$) δ 212.4, 167.5, 134.0, 132.8, 128.9, 127.4, 126.2, 125.7, 125.5, 124.1, 123.3, 52.0, 42.9, 33.4, 29.8, 29.3, 25.3. **HRMS (ESI)** Calculated for $C_{21}H_{23}O_3^+$ ($[M+H]^+$) 323.1642. Found 323.1644. **$[\alpha]_D^{25}$** = +126.9 (c = 0.41, $CHCl_3$). **HPLC** Phenomenex Lux Cellulose-2 (99:1 *n*-hexane: 2-propanol, 1 mL/min, 218 nm); tr (major) = 87.2, tr (minor) = 95.7 (83:17 e.r.)

methyl 2-((*R*)-((*R*)-2-oxocyclohexyl)(pyridin-2-yl)methyl)acrylate (3ac)

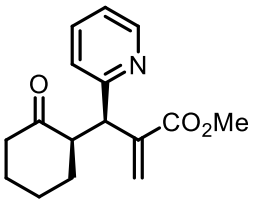

3ac *was prepared following the abovementioned procedure.*

48% yield (26 mg, 0.10 mmol), brown solid. **^{1}H NMR** (400 MHz, $CDCl_3$) δ 8.54 (1H, ddd, J = 4.81, 1.91, 0.90 Hz), 7.55 (1H, td, J = 7.64, 1.86 Hz), 7.27 (1H, dt, J = 8.17, 1.30 Hz), 7.09 (1H, ddd, J = 7.56, 4.85, 1.20 Hz), 6.18 (1H, s), 5.78 (1H, s), 4.35 (1H, d, J = 10.93 Hz), 3.74 (3H, s), 3.45 (1H, td, J = 11.30, 4.98 Hz), 2.46-2.30 (2H, m), 2.11-2.00 (1H, m), 1.81-1.73 (1H, m), 1.68-1.63 (3H, m), 0.91-0.80 (1H, m); **^{13}C NMR** (126 MHz, $CDCl_3$) δ 212.2, 167.8, 160.6, 149.8, 142.3, 136.5, 124.8, 124.1, 121.7, 55.3, 52.1, 47.0, 42.9, 33.4, 29.0, 25.1. **HRMS (ESI)** Calculated for $C_{16}H_{20}NO_3^+$ ([M+H]$^+$) 274.1438. Found 274.1448. **$[\alpha]_D^{25}$** = +58.5 (c = 1.66, $CHCl_3$). **HPLC** Phenomenex Lux Amylose-2 (80:20 *n*-hexane: 2-propanol, 1 mL/min, 218 nm); tr (minor) = 11.9, tr (major) = 15.3 (81:19 e.r.)

ethyl 2-((*S*)-((*R*)-2-oxocyclohexyl)(phenyl)methyl)acrylate (3ad)

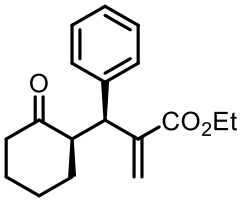

3ad *was prepared following the abovementioned procedure.*

66% yield (38 mg, 0.13 mmol), yellow solid. **^{1}H NMR** (500 MHz, $CDCl_3$) δ 7.35-7.20 (5H, m), 6.27 (1H, s), 5.63 (1H, s), 4.27 (1H, d, J = 11.28 Hz), 4.24-4.09 (2H, m), 3.12 (1H, td, J = 11.11, 5.00 Hz), 2.54-2.45 (1H, m), 2.45-2.35 (1H, m), 1.88-1.81 (1H, m), 1.80-1.69 (2H, m), 1.65-1.56 (1H, m), 1.41-1.29 (2H, m), 1.25 (3H, t, J = 7.16 Hz); **^{13}C NMR** (126 MHz, $CDCl_3$) δ 212.2, 166.9, 143.5, 140.9, 128.7, 128.6, 126.8, 122.7, 60.9, 54.9, 45.7, 42.6, 33.4, 29.2, 24.8, 14.2. **HRMS (ESI)** Calculated for $C_{18}H_{23}O_3^+$ ([M+H]$^+$) 287.1642. Found 287.1646. **$[\alpha]_D^{25}$** = +138.3 (c = 1.03, $CHCl_3$). **HPLC** Phenomenex Lux Cellulose-5 (95:5 *n*-hexane: 2-propanol, 1 mL/min, 218 nm); tr (major) = 54.7, tr (minor) = 77.8 (96:4 e.r.)

hexyl 2-((*S*)-((*R*)-2-oxocyclohexyl)(phenyl)methyl)acrylate (3ae)

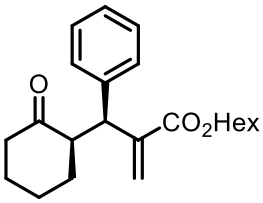

3ae *was prepared following the abovementioned procedure.*

64% yield (44 mg, 0.13 mmol), yellow oil. **^{1}H NMR** (500 MHz, $CDCl_3$) δ 7.36-7.21 (5H, m), 6.27 (1H, s), 5.63 (1H, s), 4.28 (1H, d, J = 11.19 Hz), 4.18-4.03 (2H, m), 3.12 (1H, td, J = 11.00, 4.99 Hz), 2.56-2.45 (1H, m), 2.45-2.35 (1H, m), 2.14-2.01 (1H, m), 1.90-1.81 (1H, m), 1.81-1.75 (1H, m), 1.75-1.69 (1H, m), 1.64-1.61 (2H, m), 1.42-1.29 (8H, m), 0.91 (3H, t, J = 6.8 Hz); **^{13}C NMR** (126 MHz, $CDCl_3$) δ 212.2, 166.9, 143.4, 140.8, 128.7, 128.5, 126.8, 122.7, 65.1, 54.9, 45.7, 42.6, 33.4, 31.5, 29.2, 28.6, 25.7, 24.7, 22.6, 14.1. **HRMS (ESI)** Calculated for $C_{22}H_{31}O_3^+$ ([M+H]$^+$) 343.2268. Found 343.2269. **$[\alpha]_D^{25}$** = +113.9 (c = 1.74, $CHCl_3$). **HPLC** Phenomenex Lux Cellulose-5 (80:20 *n*-hexane: 2-propanol, 1 mL/min, 218 nm); tr (major) = 15.6, tr (minor) = 24.5 (94:6 e.r.)

***rac-tert*-butyl 2-((2-oxocyclohexyl)(phenyl)methyl)acrylate (3af)**

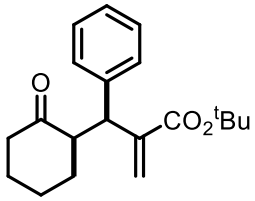

3af *was prepared following the procedure described in C.*

20% yield (13 mg, 0.04 mmol), yellow oil. **^{1}H NMR** (500 MHz, $CDCl_3$) δ 7.37-7.22 (5H, m), 6.20 (1H, s), 5.53 (1H, s), 4.26 (1H, d, *J* = 10.94 Hz), 3.08 (1H, td, *J* = 10.78, 5.03 Hz), 2.56-2.47 (1H, m), 2.46-2.35 (1H, m), 2.13-2.04 (1H, m), 1.90-1.82 (1H, m), 1.82-1.70 (2H, m), 1.70-1.58 (2H, m), 1.43 (9H, s); **^{13}C NMR** (126 MHz, $CDCl_3$) δ 212.3, 166.2, 144.8, 141.1, 128.8, 128.5, 126.7, 121.9, 80.8, 54.9, 45.6, 42.6, 33.4, 29.8, 29.2, 28.1, 28.1, 24.8. **HRMS (ESI)** Calculated for $C_{20}H_{26}NaO_3^+$ ($[M+Na]^+$) 337.1774. Found 337.1774. **HPLC** (for racemic) Phenomenex Lux Cellulose-5 (90:10 *n*-hexane: 2-propanol, 1 mL/min, 218 nm); tr = 11.4, tr = 13.6.

methyl 2-(phenyl((1*R*,4*S*)-4,7,7-trimethyl-3-oxobicyclo[2.2.1]heptan-2-yl)methyl)acrylate (3ag)

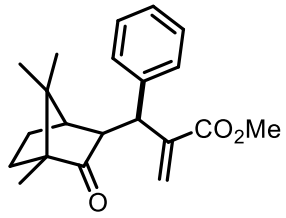

3ag *was prepared following the abovementioned procedure.*

6% yield (4 mg, 0.012 mmol), yellow oil. **^{1}H NMR** (500 MHz, $CDCl_3$) δ 7.33-7.26 (4H, m), 7.24-7.18 (1H, m), 6.29 (1H, s), 5.63 (1H, s), 4.05 (1H, d, *J* = 11.98 Hz), 3.74 (3H, s), 3.26 (1H, dd, *J* = 12.04, 4.27 Hz), 1.87-1.82 (1H, m), 1.70-1.59 (3H, m), 1.52-1.45 (1H, m), 0.93 (3H, s), 0.92 (3H, s), 0.88 (3H, s); **^{13}C NMR** (126 MHz, $CDCl_3$) δ 218.7, 167.6, 143.3, 141.6, 128.6, 128.4, 126.8, 125.4, 59.4, 52.6, 47.0, 45.4, 45.0, 30.7, 29.8, 20.7, 19.8, 19.3, 9.8. **HRMS (ESI)** Calculated for $C_{21}H_{27}O_3^+$ ($[M+H]^+$) 327.1955. Found 327.1959. **$[\alpha]_D^{25}$** = +20.6 (c = 0.35, $CHCl_3$).

methyl (*E*)-3-phenyl-2-(((1*R*,4*S*)-4,7,7-trimethyl-3-oxobicyclo[2.2.1]heptan-2-yl)methyl)acrylate (4b)

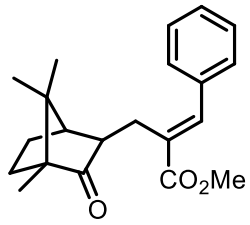

12% yield (8 mg, 0.02 mmol), yellow oil. **^{1}H NMR** (400 MHz, $CDCl_3$) δ 7.71 (1H, d, *J* = 1.09 Hz), 7.44 – 7.35 (4H, m), 7.35 – 7.27 (1H, m), 3.82 (3H, s), 3.03 (1H, ddd, *J* = 13.66, 4.34, 1.28 Hz), 2.74 – 2.65 (1H, m), 2.61 (1H, dd, *J* = 13.66, 9.94 Hz), 1.92 – 1.85 (1H, m), 1.59 – 1.50 (2H, m), 1.35 – 1.27 (1H, m), 1.18 – 1.09 (1H, m), 0.92 (3H, s), 0.86 (3H, s), 0.78 (3H, s); **^{13}C NMR** (100 MHz, $CDCl_3$) δ 220.4, 168.9, 140.1, 135.6, 131.9, 129.4, 128.7, 128.6, 58.7, 52.2, 49.6, 46.6, 45.8, 31.1, 24.4, 20.2, 19.7, 19.4, 9.7. **HRMS (ESI)** Calculated for $C_{21}H_{27}O_3^+$ ($[M+H]^+$) 327.1955. Found 327.1962. **$[\alpha]_D^{25}$** = +171.6 (c = 1.32, $CHCl_3$).

methyl 5-((3*S*,8*S*,9*S*,10*R*,13*S*,14*S*,17*S*)-3-acetoxy-10,13-dimethyl-2,3,4,7,8,9,10,11,12,13,14,15,16,17-tetradecahydro-1H-cyclopenta[a]phenanthren-17-yl)-2-methylene-5-oxo-3-phenylpentanoate (3ah)

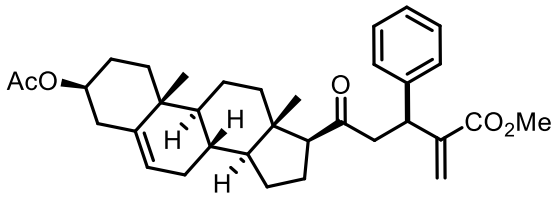

3ah *was prepared following the abovementioned procedure.*

52% yield (55 mg, 0.10 mmol), d.r. = 2:1, yellow oil. **^{1}H NMR** (400 MHz, $CDCl_3$) δ 7.39-7.22 (5H, m), 6.30 (1H, s), 5.87 (1H, s), 5.82 (1H, s), 5.38 (1H, d, *J* = 4.72 Hz), 4.67-4.54 (1H, m), 3.97-3.90 (2H, m), 3.74 (3H, m), 2.36-2.28 (2H, m), 2.17 (1H, t, *J* = 9.70 Hz), 2.03 (3H, s), 1.99-1.92 (1H, m), 1.90-1.80 (3H, m), 1.79-1.61 (3H, m), 1.58-1.51 (2H, m), 1.50-1.40 (2H, m), 1.23-1.05 (4H, m), 1.02 (3H, m), 0.99-0.91 (1H, m), 0.90-0.83 (1H, m), 0.63 (3H, m); **^{13}C NMR** (100 MHz, $CDCl_3$) δ 170.7, 166.4, 161.7, 141.1, 139.9, 139.8, 128.4, 127.8, 127.1, 125.8, 122.6, 84.6, 76.3, 74.1, 56.2, 55.4, 52.1, 50.4, 43.3, 38.5, 38.3, 37.2, 36.8, 32.2, 32.0, 27.9, 24.6, 24.4, 21.6, 21.2, 19.5, 13.0. **HRMS (ESI)** Calculated for $C_{34}H_{45}O_5^+$ ([M+H]$^+$) 533.3262. Found 533.3261. **$[\alpha]_D^{25}$** = -8.6 (c = 1.93, $CHCl_3$).

methyl 5-((3*S*,8*S*,9*S*,10*R*,13*S*,14*S*,17*S*)-3-acetoxy-10,13-dimethyl-2,3,4,7,8,9,10,11,12,13,14,15,16,17-tetradecahydro-1H-cyclopenta[a]phenanthren-17-yl)-2-methylene-5-oxo-3-phenylpentanoate (3ah')

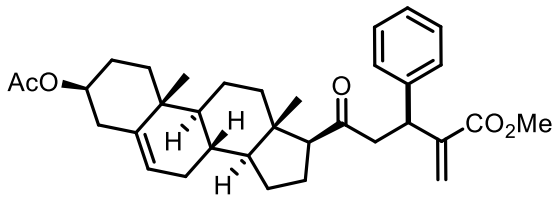

3ah' *was prepared following the abovementioned procedure.*

52% yield (55 mg, 0.10 mmol), d.r. = 1:2, yellow solid. **^{1}H NMR** (400 MHz, $CDCl_3$) δ 7.30-7.14 (5H, m), 6.29 (1H, s), 5.59 (1H, s), 5.36 (1H, d, *J* = 4.80 Hz), 4.67-4.53 (1H, m), 4.48 (1H, t, *J* = 7.39 Hz), 3.67 (3H, m), 3.02-2.86 (2H, m), 2.36 (1H, t, *J* = 9.19 Hz), 2.35-2.27 (2H, m), 2.14-2.05 (1H, m), 2.03 (3H, s), 2.00-1.92 (1H, m), 1.90-1.82 (2H, m), 1.69-1.58 (4H, m), 1.53-1.40 (4H, m), 1.20-1.05 (4H, m), 1.01 (3H, s), 0.87-0.82 (1H, m), 0.59 (3H, s); **^{13}C NMR** (100 MHz, $CDCl_3$) δ 209.1, 170.7, 167.1, 143.1, 142.0, 139.8, 128.6, 128.0, 126.8, 124.7, 122.5, 74.0, 63.1, 57.0, 52.0, 50.0, 49.3, 44.4, 42.1, 39.0, 38.2, 37.1, 36.7, 31.9, 31.8, 27.9, 24.5, 23.1, 21.6, 21.2, 19.4, 13.5. **HRMS (ESI)** Calculated for $C_{34}H_{45}O_5^+$ ([M+H]$^+$) 533.3262. Found 533.3263. **$[\alpha]_D^{25}$** = +31.4 (c = 1.97, $CHCl_3$).

methyl 2-(((8*R*,9*S*,13*S*,14*S*)-3-acetoxy-13-methyl-17-oxo-7,8,9,11,12,13,14,15,16,17-decahydro-6H-cyclopenta[a]phenanthren-16-yl)(phenyl)methyl)acrylate (3ai)

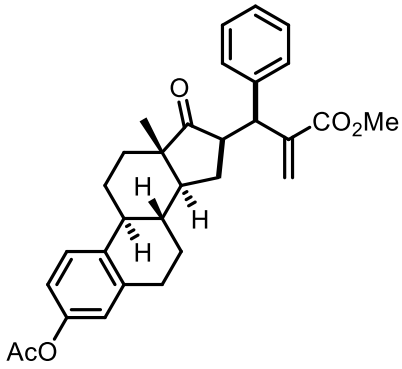

***3ai** was prepared following the abovementioned procedure.* 41% yield (40 mg, 0.08 mmol), yellow oil. *This product has been characterized as a mixture of diastereoisomers* (dr = 5:3:1).

^{1}H NMR (400 MHz, $CDCl_3$) δ (for major diastereomer) 7.31-7.10 (5H, m), 6.80-6.72 (3H, m), 6.41 (1H, s), 5.67 (1H, s), 4.59 (1H, d, *J* = 4.40 Hz), 3.62 (3H, s), 3.13-3.05 (1H, m), 2.82-2.74 (1H, m), 2.26 (3H, s), 2.26-2.18 (1H, m), 2.16-1.92 (2H, m), 1.90-1.71 (3H, m), 1.54-1.44 (1H, m), 1.44-1.26 (3H, m), 1.25-1.09 (1H, m), 1.04-0.94 (1H, m), 0.91 (3H, s), δ (for medium diastereomer) 7.31-7.10 (5H, m), 6.86-6.80 (3H, m), 6.33 (1H, s), 5.72 (1H, s), 4.19 (1H, d, *J* = 7.33 Hz), 3.69 (3H, s), 3.36-3.28 (1H, m), 2.91-2.83 (1H, m), 2.39-2.29 (1H, m), 2.28 (3H, s), 2.16-2.07 (2H, m), 1.80-1.71 (3H, m), 1.53-1.44 (1H, m), 1.44-1.26 (3H, m), 1.25-1.09 (1H, m), 0.93 (3H, s), 0.90-0.80 (1H, m), δ (for minor diastereomer) 7.31-7.10 (5H, m), 6.87-6.80 (3H, m), 6.42 (1H, s), 6.05 (1H, s), 4.11 (1H, d, *J* = 7.50 Hz), 3.67 (3H, s), 2.97-2.91 (1H, m), 2.91-2.83 (1H, m), 2.28 (3H, s), 2.26-2.19 (1H, m), 2.16-2.03 (2H, m), 1.80-1.71 (3H, m), 1.66-1.58 (1H, m), 1.44-1.27 (3H, m), 1.25-1.09 (1H, m), 1.04-0.94 (1H, m), 0.55 (3H, s); **^{13}C NMR** (100 MHz, $CDCl_3$) δ (for major diastereomer) 220.4, 170.0, 146.8, 143.0, 129.0, 128.5, 128.4, 128.3, 127.2, 126.4, 124.7, 121.7, 121.6, 118.9, 118.8, 52.1, 48.2, 47.7, 46.5, 44.1, 31.6, 29.3, 26.1, 25.5, 25.4, 21.3, 15.0, δ (for medium diastereomer) 219.5, 167.3, 148.7, 142.5, 141.2, 139.6, 138.1, 138.0, 137.5, 137.4, 126.9, 126.5, 52.1, 48.9, 48.6, 48.1, 47.9, 47.2, 44.3, 37.9, 31.8, 29.4, 27.8, 26.3, 25.7, 25.3, δ (for minor diastereomer) 219.0, 167.6, 148.6, 142.2, 140.3, 138.1, 137.4, 129.2, 128.5, 128.4, 127.0, 126.6, 53.6, 51.9, 50.6, 49.8, 49.0, 48.6, 44.4, 38.1, 36.0, 32.2, 29.5, 28.7, 26.6, 26.5, 25.8, 13.0. **HRMS (ESI)** Calculated for $C_{31}H_{35}O_5^+$ ([M+H]$^+$) 487.2479. Found 487.2489.

rac-methyl (*E*)-2-((2-oxocyclohexyl)methyl)-3-phenylacrylate (4a)

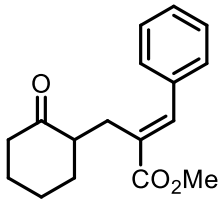

Allyl fluoride **2b** (38.8 mg, 1 equiv., 0.2 mmol) was weighted into a 5 mL vial equipped with a magnetic stirring bar and dissolved with 1 mL of distilled CH_2Cl_2 (0.2 M). Subsequently, silyl enol ether **1b** (84.8 mg, 2 equiv., 0.4 mmol) and 0.2 mL of a solution of TBAF in THF 1M were added. The reaction mixture was stirred at room temperature until full conversion of the starting material was detected by TLC analysis. The crude product was directly purified by flash column chromatography using hexane and ethyl acetate mixtures.

30% yield (16 mg, 0.6 mmol), yellow oil. **^{1}H NMR** (500 MHz, $CDCl_3$) δ 7.75 (1H, s), 7.39-7.33 (4H, m), 7.33-7.27 (1H, m), 3.81 (3H, s), 3.04 (1H, ddd, *J* = 13.55, 4.19, 1.26 Hz), 2.69-2.54 (2H, m), 2.40- 2.32 (1H, m), 2.31-2.20 (1H, m), 2.06-1.94 (2H, m), 1.76 (1H, dqd, *J* = 12.13, 3.53, 1.35 Hz), 1.65-1.58 (1H, m), 1.57-1.49 (1H, m), 1.24-1.12 (1H, m); **^{13}C NMR** (126 MHz, $CDCl_3$) δ 212.4, 168.9, 140.9, 135.8, 131.4, 129.3, 128.7, 128.5, 52.2, 49.8, 42.0, 33.3, 27.9, 26.9, 25.1. **HRMS (ESI)** Calculated for $C_{17}H_{21}O_3^+$ ([M+H]$^+$) 273.1485. Found 273.1496.

E.2. Limitations of the catalytic transformation

α,α-disubstituted silyl enol ethers

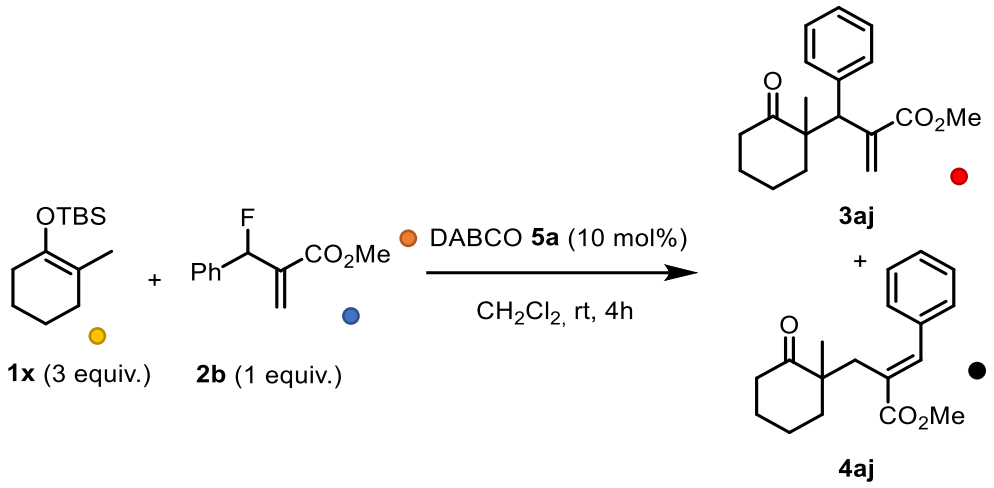

Time (h)	Conversion (%)[a]	NMR yield (%)[a]	r.r. (3aj/4aj)	d.r.
4	>98	12	1:2	>20:1

[a] Yield and conversion were determined by ^{1}H NMR spectroscopy using 1,3,5-trimethoxybenzene as the internal standard.

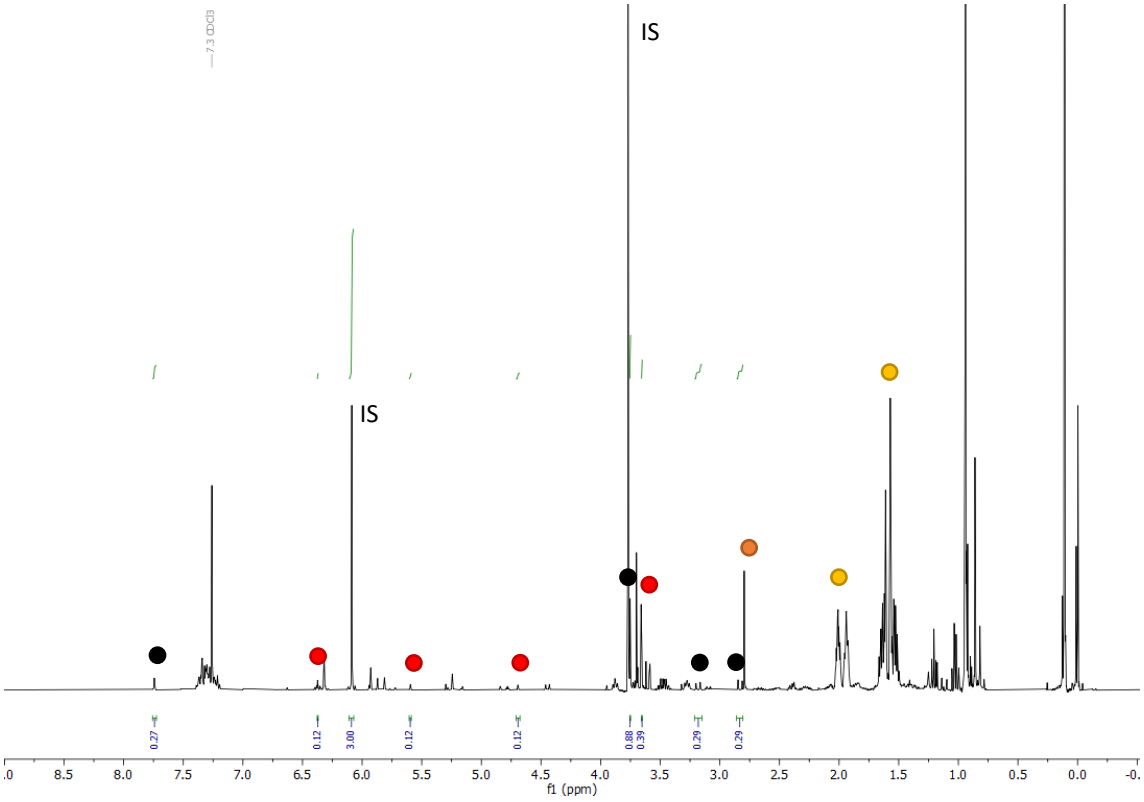

Figure S2. ^{1}H NMR spectrum of the reaction crude with DABCO.

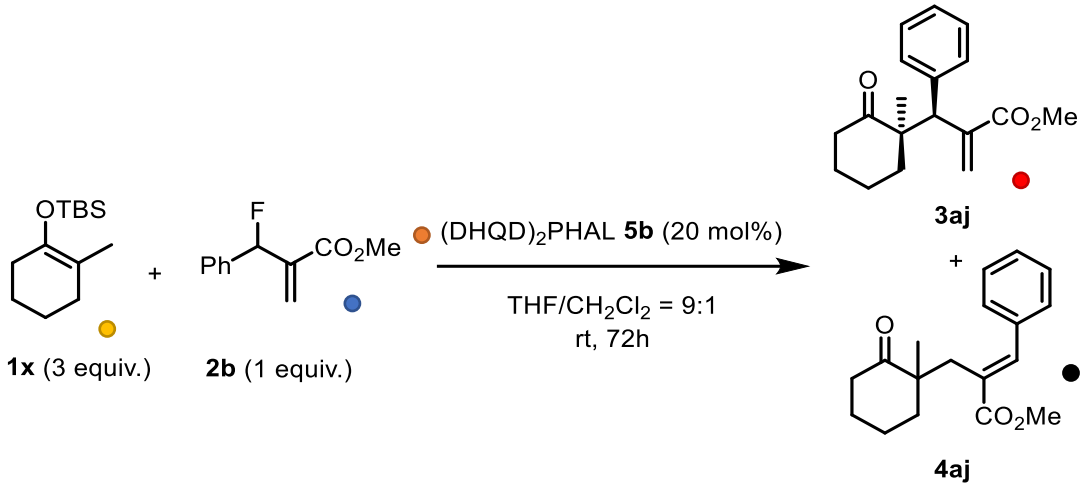

Time (h)	Conversion (%)[a]	NMR yield (%)[a]	r.r. (3aj/4aj)	d.r.
72	50	traces	1:18	n.d.

[a] Yield and conversion were determined by ^{1}H NMR spectroscopy using 1,3,5-trimethoxybenzene as the internal standard.

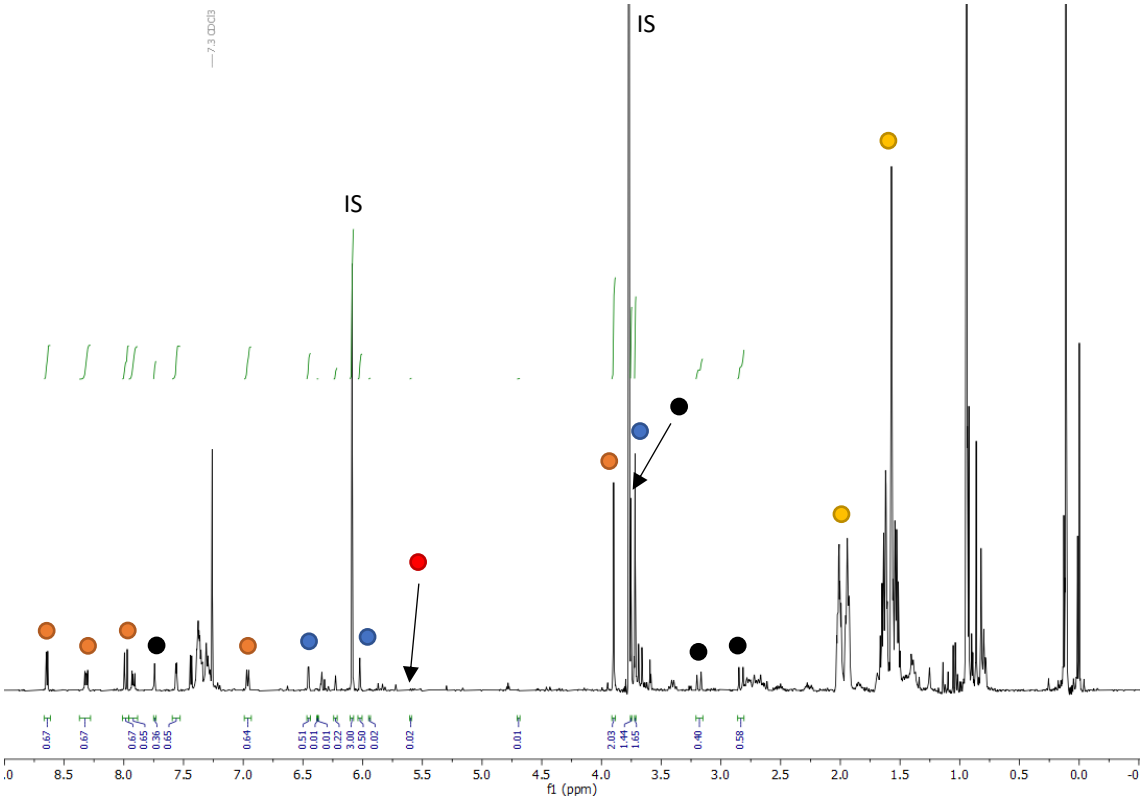

Figure S3. ^{1}H NMR spectrum of the reaction crude with $(DHQD)_2PHAL$.

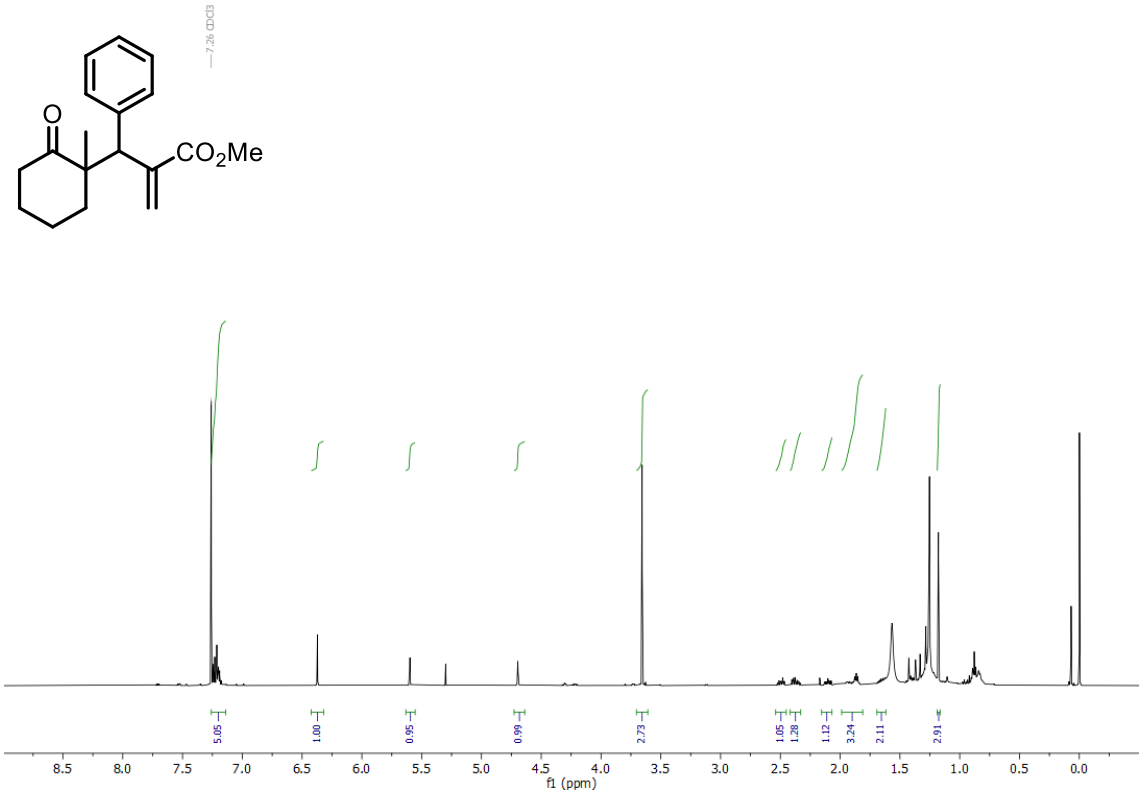

Figure S4. ^{1}H NMR spectrum of **3aj**.

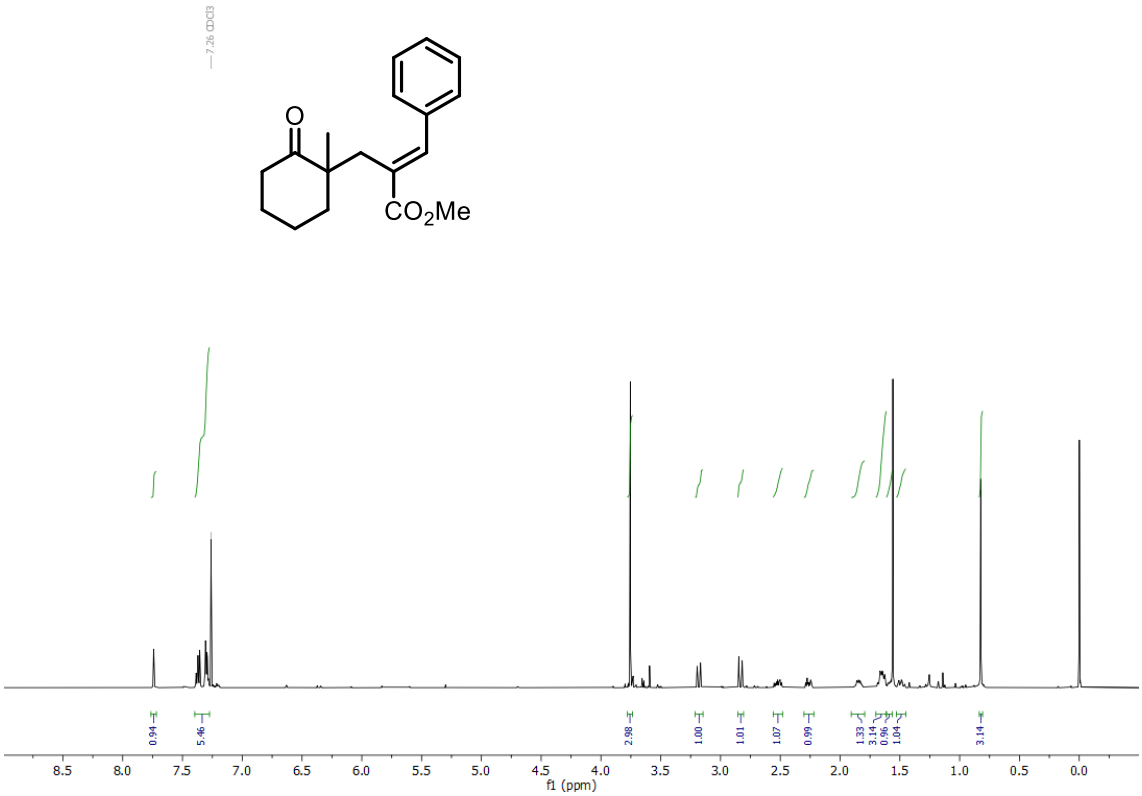

Figure S5. ^{1}H NMR spectrum of **4aj**.

Allyl fluorides bearing an aliphatic substituent

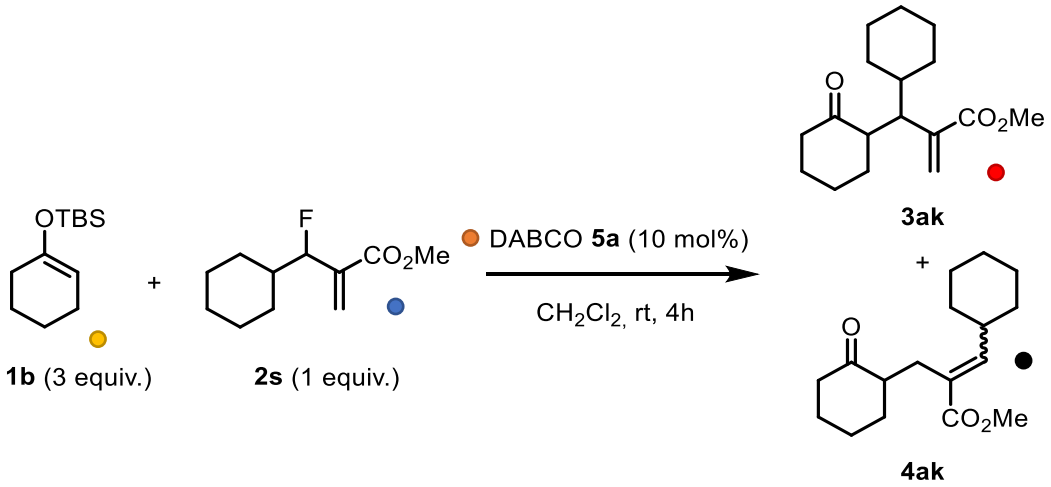

Time (h)	Conversion (%)[a]	NMR yield (%)[a]	r.r. (3ak/4ak)	d.r.
4	>98	30	2.5:1	1.6:1

[a] Yield and conversion were determined by ^{1}H NMR spectroscopy using 1,3,5-trimethoxybenzene as the internal standard.

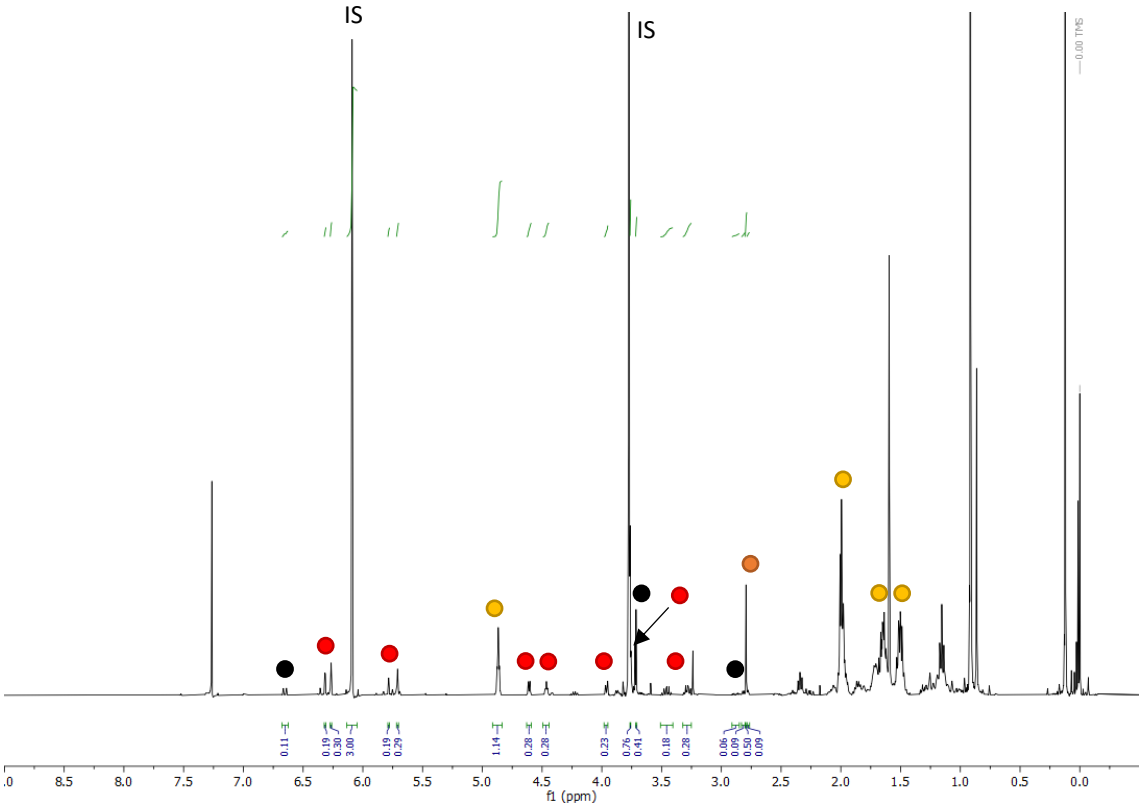

Figure S6. ^{1}H NMR spectrum of the reaction crude with DABCO.

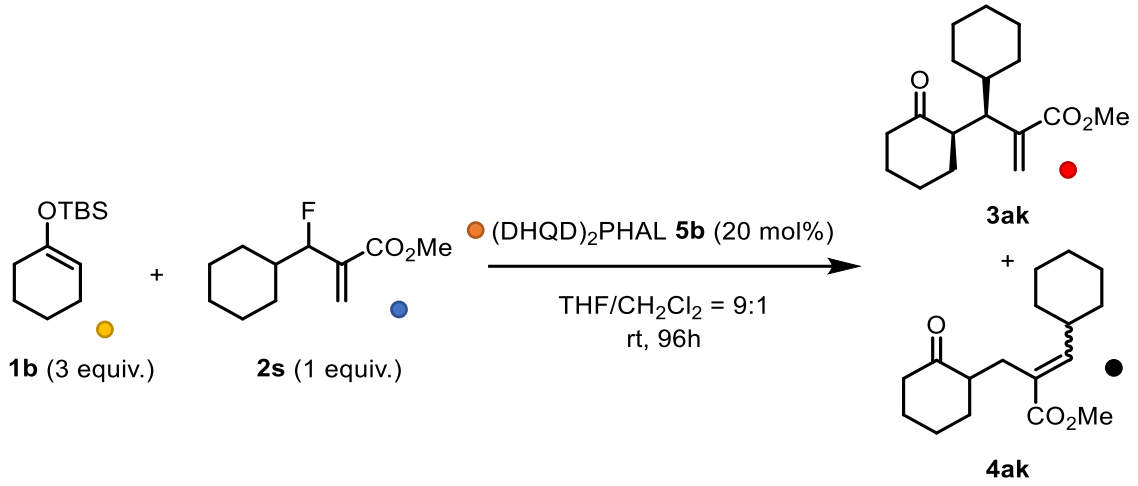

Time (h)	Conversion (%)[a]	NMR yield (%)[a]	r.r. (3ak/4ak)	d.r.
96	30	10	3.5:1	6:1

[a] Yield and conversion were determined by ^{1}H NMR spectroscopy using 1,3,5-trimethoxybenzene as the internal standard.

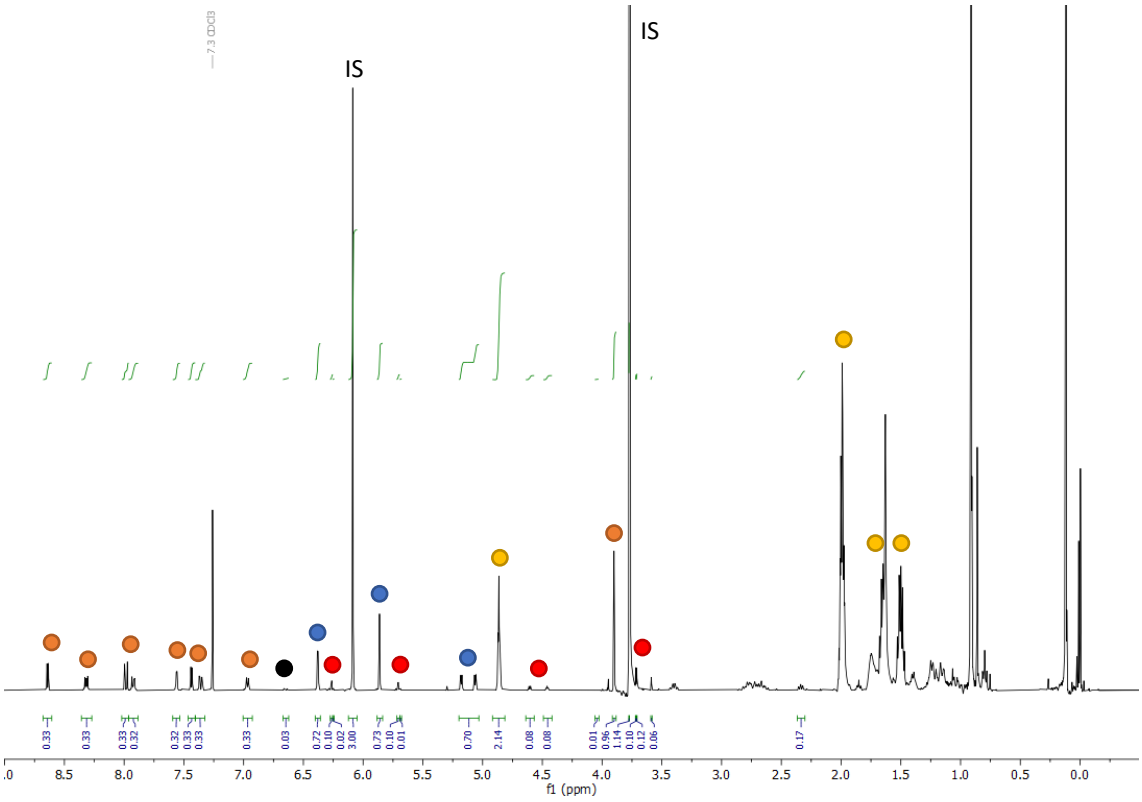

Figure S7. ^{1}H NMR spectrum of the reaction crude with $(DHQD)_2PHAL$.

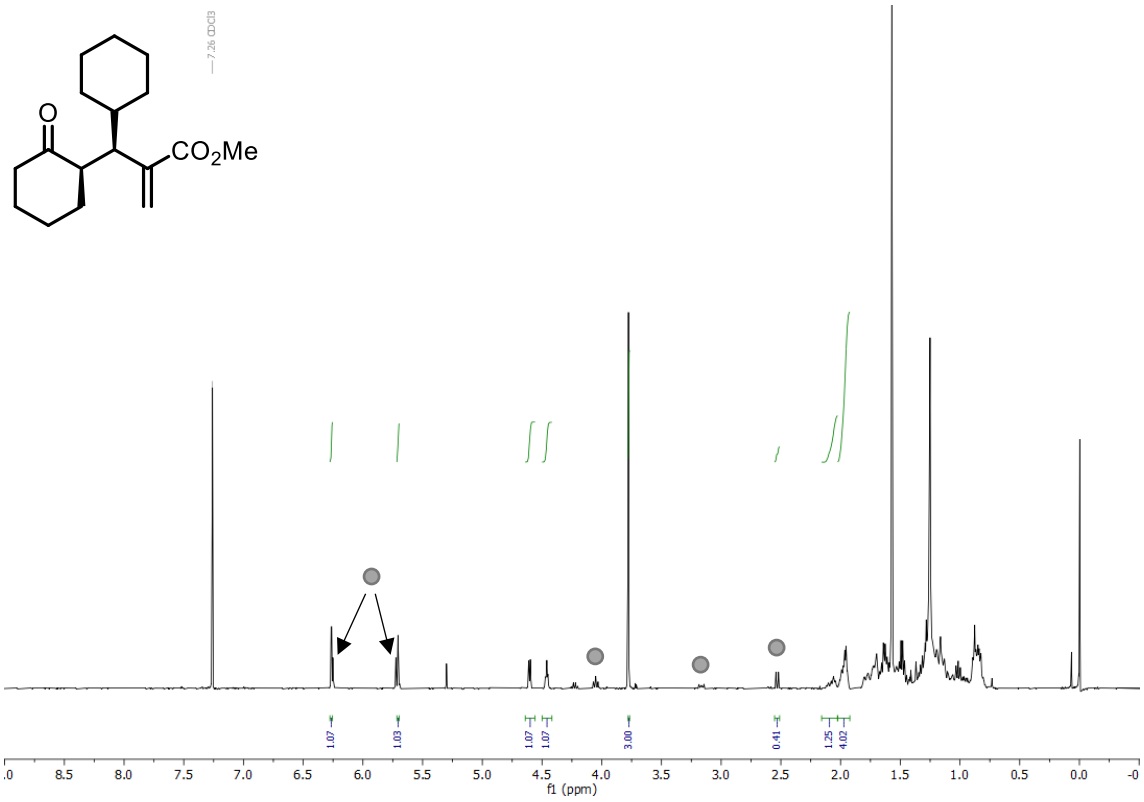

Figure S8. ^{1}H NMR spectrum of **3ak**. (Signals indicated with grey bubbles are not present in the crude mixture. They are degradation products that appear after the purification).

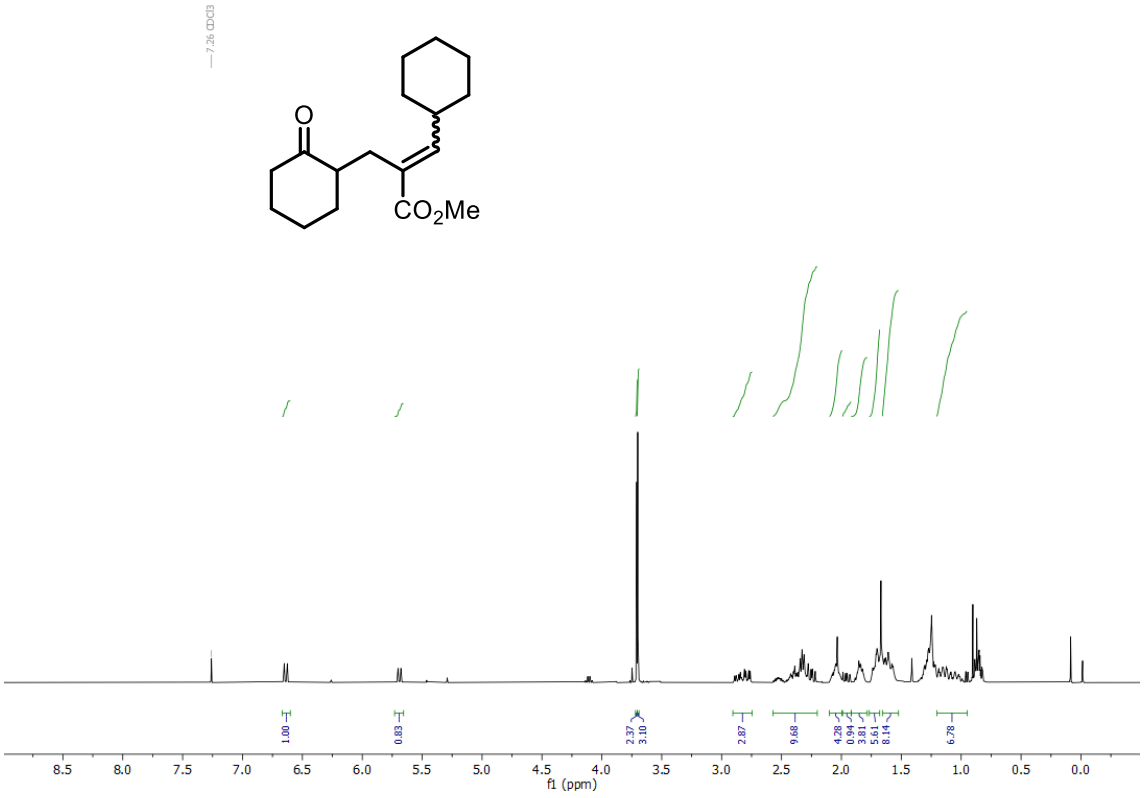

Figure S9. 1H spectrum of **4ak**.

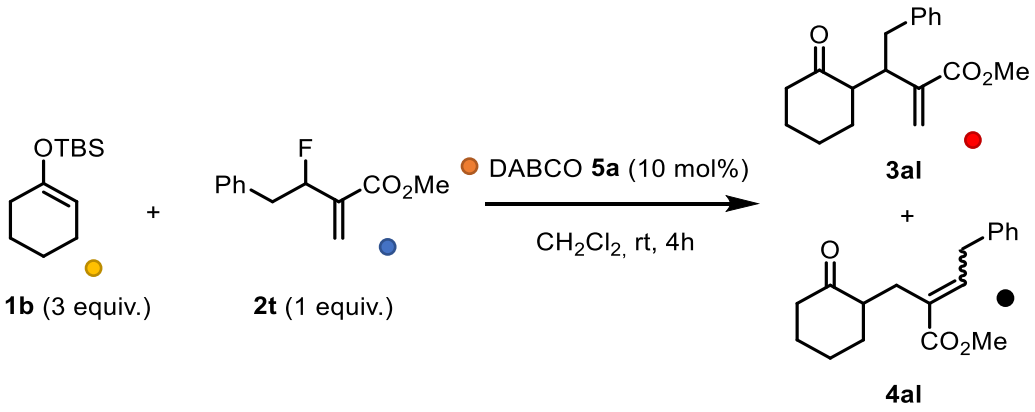

Time (h)	Conversion (%)[a]	NMR yield (%)[a]	r.r. (3al/4al)	d.r.
4	67	traces	n.d.	n.d.

[a] Yield and conversion were determined by ^{1}H NMR spectroscopy using 1,3,5-trimethoxybenzene as the internal standard.

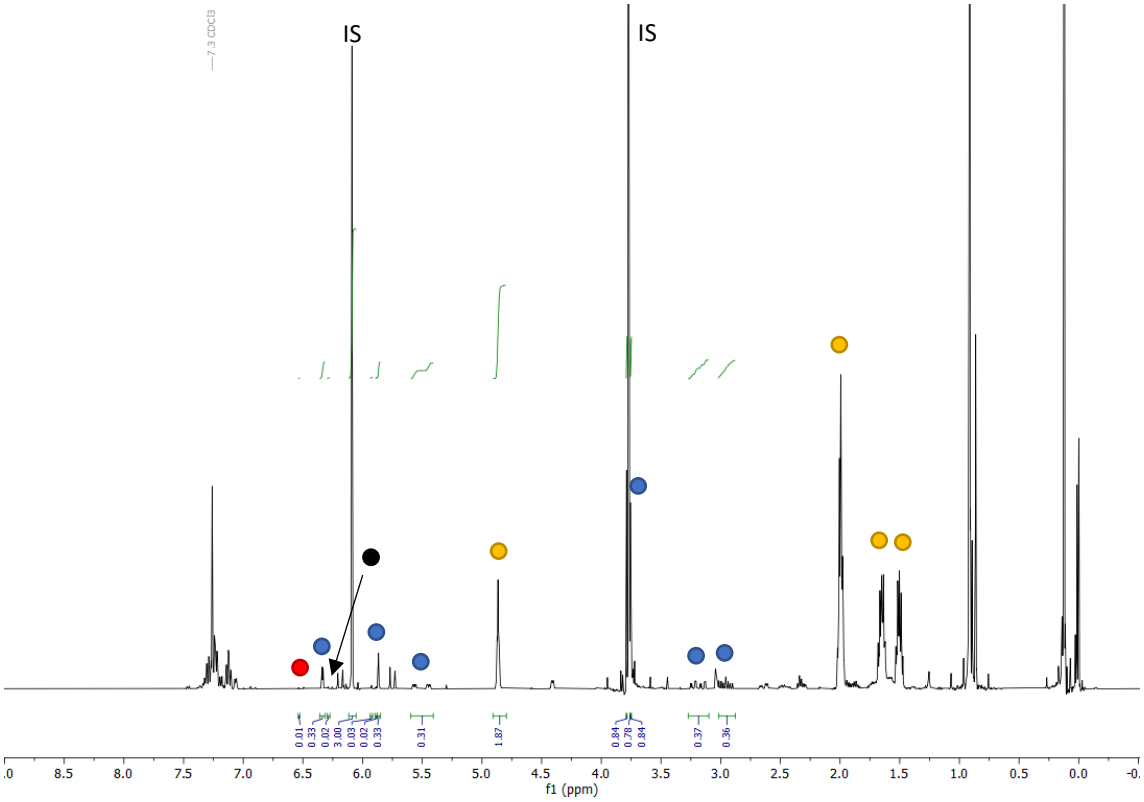

Figure S10. ^{1}H NMR spectrum of the reaction crude with DABCO.

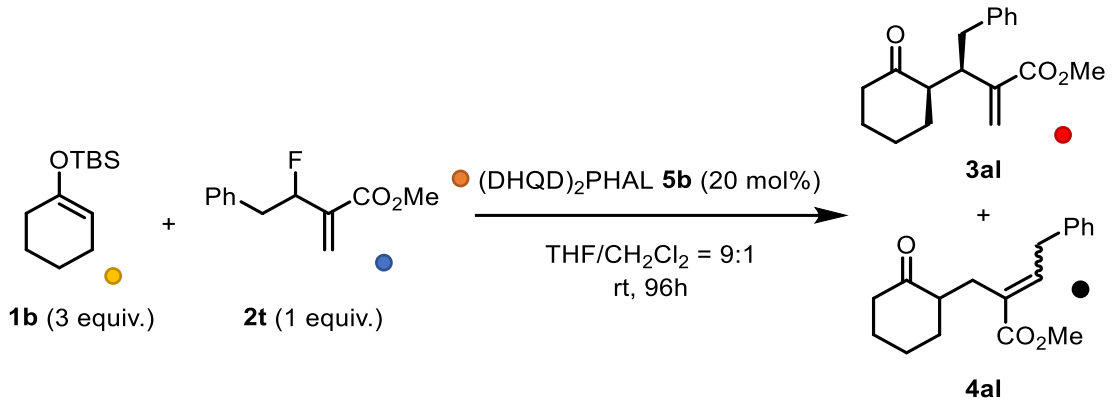

Time (h)	Conversion (%)[a]	NMR yield (%)[a]	r.r. (3al/4al)	d.r.
96	57	traces	n.d.	n.d.

[a] Yield and conversion were determined by ^{1}H NMR spectroscopy using 1,3,5-trimethoxybenzene as the internal standard.

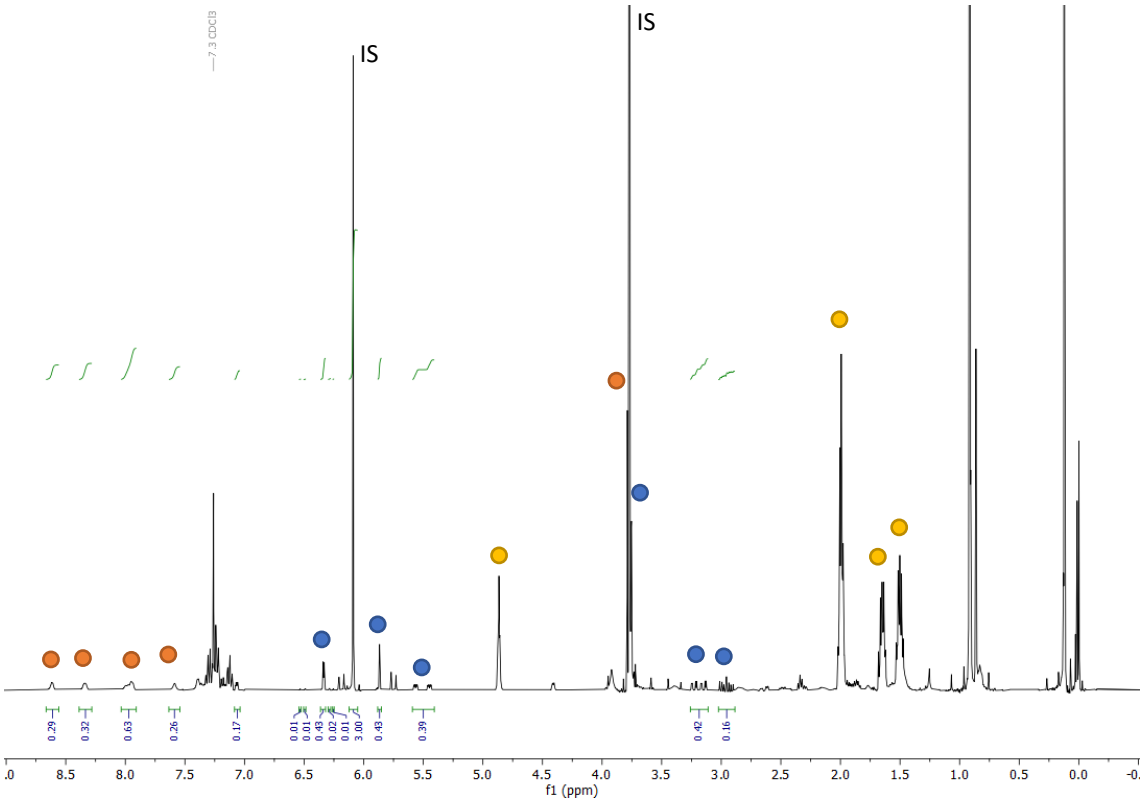

Figure S11. ^{1}H NMR spectrum of the reaction crude with $(DHQD)_2PHAL$.

F. Characterization of the catalytic species

General procedure for the characterization of catalytic species

The corresponding allyl (1 equiv., 0.1 mmol) was weighted into an NMR tube and dissolved with 0.5 mL of the corresponding deuterated solvent (0.2 M). Then, the given amount of catalyst was added. To ensure homogeneous NMR samples, the tube was initially sonicated for 1 min.

F.1. Generation of the catalytic species with DABCO – Using 1 equiv. of DABCO and allyl carbonates

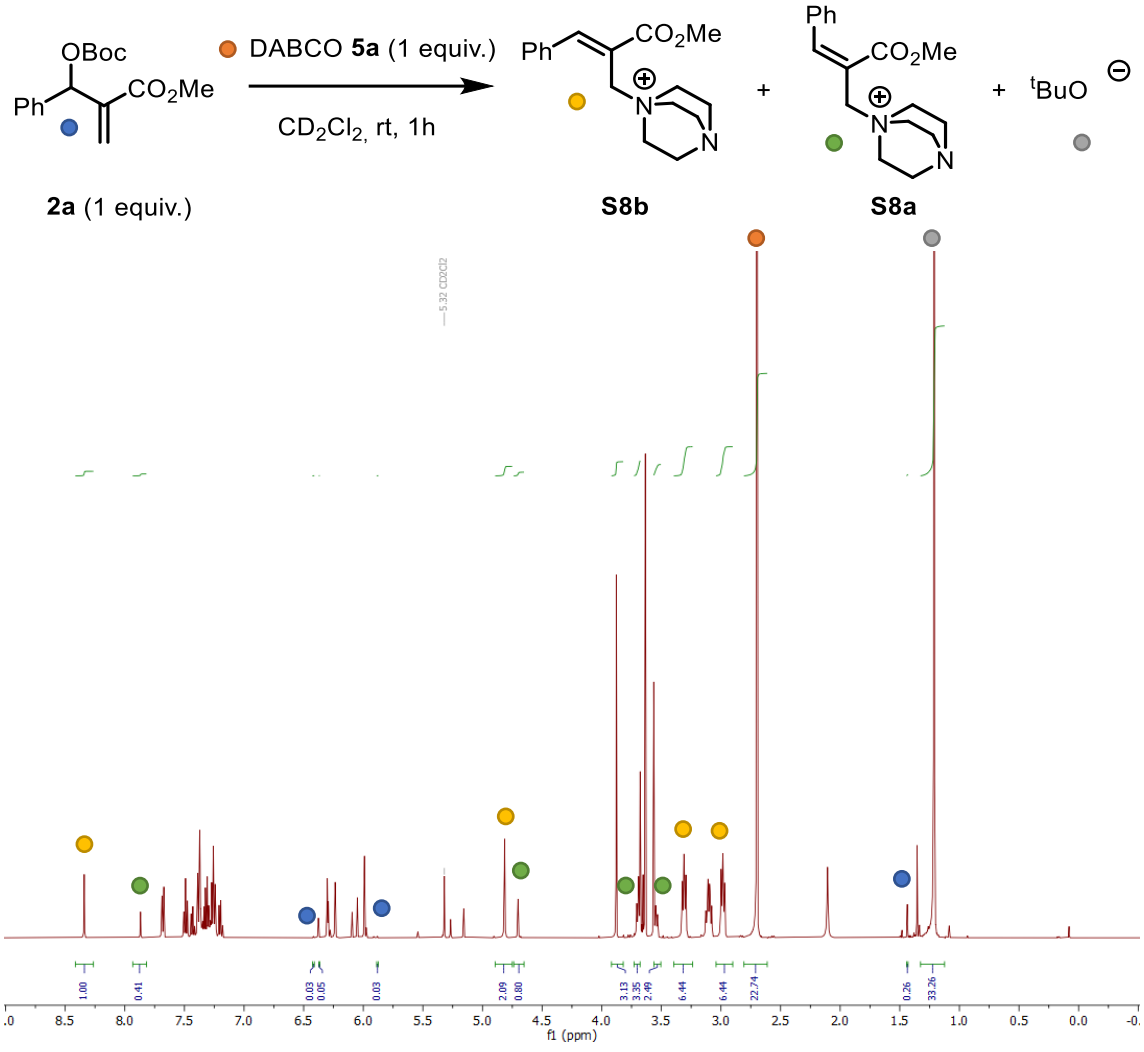

Figure S12. ^{1}H NMR spectrum at 500 MHz NMR field in CD_2Cl_2 for the formation of the catalytic species using stoichiometric amounts of DABCO **5a**.

*[In this experiment, the utilization of stoichiometric amounts of DABCO **5a** (orange bubble) leads to the formation of a 1 to 2.5 mixture of the Z- and E- isomers **S8a** and **S8b** (green and yellow bubbles respectively) of the catalytic species while consuming up to a 95% of the initial allyl carbonate **2a** (blue bubbles) after 1h.]*

F.2. Generation of the catalytic species with DABCO *– Using 20 mol% of DABCO and allyl carbonates*

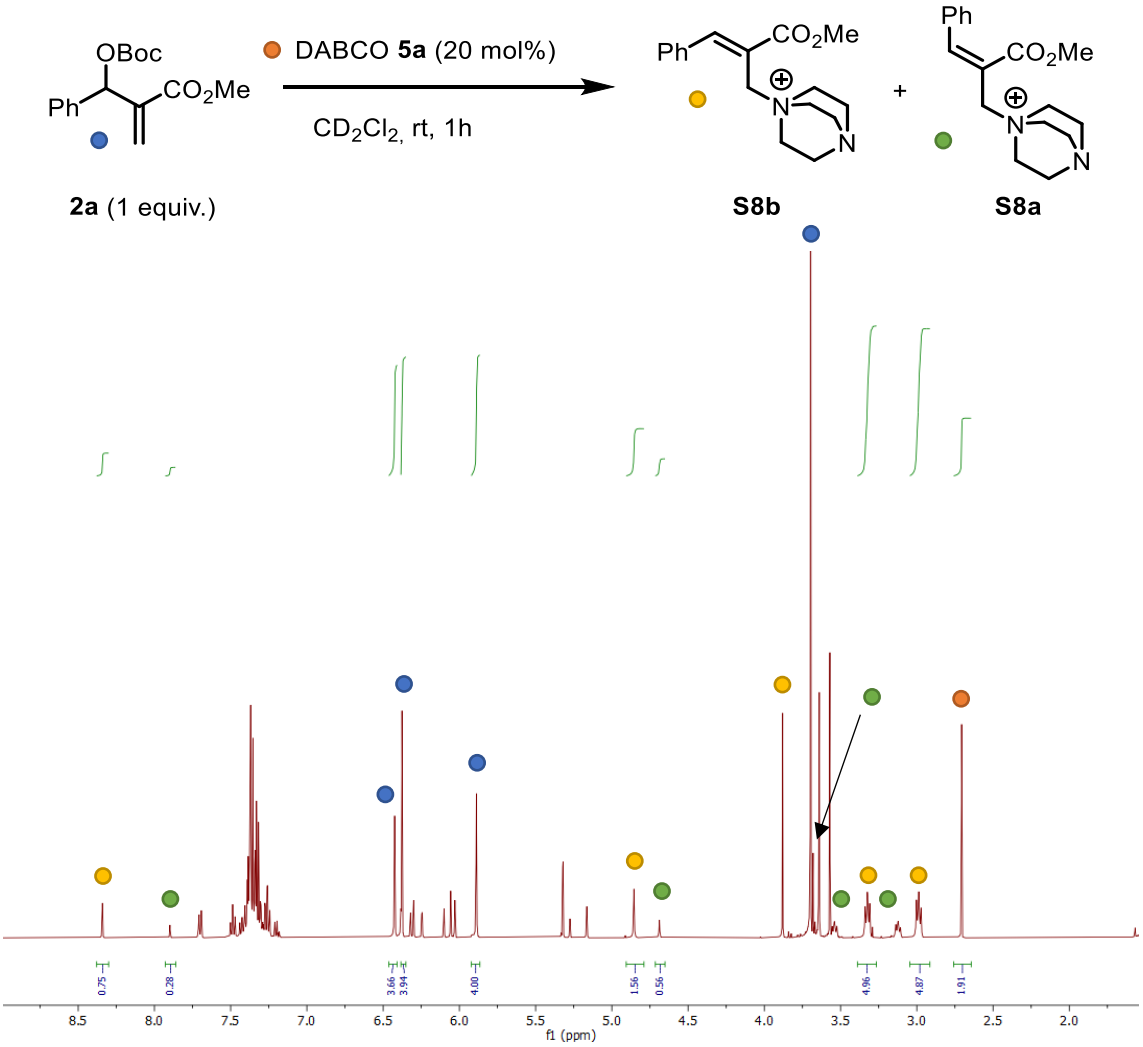

Figure S13. ^{1}H NMR spectrum at 500 MHz NMR field in CD_2Cl_2 for the formation of the catalytic species using 20 mol% of DABCO **5a**.

*[In this experiment, the utilization of catalytic amounts of DABCO **5a** (orange bubble) leads to the formation of a 1 to 3 mixture of the Z- and E- isomers **S8a** and **S8b** (green and yellow bubbles respectively) of the catalytic species while observing an 80% of the unreacted allyl carbonate **2a** (blue bubbles) after 1h.]*

F.3. Generation of the catalytic species with DABCO *– Using 1 equiv. of DABCO and allyl fluorides*

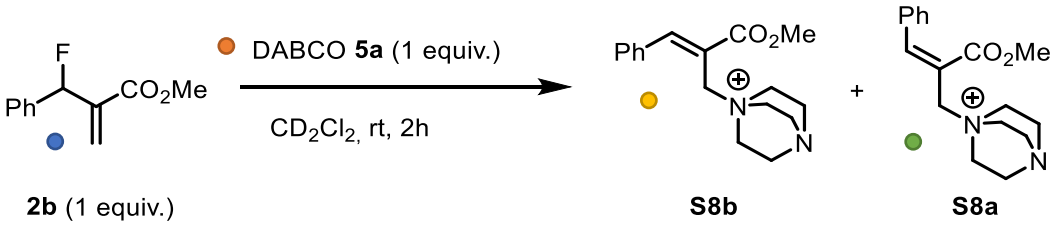

2b (1 equiv.) **S8b** **S8a**

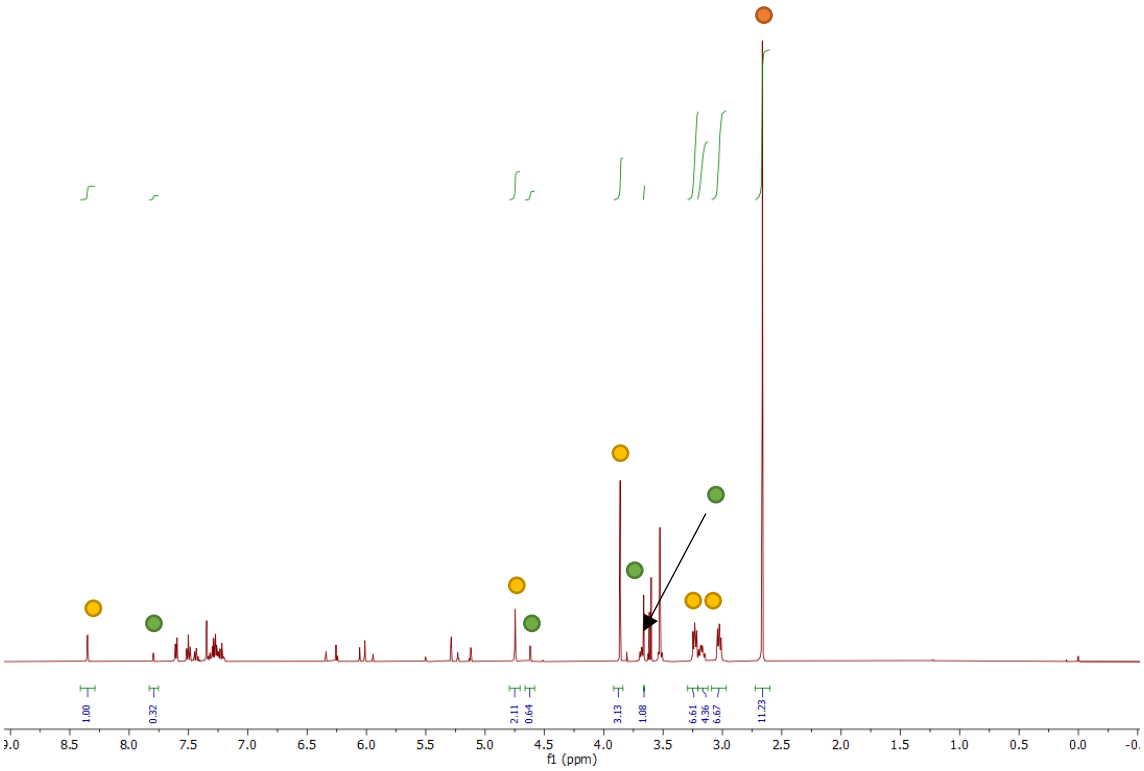

Figure S14. ^{1}H NMR spectrum at 500 MHz NMR field in CD_2Cl_2 for the formation of the catalytic species using 1 equiv. of DABCO **5a** and 1 equiv. of allyl fluoride **2b**.

*[In this experiment, the utilization of stoichiometric amounts of DABCO **5a** (orange bubble) leads to the formation of a 1 to 3 mixture of the Z- and E- isomers **S8a** and **S8b** (green and yellow bubbles respectively) of the catalytic species while observing full consumption of the initial allyl fluoride **2b** (blue bubbles) after 2h.]*

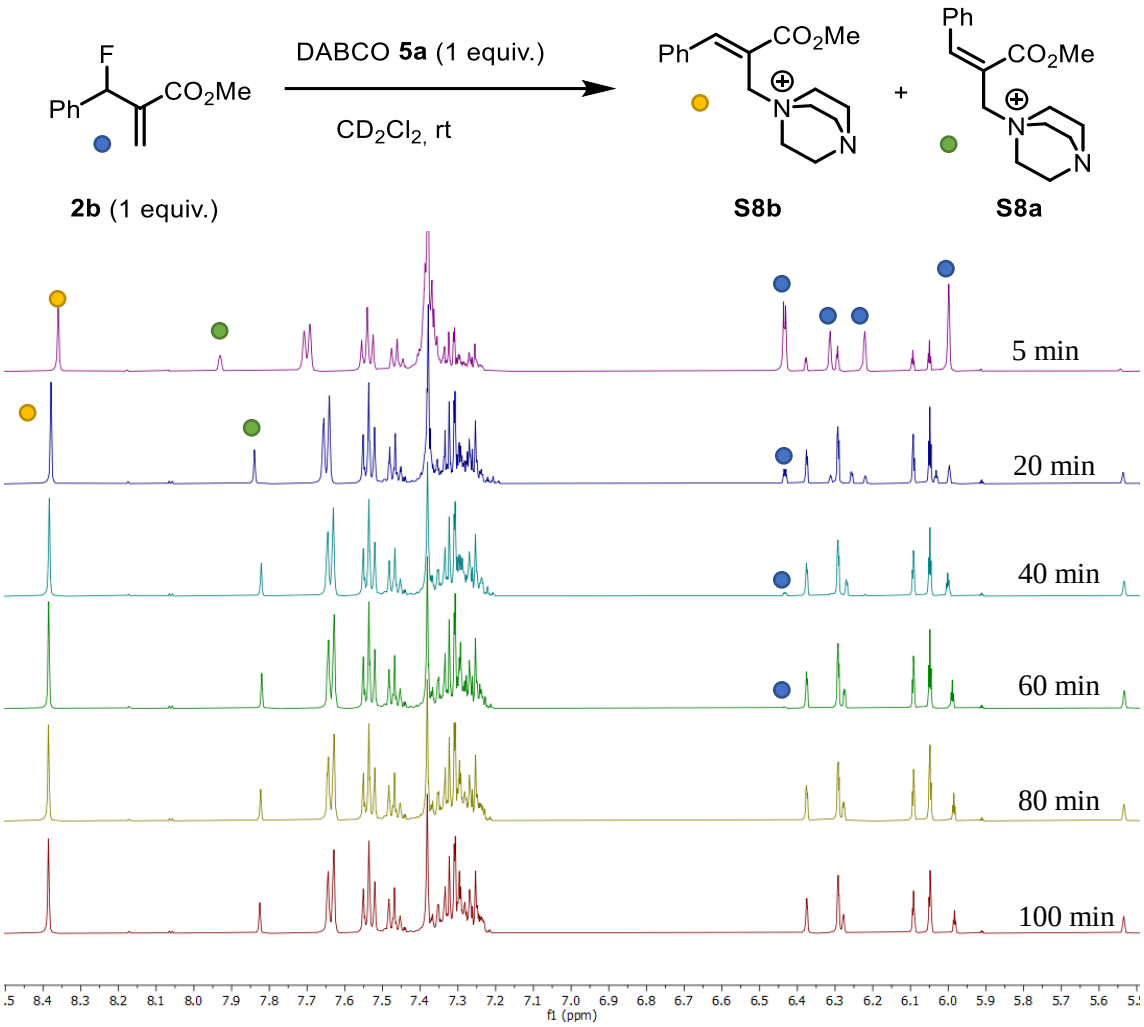

Figure S15. ^{1}H NMR spectra overtime at 500 MHz in CD_2Cl_2 for the formation of the catalytic species using 1 equiv. of DABCO **5a** and 1 equiv. of allyl fluoride **2b** over 100 min.

*[In this experiment, the utilization of stoichiometric amounts of DABCO **5a** leads to the full consumption of the initial allyl fluoride **2b** (blue bubbles) while the ratio of the Z- and E- isomers **S8a** and **S8b** (green and yellow bubbles respectively) remains stable overtime.]*

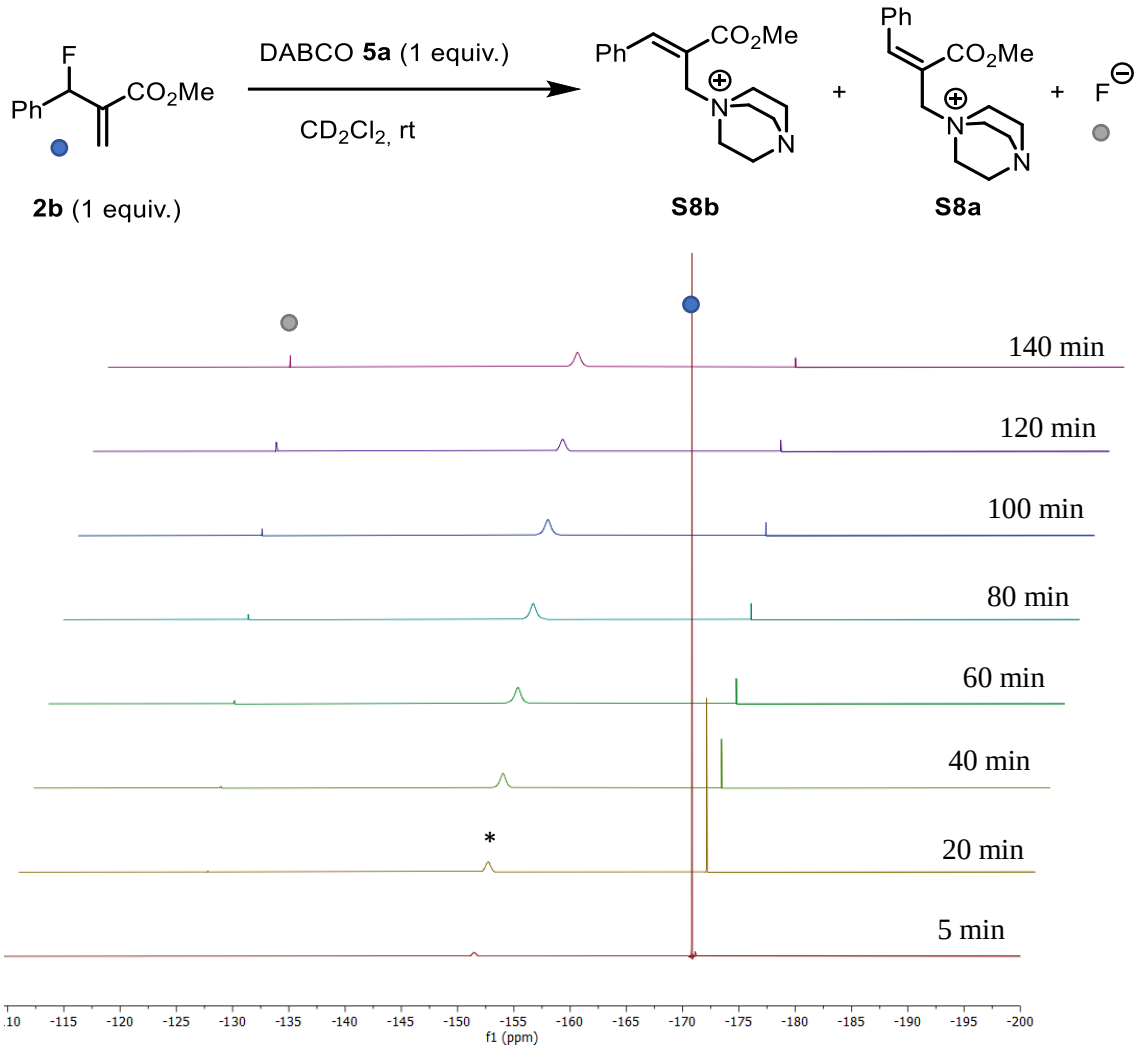

Figure S16. $^{19}F\{^{1}H\}$NMR spectra overtime at 470 MHz NMR field in CD_2Cl_2 using 1 equiv. of DABCO **5a** and 1 equiv. of allyl fluoride **2b** over 140 min.

*[In this experiment, the utilization of stoichiometric amounts of DABCO **5a** in the absence of a competitive fluorophilic trap leads to the formation of naked fluoride (grey bubbles, at -126.20 ppm), which matches with the $^{19}F\{^{1}H\}$ NMR peak of an ammonium fluoride source, such as TBAF. (The signal marked with * at -151 ppm is an artifact.[13])].*

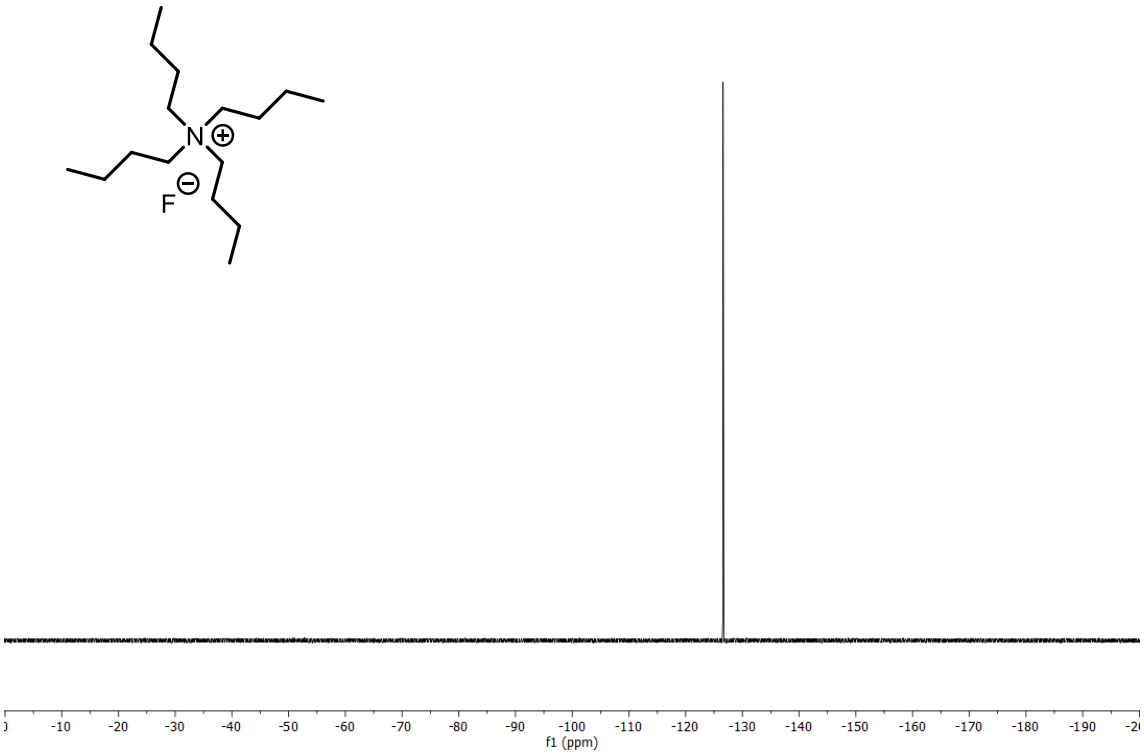

Figure S17. $^{19}F\{^{1}H\}$NMR spectra at 470 MHz NMR field in THF-d_8 of TBAF.

[^{19}F signal of TBAF appears at -126.59 ppm.]

F.4. Generation of the catalytic species with DABCO *– Using 20 mol% of DABCO and allyl fluorides*

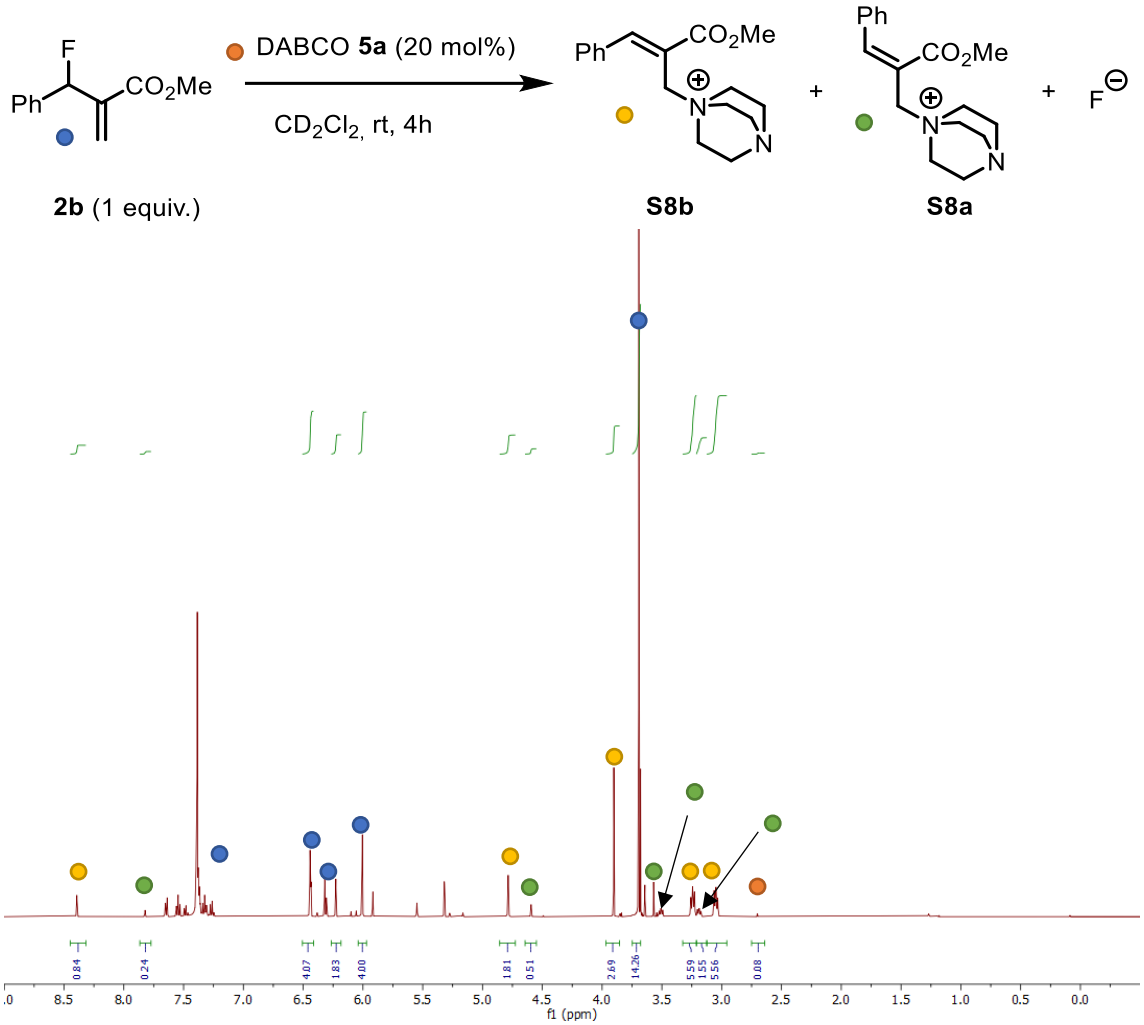

Figure S18. ^{1}H NMR spectrum at 500 MHz NMR field in CD_2Cl_2 for the formation of the catalytic species using 20 mol% of DABCO **5a** and 1 equiv. of allyl fluoride **2b**.

*[In this experiment, the utilization of catalytic amounts of DABCO **5a** (orange bubble) leads to the formation of a 1 to 3.5 mixture of the Z- and E- isomers **S8a** and **S8b** (green and yellow bubbles respectively) of the catalytic species while observing an 80% of the unreacted allyl fluoride **2b** (blue bubbles) after 4h.]*

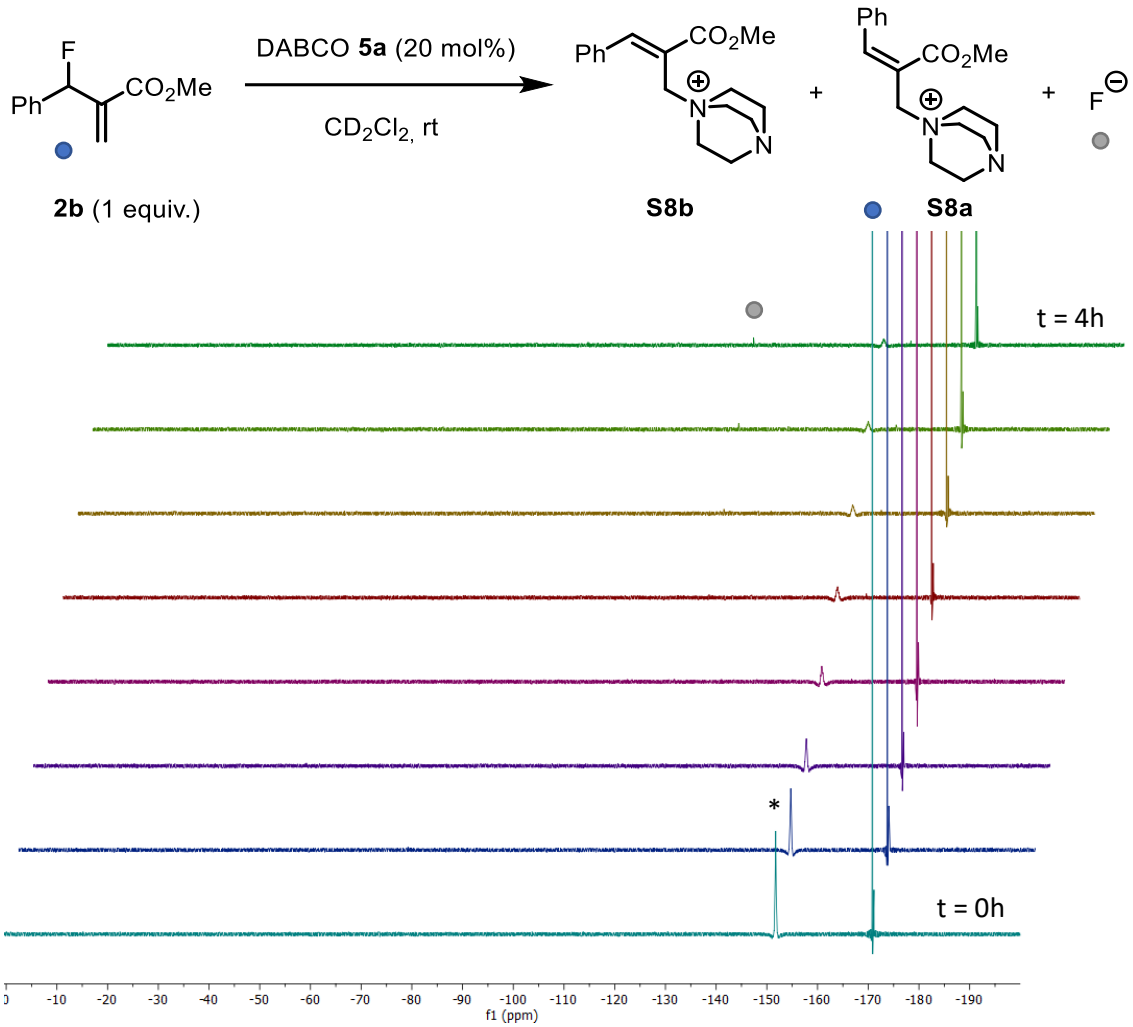

Figure S19. $^{19}F\{^{1}H\}$NMR spectra at 470 MHz NMR field in CD_2Cl_2 for the formation of the catalytic species using 20 mol% of DABCO **5a** and 1 equiv. of allyl fluoride **2b** over 4h.

*[In this experiment, the utilization of catalytic amounts of DABCO **5a** in the absence of a competitive fluorophilic trap leads to the formation of naked fluoride (grey bubble, at -126.91 ppm), which matches with the $^{19}F\{^{1}H\}$ NMR of an ammonium fluoride, such as TBAF. (The signal marked with * at -151 ppm is an artifact.[13])]*

F.5. Generation of the catalytic species with (DHQD)$_2$PHAL *– Using 20 mol% of (DHQD)$_2$PHAL and allyl carbonates*

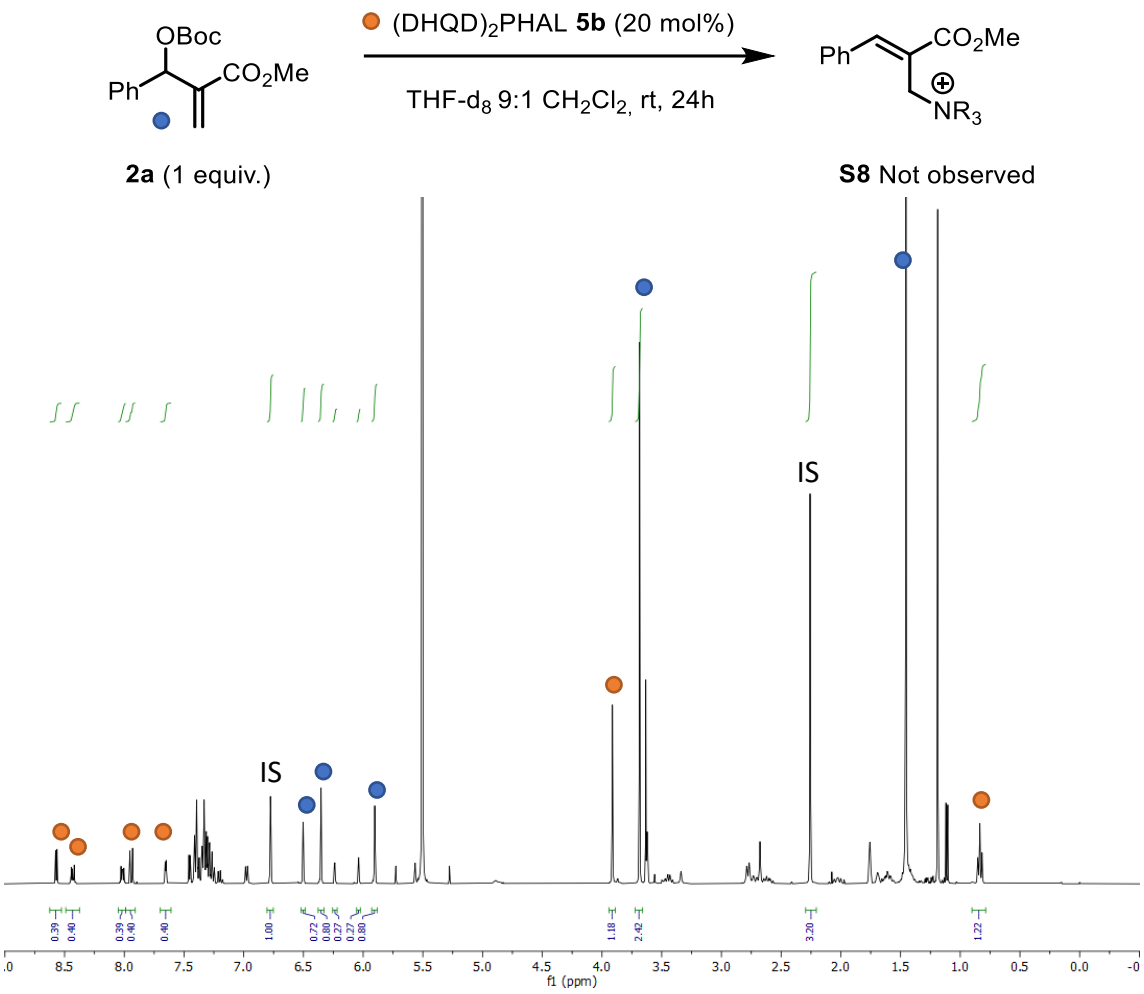

Figure S20. ^{1}H NMR spectrum at 500 MHz NMR field in THF-d_8:CD_2Cl_2 (9:1) for the formation of the catalytic species using 20 mol% of (DHQD)$_2$PHAL **5b** and 1 equiv. of allyl carbonate **2a**.

*[The utilization of catalytic amounts of (DHQD)$_2$PHAL **5b** (orange bubble) does not lead to the observation of the catalytic species **S8** after 24 h at room temperature. Moreover, 80% of the unreacted allyl carbonate **2a** (blue bubbles) is still present in the reaction mixture.]*

F.6. Generation of the catalytic species with (DHQD)$_2$PHAL *– Using 20 mol% of (DHQD)$_2$PHAL and allyl fluorides*

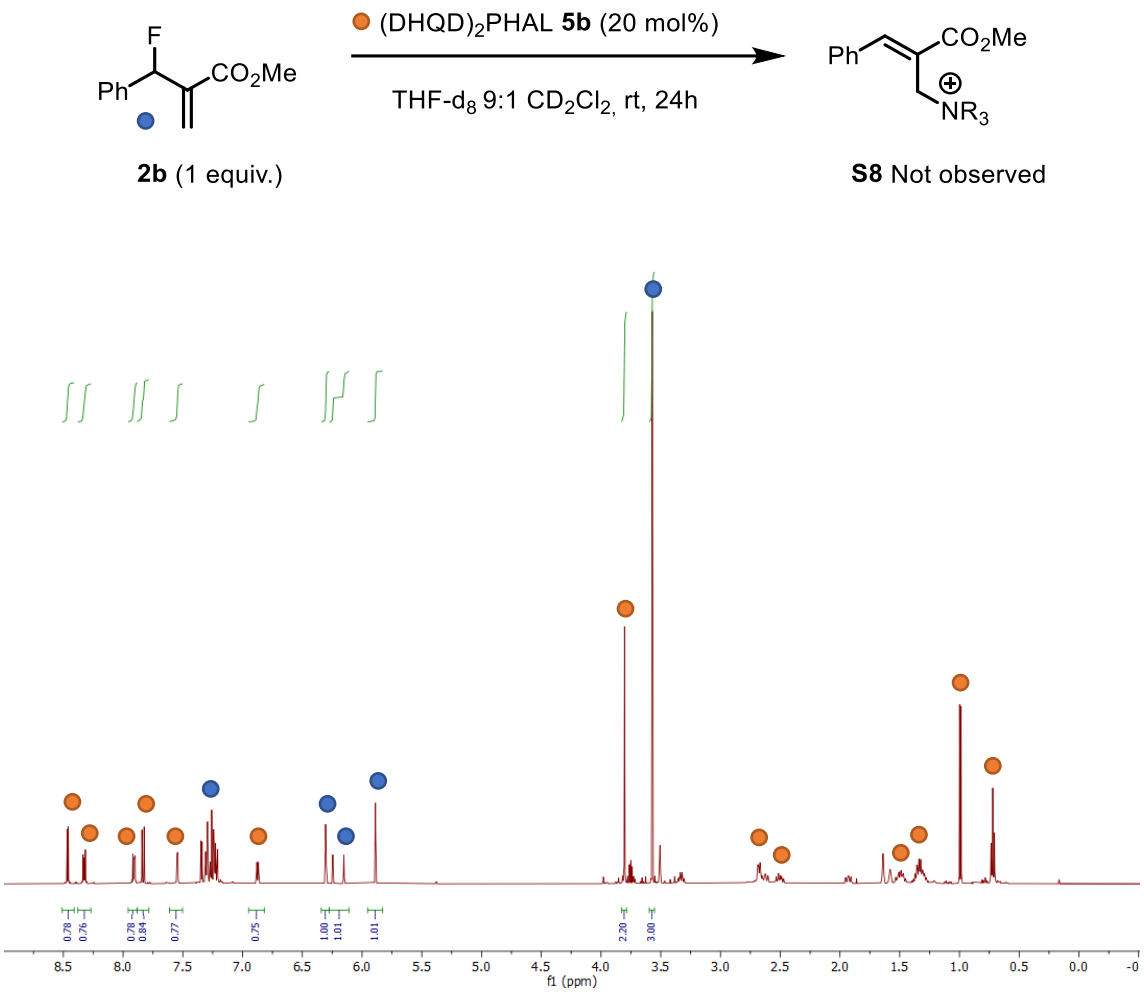

Figure S21. ^{1}H NMR spectrum at 500 MHz NMR field in THF-d_8:CD_2Cl_2 (9:1) for the formation of the catalytic species using 20 mol% of (DHQD)$_2$PHAL **5b** and 1 equiv. of allyl fluoride **2b**.

*[The utilization of catalytic amounts of (DHQD)$_2$PHAL **5b** (orange bubble) does not lead to the observation of the catalytic species **S8** after 24 h at room temperature.]*

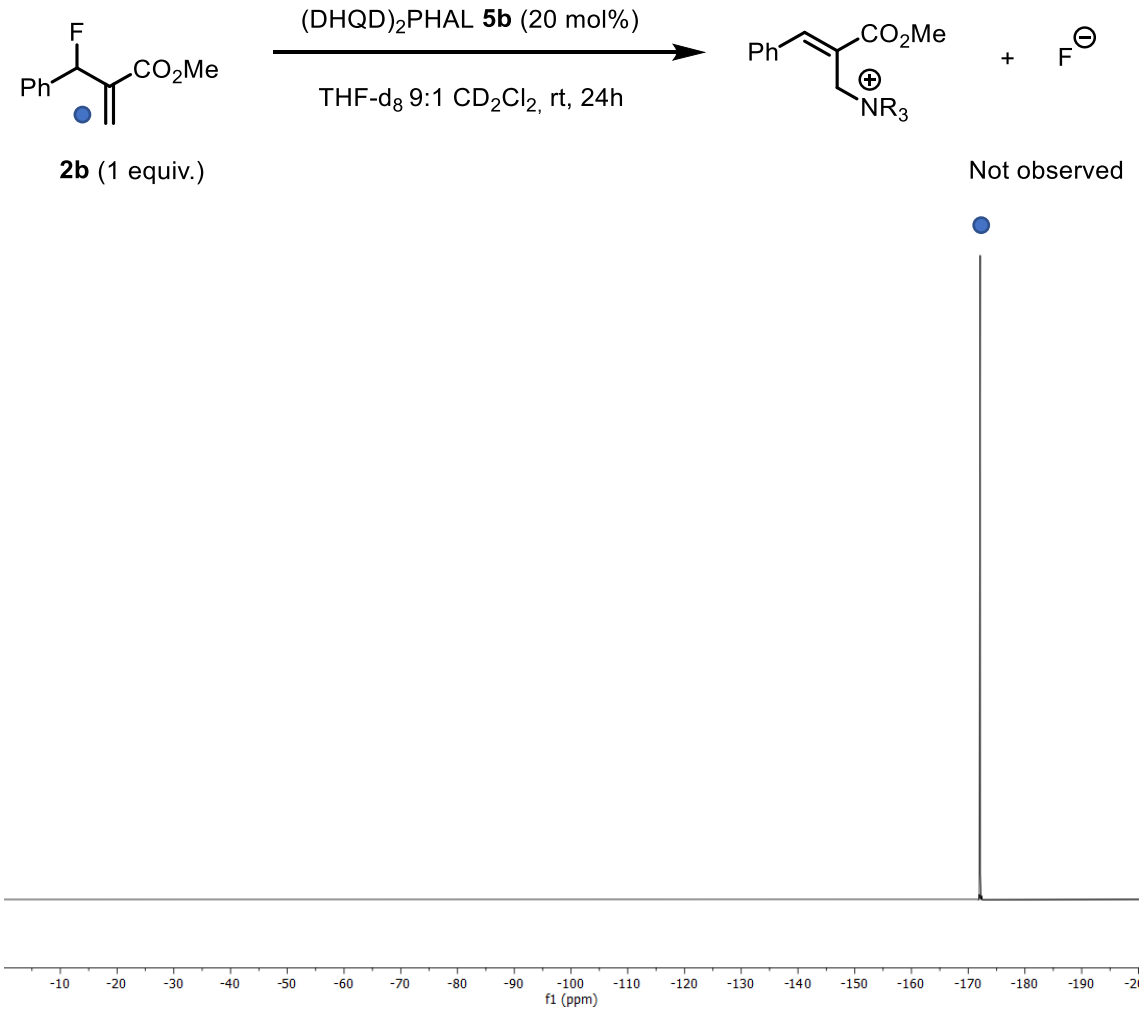

Figure S22. ^{19}F {^{1}H} NMR spectrum at 470 MHz NMR field in THF-d_8:CD_2Cl_2 (9:1) for the formation of fluoride using 20 mol% of $(DHQD)_2PHAL$ **5b** and 1 equiv. of allyl fluoride **2b**.

*[The utilization of catalytic amounts of $(DHQD)_2PHAL$ **5b** does not lead to the observation of fluoride after 24 h at room temperature.]*

G. Control experiments

General procedures

A - The corresponding allylic substrate (1 equiv., 0.1 mmol) was weighted into an NMR tube and dissolved with 0.5 mL of the corresponding deuterated solvent (0.2 M). Subsequently, the corresponding ketone/enol ether (3 equiv., 0.3 mmol) and the corresponding amount of catalyst were added (as stated in every example). To ensure homogeneous NMR samples, the tube was initially sonicated 1 min.

B - The corresponding allylic substrate (1 equiv., 0.1 mmol) was weighted into a 5 mL vial equipped with a magnetic stirring bar and dissolved with 0.5 mL of the corresponding solvent (0.2 M). Subsequently, the corresponding ketone/enol ether (3 equiv., 0.3 mmol), reagent TBAF or $LiClO_4$ (if needed) and a 10/20 mol% of catalyst were added. The reaction mixture was stirred at room temperature until the extraction of a 50 µL aliquot. The reaction aliquot was dried under vacuum pressure in a vial, where it was added 50 µL of a 0.2 M solution of 1,3,5-trimethoxybenzene in $CDCl_3$. The resulting mixture was diluted with more $CDCl_3$ and was transferred into an NMR tube.

***G.1. Control experiments** – Utilization of different leaving groups in the allylic position with cyclic ketones and DABCO*

Allyl carbonate in the presence of a cyclic ketone

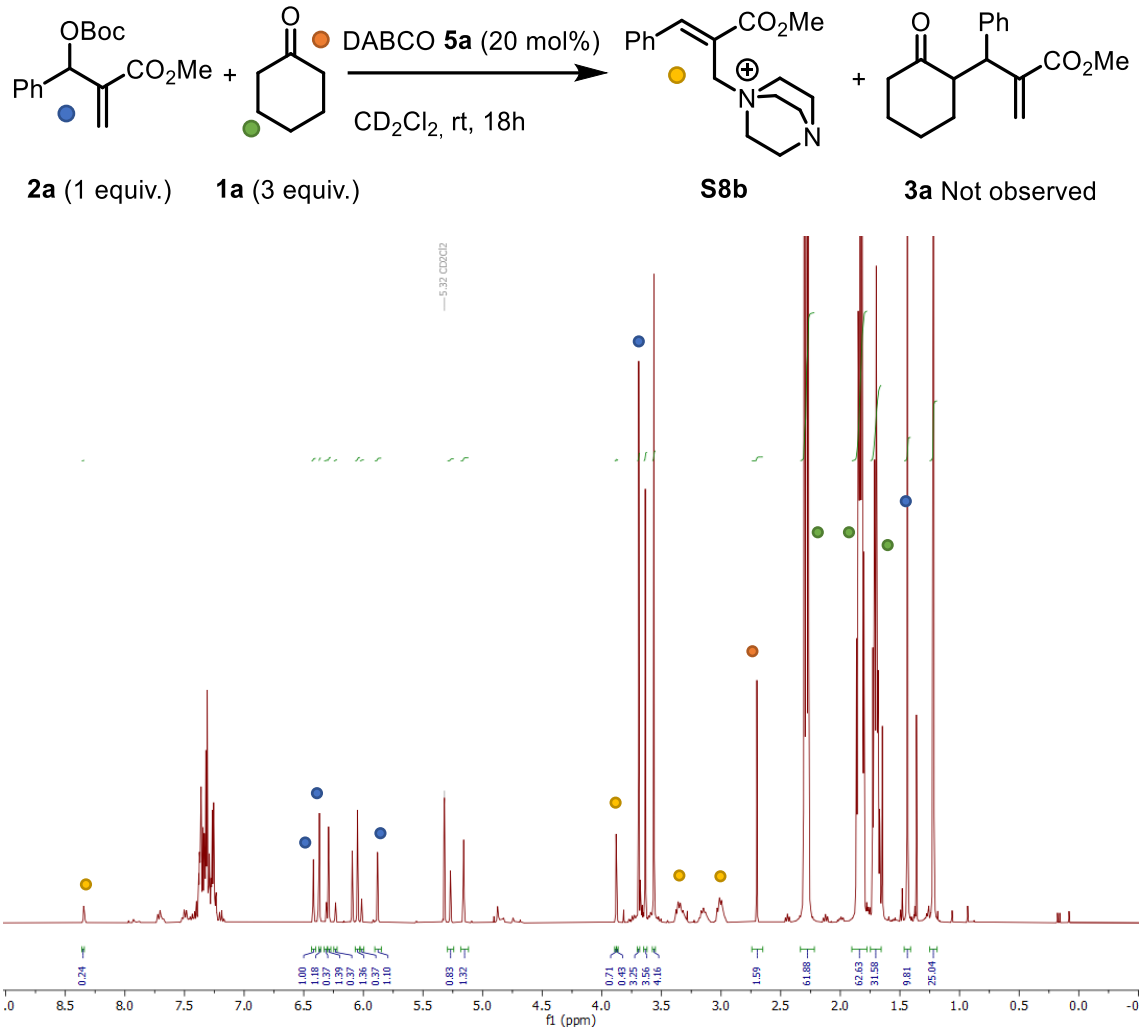

Figure S23. ^{1}H NMR spectrum at 500 MHz NMR field in CD_2Cl_2 of the reaction crude.

*[In this experiment, the utilization of catalytic amounts of DABCO **5a** (orange bubble) **leads to** the formation of the E- isomer **S8b** (yellow bubbles) of the catalytic species when allyl carbonate **2a** is used. However, even if the starting material **2a** is consumed (blue bubbles), the product **3a** is not observed.]*

*This experiment highlights the **need of a competent enol nucleophile** for the reaction to proceed.*

Allyl acetate in the presence of a cyclic ketone

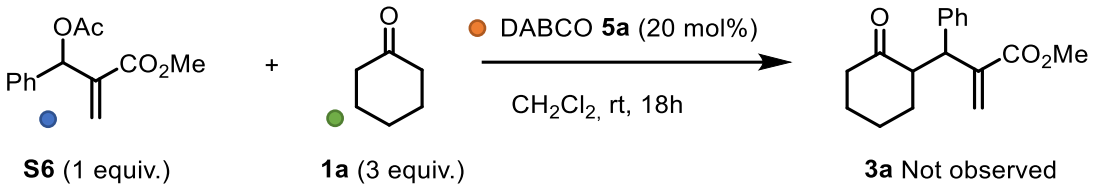

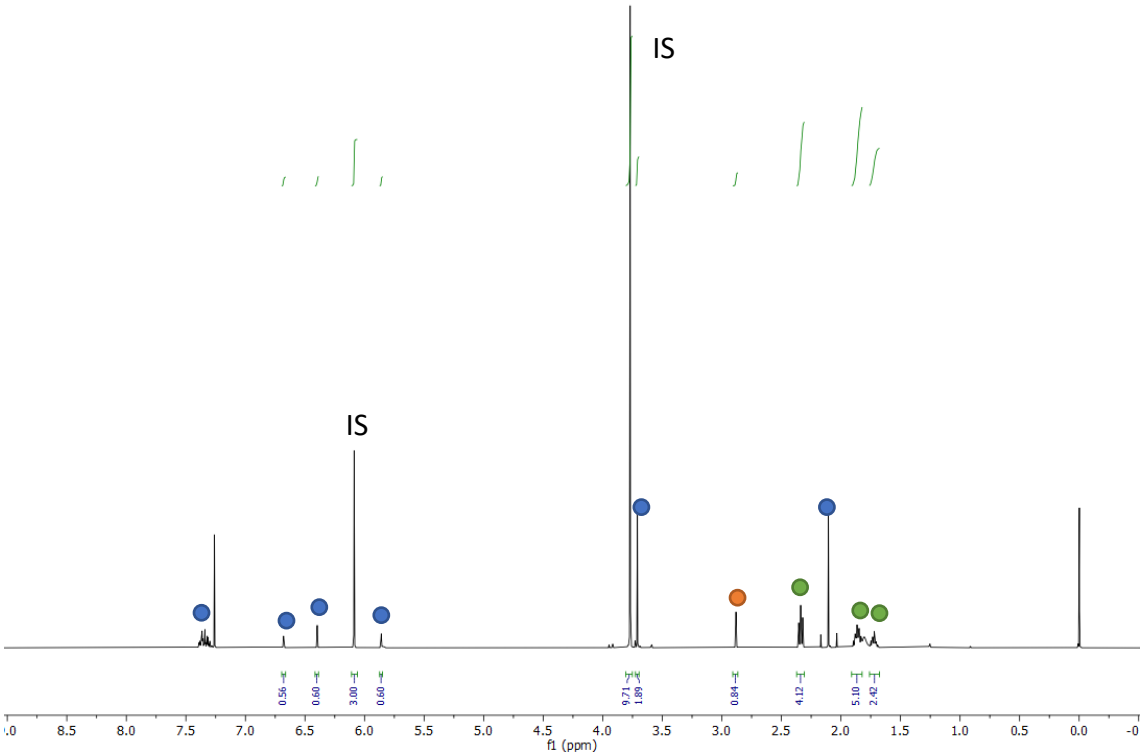

Figure S24. ^{1}H NMR spectrum at 500 MHz NMR field in CD_2Cl_2 of the reaction crude.

*[The utilization of catalytic amounts of DABCO **5a** (orange bubble) **does not lead** to the observation of the catalytic species when allyl acetate **S6** is used. Additionally, the starting material **S6** is not consumed (blue bubbles) thus the product **3a** is not observed.]*

*This experiment highlights the **need of a reactive allyl derivative** as well as a competent enol nucleophile for the reaction to proceed.*

Allyl fluoride in the presence of a cyclic ketone

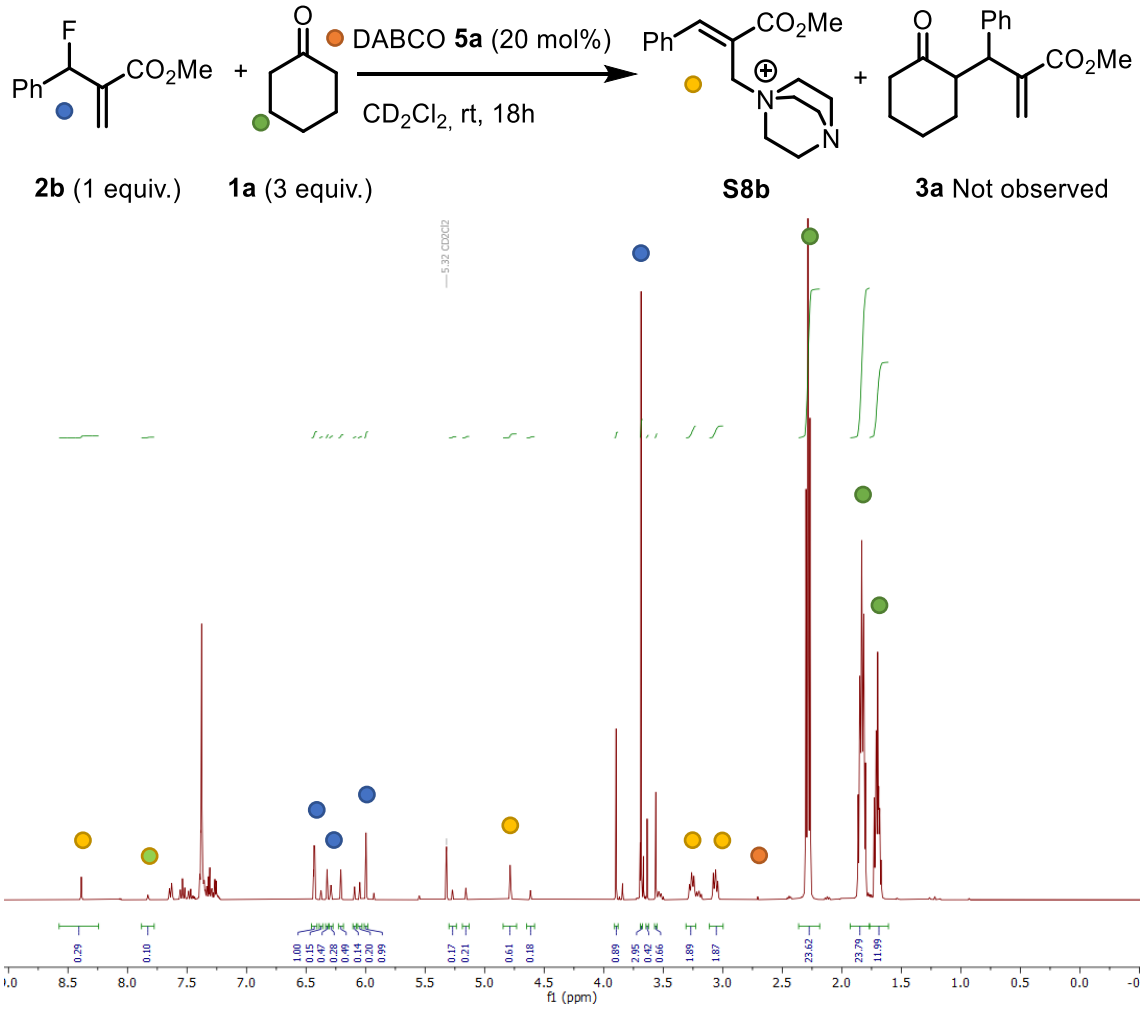

Figure S25. ^{1}H NMR spectrum at 500 MHz NMR field in CD_2Cl_2 of the reaction crude.

*[The utilization of catalytic amounts of DABCO **5a** (orange bubble) **leads to** the formation of a 1 to 3 mixture of the Z- and E- isomers **S8** (light green and yellow bubbles) of the catalytic species in the presence of allyl fluoride **2b**. However, even if the starting material **2b** is consumed (blue bubbles), the product **3a** is not observed.]*

*This experiment highlights the **need of a competent enol nucleophile** for the reaction to proceed.*

***G.2. Control experiments** – Utilization of different leaving groups in the allylic position with cyclic ketones and (DHQD)$_2$PHAL*

Allyl carbonate in the presence of a cyclic ketone

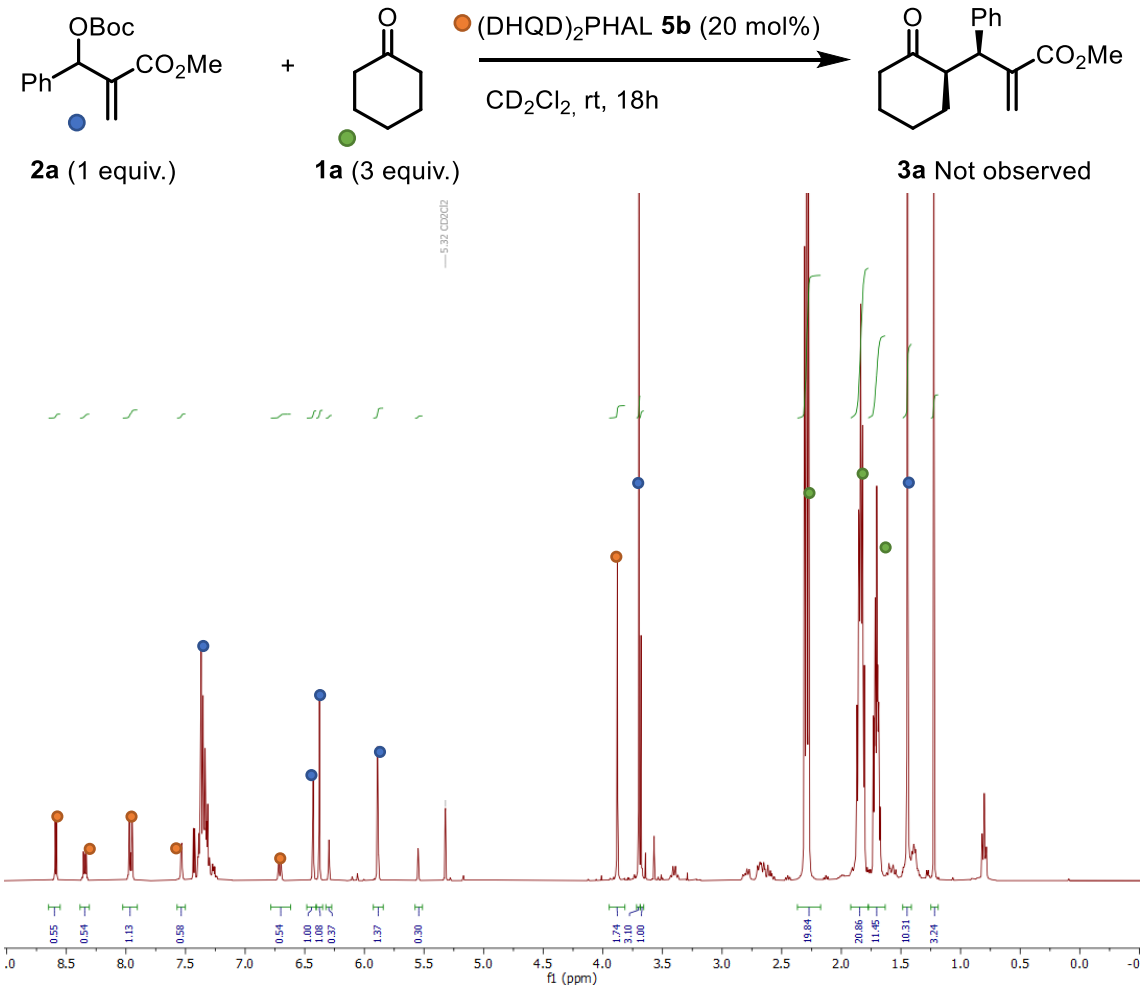

Figure S26. ^{1}H NMR spectrum at 500 MHz NMR field in CD_2Cl_2 of the reaction crude.

*[In this experiment, the utilization of catalytic amounts of (DHQD)$_2$PHAL **5b** (orange bubble) **does not lead** to the observation of the catalytic species. Additionally, the starting material **2a** is not consumed (blue bubbles) nor the product **3a** observed.]*

*This experiment highlights the **need of a competent enol nucleophile** for the reaction to proceed.*

Allyl fluoride in the presence of a cyclic ketone

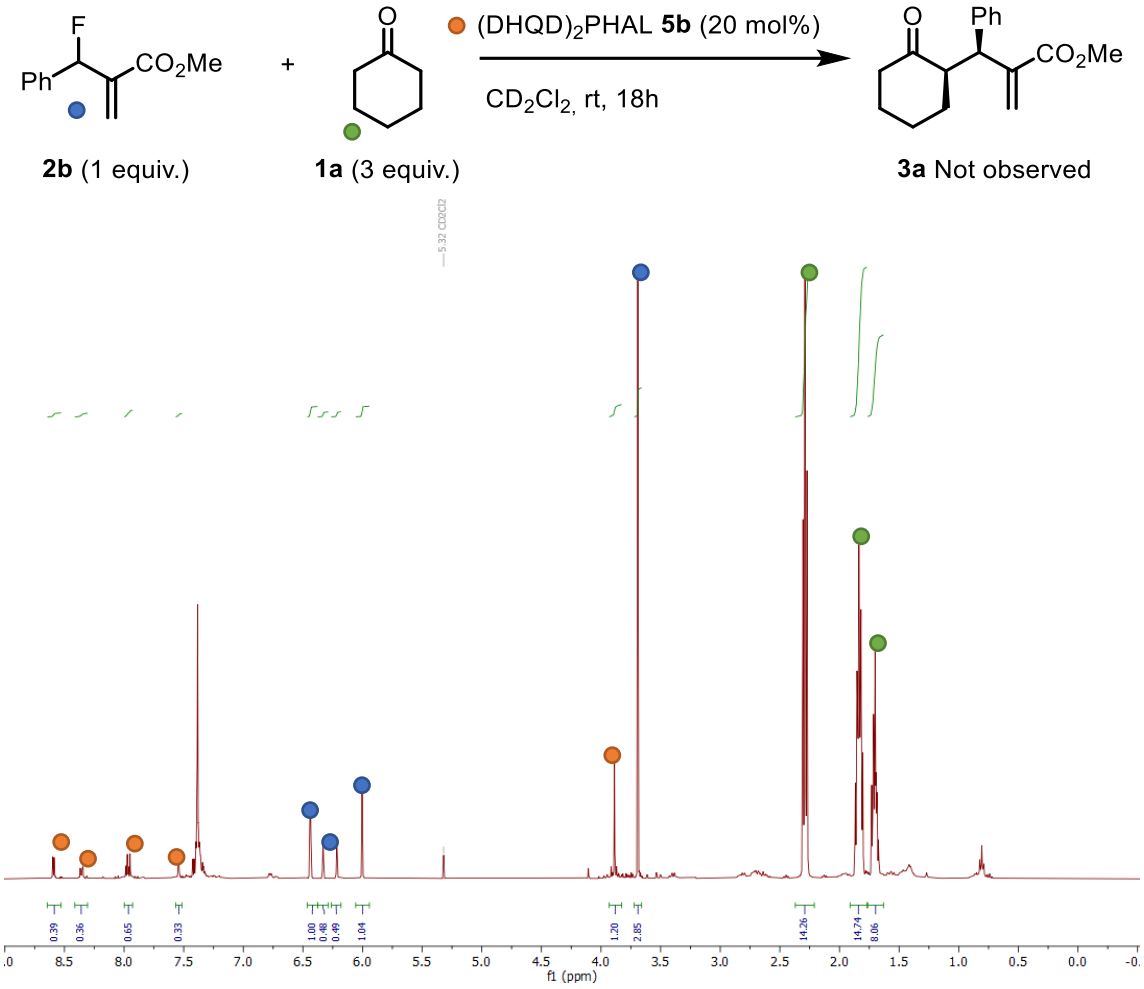

Figure S27. ^{1}H NMR spectrum at 500 MHz NMR field in CD_2Cl_2 of the reaction crude.

*[In this experiment, the utilization of catalytic amounts of (DHQD)$_2$PHAL **5b** (orange bubble) **does not lead** to the observation of the catalytic species. Additionally, the starting material **2b** is not consumed (blue bubbles) nor the product **3a** observed.]*

*This experiment highlights the **need of a competent enol nucleophile** for the reaction to proceed.*

***G.3. Control experiments** – Utilization of different enol derivatives with allyl fluorides and DABCO*

Allyl fluoride in the presence of a cyclic enol carbonate

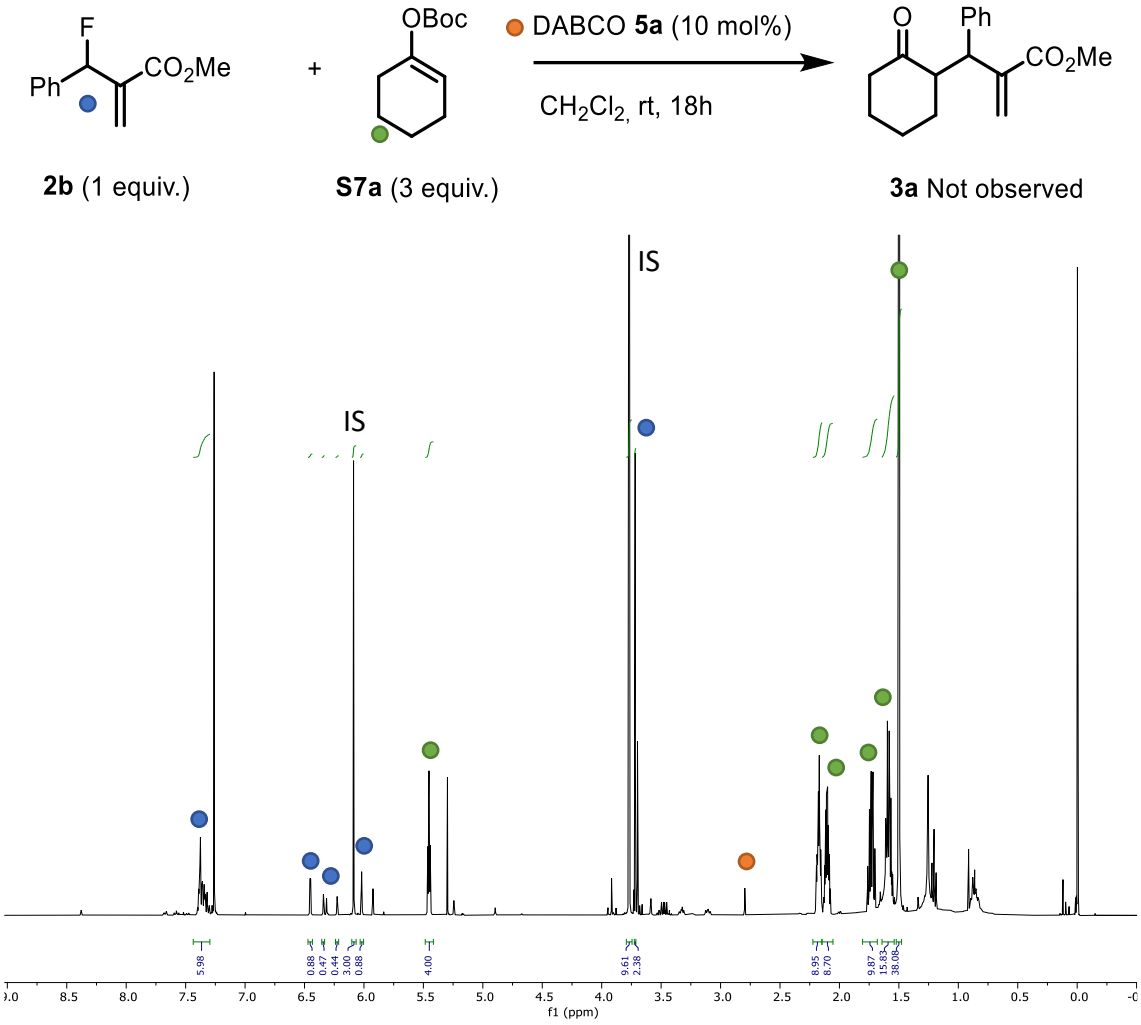

Figure S28. ^{1}H NMR spectrum at 500 MHz NMR field in $CDCl_3$ of the reaction crude.

*[In this experiment, the utilization of catalytic amounts of DABCO **5a** (orange bubble) **does not lead** to the observation of the catalytic species. Additionally, the starting material **2b** nor the enol carbonate **S7a** are consumed (blue and green bubbles respectively). In consequence, the product **3a** is not observed.]*

*This experiment highlights **the need of** a **competent fluorophilic enol derivative** for the reaction to proceed.*

Allyl fluoride in the presence of a cyclic enol acetate

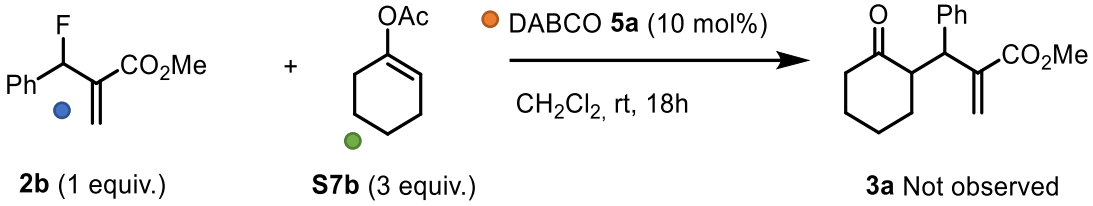

2b (1 equiv.) **S7b** (3 equiv.) **3a** Not observed

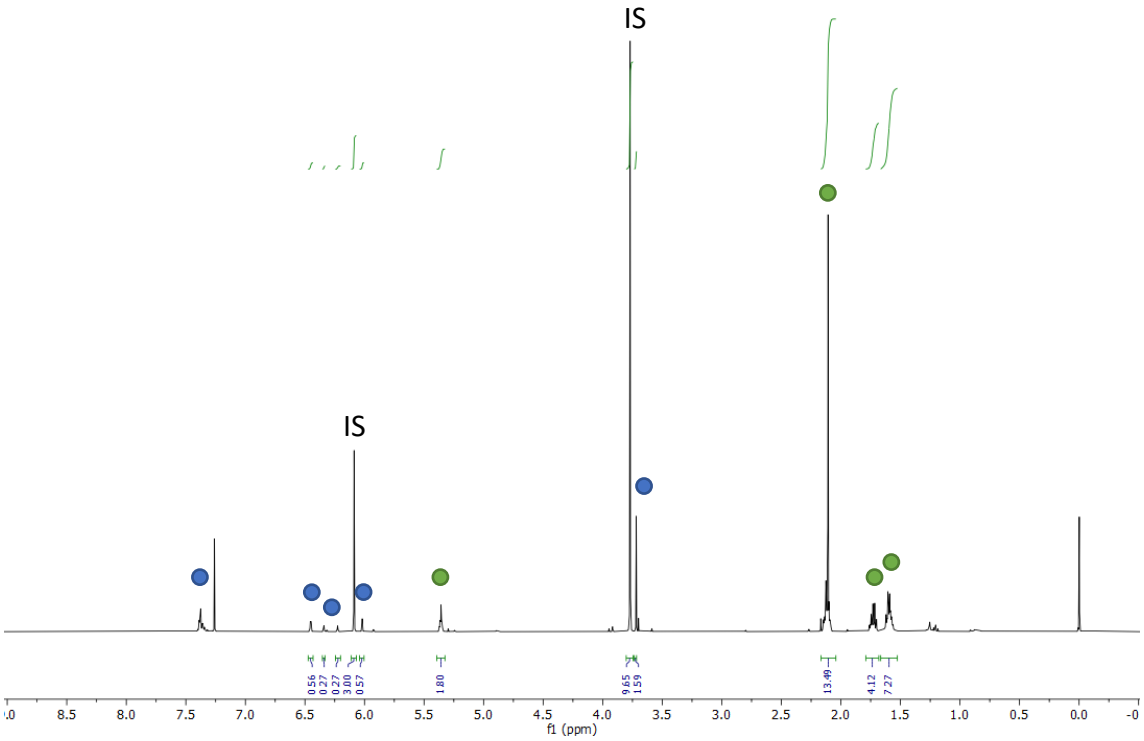

Figure S29. ^{1}H NMR spectrum at 500 MHz NMR field in $CDCl_3$ of the reaction crude.

*[In this experiment, the utilization of catalytic amounts of DABCO **5a** (orange bubble) **does not lead to** the observation of the catalytic species. Additionally, the starting material **2b** nor the enol acetate **S7b** are consumed (blue and green bubbles respectively). In consequence, the product **3a** is not observed.]*

*This experiment highlights **the need of** a **competent fluorophilic enol derivative** for the reaction to proceed.*

***G.4. Control experiments** – Utilization of enol carbonates with allyl fluorides and DABCO*

Carbonate in the presence of a cyclic silyl enol ether

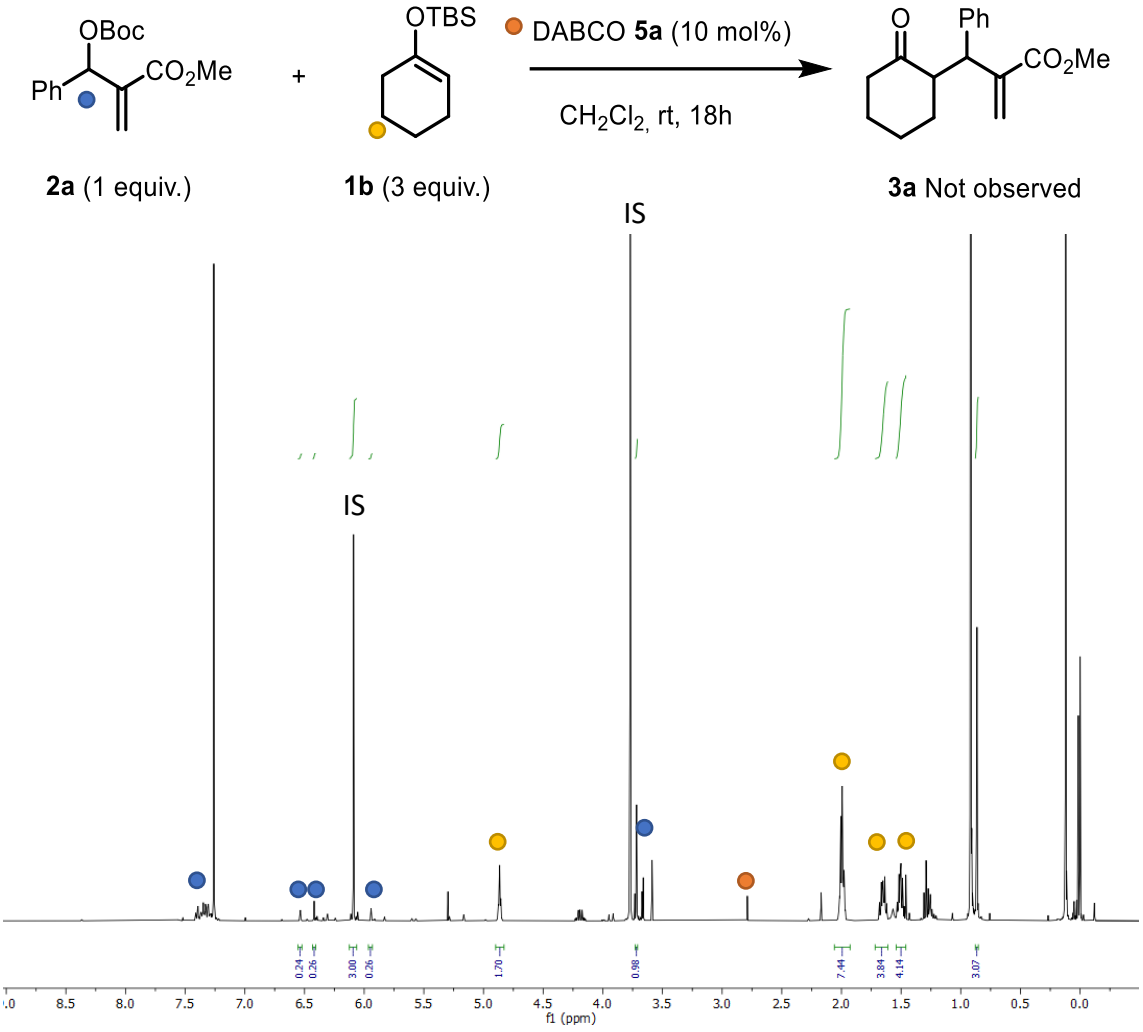

Figure S30. ^{1}H NMR spectrum at 500 MHz NMR field in $CDCl_3$ of the reaction crude.

*[In this experiment, the utilization of catalytic amounts of DABCO **5a** (orange bubble) **does not lead to** the observation of the catalytic species. Additionally, the limiting allyl carbonate **2a** nor the silyl enol ether **1b** are consumed (blue and yellow bubbles respectively). In consequence, the product **3a** is not observed.]*

*This experiment highlights **the need of** a **fluoride-mediated activation** of the silyl enol ether for the reaction to proceed.*

***G.5. Control experiments** – Activation of silyl enol ethers with external fluoride sources*

Allyl fluoride in the presence of a cyclic silyl enol ether and TBAF (without catalyst)

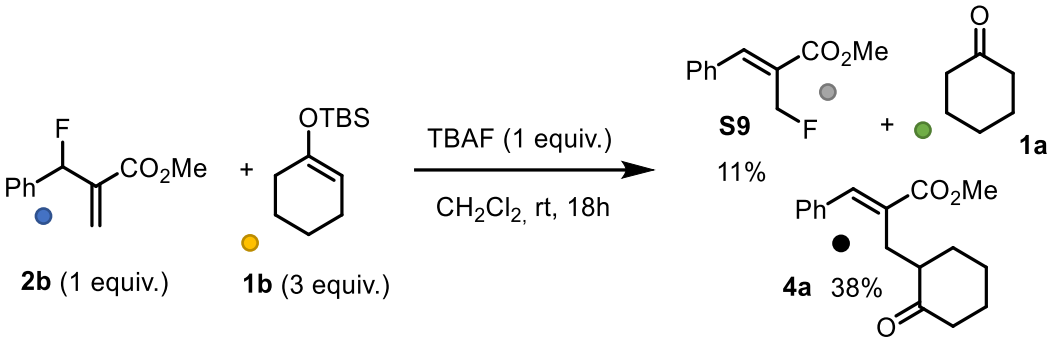

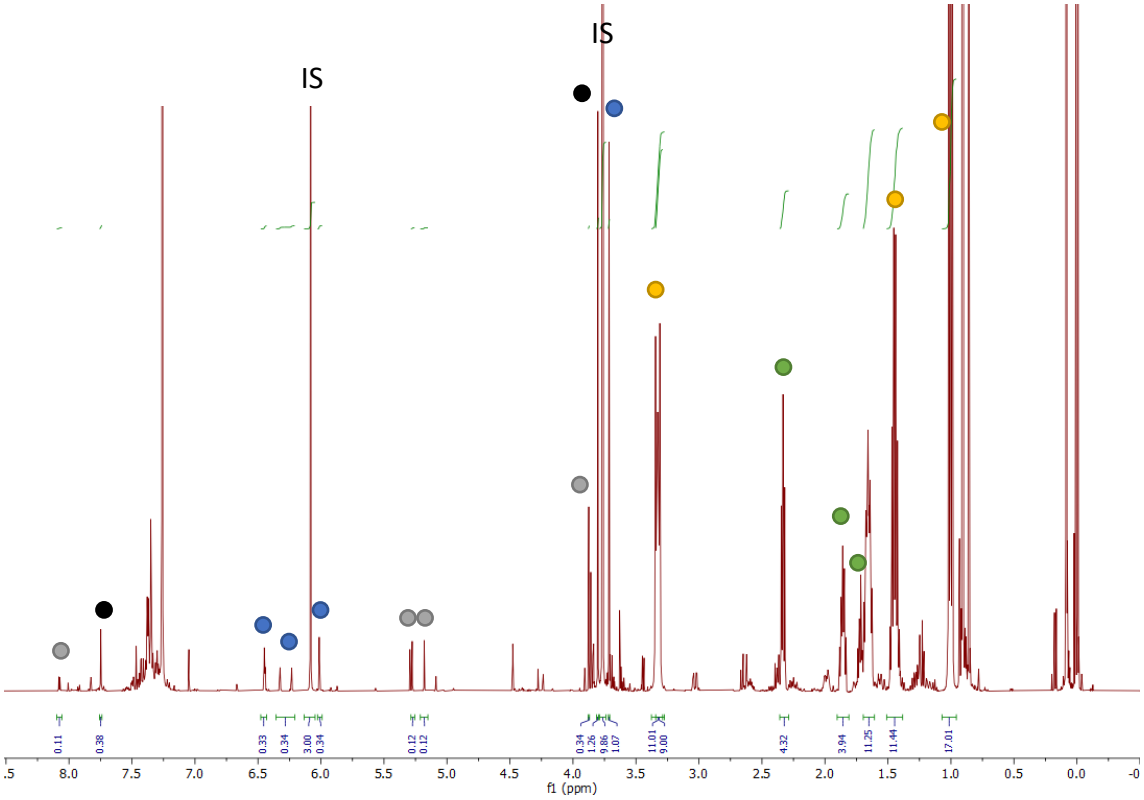

Figure S31. ^{1}H NMR spectrum at 500 MHz NMR field in $CDCl_3$ of the reaction crude.

*[In this experiment, **the absence of a Lewis base prevents the elimination of fluoride** from the allyl fluoride **2b**. However, the addition of **an external source of fluoride** (TBAF, 1 equiv.) leads to the activation of the silyl enol ether. For this reason, a **complex mixture of different regioismers** is observed. On the one hand, the regioisomer of starting material **2b** is observed in 11 % yield (grey bubbles). On the other hand, the regioisomer of the product **4a** is observed in 38% yield (black bubbles).]*

*This experiment highlights **the need of a controlled release of fluoride** in order to ensure high regioselectivities in the reaction.*

Allyl carbonate in the presence of a cyclic silyl enol ether and TBAF (with catalytic DABCO)

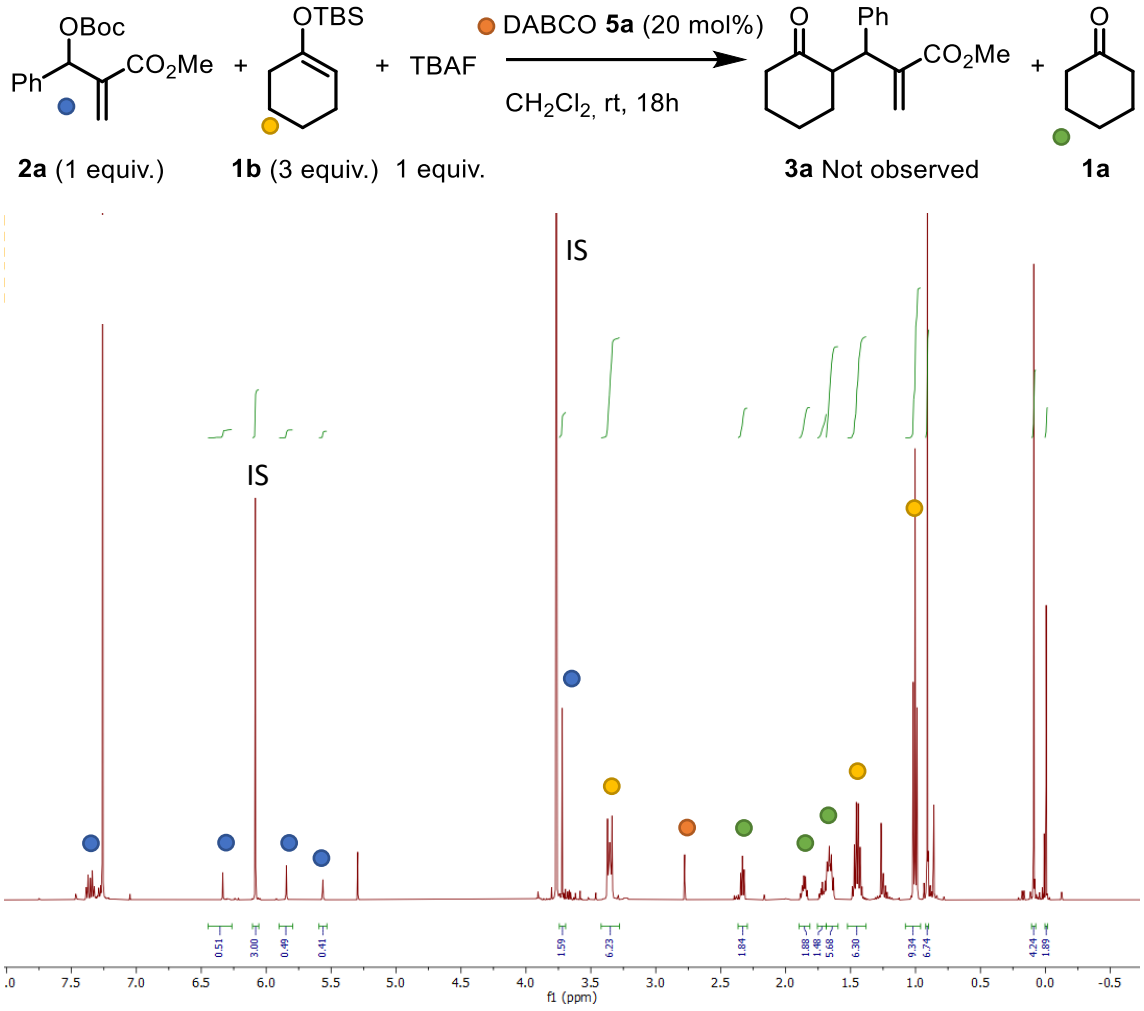

Figure S32. ^{1}H NMR spectrum at 500 MHz NMR field in $CDCl_3$ of the reaction crude.

*[In this experiment, **the presence of a Lewis base such as** DABCO **5b** (20 mol%, orange bubble) in combination with **an external source of fluoride** (TBAF, 1 equiv.) does not yield product **3a**.]*

This experiment highlights that both the formation of the ammonium catalytic species together with the enolate of the cyclohexanone do not guarantee suitable reactivity.

Allyl fluoride in the presence of a cyclic silyl enol ether and TBAF (with catalytic DABCO)

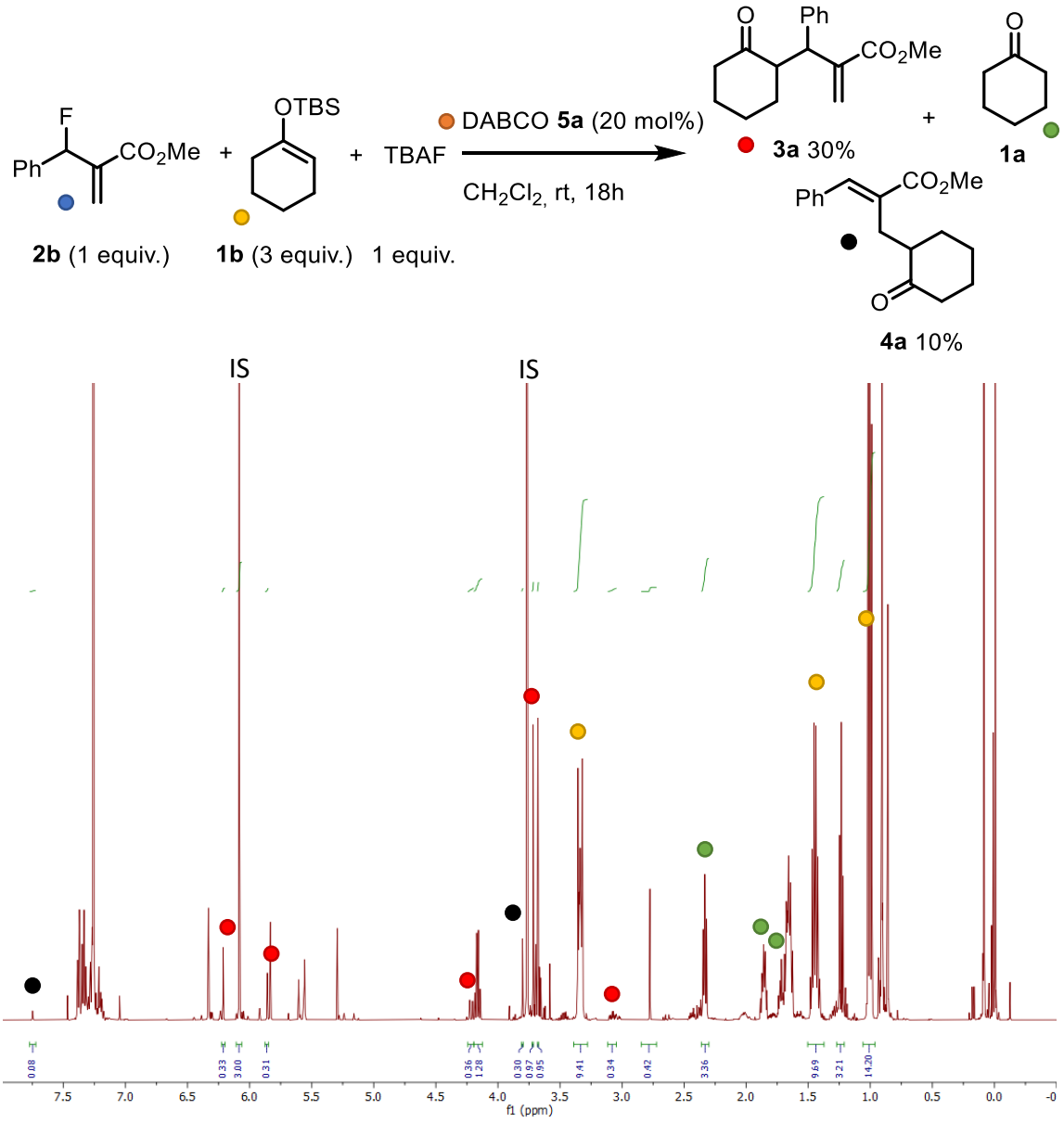

Figure S33. ^{1}H NMR spectrum at 500 MHz NMR field in $CDCl_3$ of the reaction crude.

*[In this experiment, **the presence of a Lewis base** such as DABCO (20 mol%, orange bubble) in combination with **an external source of fluoride** (TBAF, 1 equiv.) while using allyl fluorides triggers the formation of complex reaction mixtures. Additionally, full conversion of the starting material **2b** is observed (blue bubbles) yielding **complex mixture of regioismers**. On one side, product **3a** is observed in a modest 30 % yield (red bubbles). At the same time, the product regioisomer **4a** is observed in 10% yield (black bubbles).]*

*This experiment highlights **the need of a controlled release of fluoride** in order to ensure high regioselectivities in the reaction.*

Allyl carbonate in the presence of a cyclic silyl enol ether and TBAF (with catalytic (DHQD)$_2$PHAL)

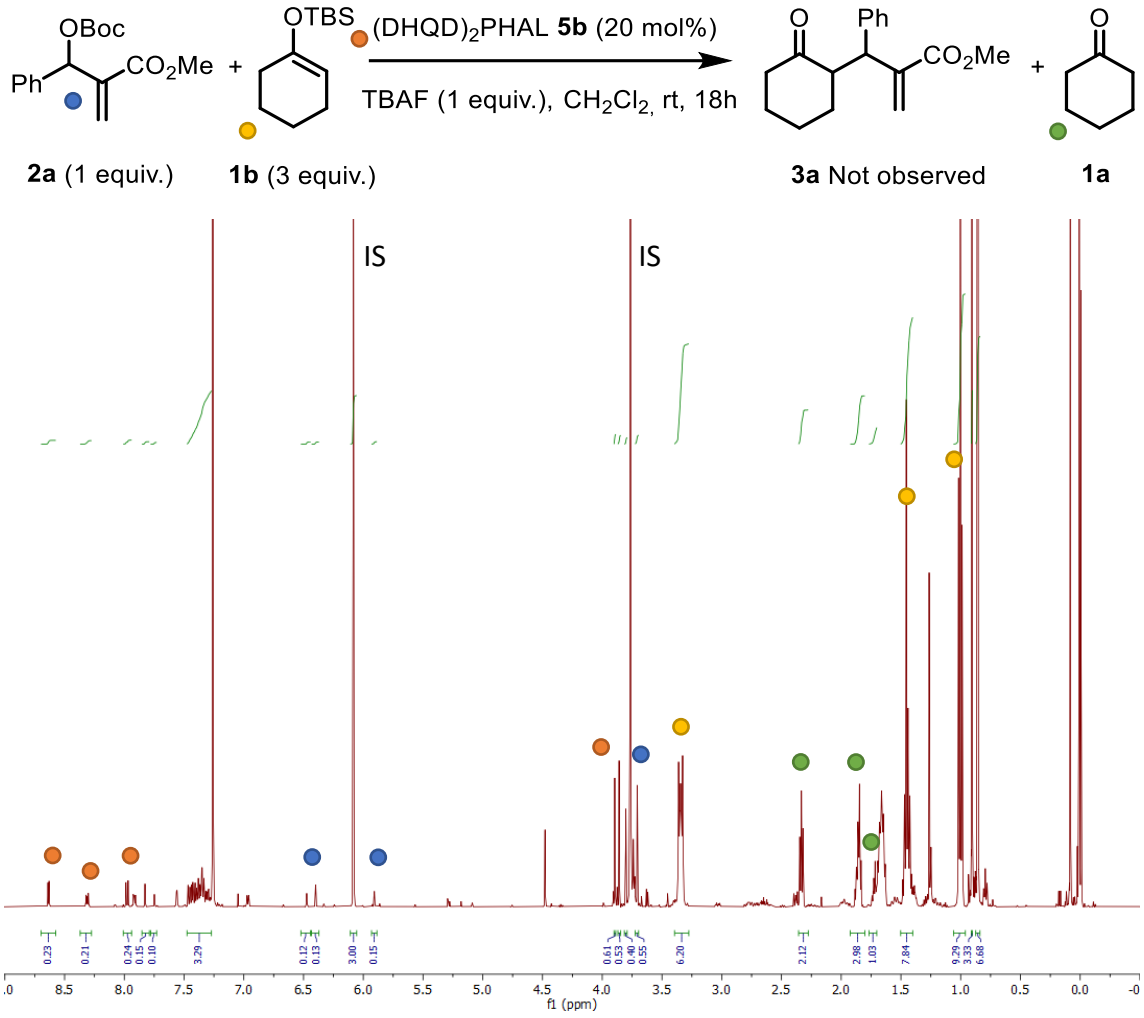

Figure S34. ^{1}H NMR spectrum at 500 MHz NMR field in $CDCl_3$ of the reaction crude.

*[In this experiment, **the presence of a chiral Lewis base** such as (DHQD)$_2$PHAL **5b** (20 mol%, orange bubble) in combination with **an external source of fluoride** (TBAF, 1 equiv.) prevents the formation of complex reaction mixtures. Additionally, no conversion of the starting allyl carbonate **2a** is observed.]*

*This experiment highlights **the need of low concentrations of naked fluoride in the reaction media** to ensure the reaction to proceed.*

Allyl fluoride in the presence of a cyclic silyl enol ether and TBAF (with catalytic (DHQD)$_2$PHAL)

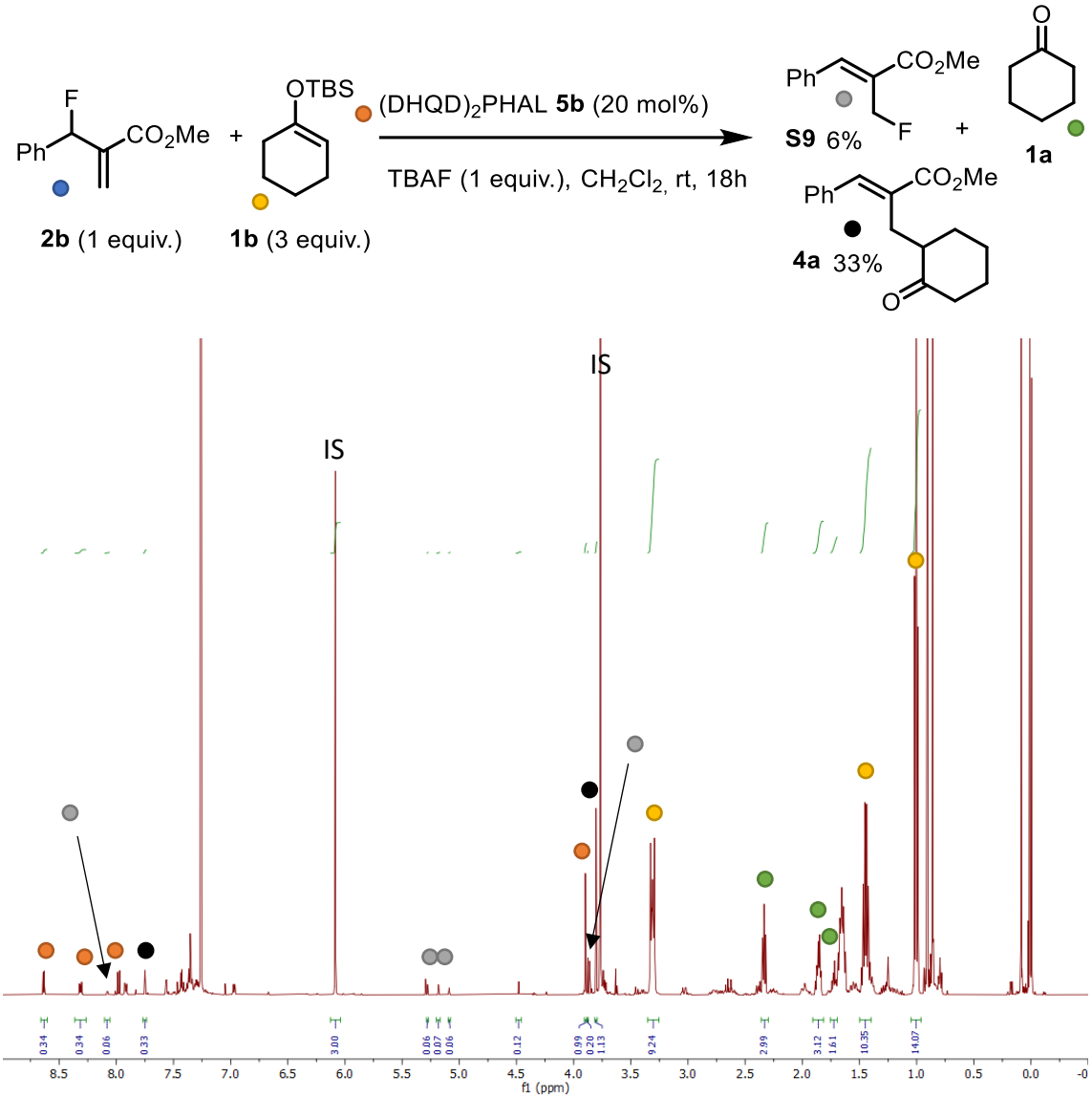

Figure S35. ^{1}H NMR spectrum at 500 MHz NMR field in $CDCl_3$ of the reaction crude.

*[In this experiment, **the presence of a chiral Lewis base** such as (DHQD)$_2$PHAL **5b** (20 mol%, orange bubble) in combination with **an external source of fluoride** (TBAF, 1 equiv.) while using allyl fluorides triggers the formation of complex reaction mixtures. Additionally, full conversion of the starting material **2b** is observed (blue bubbles) yielding **complex mixture of by-products**. On the one hand, the regioisomer of starting material **S9** is observed in 6 % yield (grey bubbles). On the other hand, the regioisomer of the product **4a** is observed in 33% yield (black bubbles).]*

*This experiment highlights **the need of a controlled release of fluoride** in order to ensure high regioselectivities in the reaction.*

***G.6. Control experiments** – Utilization of Li-salts as competitive fluorophilic traps*

Allyl fluoride **2b** (1 equiv., 0.2 mmol) was weighted into a 5 mL vial equipped with a magnetic stirring bar and dissolved with 1 mL of the corresponding solvent (0.2 M). Subsequently, the corresponding silyl enol ether **1b** (3 equiv., 0.6 mmol), $LiClO_4$ (1 equiv., 0.2 mmol) and a 10/20 mol% of catalyst were added. The reaction mixture was stirred at room temperature and a 50 µL aliquot was taken at the given time. This aliquot was dried under reduced pressure and the internal standard (1,3,5-trimethoxybenzene) was added and dissolved in $CDCl_3$.

Allyl fluoride in the presence of a cyclic silyl enol ether and $LiClO_4$ (with catalytic DABCO)

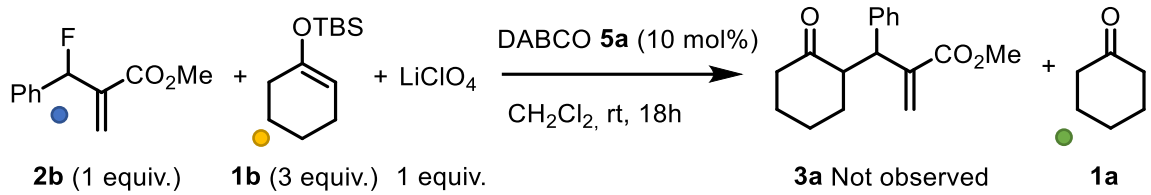

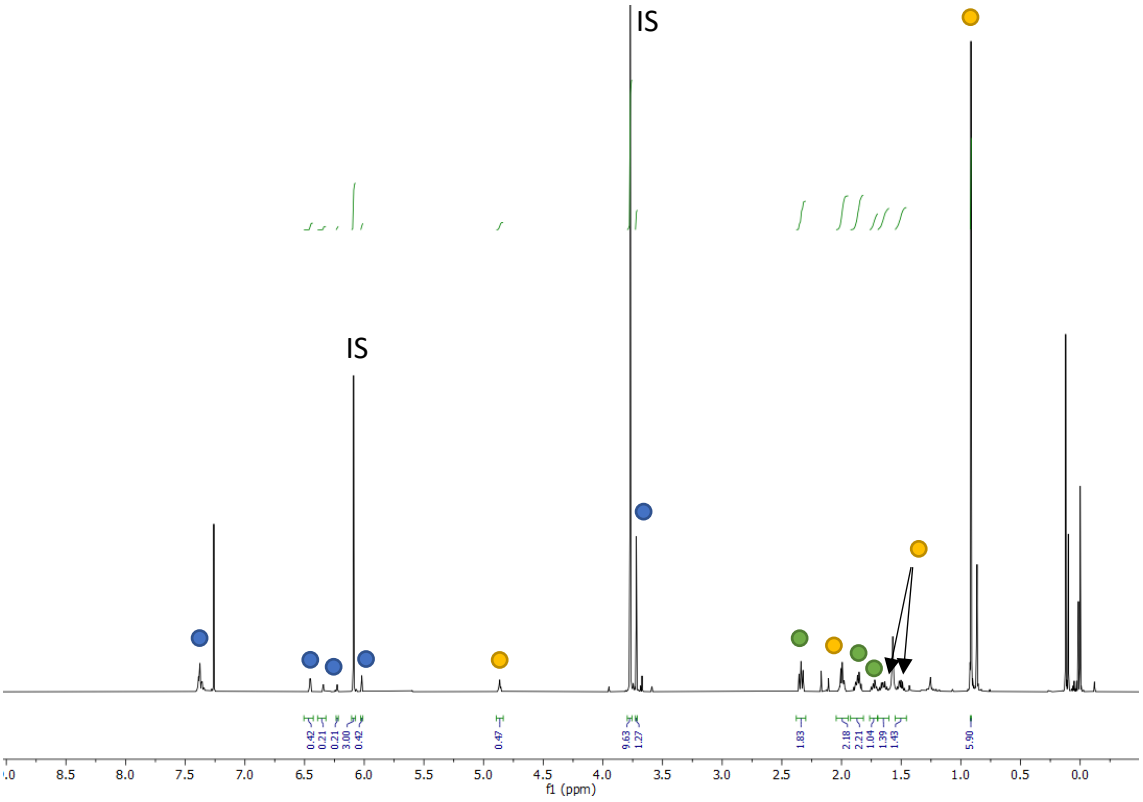

Figure S36. ^{1}H NMR spectrum at 500 MHz NMR field in $CDCl_3$ of the reaction crude.

*[In this experiment, **the presence of a Lewis base** such as DABCO **5a** (20 mol%) in combination with **$LiClO_4$** (1 equiv.) as fluorophilic trap prevents de formation of product **3a**. Additionally, 60% conversion of the starting material **2b** is observed (blue bubbles) **not yielding the desired product**.]*

*This experiment highlights **the need of Si-F interaction** for the reaction to proceed.*

Allyl fluoride in the presence of a cyclic silyl enol ether and $LiClO_4$ (with catalytic $(DHQD)_2PHAL$)

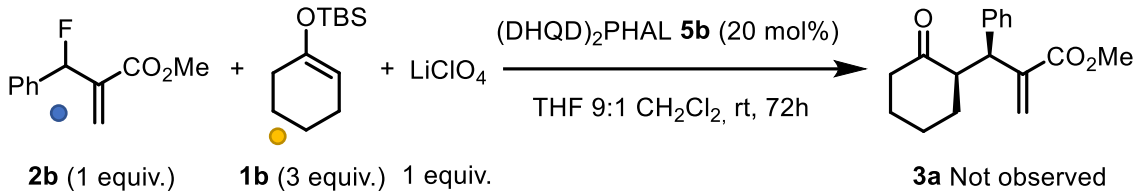

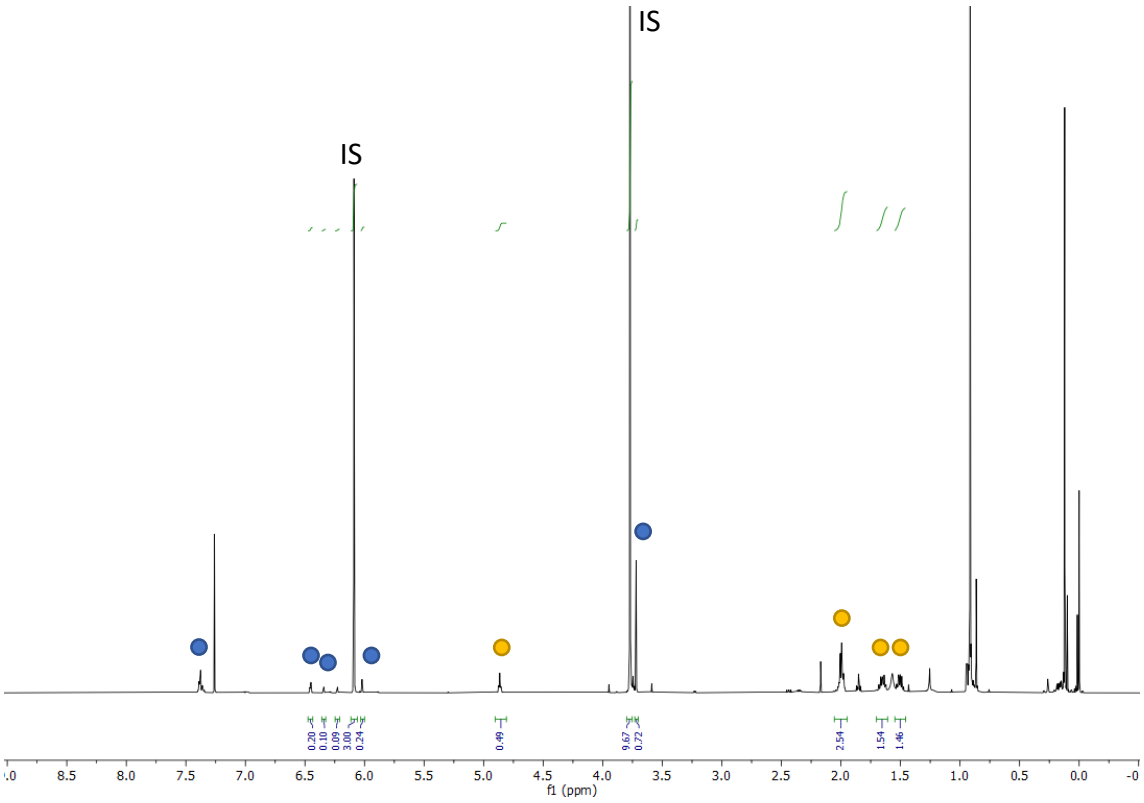

Figure S37. ^{1}H NMR spectrum at 500 MHz NMR field in $CDCl_3$ of the reaction crude.

[In this experiment, ***the presence of a chiral Lewis base*** *such as $(DHQD)_2PHAL$* ***5b*** *(20 mol%) in combination with* ***$LiClO_4$*** *(1 equiv.) as fluorophilic trap prevents de formation of product* ***3a****. Additionally, 80% conversion of the starting material* ***2b*** *is observed (blue bubbles)* ***not yielding the desired product****.]*

This experiment highlights ***the need of Si-F interaction*** *for the reaction to proceed.*

***G.7. Control experiments** – Reactivity of (DHQD)$_2$PHAL with cyclic silyl enol ethers*

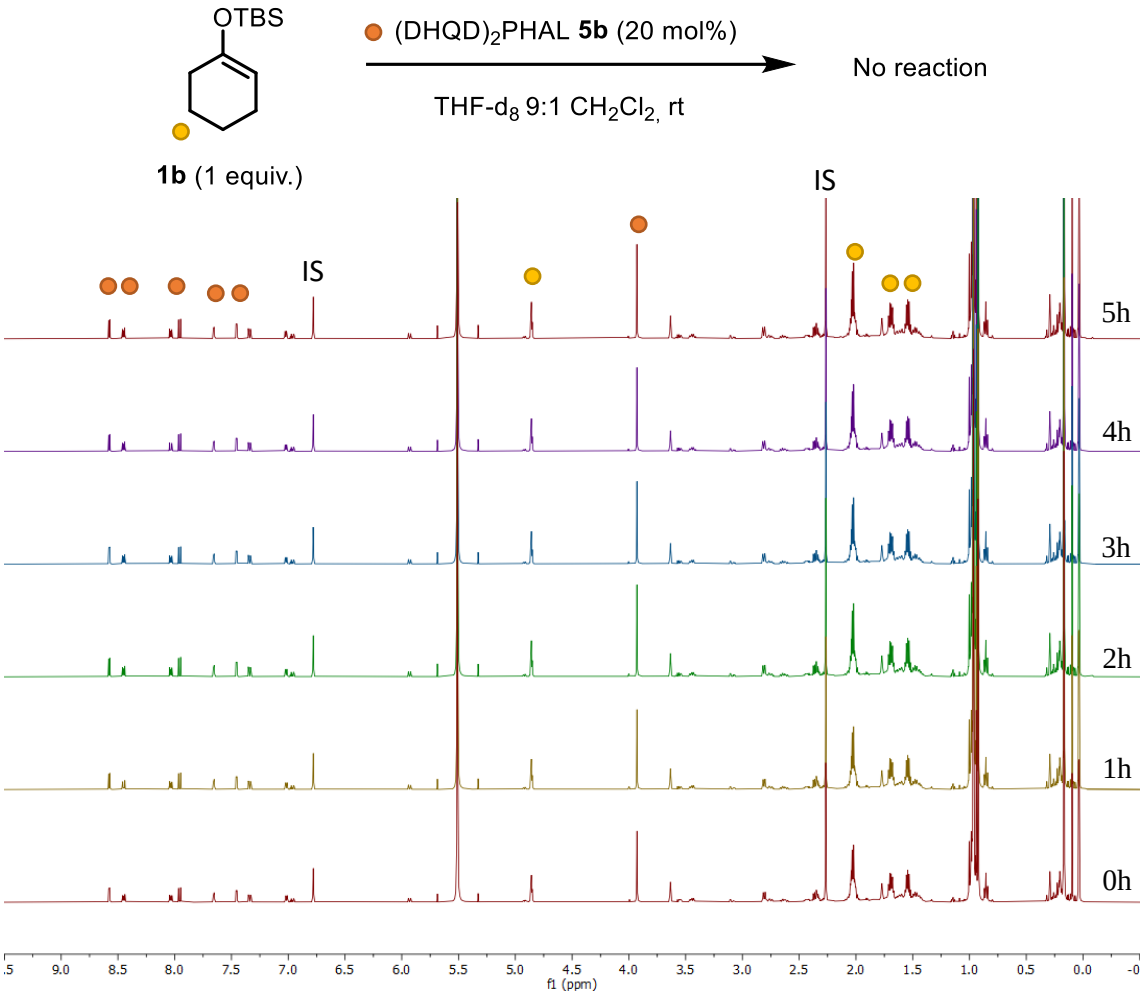

Figure S38. ^{1}H NMR spectra overtime at 500 MHz in THF_d_8:CH_2Cl_2 (9:1).

*This experiment highlights that **silyl enol ether does not react with the chiral Lewis base catalyst (DHQD)$_2$PHAL 5b.***

H. Determination of the Si-F interaction

H.1. Determination of Si-F interaction – Electrochemical studies

We used electroanalytical tools to evidence the interaction between the allyl fluoride ***2b*** *and the silyl enol ether* ***1b****.*[14] *The cyclic voltammetry experiments were carried out using a 5 mM solution of* ***1b*** *in MeCN and 0.1M of supporting electrolyte.*

Firstly, we used THF as solvent to reproduce the reaction conditions, but the oxidation potential of ***1b*** *lays outside the redox window of the solvent. In CH_2Cl_2, $LiClO_4$ is not soluble. Therefore, we used MeCN as solvent because both $TBAClO_4$ and $LiClO_4$ are completely soluble and the oxidation of* ***1b*** *falls within its redox window. Other electrolytes with BF_4^- and PF_6^- as counterions were ruled out to prevent the presence of fluorine in the solution.*

Titration using $TBAClO_4$ as supporting electrolyte

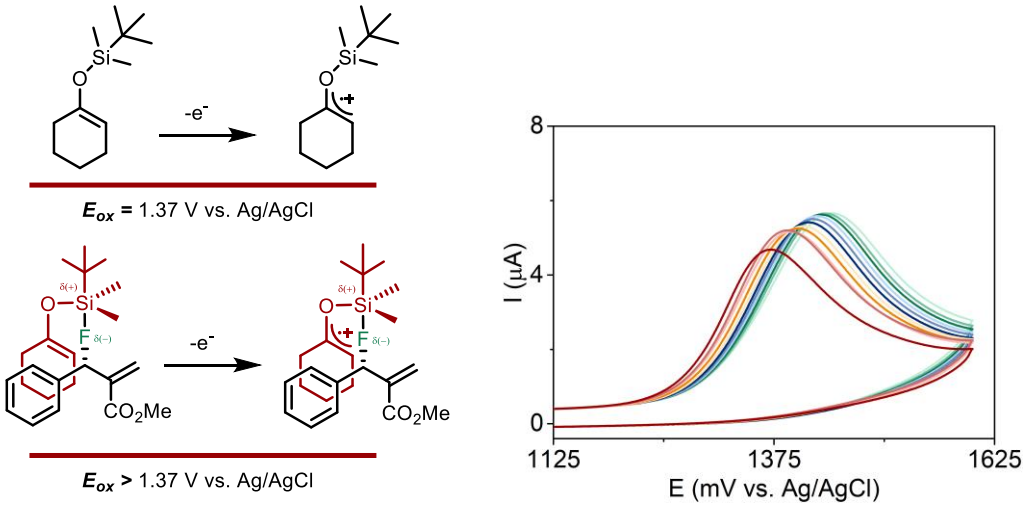

Figure S39. Anodic CV of silyl enol ether **1b** (5mM) in 0.1M $TBAClO_4$ MeCN solution with increasing equivalents of **2b**. (red line – 0 equiv.; pale green line – 5.0 equiv.) GC electrode. Scan rate 100 mV/s, potential refers to Ag/AgCl at room temperature using a platinum wire as a counter electrode.

[In this experiment, ***the cathodic shift*** *of the oxidation potential of* ***1b*** *in the presence of aliquots of* ***2b highlights the presence of an interaction*** *between allyl fluorides and fluorophilic species. This observation is consistent with the formation of the pentacoordinated complex whose central silicon atom becomes inherently electron-deficient due to hypervalent bonding. Therefore, the electron-deficient silicon atom reduces the electron density on the enol ether moiety making it more difficult to oxidize.]*

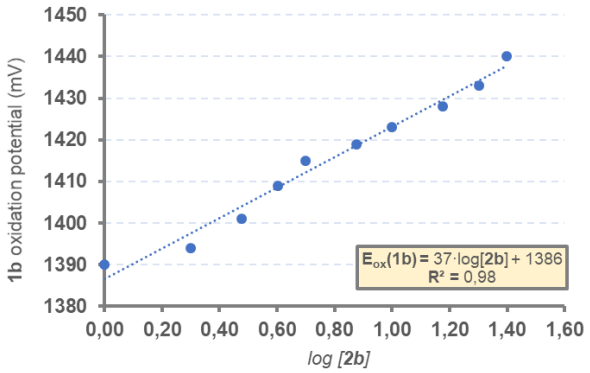

Figure S40. Plot of the shift in the potential of **1b** measured by CV against log of the concentration of **2b**.

We tried to deduce the stoichiometry of the complex by using the Nernst binding stoichiometry of the CV reported in Figure S39. As observable in Figure S40, the slope is 37 mV/dec, far from the ideal 59 mV/dec at 298K observed for a 1 to 1 complex stoichiometry.

Titration using $LiClO_4$ as supporting electrolyte

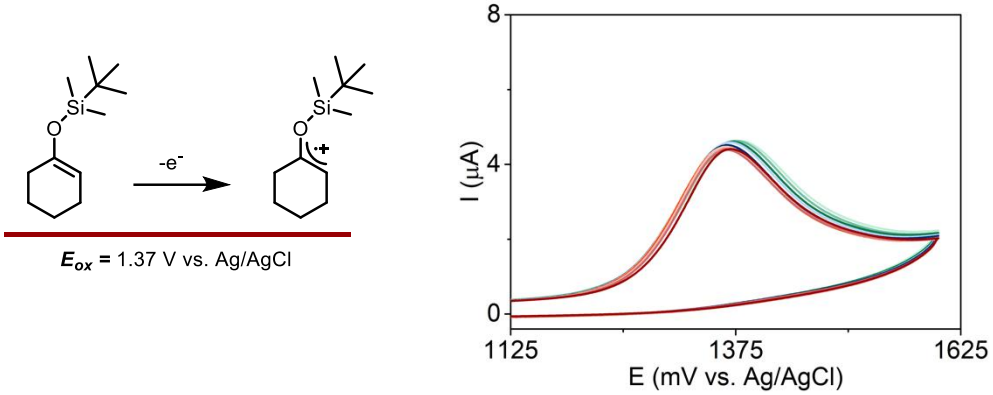

Figure S41. Anodic CV of silyl enol ether **1b** (5mM) in 0.1M $LiClO_4$ MeCN solution with increasing equivalents of **2b**. (red line – 0 equiv.; pale green line – 5.0 equiv.) GC electrode. Scan rate 100 mV/s, potential refers to Ag/AgCl at room temperature using a platinum wire as a counter electrode.

*[In this experiment, **the absence of cathodic shift** of the oxidation potential of **1b** in the presence of aliquots of **2b highlights the absence of an interaction** between allyl fluorides and fluorophilic species due to **the presence of $LiClO_4$ as fluorophilic trap.**]*

H.2. Determination of Si-F interaction – ^{19}F NMR Titration

*Another method to evidence the interaction between the allyl fluoride **2b** and the silyl enol ether **1b** is the utilization of ^{19}F NMR due to the high sensitivity of this nucleus.[15]*

General Procedure for the ^{19}F NMR titration

In an NMR tube, 0.1 mmol of **2b** were dissolved in 0.5mL of deuterated solvent. Then, the $^{19}F\{^{1}H\}$ NMR spectrum of the previously mentioned solution was measured. Increasing equivalents of **1b** were added to the NMR tube.

The spectra were referenced through an external shift referencing the residual peak of the corresponding deuterated solvent in the ^{1}H NMR spectra by using the xiref command.

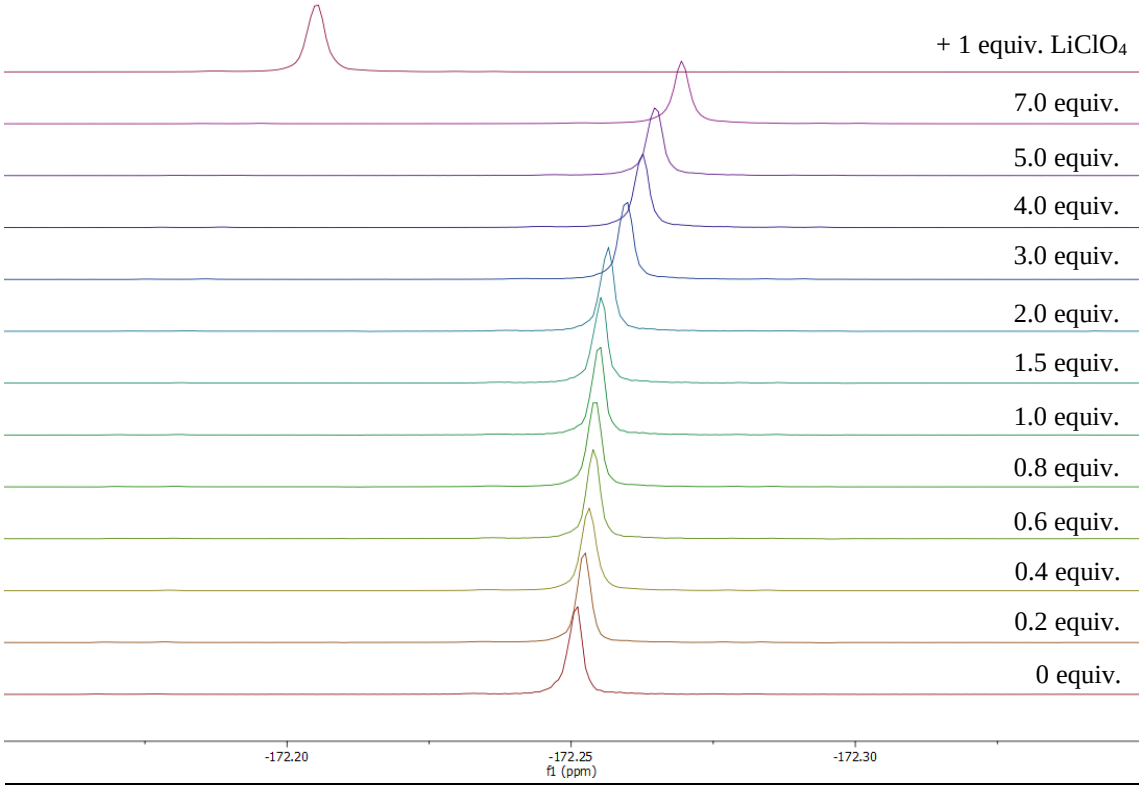

Figure S42. $^{19}F\{^{1}H\}$ NMR spectra at 470 MHz NMR field in THF_d_8 of **2b** (bottom) with increasing equivalents of **1b** (from 0.2 to 7 equiv.)

*[In this experiment, **the shift of the $^{19}F\{^{1}H\}$ signal of 2b** in the presence of increasing amounts of **1b highlights the presence of an interaction** between an allyl fluoride and fluorophilic species. When the solution is quenched with $LiClO_4$, the peak shifts towards higher chemical shifts.]*

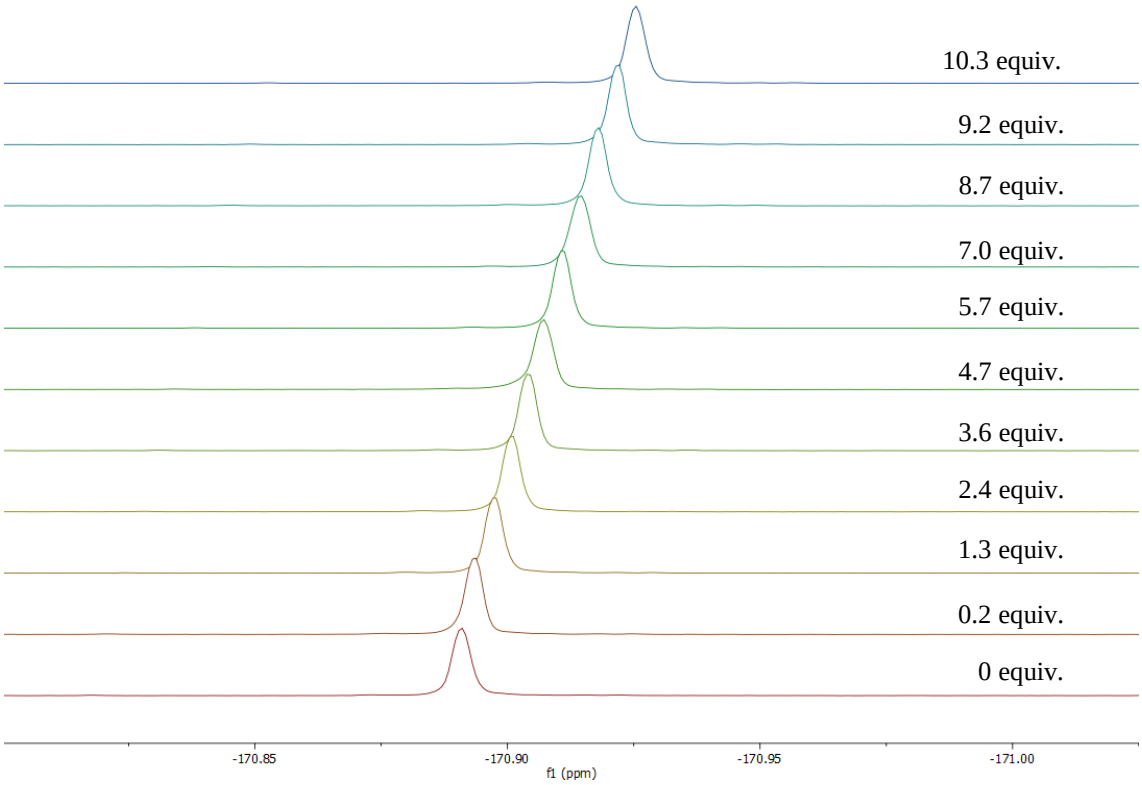

Figure S43. $^{19}F\{^{1}H\}$ NMR spectra at 470 MHz NMR field in CD_2Cl_2 of **2b** (bottom) with increasing equivalents of **1b** (from 0.2 to 10.3 equiv.)

[In this experiment, ***the shift of the $^{19}F\{^{1}H\}$ signal of 2b*** *in the presence of increasing amounts of* ***1b highlights the presence of an interaction*** *between allyl fluorides and fluorophilic species. The experiment in the presence of Li^+ salts could not be performed due to its insolubility in CD_2Cl_2.]*

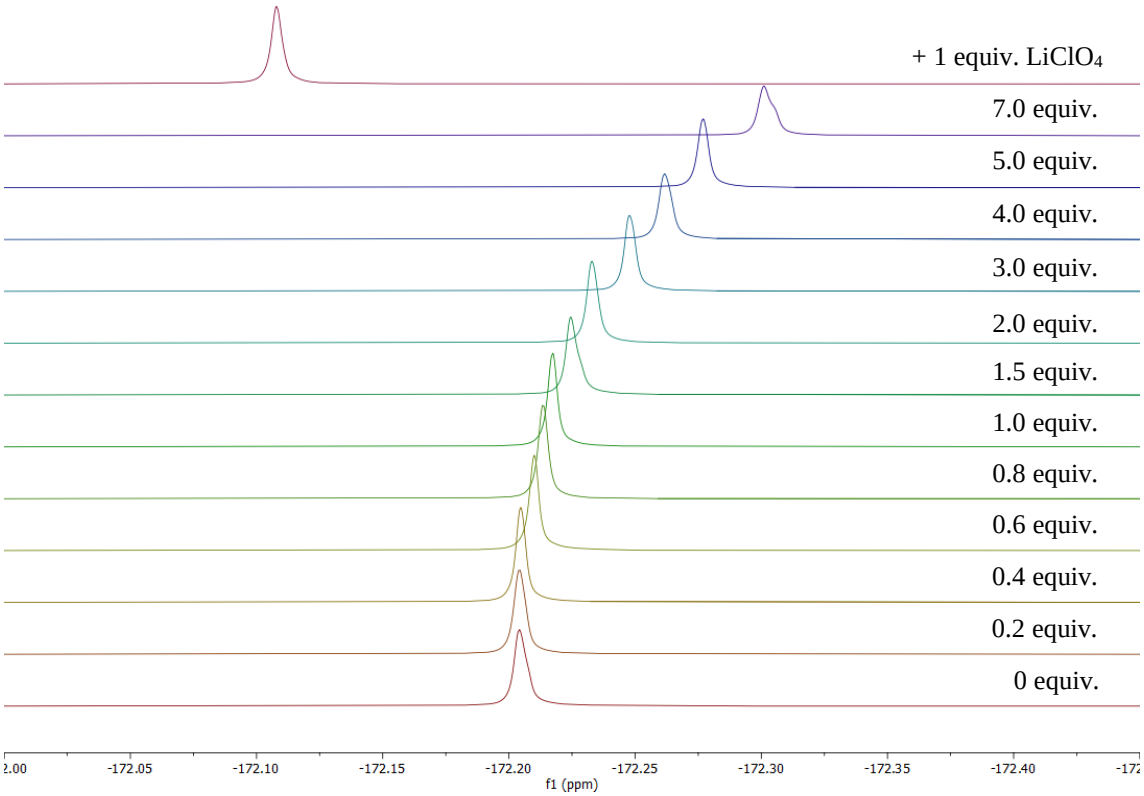

Figure S44. $^{19}F\{^{1}H\}$ NMR spectra at 470 MHz NMR field in THF_d_8/CD_2Cl_2 (9:1) of **2b** (bottom) with increasing equivalents of **1b** (from 0.2 to 7 equiv.).

*[In this experiment, **the shift of the $^{19}F\{^{1}H\}$ signal of 2b** in the presence of increasing amounts of **1b highlights the presence of an interaction** between an allyl fluoride and fluorophilic species under reaction conditions (THF_d_8/CD_2Cl_2 = 9:1). When the solution is quenched with $LiClO_4$, the peak shifts towards higher chemical shifts.]*

Although both Li^+ and the Si atom in SEE **1b** are both acting as Lewis acids in their interaction with the fluorine atom of **2b**, they are very different in nature and affect the ^{19}F resonance in different ways:

- In the case of the Li cation, there is a net charge transfer from F to Li, that explains the downfield shift (from -172.21 ppm to -172.11 ppm) upon addition of $LiClO_4$ (Figure S44) to a THF_d_8/CD_2Cl_2=9:1 solution of **2b**.

- On the other hand, the interaction with **1b** leads to the formation of a pentacoordinated TBP intermediate **B**. The upfield shift experienced by the ^{19}F nucleus upon addition of increasing amounts of **1b** is what should be expected from its apical position: in hypervalent TBP complexes, the two apical ligands give rise to hypervalent three-center four-electron bonds that increases the positive charge on the silicon and the negative charge in the apical ligands with respect to the separated fragments.

Attempt to determine Ka

We tried to deduce the stoichiometry of the complex using the ^{19}F NMR titrations. All the attempts to find the K_a of such complex failed. ^{19}F NMR titrations at low concentrations of **2b** (**[i]**=0.01M) showed a linear shift even after the addition of 300 equivalents of **1b** (from 0.01 M to 3M). Thus, we conclude that the association constant is <<1 and complex saturation was never reached**.**

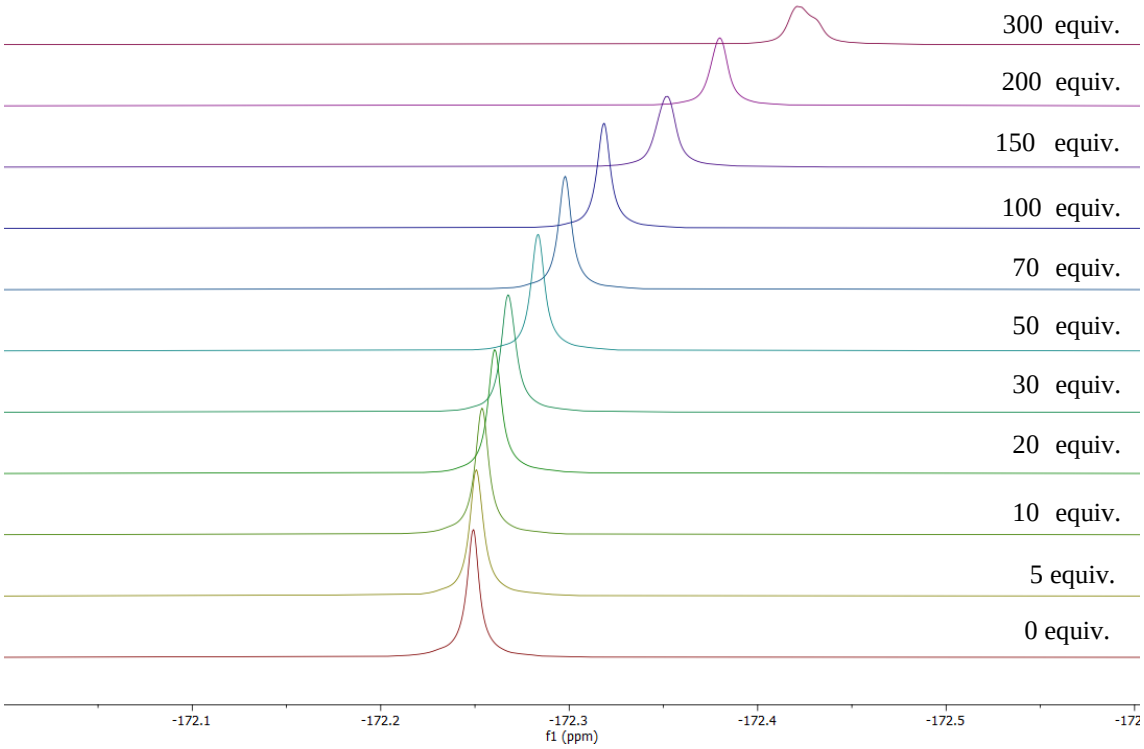

Figure S45. $^{19}F\{^{1}H\}$ NMR spectra at 470 MHz NMR field in THF_d_8/CD_2Cl_2 (9:1) of **2b** (bottom) with increasing equivalents of **1b** (from 0.2 to 7 equiv.).

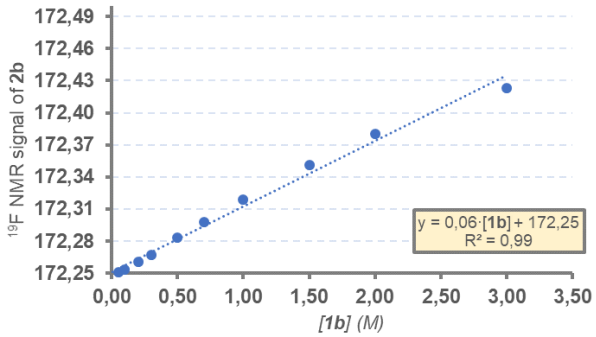

Figure S46. Plot of the shift of the ^{19}F resonance of **2b** against the concentration of **1b**.

^{19}F NMR of an alternative allyl fluoride

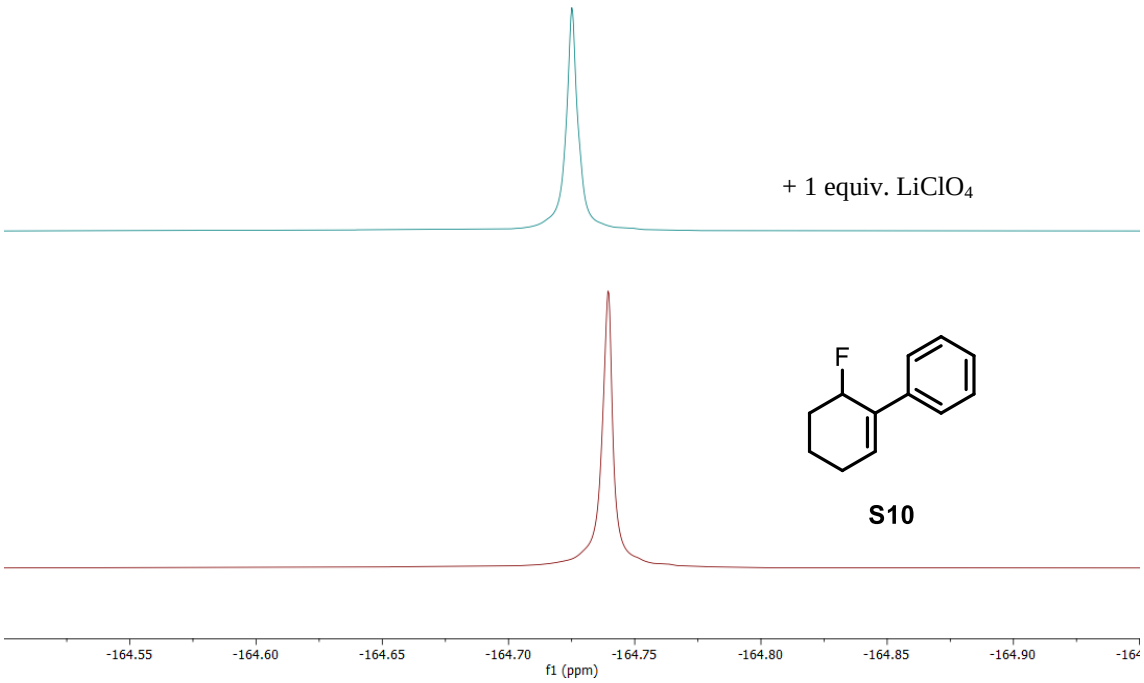

Figure S47. $^{19}F\{^{1}H\}$ NMR spectra at 470 MHz NMR field in THF_d_8/CD_2Cl_2 (9:1) of **S10** (bottom) with 1 equivalent of $LiClO_4$.

*[We have treated a solution of 2-phenyl-3-fluorociclohexene **S10**, an allyl fluoride without ester groups, in THF_d_8/CD_2Cl_2 = 9:1 with $LiClO_4$ and we have also observed a downfield shift of the ^{19}F resonance. The magnitude of the shift is however smaller (from -164,74 ppm to -164,72 ppm) than that observed for **2b** (from -172.21 ppm to -172.11 ppm), a fact that can be attributed to the stabilization of the corresponding Lewis acid/base complex between **2b** and Li^+ by a chelate effect with the ester moiety of **2b**.]*

H3. Detailed discussion of the proposed structure for hypervalent intermediate B

Our experimental observations of an anodic shift in the oxidation potential of SEE **1b** upon sequential addition of allylic fluoride **2b** (Figure S39), together with a shift in the fluorine resonance in **2b** towards higher fields with increasing amounts of **1b**, can be accommodated within a trigonal bipyramid (TBP) geometry for **B**. In such spatial configuration, the weak sigma-donor fluorine atom (the most electronegative atom of the substituents) occupies an apical position by hypervalent bonding. The oxygen atom of the SEE moiety occupies an equatorial position that facilitates back π-bonding between the enol ether moiety and the electron-depleted silicon atom.[16]

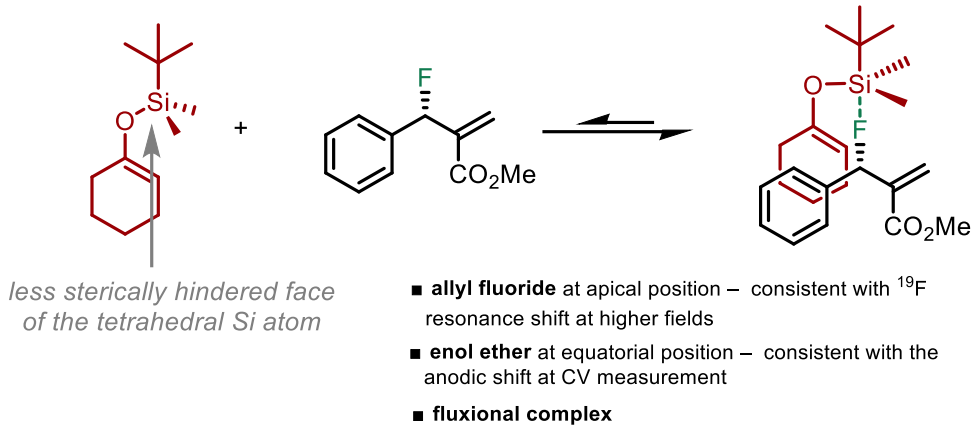

Such configuration can be rationalized considering the role of the substituents attached to the Si atom. While for steric reasons in a TBP complex the bulky *tert*-butyl group would prefer an equatorial position and the methyl group would preferentially occupy an apical one, most probably the approach of the allyl fluoride to the tetrahedral Si atom in **1b** takes place through the less hindered face of the tetrahedron (*i.e.* the one that is opposite to the *tert*-butyl group). In this scenario, the *tert*-butyl group and **2b** would initially occupy the apical positions and the enol ether moiety an equatorial position in a TBP geometry. In any case, complex **B** is certainly fluxional and in fast interchange between equatorial and apical positions. This structural flexibility will take easily place either through Berry pseudorotation or turnstyle mechanisms.[16a] While it is true that with this geometry the SEE moiety becomes less nucleophilic, this does not preclude the activation of the S_Ni pathway by the nucleophilic catalyst. A complex in which both O and F atoms occupy apical positions would not be productive since the reactive centers would not be in enough proximity to favor reactivity.

I. Kinetic profiles

I.1. Kinetic profiles – Synthesis of the enantiopure (*R*)-2b

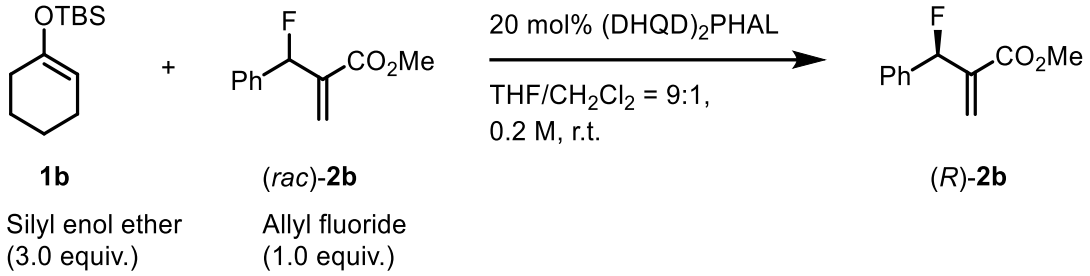

Allyl fluoride **2b** (1 equiv., 0.2 mmol) was weighted into a 5 mL vial equipped with a magnetic stirring bar and dissolved with 1 mL of a 9:1 = THF/CH_2Cl_2 mixture (0.2 M). Subsequently, the silyl enol ether **1b** (3 equiv., 0.6 mmol) and a 20 mol% of $(DHQD)_2PHAL$ were added. The reaction mixture was stirred at room temperature until the 50% conversion of the allyl fluoride. The reaction crude was directly purified by flash column chromatography using hexane and ethyl acetate mixtures. The e.r. (98:2) was determined by chiral GC and the absolute (*R*)-configuration was determined by chemical correlation $[\alpha]_D^{25}$ = -52.3 (c = 1.32, $CHCl_3$).[4]

GC Chromatogram of (*R*)-2a

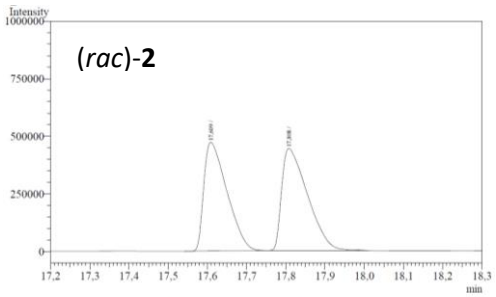

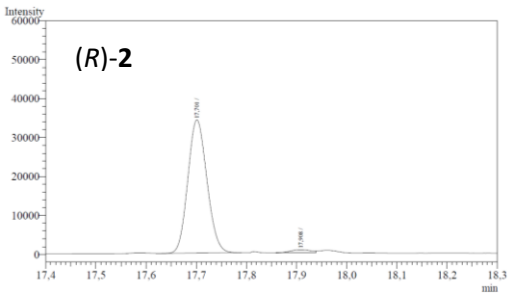

I.2. Kinetic profiles – Synthesis of the enantiopure (*S*)-2b

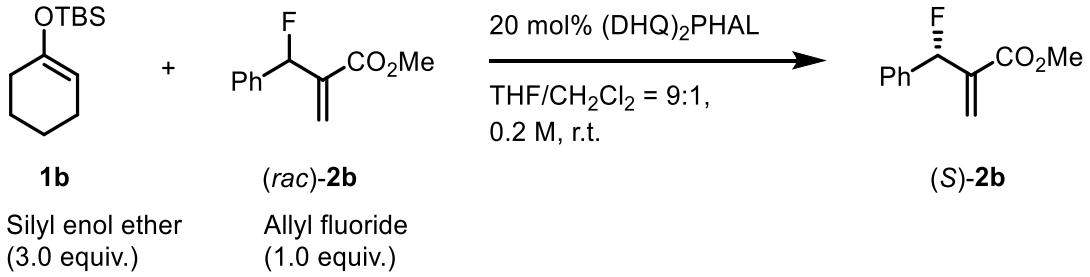

1b (*rac*)-**2b** (*S*)-**2b**

Silyl enol ether (3.0 equiv.) Allyl fluoride (1.0 equiv.)

Allyl fluoride **2b** (1 equiv., 0.2 mmol) was weighted into a 5 mL vial equipped with a magnetic stirring bar and dissolved with 1 mL of a 9:1 = THF/CH_2Cl_2 mixture (0.2 M). Subsequently, the silyl enol ether **1b** (3 equiv., 0.6 mmol) and a 20 mol% of $(DHQ)_2PHAL$ were added. The reaction mixture was stirred at room temperature until the 50% conversion of the allyl fluoride. The reaction crude was directly purified by flash column chromatography using hexane and ethyl acetate mixtures. The e.r. (88:12) was determined by chiral GC.

GC Chromatogram of (*S*)-2a

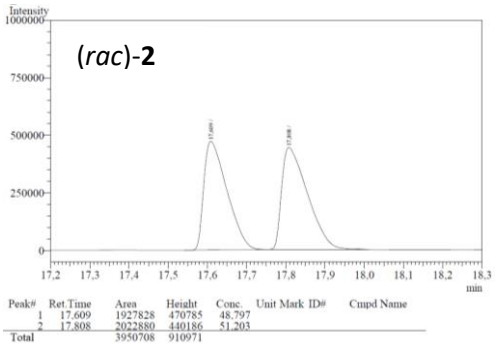

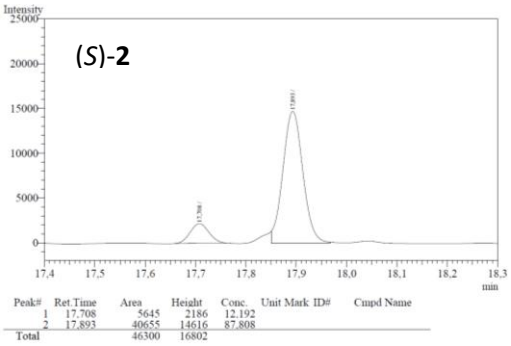

I.3. Kinetic profiles

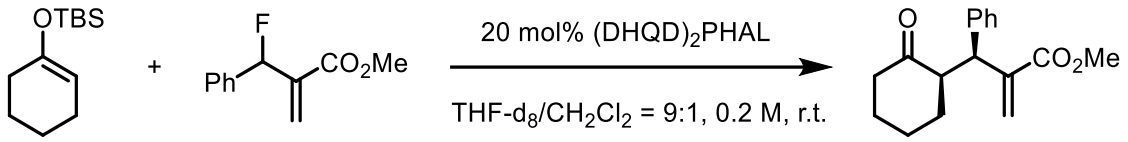

1b (*rac*)-**2b** **3a**

Silyl enol ether (3.0 equiv.) Allyl fluoride (1.0 equiv.)

Allyl fluoride **2b** (1 equiv., 0.4 mmol) was weighted into a 5 mL vial equipped with a magnetic stirring bar and dissolved with 2 mL of a 9:1 = THF-d_8/CH_2Cl_2 mixture (0.2 M). Subsequently, silyl enol ether **1b** (3 equiv., 1.2 mmol) and a 20 mol% of $(DHQD)_2PHAL$ were added. Immediately, 0.5 mL of the reaction mixture was transferred to an NMR tube and the other 1.5 mL of solution were stirred in the same vial at room temperature. Conversion of **2b** was analyzed by *in situ* ^{1}H and ^{19}F NMR, and the enantiomeric excess of **2b** and **3a** were analyzed by chiral GC and HPLC, respectively.

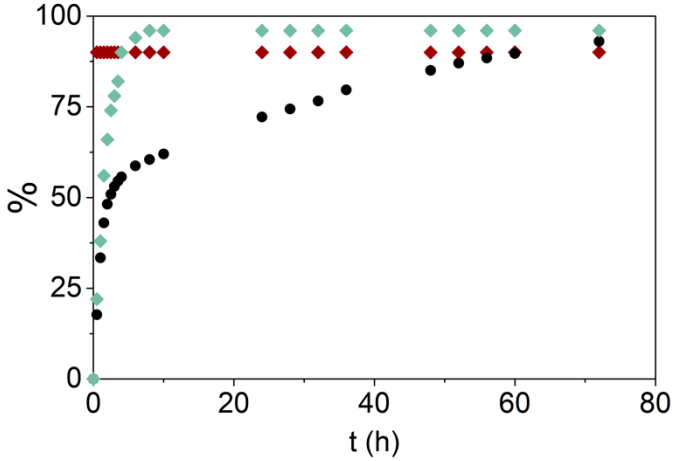

Figure S48. Reaction conversion (black dots) and enantiomeric excess of **2b** (green diamonds) and **3a** (red diamonds).

*[This experiment demonstrates that the reaction proceeds through a dynamic kinetic resolution of the racemic allyl fluoride **2b**. The reaction exhibits an initial fast regime where only the (S)-**2b** is consumed. Around 50% of conversion, the remaining allyl fluoride **2b** is essentially in its (R) form and the reaction kinetics shifts to a second, slower regime controlled by the racemization of the remaining (R)-**2b**. The enantiomeric excess of the product does not change during the reaction.]*

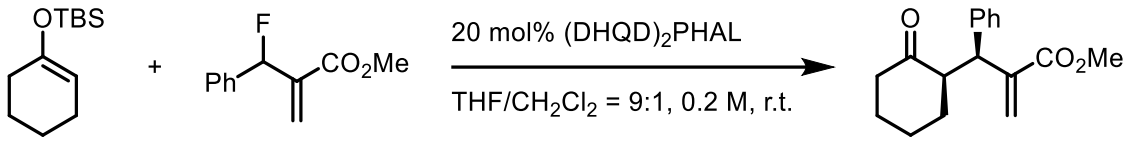

1b (*rac/R/S*)-**2b** **3a**

Silyl enol ether (3.0 equiv.) Allyl fluoride (1.0 equiv.)

The corresponding allyl fluoride **2b** (1 equiv., 0.05 mmol) was weighted into a 5 mL vial equipped with a magnetic stirring bar and dissolved with 0.25 mL of a 9:1 = THF/CH_2Cl_2 mixture (0.2 M). Subsequently, the corresponding silyl enol ether **1b** (3 equiv., 0.15 mmol) and a 20 mol% of $(DHQD)_2PHAL$ were added. The reaction mixture was stirred at room temperature. Conversion and ee of the 3 reactions were analyzed by conventional and chiral GC chromatography respectively.

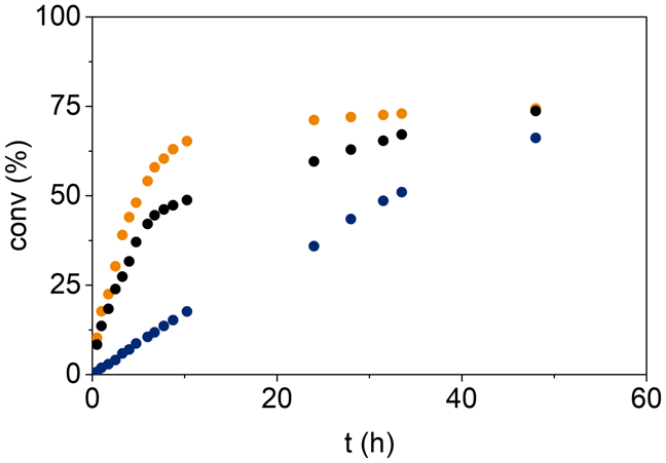

Figure S49. Kinetic profiles (conv. vs time) analyzed by GC of three different reactions using (*rac*)-**2b** (black dots), (*R*)-**2b** (blue dots) and (*S*)-**2b** (yellow dots) as starting allyl fluoride.

*[This experiment shows the different reaction regimes using an allyl fluoride with different enantiomeric compositions. The reaction conversion starting from highly-enantioenriched (R)-**2b** (R/S=98:2) proceeds through a single, slow regime controlled by substrate racemization (blue). The kinetic profile employing a scalemic mixture of the (S)-**2b** (R/S=12:88) features a faster initial regime up to 70% conversion (yellow). The reaction conversion starting from (rac)-**2b** starts with an initial fast regime changing at 50% conversion to a slow regime controlled by substrate racemization (black).]*

I.4. Racemization of the allyl fluoride

The two experiments shown below were performed to study the racemization of the allyl fluoride.

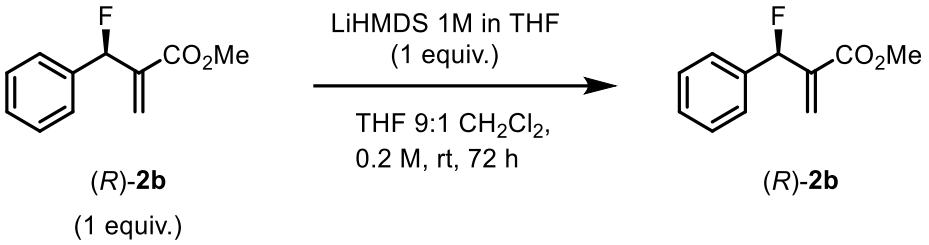

(*R*)-**2b**
(1 equiv.)

(*R*)-**2b**

[Using a strong non-nucleophilic base, such as LiHMDS, no racemization of the allyl fluoride was observed by chiral GC.]

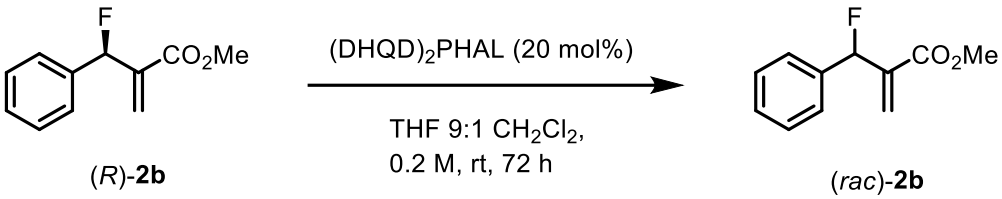

(*R*)-**2b**

(*rac*)-**2b**

*[A highly-enantioenriched sample of the allyl fluoride (R)-**2b** (R/S)=98:2 was racemized in 72 h under the effect of catalytic amounts (20 mol%) of (DHQD)$_2$PHAL (**5b**), as determined by chiral GC.[17]]*

I.5. Identification of the catalyst resting state

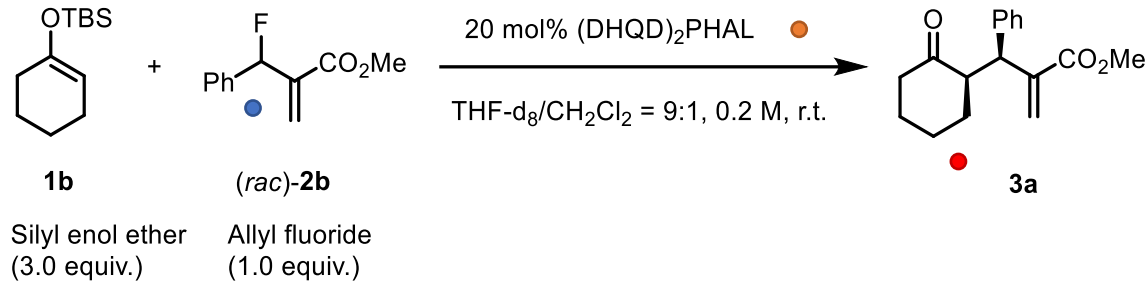

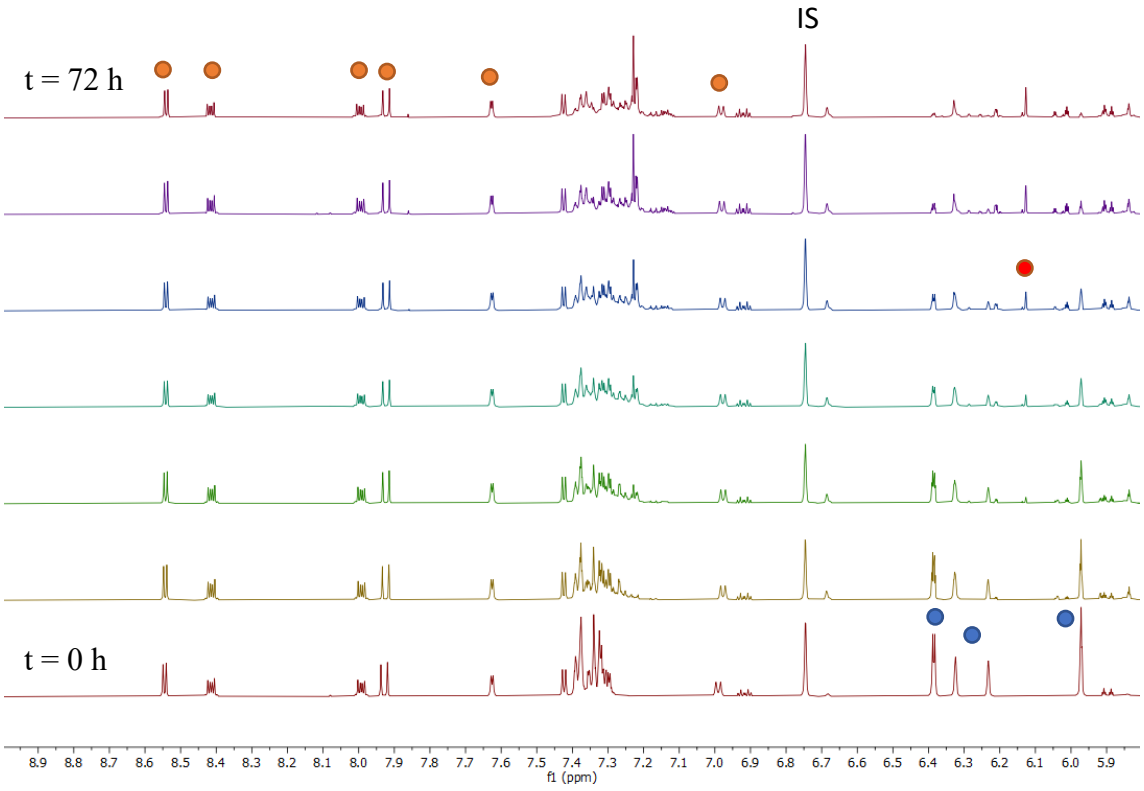

Figure S50. Stacked ^{1}H NMR spectra at 500 MHz NMR field, acquired at regular intervals of time, of the catalytic reaction *in situ* monitored into the NMR tube over 72h.

*[The sole detectable catalytic species during the whole reaction course is the free catalyst (DHQD)$_2$PHAL (**5b**)]*

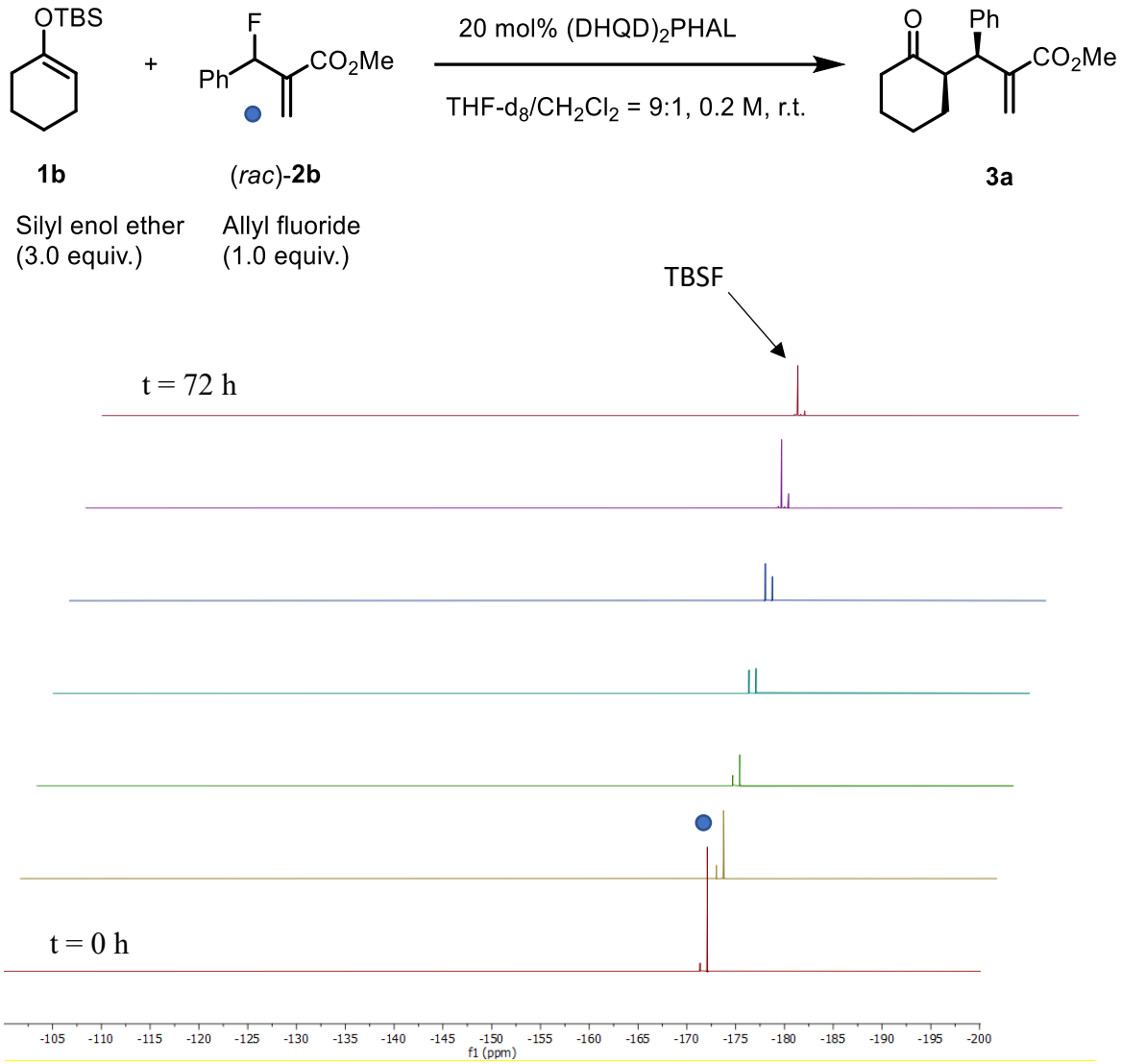

Figure S51. Stacked $^{19}F\{^{1}H\}$ NMR spectra at 470 MHz NMR field, acquired at regular intervals of time, of the catalytic reaction *in situ* monitored into the NMR tube over 72h.

[During the reaction course, fluoride anion is not detected]

J. Mechanistic consideration

The kinetic data acquired during the development of this project (Figure 4A of the manuscript and section I of the SI) could in principle fit with two different mechanistic scenarios shown in the figure below (S52).

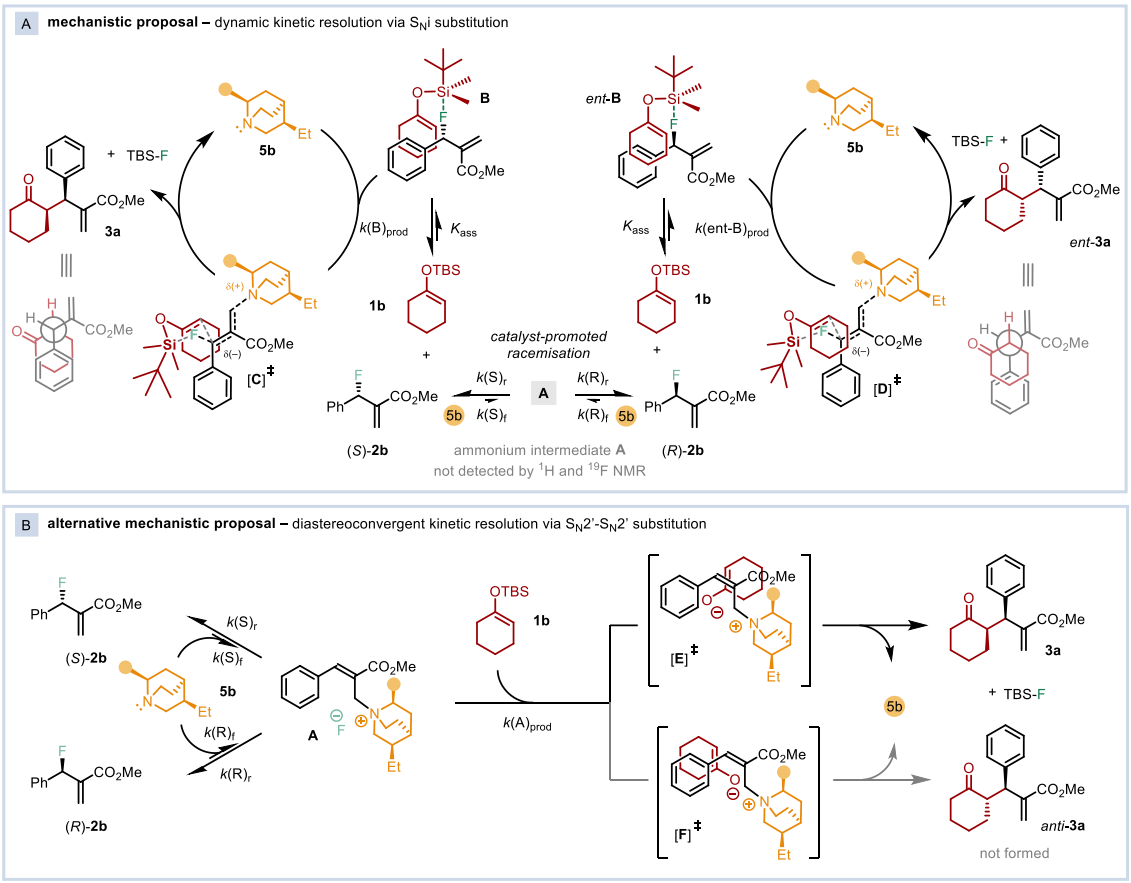

Figure S52. Schemes of the two plausible mechanistic scenarios.

On the one hand, the proposed dynamic kinetic resolution via S_Ni substitution (figure S52, A), and on the other hand a diastereoconvergent kinetic resolution via two consecutive S_N2'-S_N2' substitutions (figure S52, B). Both mechanisms involve the reversible, endoergic formation of the chiral quaternary ammonium intermediate **A**. In the first one, **A** is involved in the catalyst-promoted racemization of **2b**; in the second one **A** is the immediate precursor of the allylation product **3a**.

<u>*Scenario A*</u> – according to the Si–F interaction between substrates **1b** and **2b**, the reaction should proceed via intermediate B where $k(B)_{prod}$ would determine the first reaction regime while $k(R)_f$ would control the second, slower reaction regime. This is $k(B)_{prod} > k(R)_f >> k(ent\text{-}B)_{prod}$.

<u>*Scenario B*</u> – the fast initial regime would be governed by $k(S)_f$ and the slower regime by $k(R)_f$. The fact that intermediate **A** has not been detected nor by mixing **2b** with **5b** neither upon *in-situ* monitoring the reaction by ^1H and ^{19}F NMR, means that in any case $k(A)_{prod} >> k(S)_f > k(R)_f$ with $k(R)_r >> k(R)_f$ and $k(S)_r >> k(S)_f$.

Although we cannot rule out any of the two possible scenarios, based on a series of experimental evidence detailed below, including the reaction stereochemical outcome and diverse control experiments, along with key the literature precedents, such as the pioneering methodologies using allyl fluorides in a Lewis-base catalysed asymmetric allylic alkylation reported by Shibata,[18] we believe that the most likely mechanistic scenario is the one depicted in scheme S52A.

We think that the following experimental observations support our mechanistic proposal:

- *Observation* – The reaction between rac-**2b** and **1b** catalysed by **5b** is highly diastereoselective, affording exclusively the *syn*-allylated ketone **3a.**

  Hypothesis – This fact might indicate that the reaction proceeds via a highly-ordered transition state, such as the chair-like six-membered transition state **C** proposed in scenario A. Conversely, the nucleophilic attack of the enolate upon intermediate **A** (scenario B) is more likely to proceed with poor control over the two prochiral faces of the nucleophile (e.g. transition states E and F), which would lead to the formation of products **3a** in poor diastereocontrol.

- *Observation* – The reaction between rac-**2b** and **1b** catalysed by DABCO is also highly diastereoselective, affording the racemic product **3a** as a single diastereoisomer (>20:1). By in-situ NMR, we observed that upon mixing **2b** with 20 mol% of DABCO the corresponding achiral ammonium intermediate **A** (not shown in scheme S52) is formed as a 75:25 *E*/*Z* mixture and the equilibria is completely shifted towards **A** in 4h (section F4 of SI).

  Hypothesis – It is reasonable to think that intermediate **A** derived from DABCO will be less sterically hindered than the corresponding species **A** derived from **5b**. In this scenario, a highly diastereoselective attack of the nucleophilic enolate to electrophilic species **A** (which moreover is a diastereomeric mixture of *E*/*Z* isomers) via an open transition state is unlikely.

- *Observation* – In section F2 we demonstrate that when allyl carbonate **2a** is used instead of allyl fluoride **2b**, the formation of the corresponding ammonium species **A** with 20 mol% of DABCO is much faster (1h vs. 4h). In addition, in this case, the formation of **A** is irreversible due to decomposition of the leaving group (forming *tert*-butoxide anion and carbon dioxide). On the other hand, we performed the control experiment using allyl carbonate **2a** (1 equiv.) with SEE **1b** (3 equiv.) catalysed by 20 mol% of DABCO together with 1 equiv. of TBAF (figure S22), and no traces of product **3a** were observed after 18h.

  Conclusion – This fact points out that the presence of intermediate **A** together with the nucleophilic SEE do not guarantee suitable reactivity, highlighting therefore that the Si–F interaction plays a pivotal role in the observed reactivity.

K. Derivatizations

K.1. Hydrogenation – Reduction of the terminal alkene

Hydrogenation on Pd/C

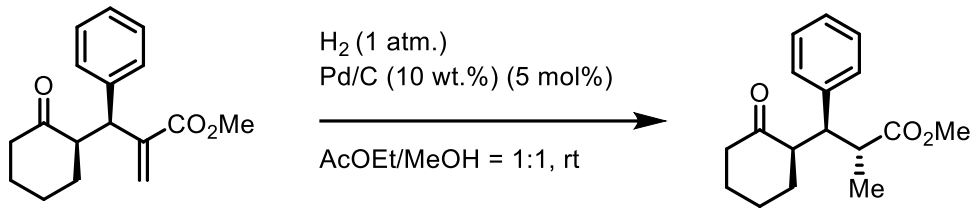

3a (1 equiv.) **6a**

The reaction was carried out following the previously described procedure[2]

To a solution of compound **3a** (0.2 mmol) in 2 mL of a AcOEt/MeOH = 1:1 mixture (0.1 M) was added 10 wt.% Pd/C (0.05 equiv.). The hydrogenation was carried out under a hydrogen atmosphere at room temperature and atmospheric pressure until full conversion of the starting material was detected by TLC analysis. Then, the reaction mixture was filtered through Celite and the filtrate was concentrated under vacuum. Purification of the residue by flash column chromatography using hexane and ethyl acetate mixtures afforded the desired reduced product **6a** (>98% yield, d.r. =2:1) as a colourless oil.

.

methyl (2R,3R)-2-methyl-3-((R)-2-oxocyclohexyl)-3-phenylpropanoate (6a)

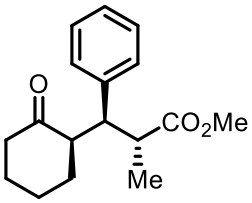

^{1}H NMR (400 MHz, $CDCl_3$) δ 7.19-7.16 (3H, m), 7.08-7.04 (2H, m), 3.54 (3H, s), 3.24-3.10 (3H, m), 3.51-3.38 (2H, m), 2.11-2.00 (1H, m), 1.79-1.68 (2H, m), 1.68-1.61 (1H, m), 1.60-1.51 (1H, m), 1.17-1.07 (1H, m), 1.05 (3H, d, J = 6.80 Hz); **^{13}C NMR** (100 MHz, $CDCl_3$) δ 213.7, 175.5, 139.5, 129.4, 128.2, 126.9, 52.7, 51.4, 48.6, 43.1, 41.8, 33.7, 29.2, 25.5, 15.9. **HRMS (ESI)** Calculated for $C_{17}H_{23}O_3^+$ ($[M+H]^+$) 275.1642. Found 275.1642. **$[\alpha]_D^{25}$** = +42.6 (c = 0.88, $CHCl_3$).

Ir-mediated hydrogenation

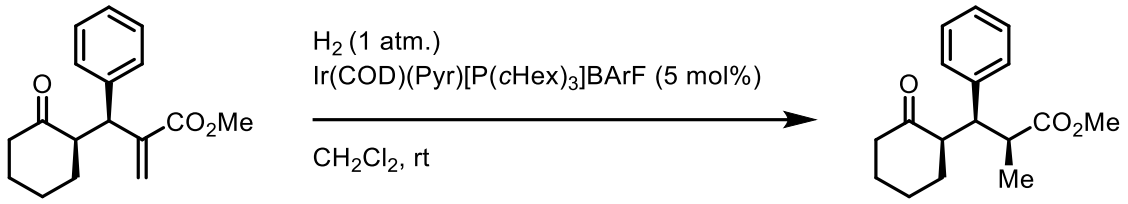

3a (1 equiv.) **6b**

To a solution of compound **3a** (54.6 mg, 1 equiv., 0.2 mmol) in 2 mL of CH_2Cl_2 (0.1 M) was added Ir(COD)(Pyr)[P(*c*Hex)$_3$]BArF (16.5 mg, 0.05 equiv., 0.01 mmol). The hydrogenation was carried out under hydrogen atmosphere at room temperature and atmospheric pressure until full conversion of the starting material was detected by TLC analysis. Then, the reaction mixture was filtered through Celite and the filtrate was concentrated under vacuum. Purification of the residue by flash column chromatography using hexane and ethyl acetate mixtures afforded the desired reduced product **6b** (92% yield, d.r. =10:1) as a yellow oil.

methyl (2S,3R)-2-methyl-3-((R)-2-oxocyclohexyl)-3-phenylpropanoate (6b)

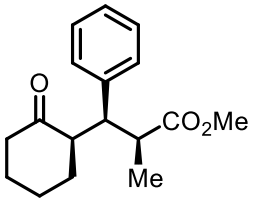

^{1}H NMR (400 MHz, $CDCl_3$) δ 7.32-7.10 (5H, m), 3.62 (3H, s), 2.95-2.83 (1H, m), 2.76 (1H, td, *J* = 9.36, 4.77 Hz), 2.52-2.43 (1H, m), 2.38-2.28 (1H, m), 1.97-1.85 (1H, m), 1.79-1.66 (3H, m), 1.58-1.46 (1H, m), 1.29-1.16 (2H, m), 0.94 (3H, d, *J* = 6.98 Hz); **^{13}C NMR** (100 MHz, $CDCl_3$) δ 212.9, 176.1, 139.3, 129.5, 128.4, 126.9, 53.7, 51.7, 46.9, 43.1, 41.9, 31.9, 28.3, 24.1, 14.5. **HRMS (ESI)** Calculated for $C_{17}H_{23}O_3^+$ ($[M+H]^+$) 275.1642. Found 275.1642. $\mathbf{[\alpha]_D^{25}}$ = +55.2 (c = 1.35, $CHCl_3$).

Determination of the relative configuration of diastereomers 6a and 6b by NMR spectroscopy

In the ^{1}H NMR spectra of compound **6a** performed in $CDCl_3$, the signals of protons 2, 3 and 4 overlap in an a complex multiplet, making it impossible to assign them by COSY and to study their relative configuration by NOESY. Gratifyingly, when the ^{1}H NMR spectra of compound **6a** was recorded in toluene_d_8, the resonances of protons 2, 3 and 4 appear well resolved, thus allowing to determine their relative configuration by 2D-NMR.

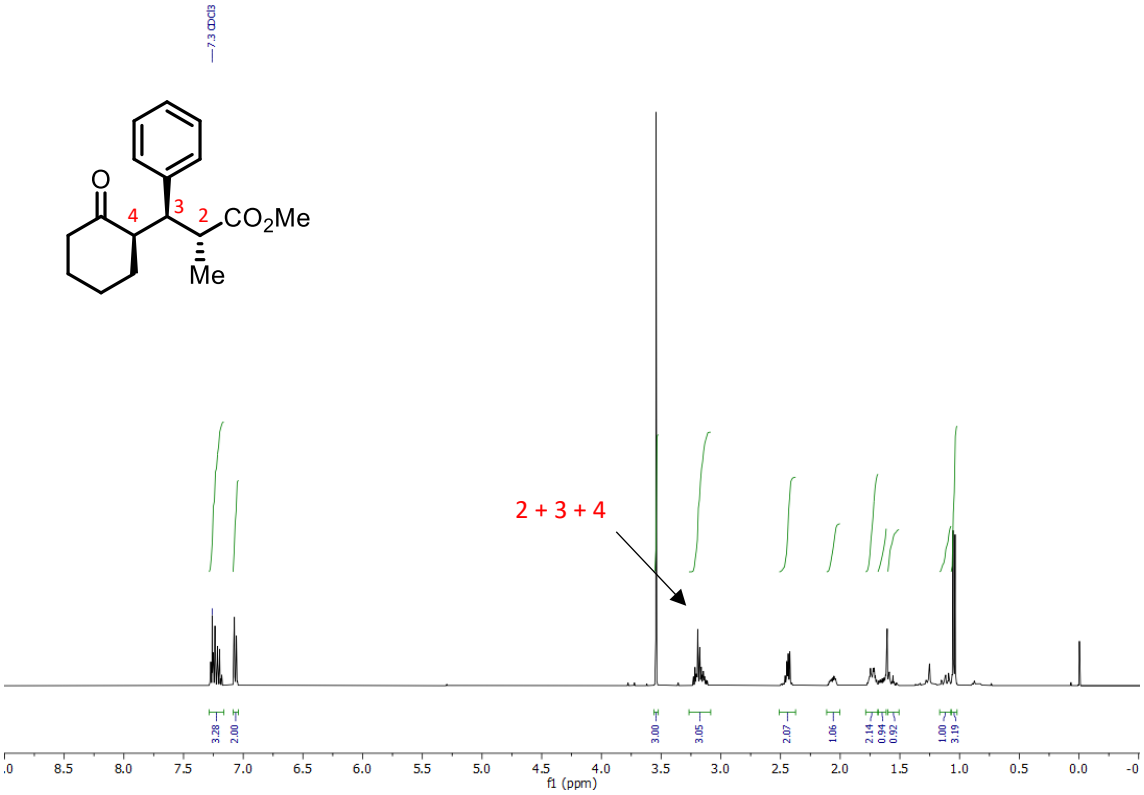

Figure S53. ^{1}H NMR spectrum of **6a** at 400 MHz in $CDCl_3$.

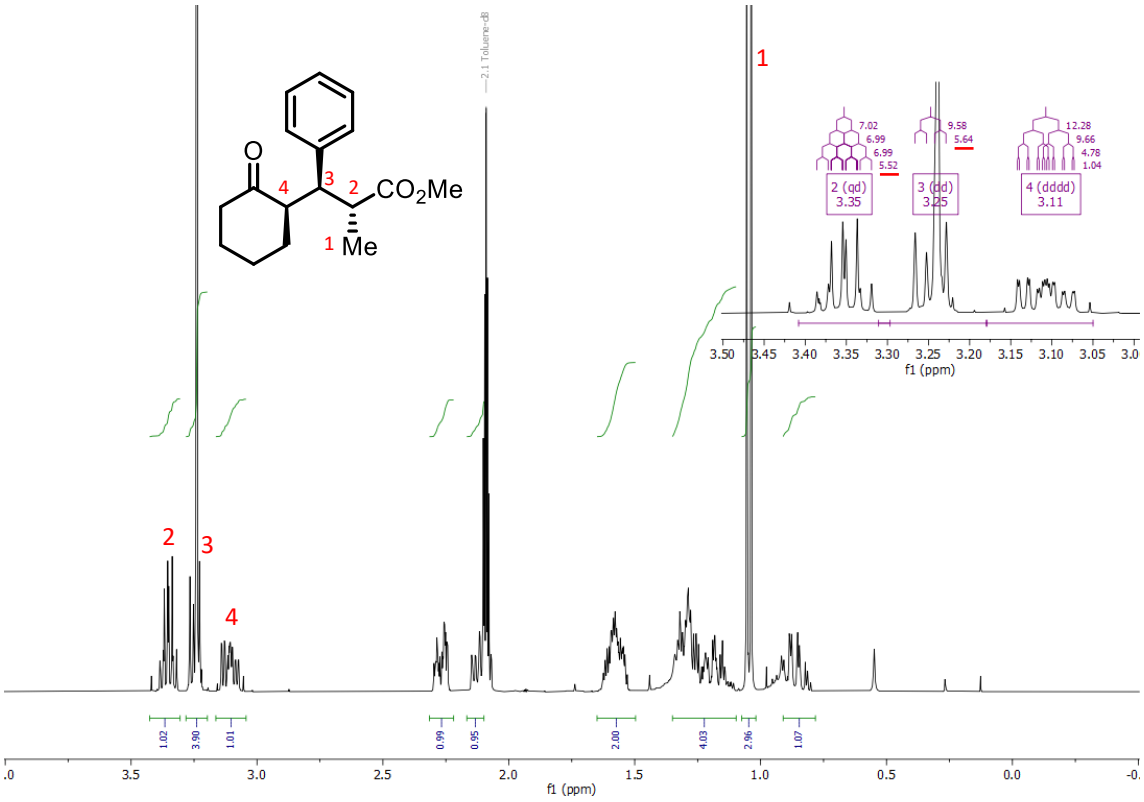

Figure S54. ^{1}H NMR spectrum of **6a** at 400 MHz in toluene_d$_8$.

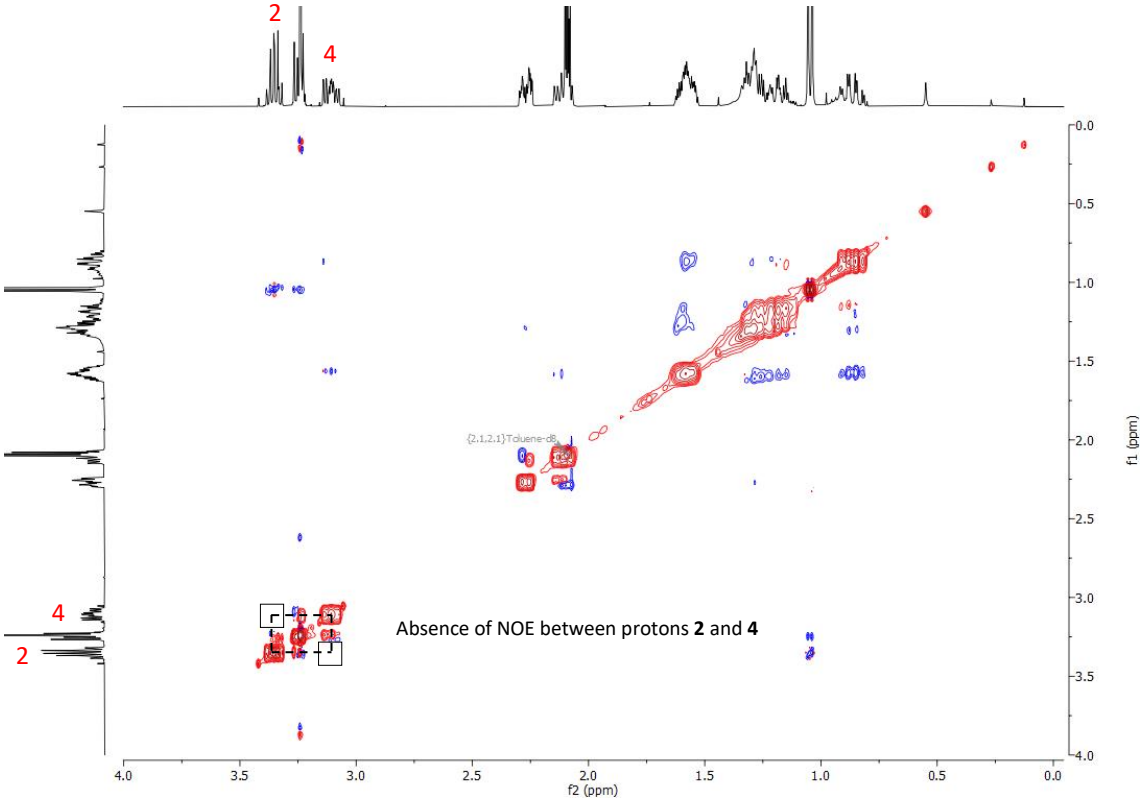

Figure S55. 2D NOESY spectrum of **6a** at 400 MHz in toluene_d$_8$.

*[The absence of NOE contact between protons **2** and **4** confirms their anti-configuration in **6a**. The analysis of the coupling constants also confirms the anti-configuration of **6a**: $J_{(2\text{-}3)}$ = 5.6 Hz.]*

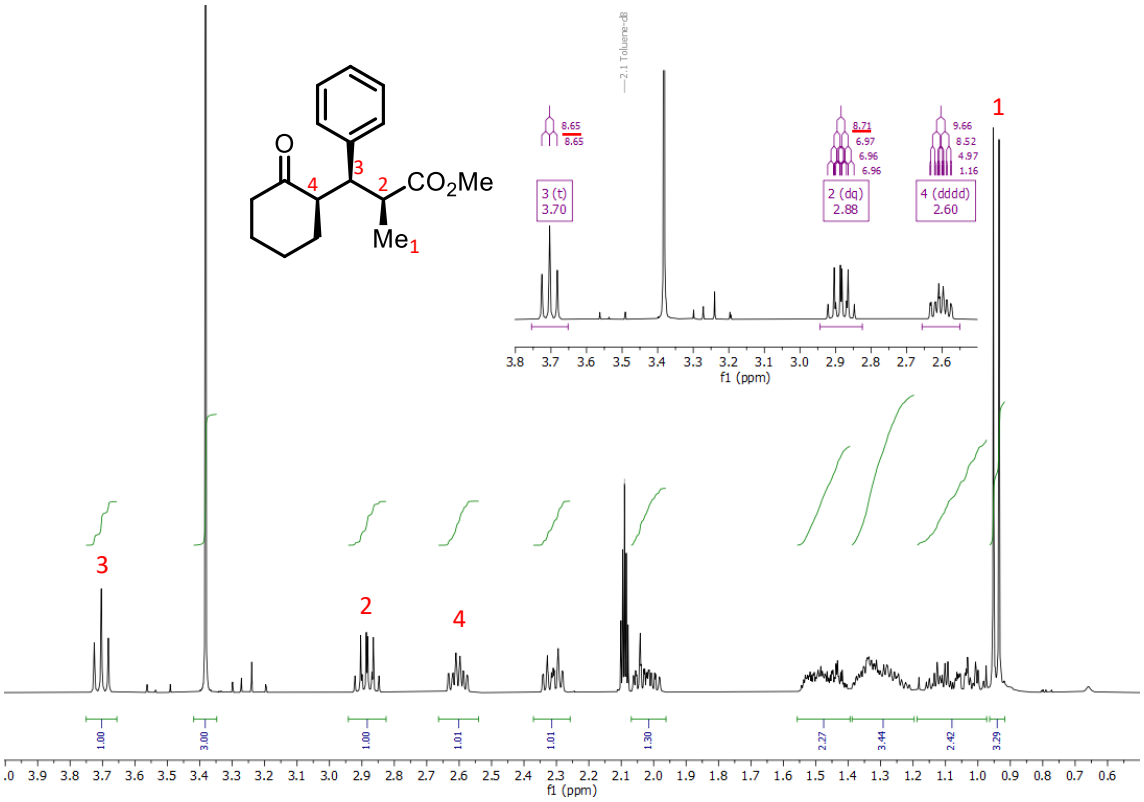

Figure S56. ^{1}H NMR spectrum of **6b** at 400 MHz in toluene_d$_8$.

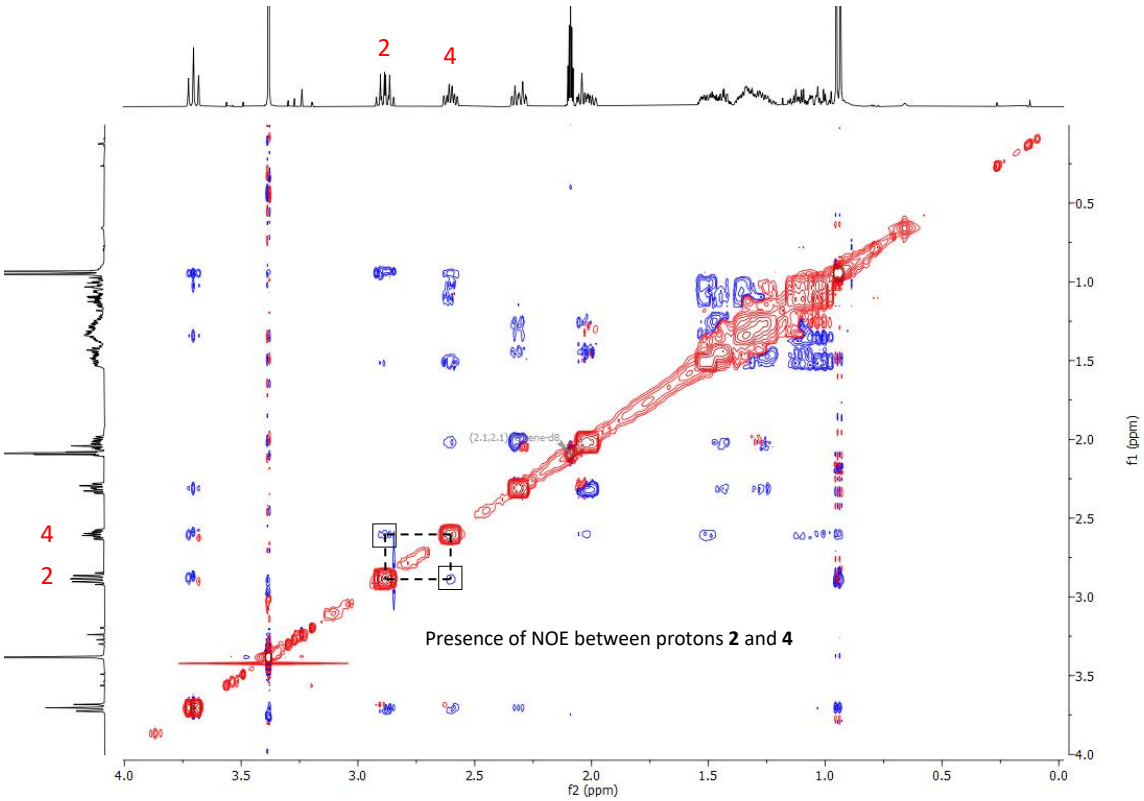

Figure S57. 2D NOESY spectrum of **6b** at 400 MHz in toluene_d$_8$.

*[The presence of NOE contact between protons **2** and **4** confirms the all-syn configuration of product **6b**. The analysis of the coupling constants also confirms the sin-configuration of **6b**: $J_{(2\text{-}3)}$ = 8.7 Hz.]*

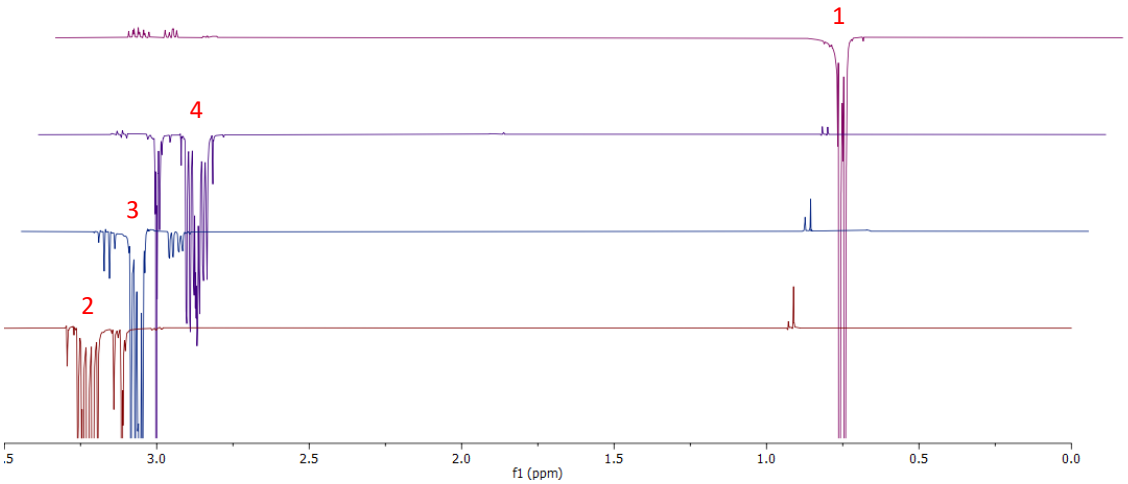

Figure S58. 1D NOE stacked spectra of **6a** at 400 MHz in toluene_d_8.

*[When proton **4** is irradiated, proton **2** is not in antiphase and vice versa. Therefore, there is no NOE contact between protons **2** and **4**. 1D NOE spectra confirm the assigned anti-configuration for **6a**.]*

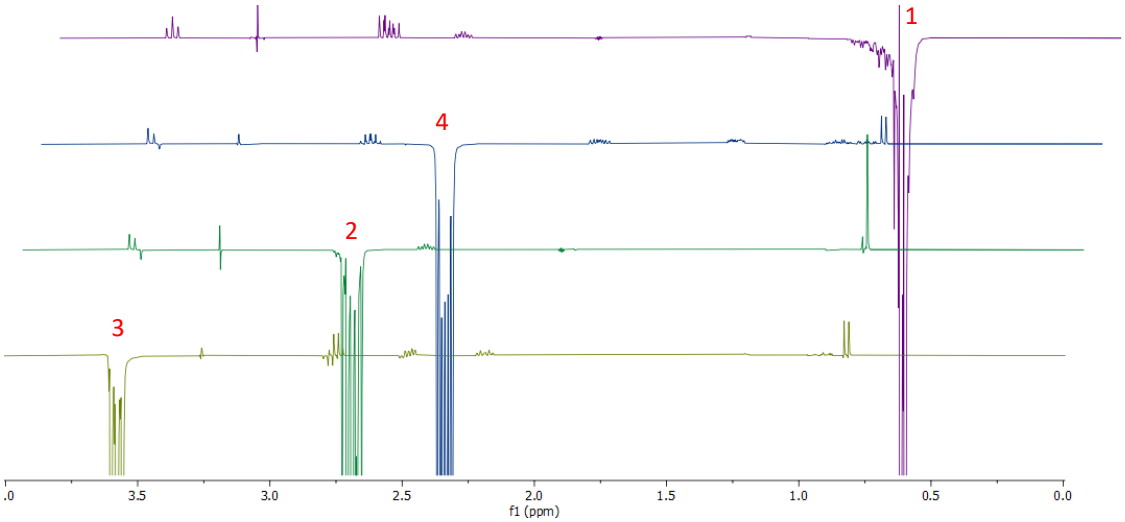

Figure S59. 1D NOE stacked spectra of **6b** at 400 MHz in toluene_d_8.

*[When proton **4** is irradiated, proton **2** is in antiphase and vice versa. Therefore, there is NOE contact between protons **2** and **4**. 1D NOE spectra confirm the assigned syn-configuration for **6b**.]*

K.2.Reduction and cyclization

Reduction of the ketone

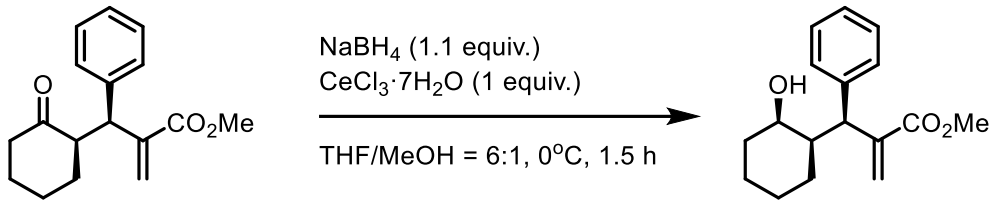

3a (1 equiv.) **8**

To a solution of compound **3a** (54,6 mg, 1 equiv., 0.2 mmol) in 4 mL of a mixture THF/MeOH = 6:1 (0.05 M) was added $CeCl_3 \cdot 7H_2O$ (74,5 mg, 1 equiv., 0.2 mmol). The solution was cooled to 0 ºC and $NaBH_4$ (8.3 mg, 1..1 equiv., 0.22 mmol) was added. The reaction was carried at 0 ºC until full conversion of the starting material was detected by TLC analysis. Then, the reaction mixture was quenched with a saturated solution of NH_4Cl (4 mL) and extracted with CH_2Cl_2 (2 x 4 mL). The organic layers were collected, dried with anhydrous $MgSO_4$ and concentrated under reduced pressure. The resulting crude was purified by flash column chromatography using hexane and ethyl acetate mixtures affording the desired product **8** (75% yield, d.r. >20:1) as a yellow oil.

methyl 2-((S)-((1R,2R)-2-hydroxycyclohexyl)(phenyl)methyl)acrylate (8)

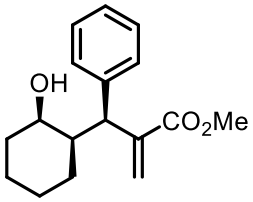

^{1}H NMR (400 MHz, $CDCl_3$) δ 7.31-7.15 (5H, m), 6.33 (1H, s), 5.75 (1H, s), 3.98 (1H, bs), 3.89 (1H, d, *J* = 11.71 Hz), 3.74 (3H, s), 2.33 (1H, d, *J* = 4.23 Hz), 2.00 (1H, tdd, *J* = 11.71, 3.90, 2.14 Hz), 1.94-1.85 (1H, m), 1.69-1.53 (2H, m), 1.52-1.39 (2H, m), 1.32-1.19 (5H, m); **^{13}C NMR** (100 MHz, $CDCl_3$) δ 169.0, 142.8, 142.3, 128.7, 128.6, 126.6, 126.4, 66.4, 52.4, 48.6, 46.0, 33.5, 26.2, 25.1, 19.9. **HRMS (ESI)** Calculated for $C_{17}H_{22}NaO_3^+$ ([M+Na]$^+$) 297.1461. Found 297.1462. **$[\alpha]_D^{25}$** = -11.5 (c = 0.60), $CHCl_3$).

Determination of the relative configuration of 8 by 2D NOESY

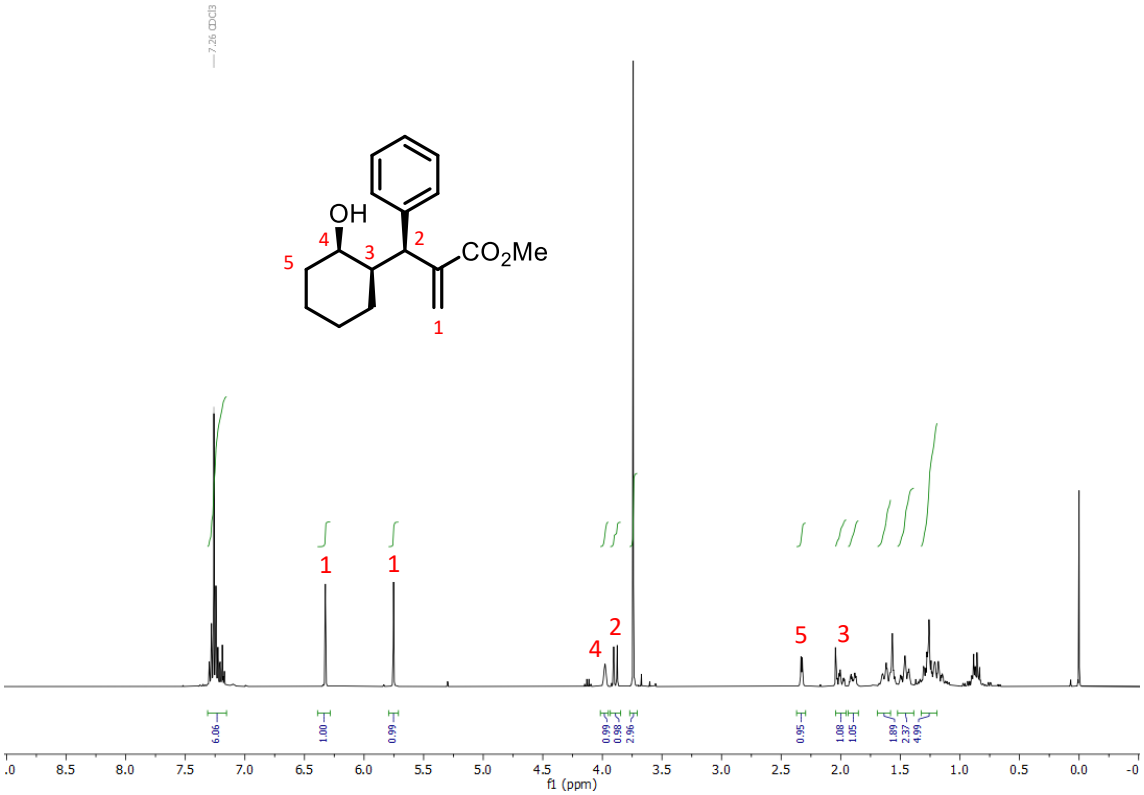

Figure S60. ^{1}H NMR spectrum of **8** at 400 MHz in $CDCl_3$.

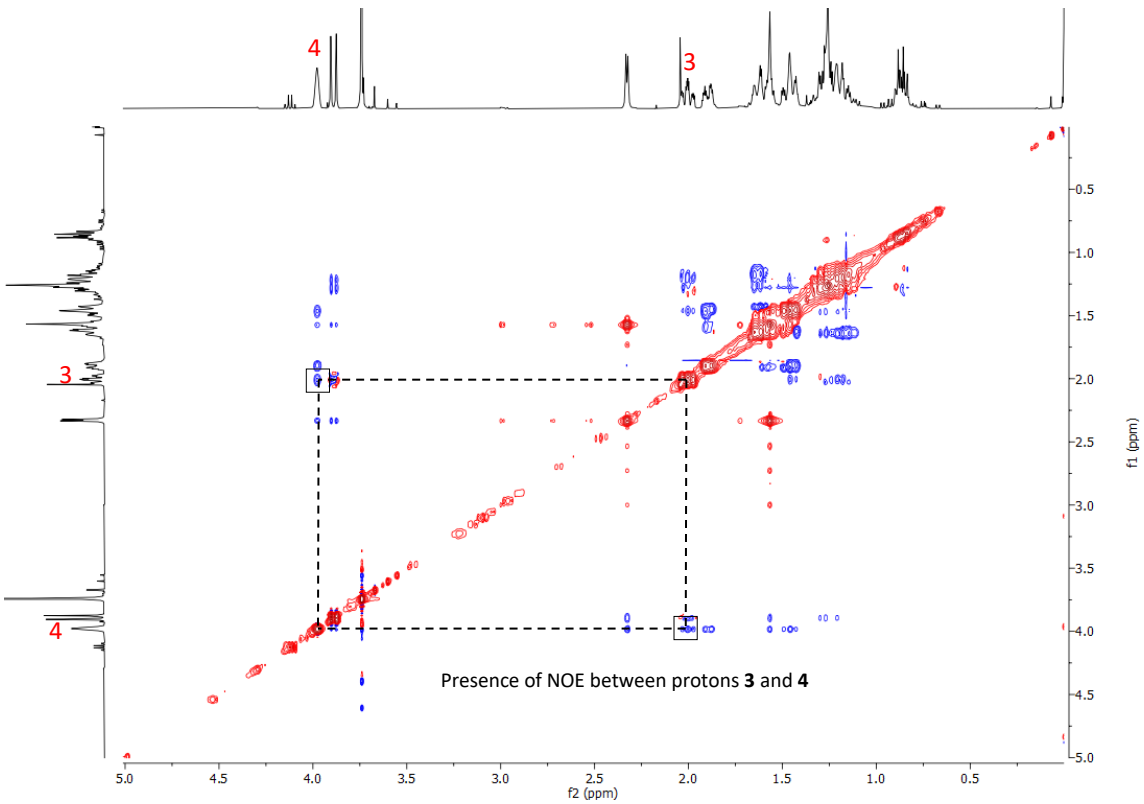

Figure S61. 2D NOESY spectrum of **8** at 400 MHz in $CDCl_3$.

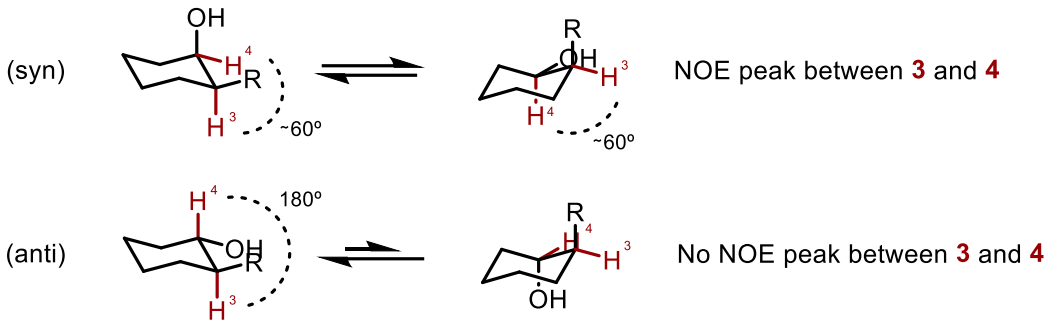

The most favoured conformation for the *anti*-product is the one with the protons **3** and **4** in axial position (no NOE peak) while the bulkier groups (R and OH) are in equatorial position. In the NOESY spectrum, there is a NOE contact between proton **3** and **4**. Therefore, the alcohol moiety in **8** is in *syn*-configuration respect the other two stereocenters.

Lactonization

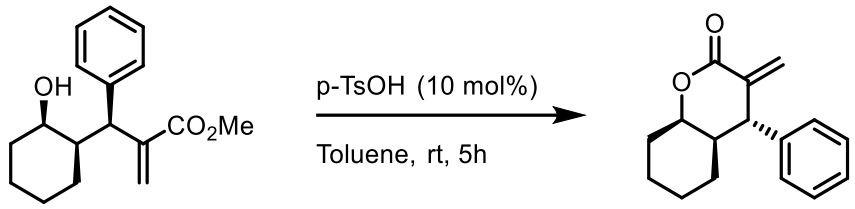

8 (1 equiv.) **7**

To a solution of compound **8** (41.2 mg, 1 equiv., 0.15 mmol) in 1.5 mL of toluene (0.1 M) was added p-TsOH (3.8 mg, 0.1 equiv., 0.02 mmol). The lactonization was carried out at room temperature until full conversion of the starting material was detected by TLC analysis. Then, the reaction mixture was directly purified by flash column chromatography using hexane and ethyl acetate mixtures affording the desired product **7** (85% yield) as a colourless solid.

(4S,4aR,8aR)-3-methylene-4-phenyloctahydro-2H-chromen-2-one (7)

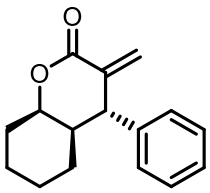

^{1}H NMR (400 MHz, $CDCl_3$) δ 7.38-7.29 (2H, m), 7.28-7.22 (1H, m), 7.18-7.11 (2H, m), 6.71 (1H, t, *J* = 4.16 Hz), 5.55 (1H, t, *J* = 1.47 Hz), 4.47 (1H, dt, *J* = 5.29, 2.93 Hz), 3.81 (1H, d, *J* = 3.97 Hz), 2.08-1.92 (2H, m), 1.79-1.68 (1H, m), 1.68-1.75 (2H, m), 1.53-1.43 (3H, m), 1.43-1.32 (1H, m); **^{13}C NMR** (100 MHz, $CDCl_3$) δ 166.2, 142.8, 135.5, 132.2, 128.9, 127.9, 127.1, 75.2, 48.6, 41.5, 30.4, 27.0, 24.2, 20.3. **HRMS (ESI)** Calculated for $C_{16}H_{19}O_2^+$ ($[M+H]^+$) 243.1383. Found 243.1380. **$[\alpha]_D^{25}$** = -91.5 (c = 2.05, $CHCl_3$).

Determination of the relative configuration 7 by 2D NOESY

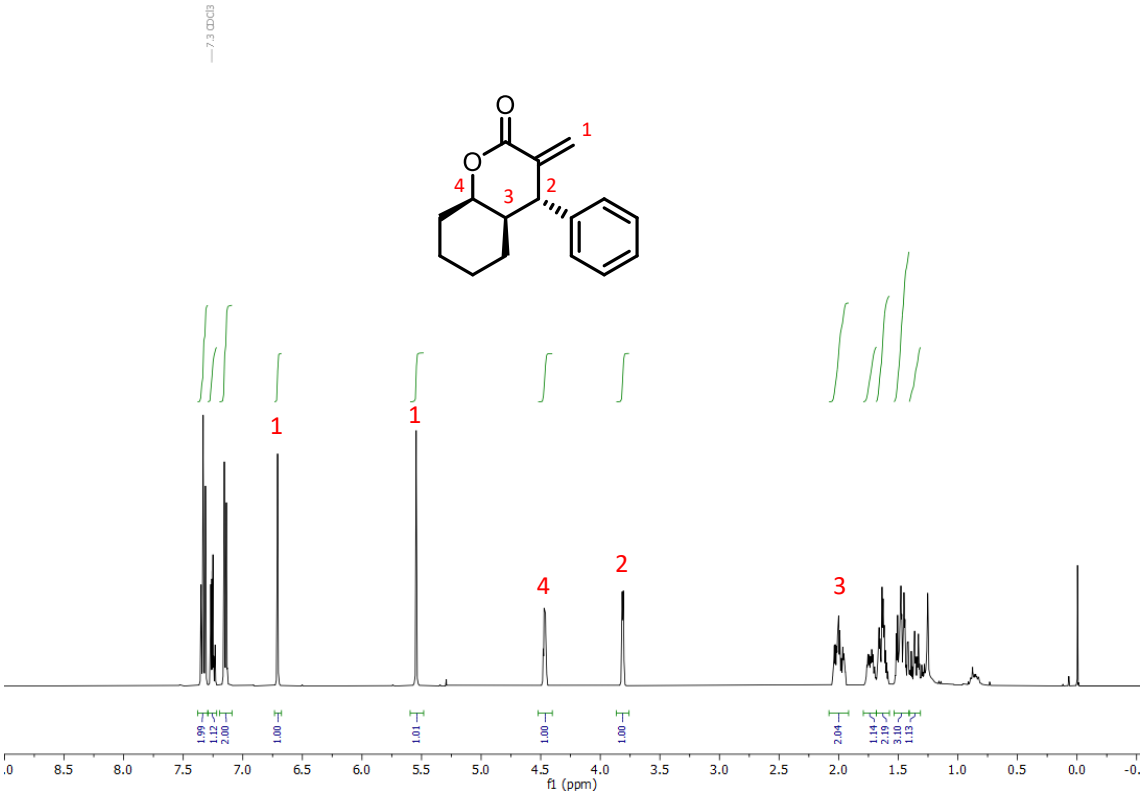

Figure S62. ^{1}H NMR spectrum of **7** at 400 MHz in $CDCl_3$.

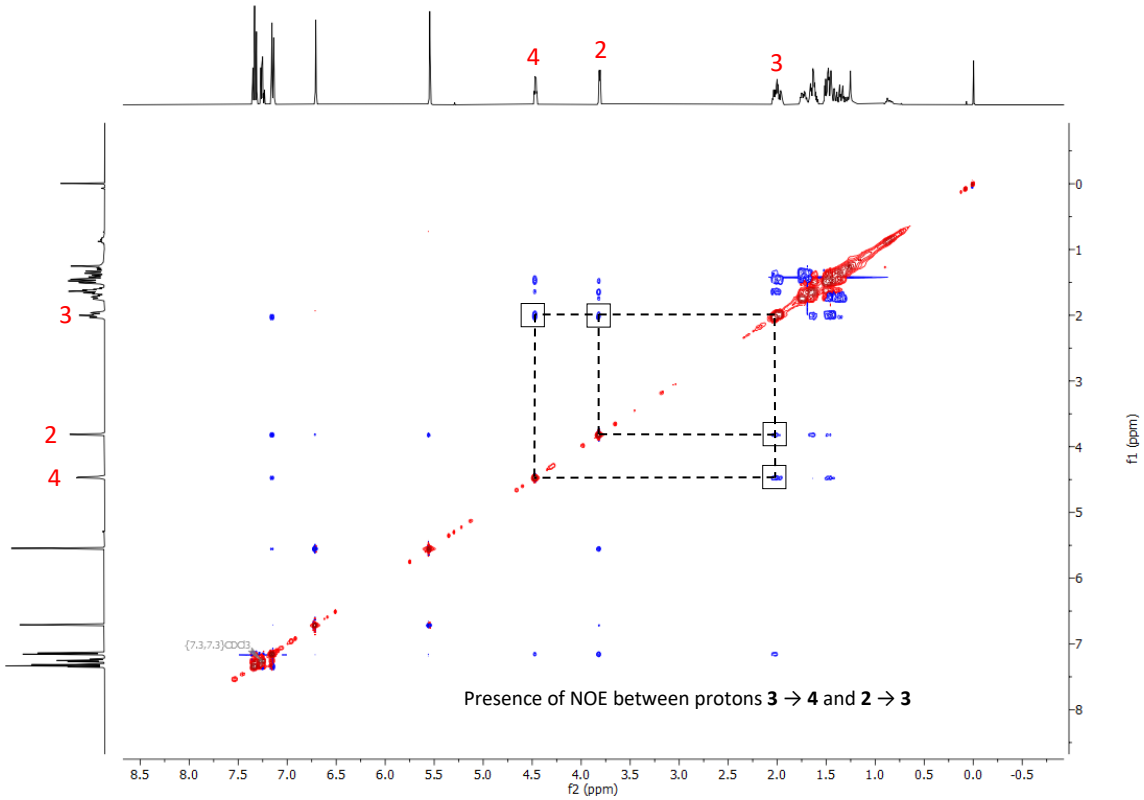

Figure S63. 2D NOESY spectrum of **7** at 400 MHz in $CDCl_3$.

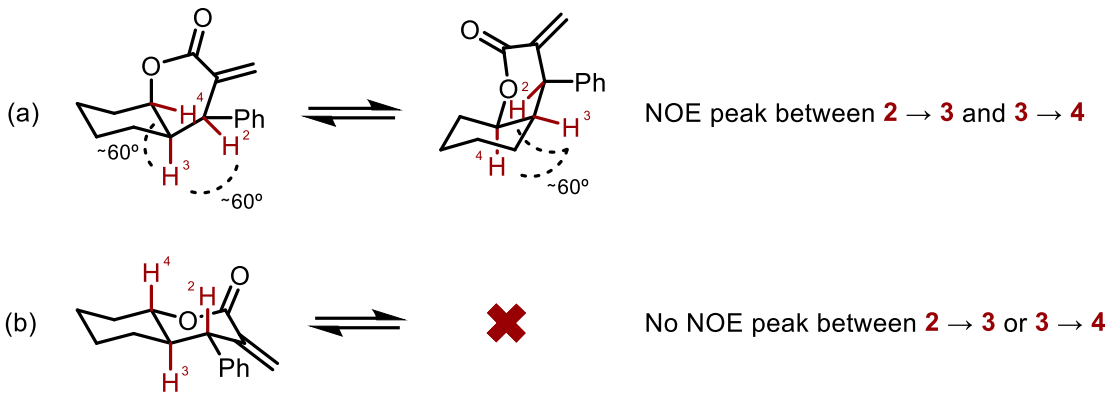

Protons **2** – **3** and **3** – **4** for lactone (a) are at *ca.* 60° in both conformers. In the NOESY spectrum, there are NOE contacts between protons **2** – **3** and **3** – **4**. Conversely, lactone (b) should show a NOE peak between protons **2** – **4**, which is not observed in the NOESY spectrum. Therefore, lactone **7** possesses a *cis*-decalin-like structure.

L. References

[1] Waligora, L.; Galinski, M.; Lewandowski, A. *Electroanalysis*, **2009**, *21*, 2221-2227.

[2] Companyó, X.; Geant, P.-Y.; Mazzanti, A.; Moyano, A.; Rios, R. *Tetrahedron* **2014**, *70*, 75-83.

[3] (a) Santos, M. S.; Coelho, F. *RSC Adv*. **2012**, *2*, 3237-3241. (b) Huang, F-F.; Lin, S-Y.; Liu, X-L.; Huang, X.; Sheng, S-R. *Synthesis* **2007**, *9*, 1373-1377. (c) Helppi, M. A.; Lehmkuhler, A. L.; Marchi, J. M.; Schmidt, C. M.; Yip-Schneider, M. T.; Ramachandran, P. V.; *Bioorg. Med. Chem. Lett*. **2015**, *25*, 4270-4273. (d) Rasson, C.; Stouse, A.; Boreux, A.; Cirriez, V.; Riant, O. *Chem. Eur. J.* **2018**, *24*, 9234-9237. (e) Jacobsen, E.; Chavda, M. K.; Zikpi, K. M.; Waggoner, S. L.; Passini, D. J.; Wolfe, J. A.; Larson, R.; Beckley, C.; Hamaker, C. G.; Hitchcock, S. R. *Tetr. Lett.*, **2017**, *58*, 3073-3077. (f) Akins, N. S.; Mishra, N.; Harris, H. M.; Dudhipala, N.; Kim, S. J.; Keasling, A. W.; Majumdar, S.; Zjawiony, J. K.; Paris, J. J.; Ashpole, N. M.; Le, H. V. *Chem. Med. Chem*., **2022**, *17*, e202100684. (g) Fort, Y.; Berthe, M. C.; Caubere, P. *Tetrahedron*, **1992**, *48*, 6371-6384. (h) Poly, W.; Schomburg, D.; Hoffmann, H. M. R. *J. Org. Chem*. **1988**, *53*, 3701-3710.

[4] Nishimine, T.; Fukushi, K.; Shibata, N.; Taira, H.; Tokunaga, E.; Yamano, A.; Shiro, M.; Shibata, N *Angew. Chem. Int. Ed.*, **2014**, *53*, 517-520.

[5] (a) Zi, Y.; Lange, M.; Schultz, C.; Vilotijevic, I. *Angew. Chem. Int. Ed*., **2019**, *58*, 10727-10731. (b) Nishimine, T.; Taira, H.; Tokunaga, E.; Shiro, M.; Shibata, N. *Angew. Chem. Int. Ed.*, **2016**, *55*, 359-363.

[6] Loy, N.; Subin, C.; Kim, S.; Park, C-M. *Chem. Commun*. **2016**, *52*, 7336-7339.

[7] (a) Ohmatsu, K.; Nakashima, T.; Sato, M.; Ooi, T. *Nat. Commun*. **2019**, 10, 2706-2713. (b) Yu, J-Q.; Wu, H-C.; Corey, E. J. *Org. Lett*, **2005**, *7*, 1415-1417. (c) Zhang, J.; Wang, L.; Liu, Q.; Yang, Z.; Huang, Y. *Chem. Commun*. **2013**, *49*, 11662-11664. (d) Khan, I.; Reed-Berendt, B. G.; Melen, R. L.; Morrill, L. C. *Angew. Chem. Int. Ed*. **2018**, *57*, 12356-12359. (e) Kang, T.; Cao, W.; Hou, L.; Tang, Q.; Zou, S.; Liu, X.; Feng, X. *Angew. Chem. Int. Ed*. **2019**, *58*, 2464-2468. (f) US 4992591, A, **1991** – MERCK & CO INK. (g) Hayashi, M.; Shibuya, M.; Iwabuchi, Y. *Synlett* **2012**, *23*, 1025-1030.

[8] (a) Sousa e Silva, F. C.; Van, N. T.; Wengryniuk, S. E. *J. Am. Chem. Soc.* **2020**, *142*, 64–69. (b) Takasu, K.; Ishii, T.; Inanaga, K.; Ihara, M.; *Org. Synth*. **2006**, 83, 193-199.

[9] Huang, J.; Zhang, R.; Wu, X.; Dong, G.; Xia, Y. *Org. Lett.* **2022**, *24*, 2436-2440.

[10] (a) Vogt, C. D.; Bart, A. G.; Yadav, R.; Scott, E. E.; Aubé, J. *Org. Biomol. Chem.* **2021**, *19*, 7664-7669. (b) Orban, J.; Turner, J. V.; Twitchin, B. *Tetr. Lett*. **1984**, *25*, 5099-5102.

[11] Wang, W-X.; Zhang, Q-Z.; Zhang, T-Q.; Li, Z-S.; Zhang, W.; Yu, W. *Adv. Synth. Catal*. **2015**, *357*, 221-226.

[12] Jameleddine, K.; Yakdhan, K.; Jamil, K.; Bechir, B. H.; Denis, G. *Synth. Comm*. **2002**, *32*, 2719-2722.

[13] Sun, H.; DiMagno, S. G. *J. Am. Chem. Soc*. **2005**, *127*, *7*, 2050-2051.

[14] Sandford, C.; Edwards, M. A.; Klunder, K. J.; Hickey, D. P.; Li, M.; Barman, K.; Sigman, M. S.; White, H. S.; Minteer, S. D. *Chem. Sci.* **2019**,*10*, 6404-6422.

[15] Veronesi, M.; Vulpetti, A.; Dalvit, C. *J. Mag. Resson. Open* **2022**, *12-13*, 100070.

[16] (a) Tandura, S. N.; Voronkov, M. G.; Alekseev, N. V. *Top. Curr. Chem.* **1986**, *131*, 99-189. (b) Denmark, S. E.; Beutner, G. L. *Angew. Chem. Int. Ed.* **2008**, *47*, 1560-1638.

[17] Sumii, Y.; Nagasaka, T.; Wang, J.; Uno, H.; Shibata, N. *J. Org. Chem*. **2020**, *85*, 15699-15707.

[18] (a) Okusu, S.; Okazaki, H.; Tokunaga, W.; Soloshonok, V. A.; Shibata, N. *Angew. Chem. Int. Ed.* **2016**, *55*, 6744-6748. (b) Nishimine, T.; Taira, H.; Mori, S.; Matsubara, O.; Tokunaga, E.; Akiyama, H.; Soloshonok, V. A.; Shibata, N. *Chem. Commun.* **2017**, *53*, 1128-1131.

M. Determination of the absolute configuration. X-Ray Crystallographic Data of compound 3w

A colourless prism-like specimen of $C_{17}H_{19}BrO_3$, approximate dimensions 0.063mm x 0.118mm x 0.306mm, was used for the X-ray crystallographic analysis. The X-ray intensity data were measured. The integration of the data using an orthorhombic unit cell yielded a total of 38606 reflections to a maximum θ angle of 30.56° (0.70Å resolution), of which 4799 were independent (average redundancy 8.045, completeness = 99.7%, R_{int} = 5.48%, R_{sig} = 4.01%) and 4258 (88.73%) were greater than $2\sigma(F^2)$. The final cell constants of a = 9.3235(17)Å, b = 9.838(2)Å, c = 17.181(4)Å, volume = 1575.9(6)Å^3, are based upon the refinement of the XYZ-centroids of reflections above 20 σ(I). The calculated minimum and maximum transmission coefficients (based on crystal size) are 0.5995 and 0.7461.

The structure was solved and refined using the Bruker SHELXTL Software Package, using the space group P 21 21 21, with Z = 4 for the formula unit $C_{17}H_{19}BrO_3$.The final anisotropic full-matrix least-squares refinement on F^2 with 191 variables converged at R1 = 2.53%, for the observed data and wR2 =5.24% for all data. The goodness-of-fit was 1.024. The largest peak in the final difference electron density synthesis was 0.271e$^-$/Å^3 and the largest hole was -0.473e$^-$/Å^3 with an RMS deviation of 0.061e$^-$/Å^3. On the basis of the final model, the calculated density was 1.480g/cm^3 and F(000), 720 e$^-$.

The specific refinement details are embedded in the CIF files given as Supplementary Materials and that have been deposited with the Cambridge Crystallographic Data Centre as supplementary publication (CCDC 2226509).

Table S5. Crystal data and structure refinement for **3w**.

Identification code	**3w**
Empirical formula	C_{17} H_{19} Br O_3
Formula weight	351.23
Temperature	100(2) K
Wavelength	0.71073 Å
Crystal system	Orthorhombic
Space group	P 21 21 21
Unit cell dimensions	a = 9.3235(17) Å α= 90°. b = 9.838(2) Å β= 90°. c = 17.181(4) Å γ = 90°.
Volume	1575.9(6) Å^3
Z	4
Density (calculated)	1.480 Mg/m^3
Absorption coefficient	2.616 mm^{-1}
F(000)	720
Crystal size	0.306 x 0.118 x 0.063 mm^3
Theta range for data collection	2.371 to 30.555°.
Index ranges	-13<=h<=12, -13<=k<=14, -24<=l<=24
Reflections collected	38606
Independent reflections	4799 [R(int) = 0.0548]
Completeness to theta = 25.242°	100.0 %
Absorption correction	Semi-empirical from equivalents
Max. and min. transmission	0.7461 and 0.5995
Refinement method	Full-matrix least-squares on F^2
Data / restraints / parameters	4799 / 0 / 191
Goodness-of-fit on F^2	1.024

Final R indices [I>2sigma(I)]	R1 = 0.0253, wR2 = 0.0490
R indices (all data)	R1 = 0.0348, wR2 = 0.0524
Absolute structure parameter	0.010(4)
Extinction coefficient	n/a
Largest diff. peak and hole	0.271 and -0.473 e.Å^{-3}

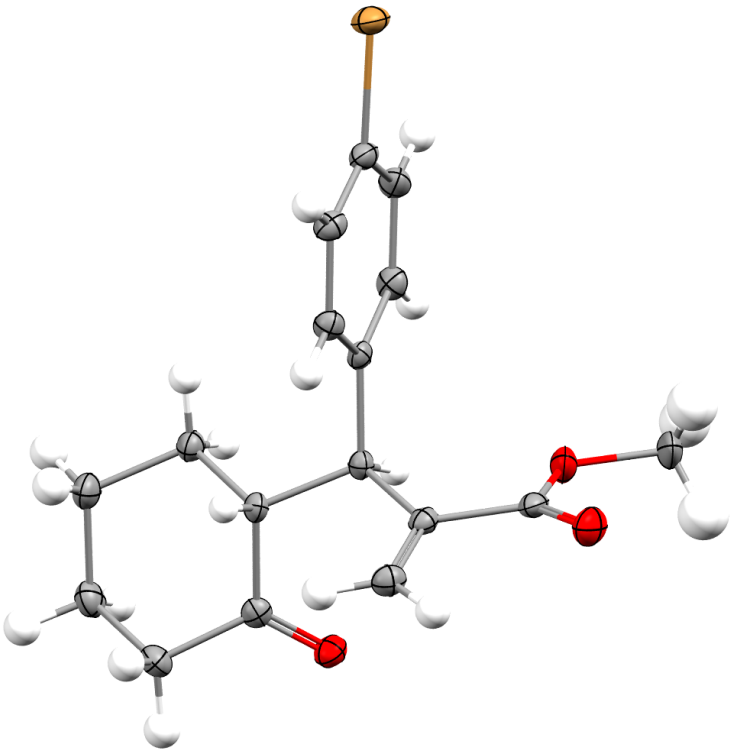

Figure S64. Crystal structure of compound **3w**. Thermal ellipsoids drawn at the 50% probability level.

Table S6. Atomic coordinates (x 10^4) and equivalent isotropic displacement parameters ($Å^2$x 10^3) for **3w**. U(eq) is defined as one third of the trace of the orthogonalized U^{ij} tensor.

	x	y	z	U(eq)
Br(1)	10643(1)	6850(1)	4350(1)	26(1)
O(1)	8686(2)	1341(2)	6468(1)	25(1)
O(2)	4455(2)	1856(2)	7145(1)	21(1)
O(3)	9675(2)	1953(2)	7605(1)	29(1)
C(1)	9826(3)	356(3)	6379(2)	34(1)
C(2)	8738(2)	2076(2)	7123(1)	18(1)
C(3)	7505(2)	3043(3)	7190(1)	16(1)
C(4)	6669(2)	3359(2)	6452(1)	14(1)
C(5)	7599(2)	4240(2)	5924(1)	14(1)
C(6)	7923(3)	3825(2)	5170(1)	18(1)
C(7)	8818(3)	4598(3)	4689(1)	21(1)
C(8)	9371(3)	5800(2)	4977(1)	18(1)
C(9)	5203(2)	4015(2)	6616(1)	14(1)
C(10)	4204(2)	3063(3)	7054(1)	16(1)
C(11)	2797(2)	3695(3)	7288(1)	21(1)
C(12)	2000(2)	4113(3)	6539(1)	23(1)
C(13)	2932(3)	5045(3)	6039(2)	23(1)
C(14)	4405(2)	4417(2)	5864(1)	18(1)
C(15)	7259(2)	3585(2)	7883(1)	20(1)
C(16)	8170(2)	5458(2)	6191(1)	17(1)
C(17)	9056(2)	6250(2)	5722(1)	18(1)

Table S7. Bond lengths [Å] and angles [°] for **3w**.

Br(1)-C(8)	1.906(2)
O(1)-C(2)	1.339(3)
O(1)-C(1)	1.446(3)
O(2)-C(10)	1.220(3)
O(3)-C(2)	1.210(3)
C(1)-H(1)	0.9800
C(1)-H(13)	0.9800
C(1)-H(14)	0.9800
C(2)-C(3)	1.496(3)
C(3)-C(15)	1.324(3)
C(3)-C(4)	1.522(3)
C(4)-C(5)	1.526(3)
C(4)-C(9)	1.538(3)
C(4)-H(3)	1.0000
C(5)-C(16)	1.389(3)
C(5)-C(6)	1.390(3)
C(6)-C(7)	1.399(3)
C(6)-H(2)	0.9500
C(7)-C(8)	1.382(3)
C(7)-H(19)	0.9500
C(8)-C(17)	1.386(3)
C(9)-C(10)	1.520(3)

C(9)-C(14)	1.543(3)
C(9)-H(4)	1.0000
C(10)-C(11)	1.507(3)
C(11)-C(12)	1.541(3)
C(11)-H(12)	0.9900
C(11)-H(11)	0.9900
C(12)-C(13)	1.527(3)
C(12)-H(10)	0.9900
C(12)-H(5)	0.9900
C(13)-C(14)	1.536(3)
C(13)-H(6)	0.9900
C(13)-H(7)	0.9900
C(14)-H(8)	0.9900
C(14)-H(9)	0.9900
C(15)-H(15)	0.9500
C(15)-H(16)	0.9500
C(16)-C(17)	1.393(3)
C(16)-H(17)	0.9500
C(17)-H(18)	0.9500

C(2)-O(1)-C(1)	115.1(2)
O(1)-C(1)-H(1)	109.5
O(1)-C(1)-H(13)	109.5
H(1)-C(1)-H(13)	109.5
O(1)-C(1)-H(14)	109.5
H(1)-C(1)-H(14)	109.5
H(13)-C(1)-H(14)	109.5
O(3)-C(2)-O(1)	123.2(2)
O(3)-C(2)-C(3)	124.4(2)
O(1)-C(2)-C(3)	112.38(18)
C(15)-C(3)-C(2)	117.3(2)
C(15)-C(3)-C(4)	125.4(2)
C(2)-C(3)-C(4)	117.30(19)
C(3)-C(4)-C(5)	108.71(17)
C(3)-C(4)-C(9)	112.82(17)
C(5)-C(4)-C(9)	112.08(17)
C(3)-C(4)-H(3)	107.7
C(5)-C(4)-H(3)	107.7
C(9)-C(4)-H(3)	107.7
C(16)-C(5)-C(6)	118.5(2)
C(16)-C(5)-C(4)	120.8(2)
C(6)-C(5)-C(4)	120.7(2)
C(5)-C(6)-C(7)	121.3(2)
C(5)-C(6)-H(2)	119.3
C(7)-C(6)-H(2)	119.3
C(8)-C(7)-C(6)	118.5(2)
C(8)-C(7)-H(19)	120.8
C(6)-C(7)-H(19)	120.8
C(7)-C(8)-C(17)	121.6(2)
C(7)-C(8)-Br(1)	119.61(17)
C(17)-C(8)-Br(1)	118.73(17)
C(10)-C(9)-C(4)	112.10(18)
C(10)-C(9)-C(14)	106.12(17)
C(4)-C(9)-C(14)	112.47(17)
C(10)-C(9)-H(4)	108.7

C(4)-C(9)-H(4)	108.7
C(14)-C(9)-H(4)	108.7
O(2)-C(10)-C(11)	122.3(2)
O(2)-C(10)-C(9)	123.07(19)
C(11)-C(10)-C(9)	114.3(2)
C(10)-C(11)-C(12)	107.92(19)
C(10)-C(11)-H(12)	110.1
C(12)-C(11)-H(12)	110.1
C(10)-C(11)-H(11)	110.1
C(12)-C(11)-H(11)	110.1
H(12)-C(11)-H(11)	108.4
C(13)-C(12)-C(11)	110.8(2)
C(13)-C(12)-H(10)	109.5
C(11)-C(12)-H(10)	109.5
C(13)-C(12)-H(5)	109.5
C(11)-C(12)-H(5)	109.5
H(10)-C(12)-H(5)	108.1
C(12)-C(13)-C(14)	112.2(2)
C(12)-C(13)-H(6)	109.2
C(14)-C(13)-H(6)	109.2
C(12)-C(13)-H(7)	109.2
C(14)-C(13)-H(7)	109.2
H(6)-C(13)-H(7)	107.9
C(13)-C(14)-C(9)	111.67(18)
C(13)-C(14)-H(8)	109.3
C(9)-C(14)-H(8)	109.3
C(13)-C(14)-H(9)	109.3
C(9)-C(14)-H(9)	109.3
H(8)-C(14)-H(9)	107.9
C(3)-C(15)-H(15)	120.0
C(3)-C(15)-H(16)	120.0
H(15)-C(15)-H(16)	120.0
C(5)-C(16)-C(17)	121.3(2)
C(5)-C(16)-H(17)	119.4
C(17)-C(16)-H(17)	119.4
C(8)-C(17)-C(16)	118.8(2)
C(8)-C(17)-H(18)	120.6
C(16)-C(17)-H(18)	120.6

Symmetry transformations used to generate equivalent atoms:

Table S8. Anisotropic displacement parameters ($Å^2 x\ 10^3$) for **3w**. The anisotropic displacement factor exponent takes the form: $-2\pi^2[\ h^2\ a^{*2}U^{11} + ...\ + 2\ h\ k\ a^*\ b^*\ U^{12}\ ]$

	U^{11}	U^{22}	U^{33}	U^{23}	U^{13}	U^{12}
Br(1)	24(1)	29(1)	25(1)	11(1)	3(1)	-3(1)
O(1)	27(1)	24(1)	24(1)	3(1)	2(1)	13(1)
O(2)	21(1)	17(1)	23(1)	2(1)	-1(1)	-2(1)
O(3)	20(1)	37(1)	30(1)	9(1)	-6(1)	4(1)
C(1)	36(1)	31(2)	35(2)	10(1)	13(1)	21(1)
C(2)	16(1)	20(1)	19(1)	8(1)	1(1)	-1(1)
C(3)	15(1)	15(1)	18(1)	3(1)	-1(1)	-2(1)
C(4)	14(1)	13(1)	15(1)	-1(1)	-1(1)	2(1)
C(5)	13(1)	15(1)	14(1)	2(1)	-2(1)	2(1)
C(6)	22(1)	16(1)	18(1)	-2(1)	-1(1)	0(1)
C(7)	25(1)	22(1)	16(1)	0(1)	2(1)	4(1)
C(8)	16(1)	20(1)	19(1)	7(1)	0(1)	0(1)
C(9)	15(1)	12(1)	16(1)	-1(1)	-1(1)	1(1)
C(10)	16(1)	19(1)	13(1)	-2(1)	-3(1)	0(1)
C(11)	17(1)	24(1)	24(1)	1(1)	4(1)	1(1)
C(12)	15(1)	27(1)	26(1)	0(1)	-1(1)	2(1)
C(13)	19(1)	24(1)	27(1)	6(1)	-2(1)	5(1)
C(14)	17(1)	18(1)	19(1)	2(1)	-2(1)	2(1)
C(15)	20(1)	22(1)	17(1)	1(1)	-3(1)	-2(1)
C(16)	19(1)	18(1)	15(1)	-1(1)	-1(1)	0(1)
C(17)	18(1)	18(1)	19(1)	2(1)	-3(1)	-3(1)

Table S9. Hydrogen coordinates (x 10^4) and isotropic displacement parameters ($Å^2$x 10^3) for **3w**.

	x	y	z	U(eq)
H(1)	10752	825	6370	51
H(13)	9693	-142	5890	51
H(14)	9803	-283	6816	51
H(3)	6492	2480	6176	17
H(2)	7528	3000	4978	22
H(19)	9040	4303	4177	25
H(4)	5355	4851	6937	17
H(12)	2968	4502	7620	26
H(11)	2215	3034	7586	26
H(10)	1746	3290	6238	27
H(5)	1101	4590	6678	27
H(6)	3069	5921	6313	28
H(7)	2430	5234	5543	28
H(8)	4992	5079	5569	21
H(9)	4276	3601	5534	21
H(15)	7855	3356	8312	24
H(16)	6486	4203	7951	24
H(17)	7952	5755	6703	21
H(18)	9436	7084	5909	22

Table S10. Torsion angles [°] for **3w**.

C(1)-O(1)-C(2)-O(3)	1.1(3)
C(1)-O(1)-C(2)-C(3)	-178.1(2)
O(3)-C(2)-C(3)-C(15)	-14.6(4)
O(1)-C(2)-C(3)-C(15)	164.6(2)
O(3)-C(2)-C(3)-C(4)	163.3(2)
O(1)-C(2)-C(3)-C(4)	-17.4(3)
C(15)-C(3)-C(4)-C(5)	106.4(2)
C(2)-C(3)-C(4)-C(5)	-71.3(3)
C(15)-C(3)-C(4)-C(9)	-18.5(3)
C(2)-C(3)-C(4)-C(9)	163.69(19)
C(3)-C(4)-C(5)-C(16)	-55.6(3)
C(9)-C(4)-C(5)-C(16)	69.8(2)
C(3)-C(4)-C(5)-C(6)	122.9(2)
C(9)-C(4)-C(5)-C(6)	-111.8(2)
C(16)-C(5)-C(6)-C(7)	0.9(3)
C(4)-C(5)-C(6)-C(7)	-177.6(2)
C(5)-C(6)-C(7)-C(8)	-0.5(3)
C(6)-C(7)-C(8)-C(17)	-0.2(4)
C(6)-C(7)-C(8)-Br(1)	178.02(17)
C(3)-C(4)-C(9)-C(10)	-64.2(2)
C(5)-C(4)-C(9)-C(10)	172.66(17)
C(3)-C(4)-C(9)-C(14)	176.27(19)
C(5)-C(4)-C(9)-C(14)	53.2(2)
C(4)-C(9)-C(10)-O(2)	-11.5(3)
C(14)-C(9)-C(10)-O(2)	111.7(2)
C(4)-C(9)-C(10)-C(11)	175.27(18)
C(14)-C(9)-C(10)-C(11)	-61.6(2)
O(2)-C(10)-C(11)-C(12)	-111.5(2)
C(9)-C(10)-C(11)-C(12)	61.8(2)
C(10)-C(11)-C(12)-C(13)	-55.3(3)
C(11)-C(12)-C(13)-C(14)	54.0(3)
C(12)-C(13)-C(14)-C(9)	-55.3(3)
C(10)-C(9)-C(14)-C(13)	56.0(2)
C(4)-C(9)-C(14)-C(13)	178.89(19)
C(6)-C(5)-C(16)-C(17)	-0.4(3)
C(4)-C(5)-C(16)-C(17)	178.06(19)
C(7)-C(8)-C(17)-C(16)	0.7(3)
Br(1)-C(8)-C(17)-C(16)	-177.59(16)
C(5)-C(16)-C(17)-C(8)	-0.4(3)

Symmetry transformations used to generate equivalent atoms

Table S11. Hydrogen bonds for **3w**.

D-H...A	d(D-H)	d(H...A)	d(D...A)	<(DHA)
C(9) --H(4) ..O(2) [1-x,1/2+y,3/2-z]	1.00	2.53	3.527(3)	174
C(11) --H(11) ..O(3) [-1+x,y,z]	0.99	2.60	3.421(3)	141
C(7) --H(19) ..O(2) [1/2+x,1/2-y,1-z]	0.95	2.57	3.512(3)	171

C(4) - C(3) C(5) C(9) H(3) sp3 S
C(9) - C(4) C(10) C(14) H(4) sp3 R

N. NMR Spectra

N.1. NMR spectra of allyl fluorides

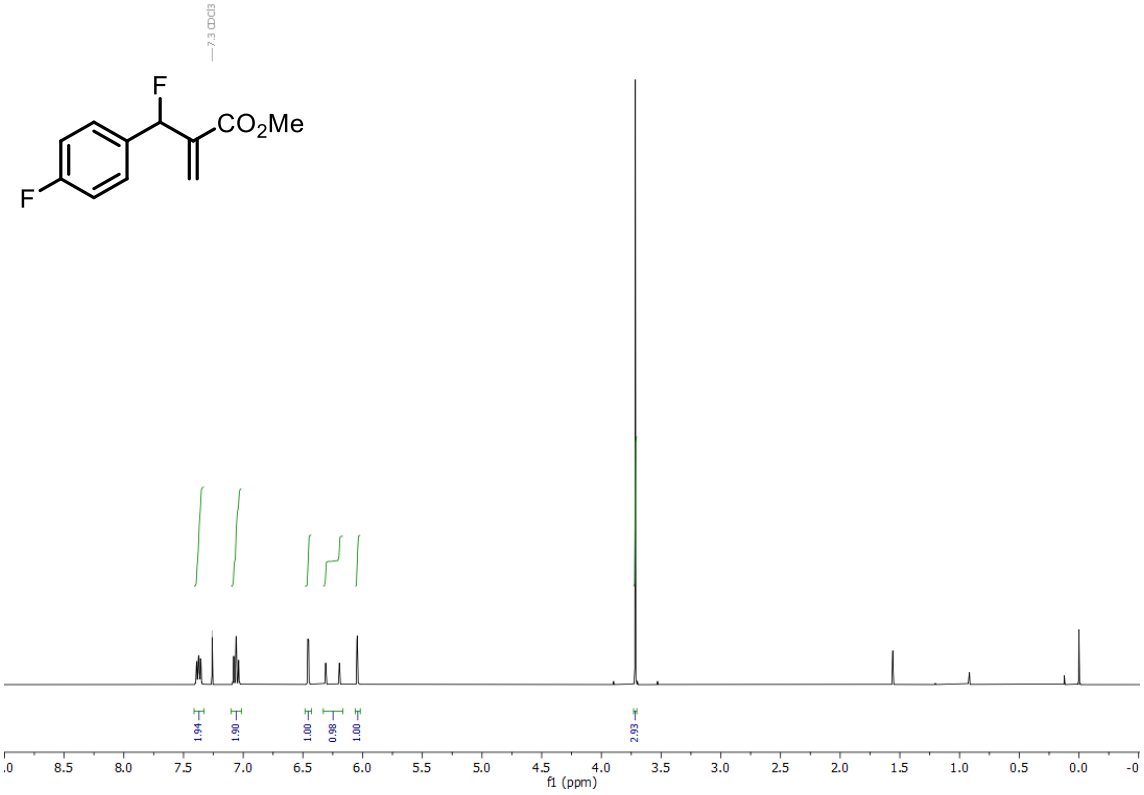

^{1}H NMR spectra of **2c**.

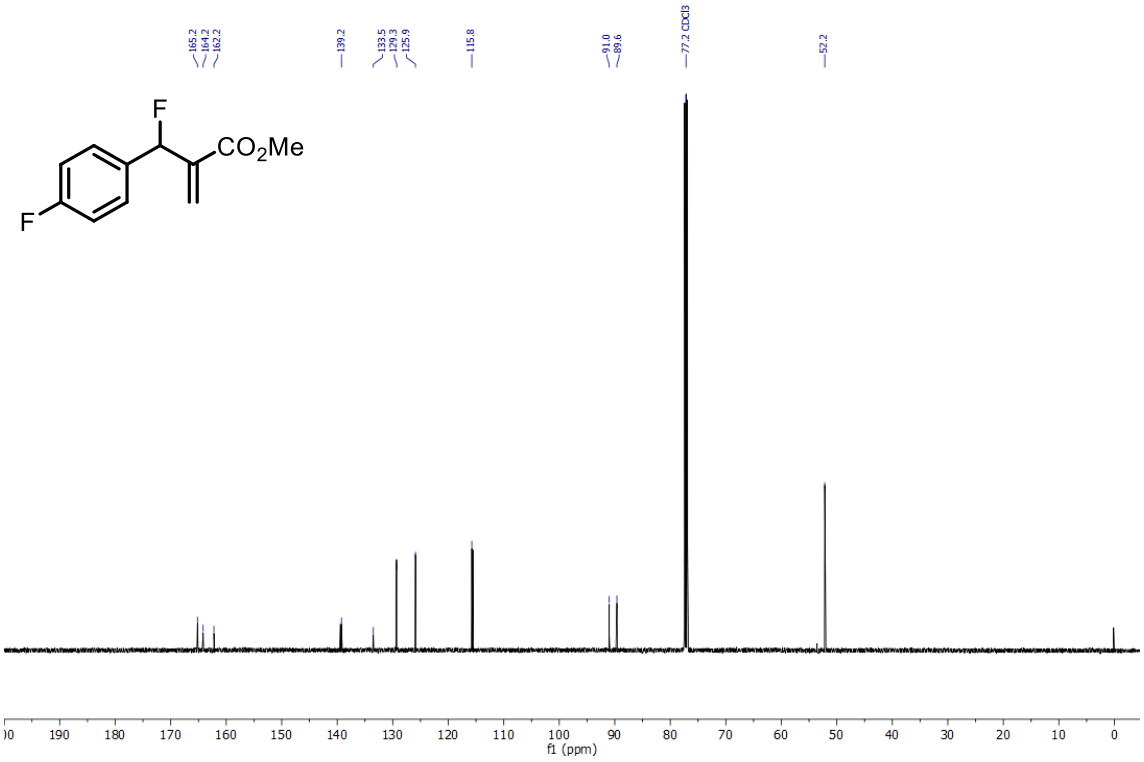

^{13}C NMR spectra of **2c**.

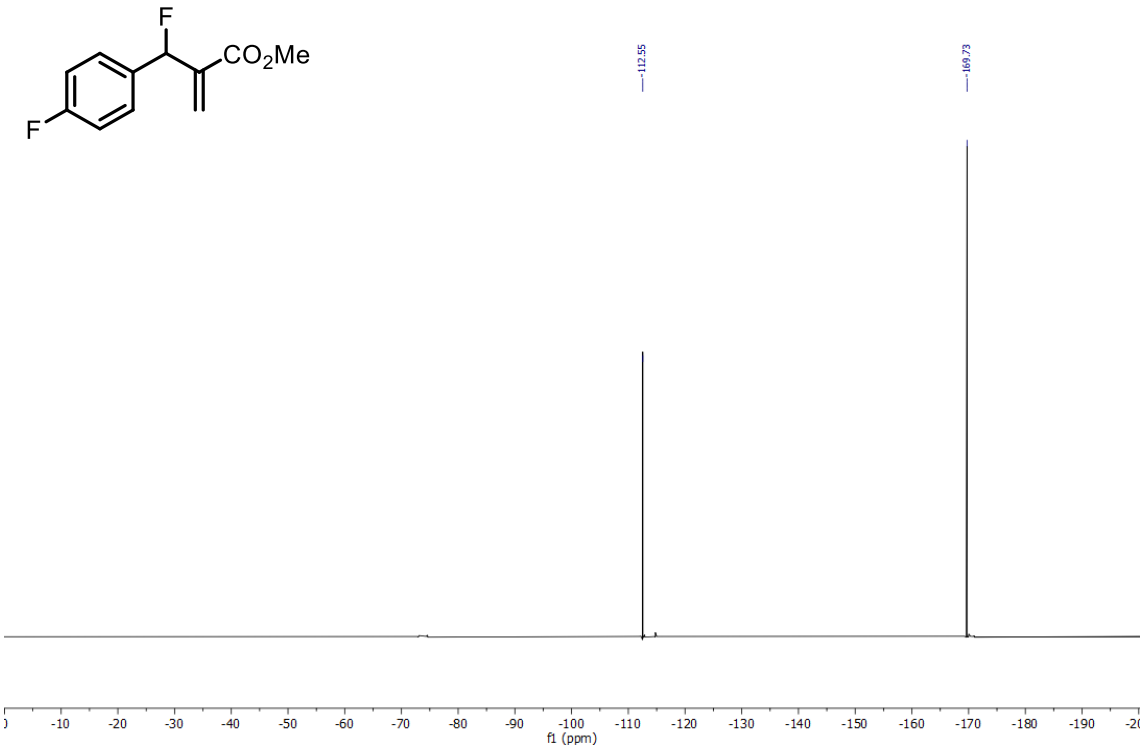

^{19}F NMR spectra of **2c**.

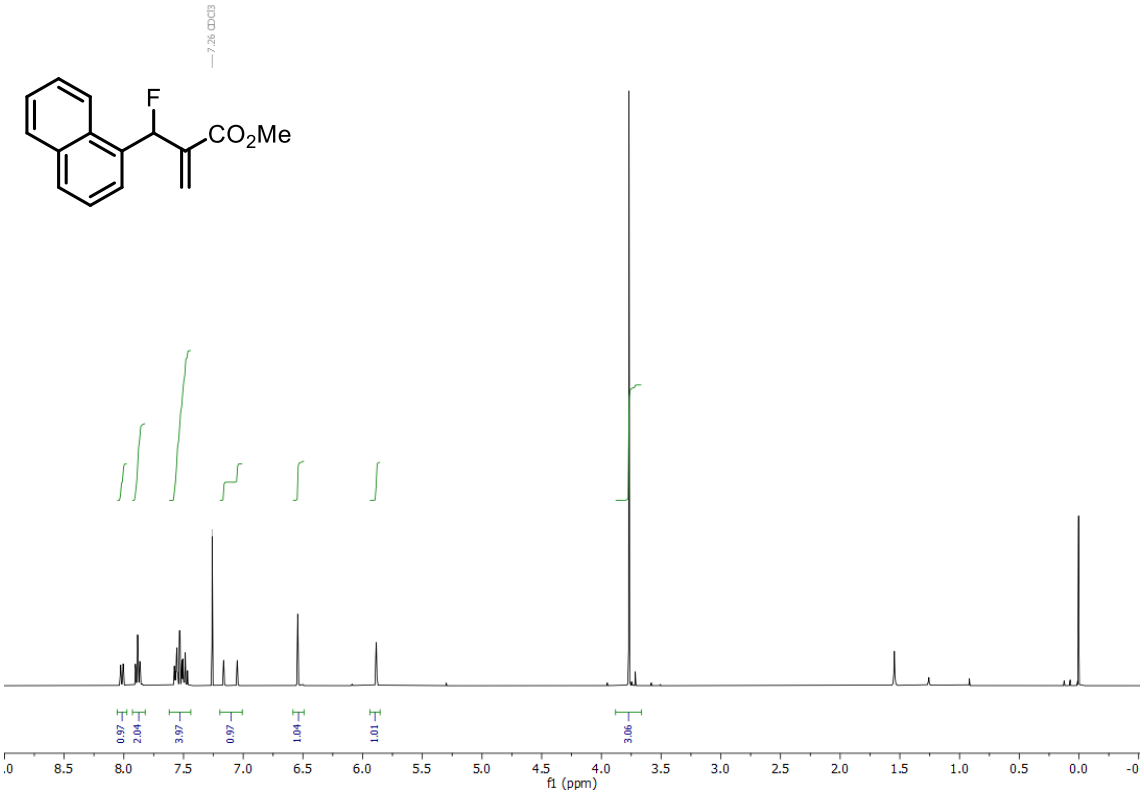

^{1}H NMR spectra of **2n**.

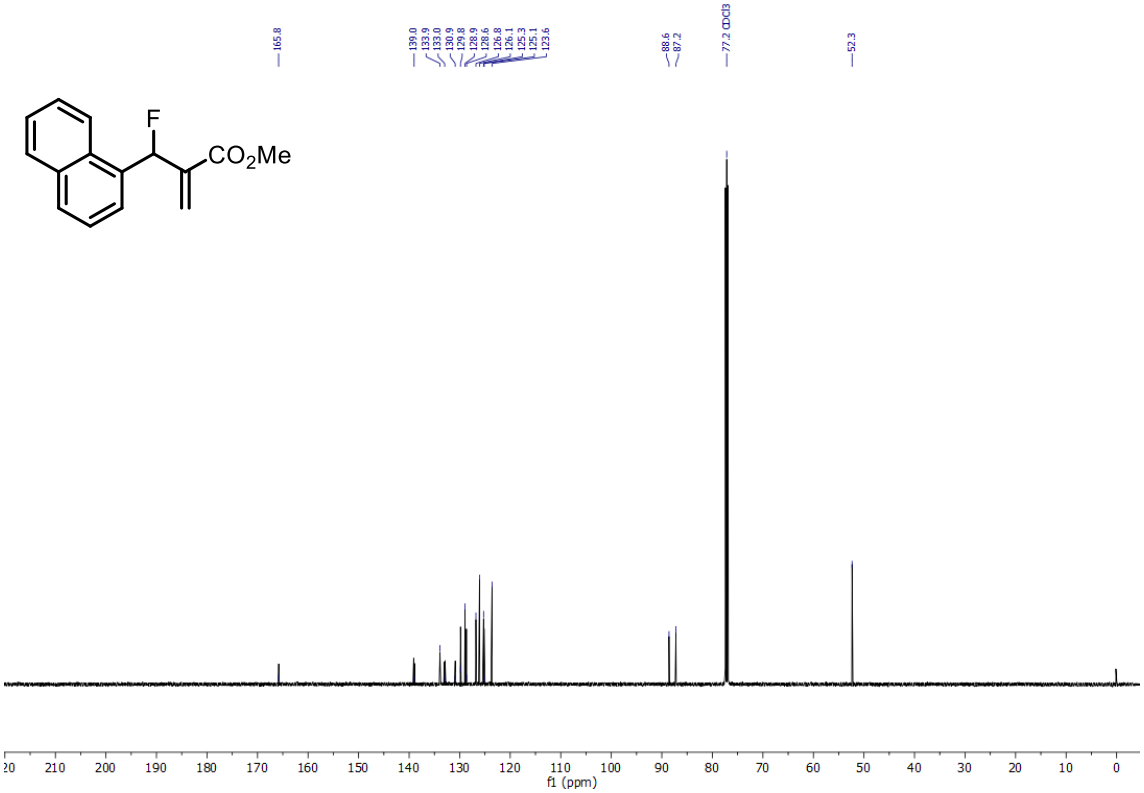

^{13}C NMR spectra of **2n**.

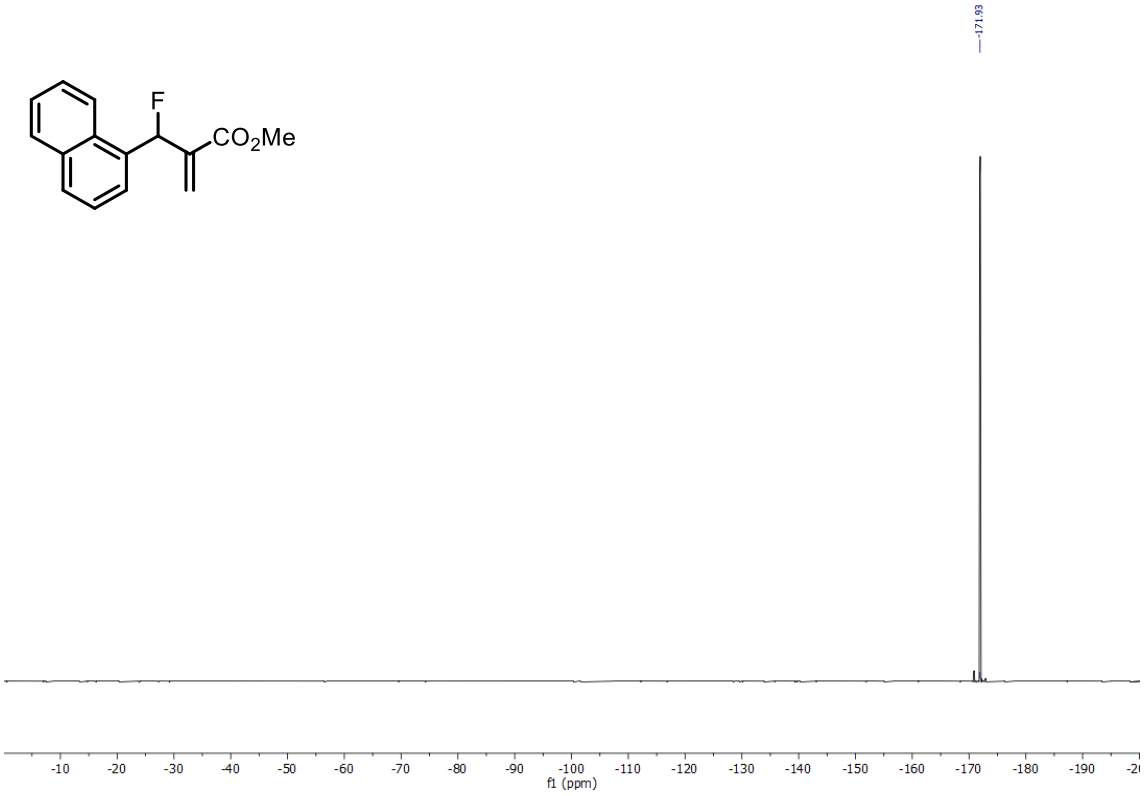

^{19}F NMR spectra of **2n**.

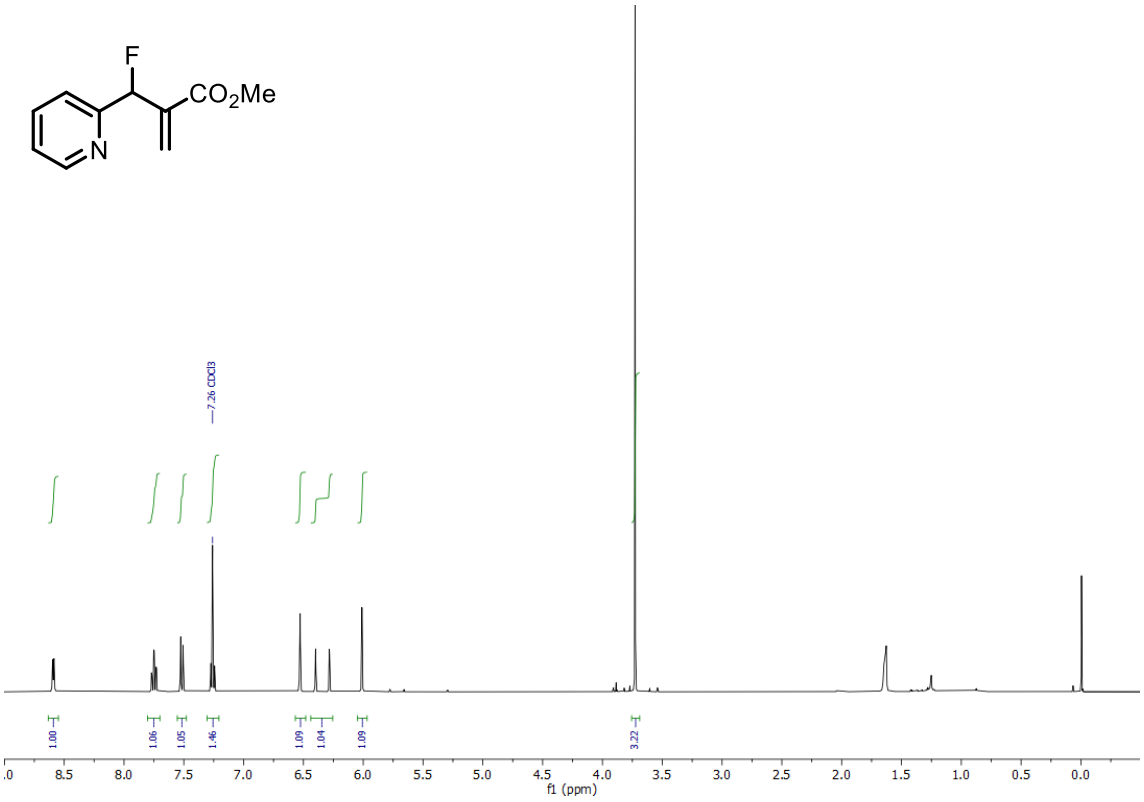

^{1}H NMR spectra of **2o**.

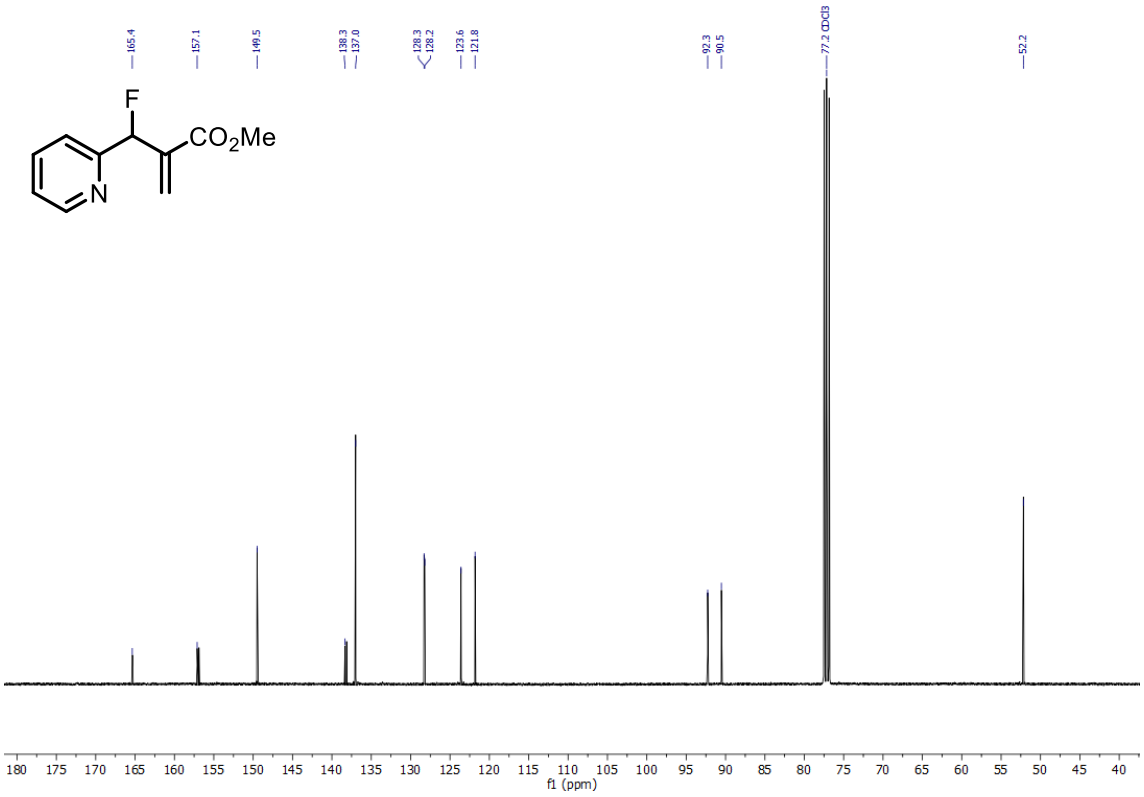

^{13}C NMR spectra of **2o**.

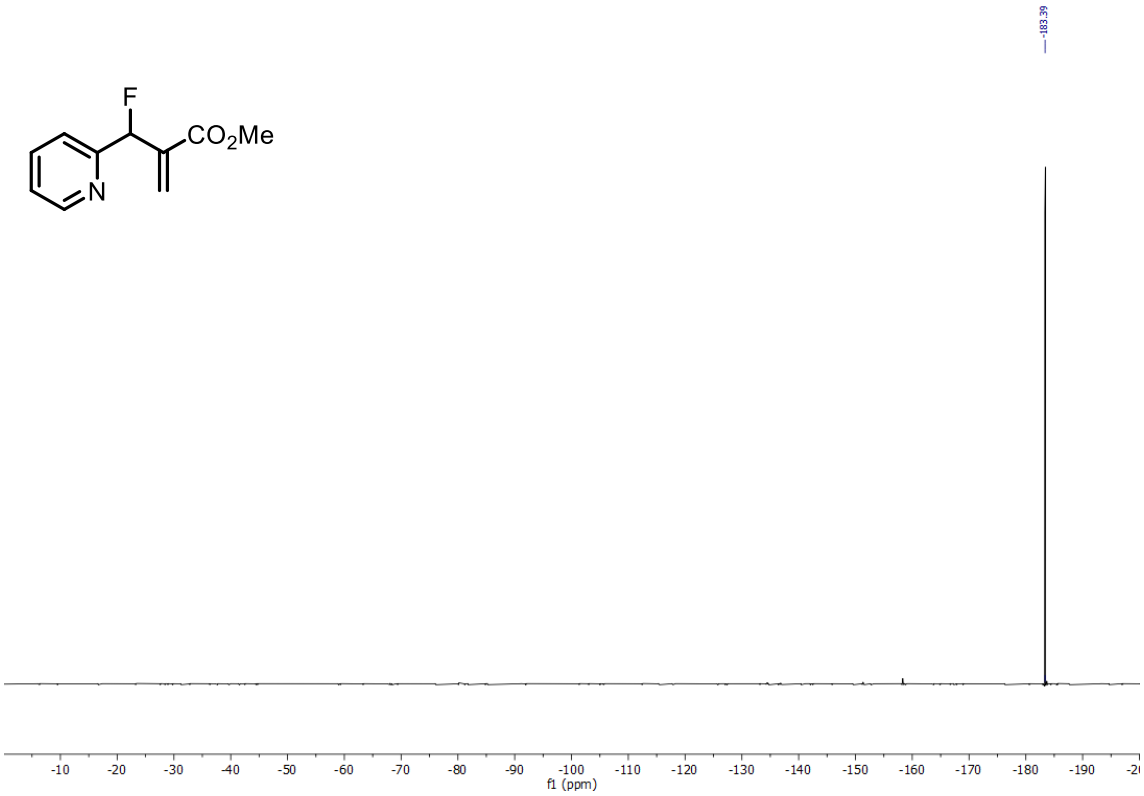

^{19}F NMR spectra of **2o**.

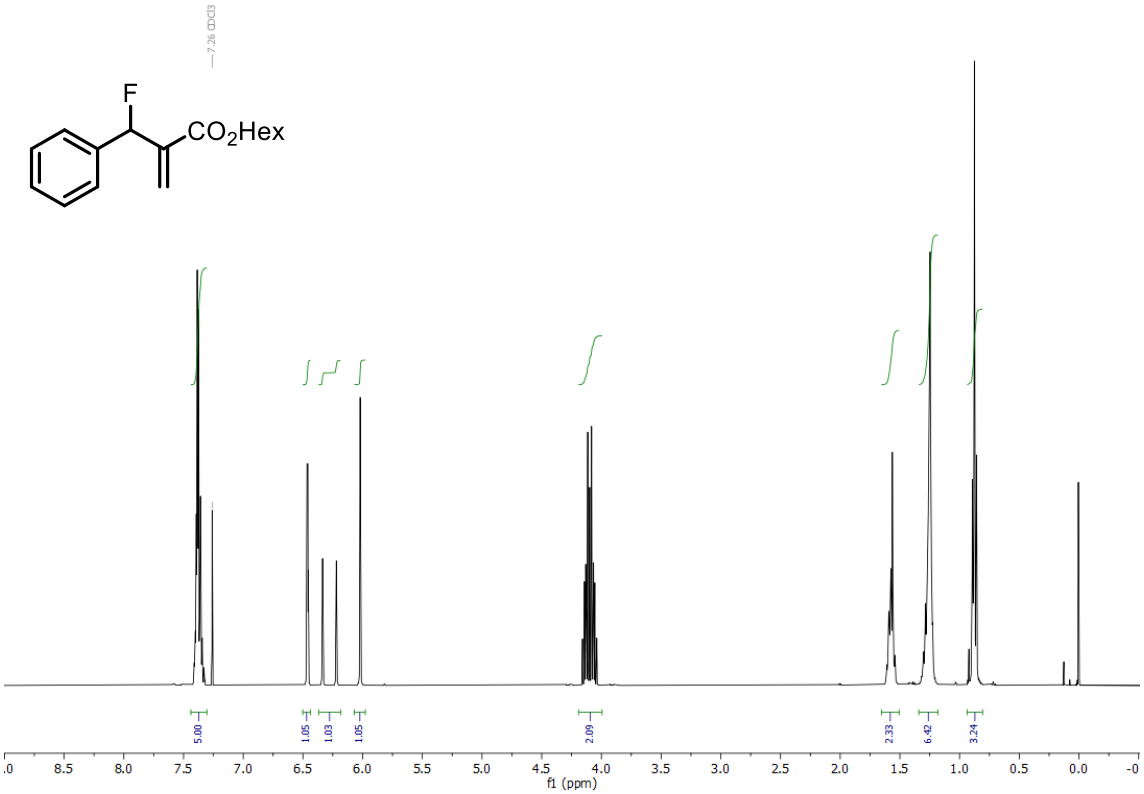

^{1}H NMR spectra of **2q**.

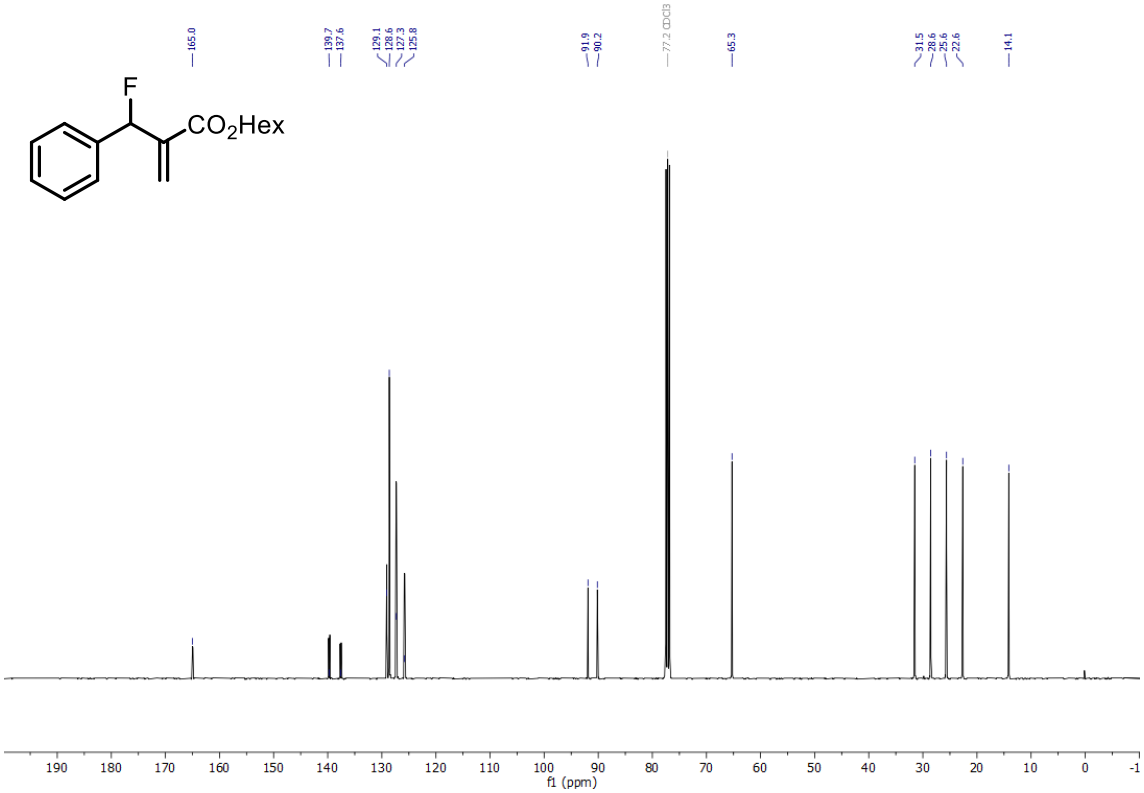

^{13}C NMR spectra of **2q**.

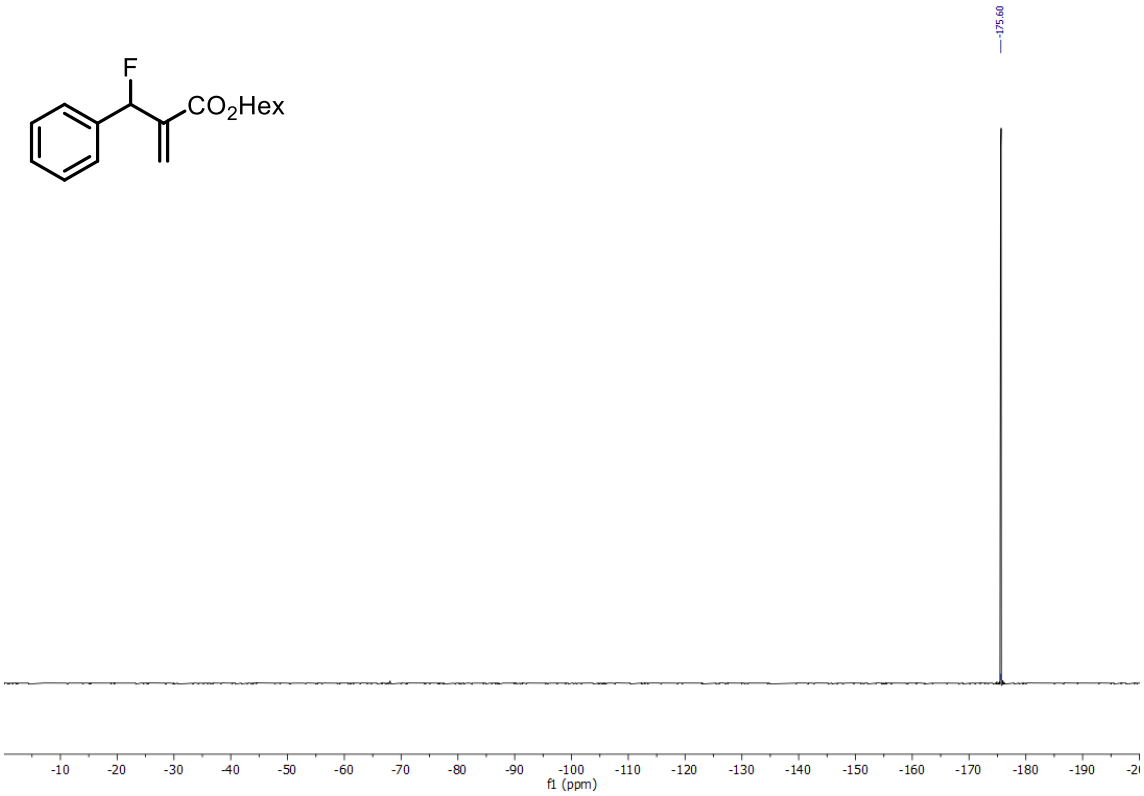

^{19}F NMR spectra of **2q**.

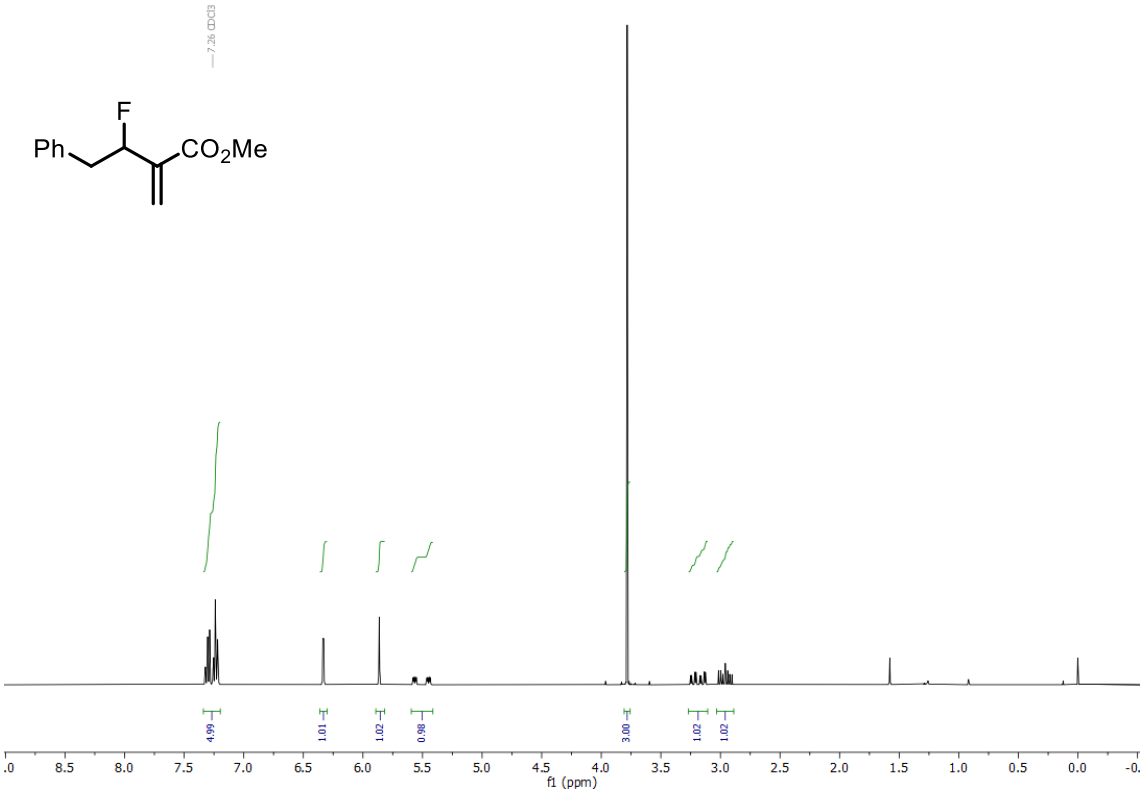

^{1}H NMR spectra of **2t**.

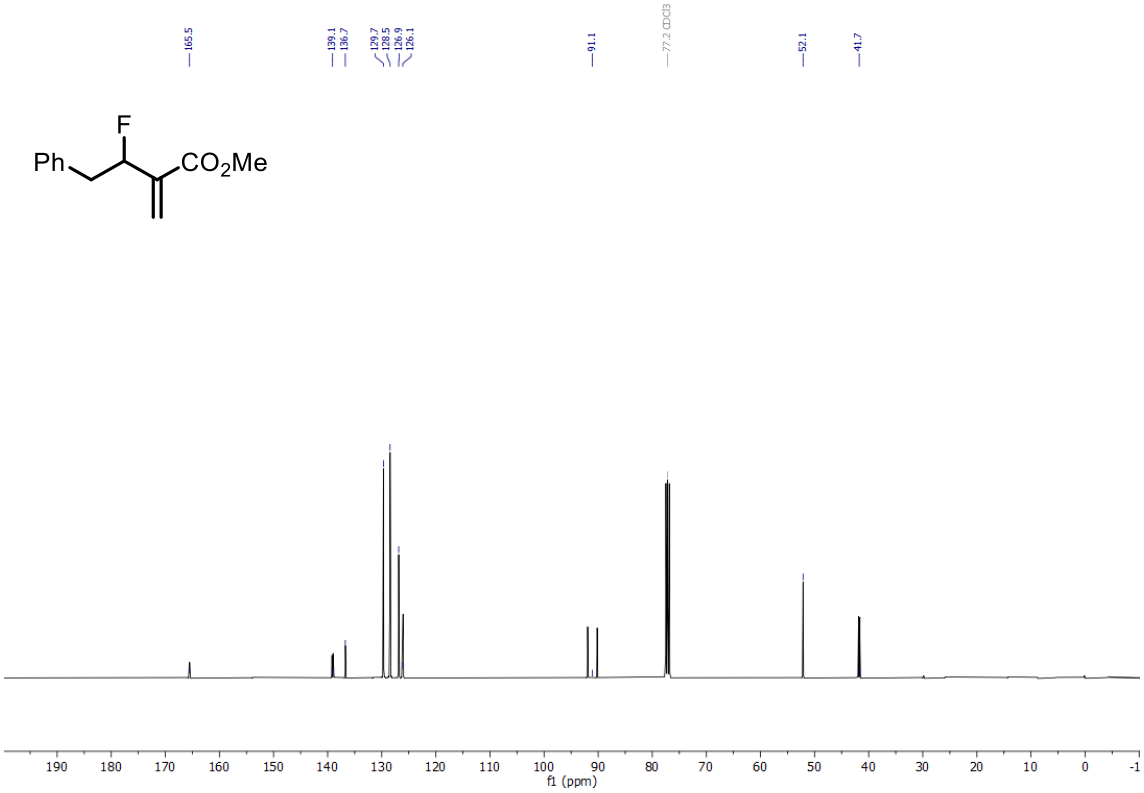

^{13}C NMR spectra of **2t**.

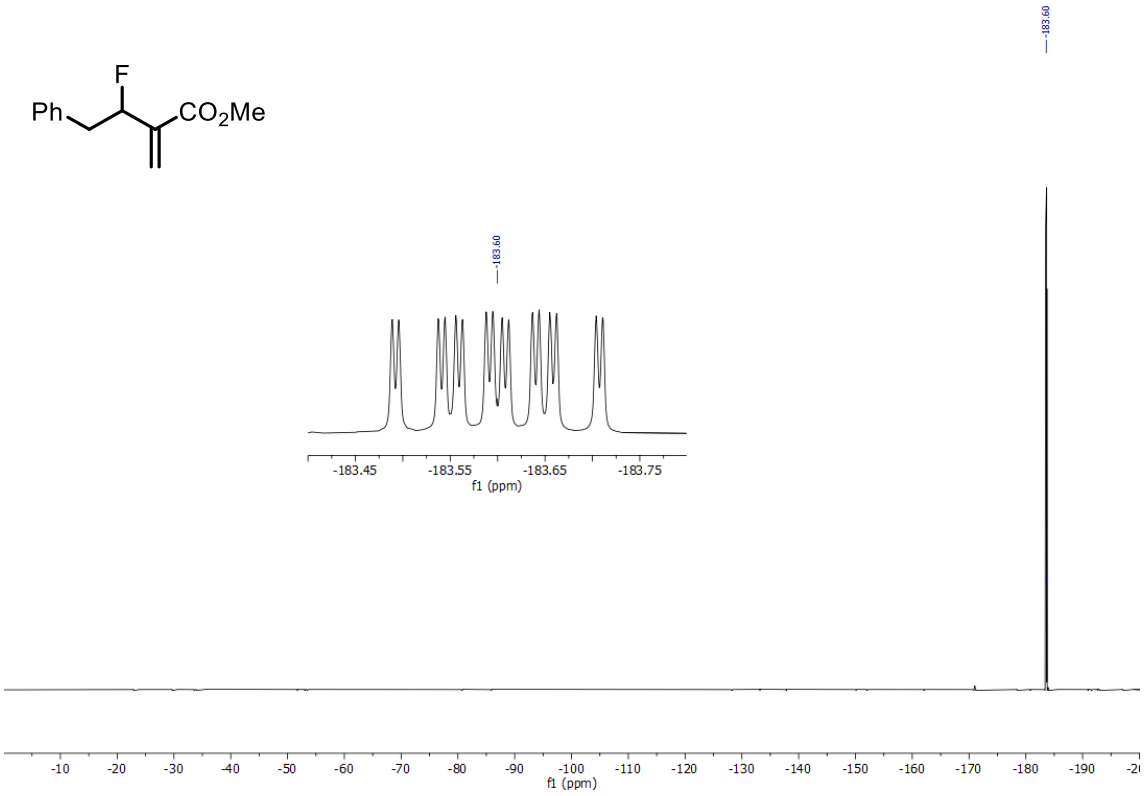

^{19}F NMR spectra of **2t**.

N.2. NMR spectra of silyl enol ethers

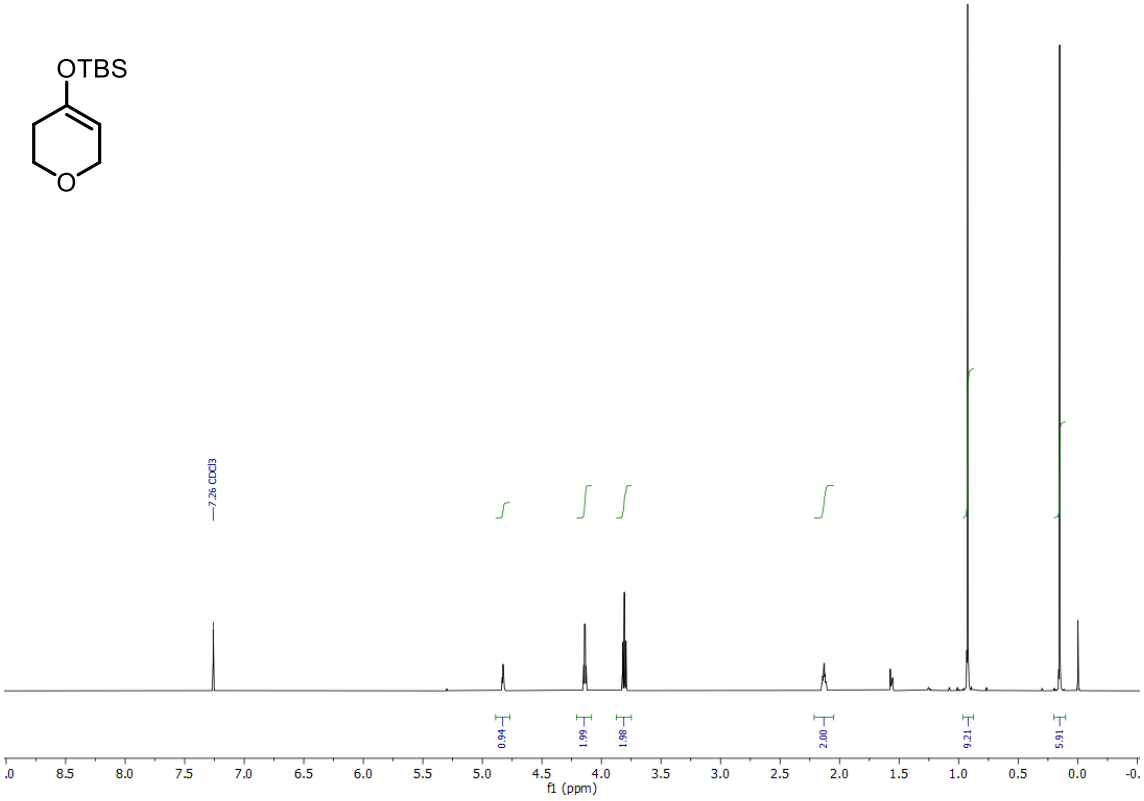

^{1}H NMR spectra of **1h**.

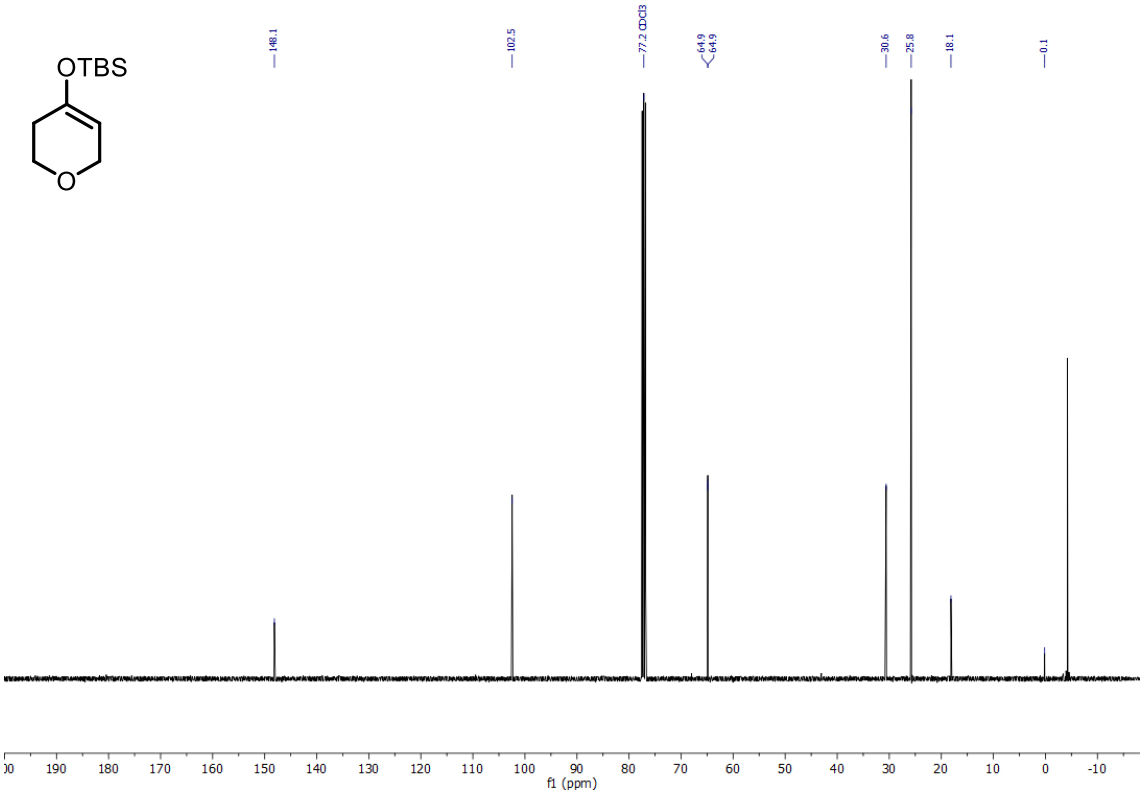

^{13}C NMR spectra of **1h**.

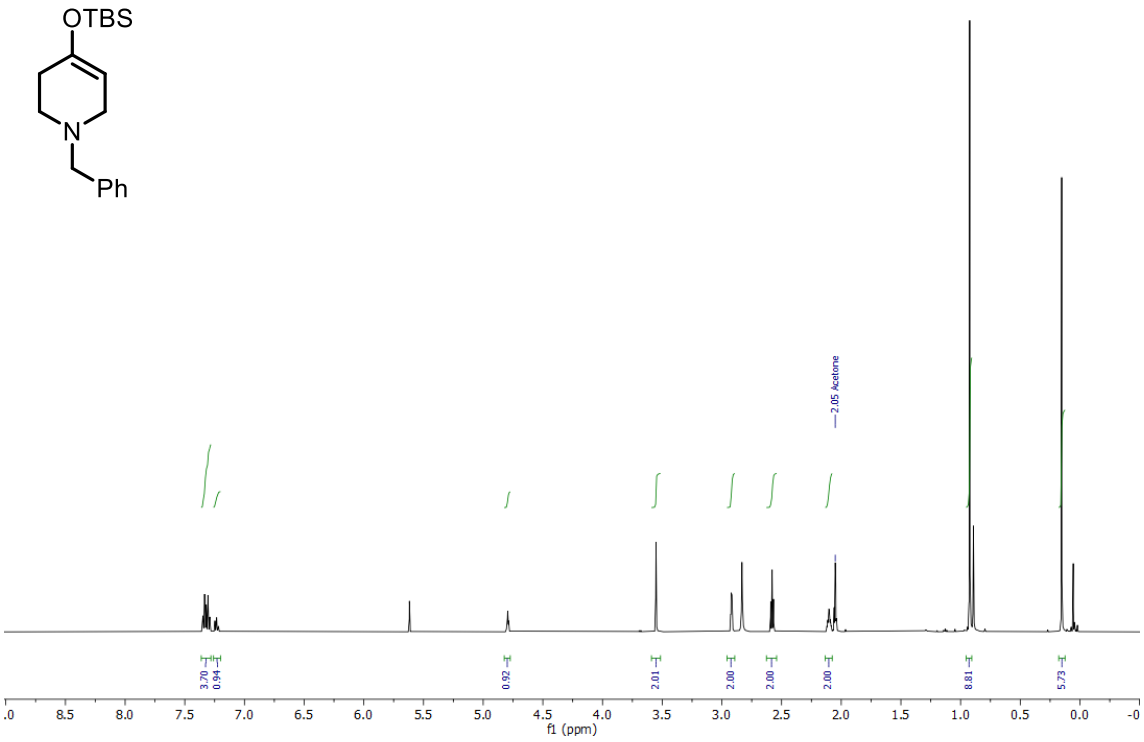

^{1}H NMR spectra of **1r**.

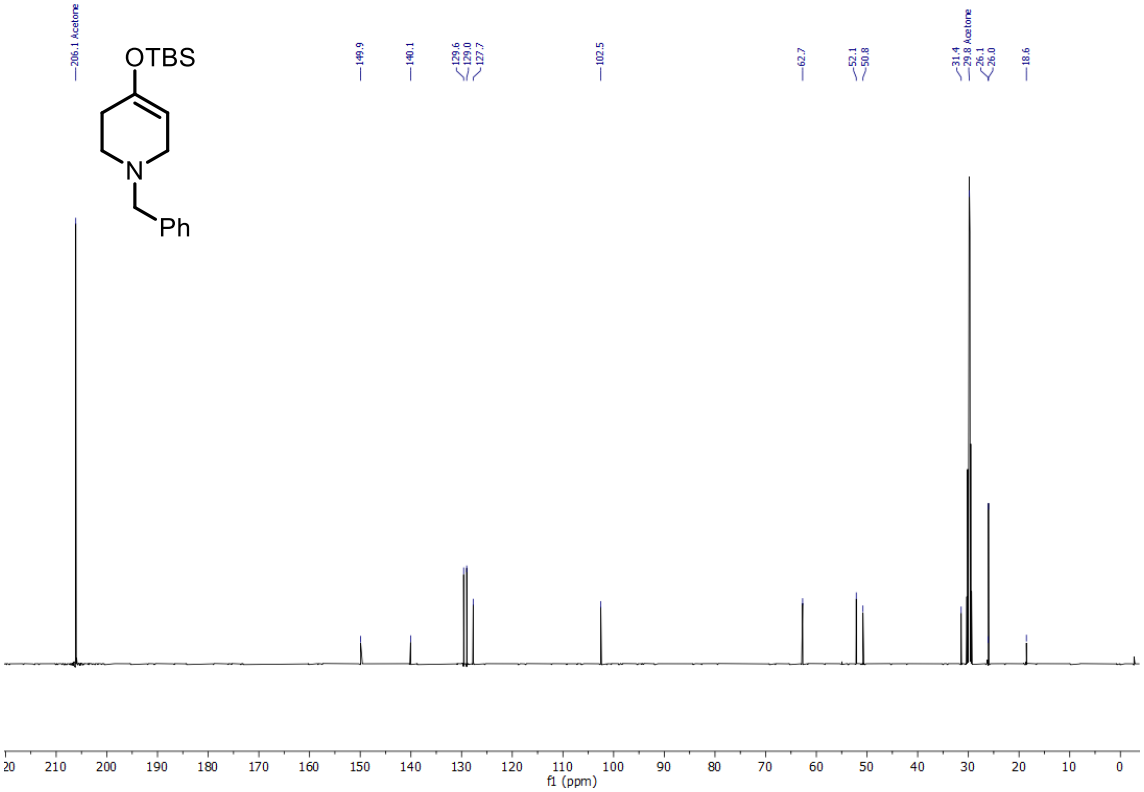

^{13}C NMR spectra of **1r**.

N.3. NMR spectra of enol carbonate

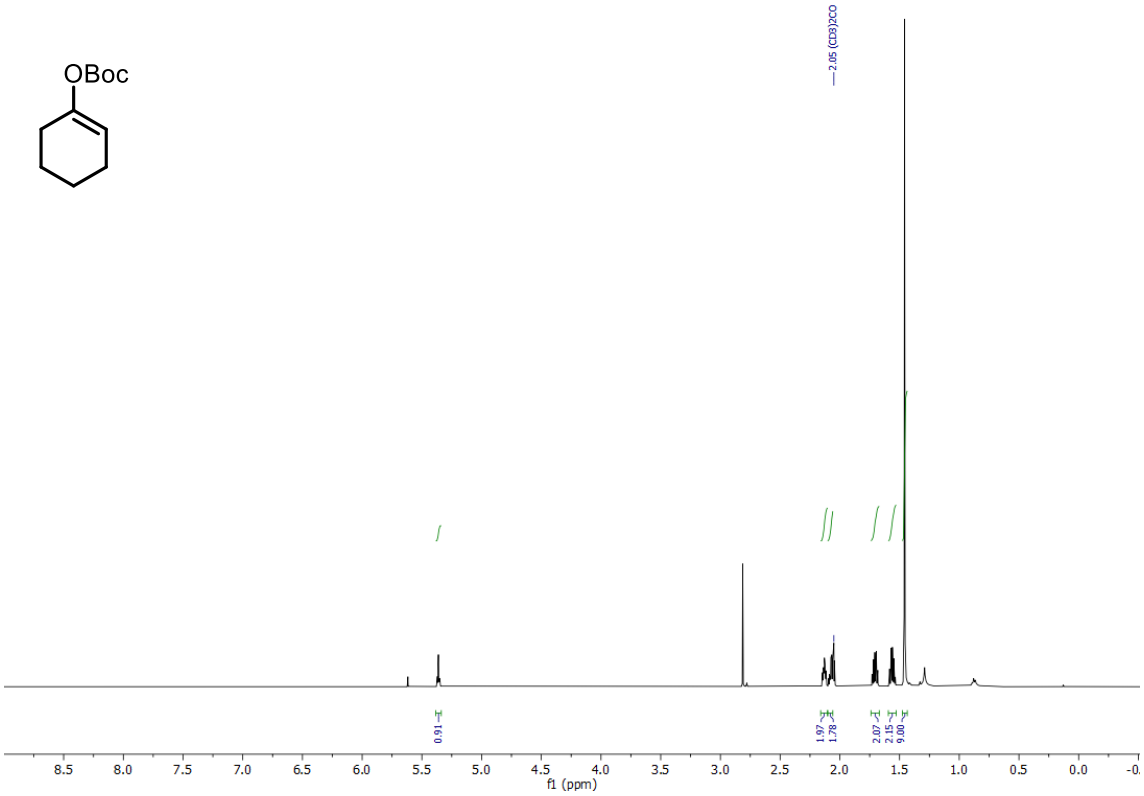

^{1}H NMR spectra of **S7a**.

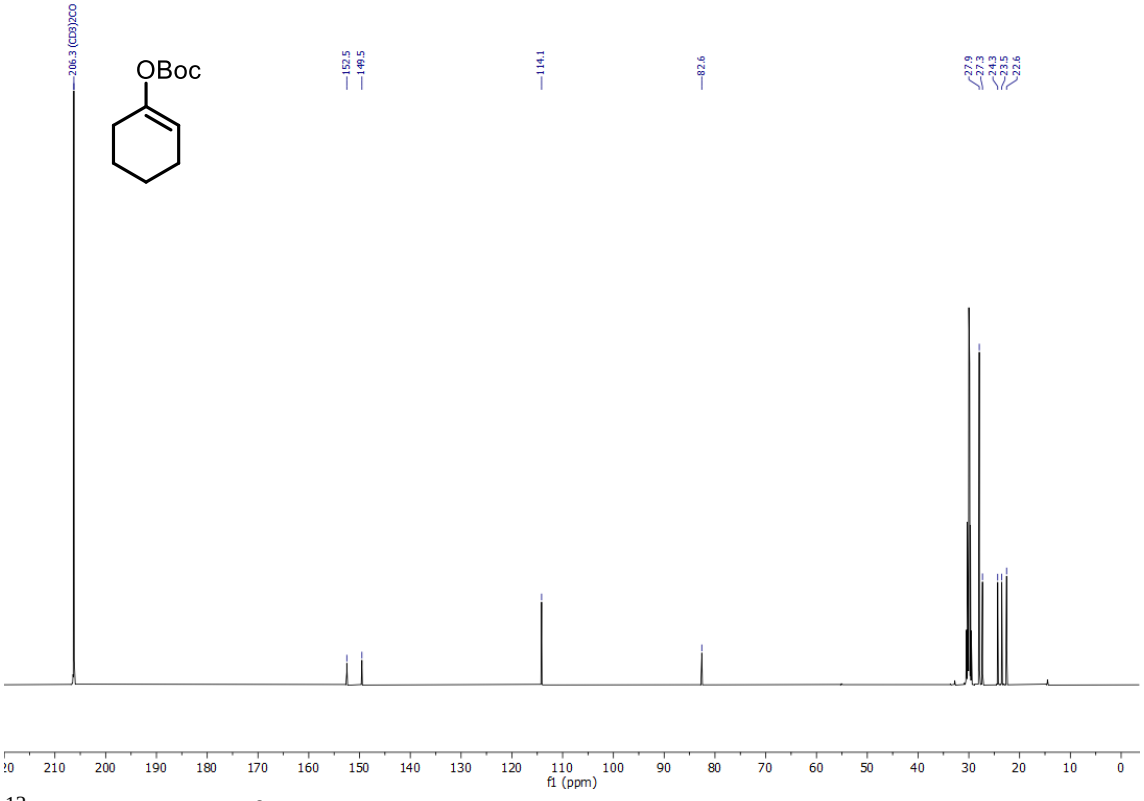

^{13}C NMR spectra of **S7a**.

N.4. NMR spectra of products 3a-ae and 4a

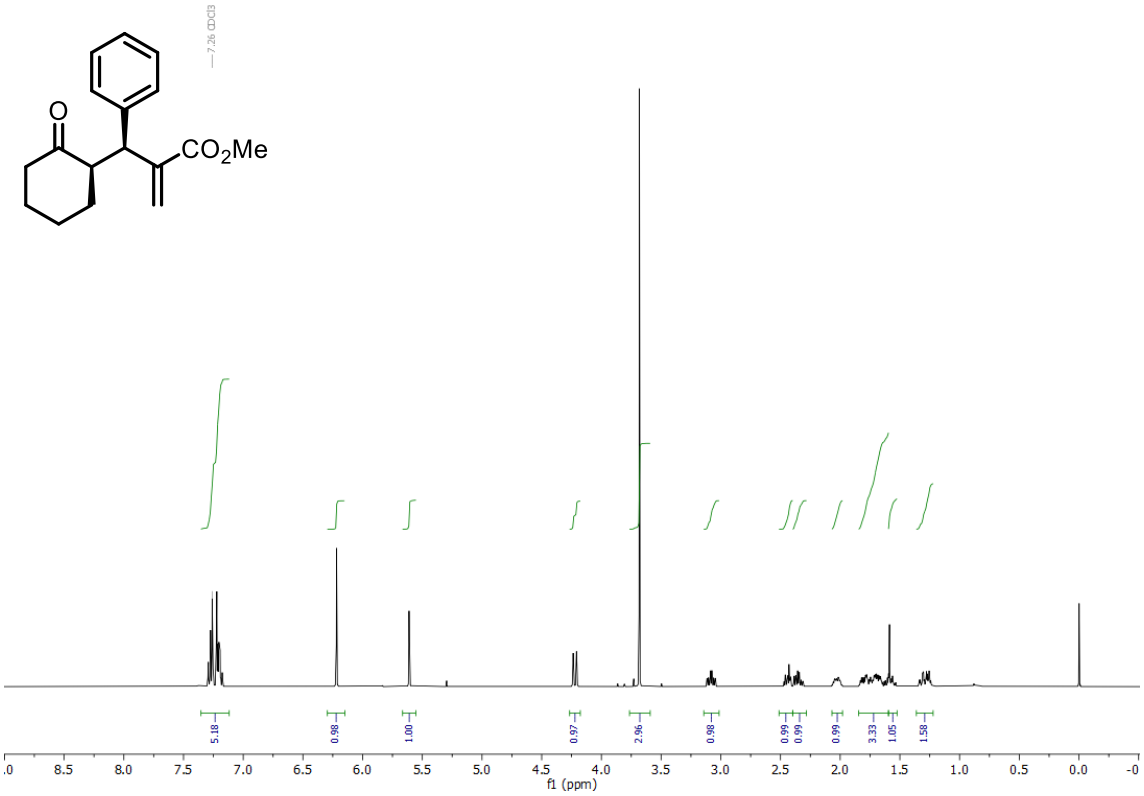

^{1}H NMR spectra of **3a**.

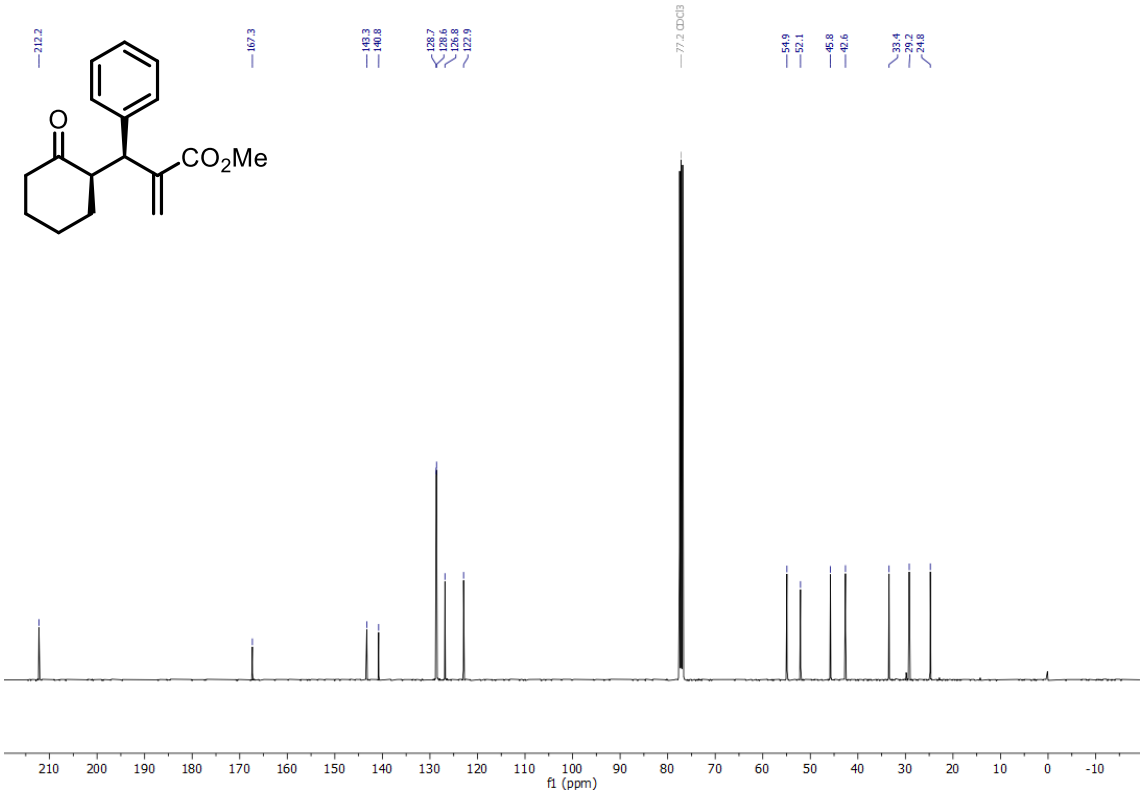

^{13}C NMR spectra of **3a**.

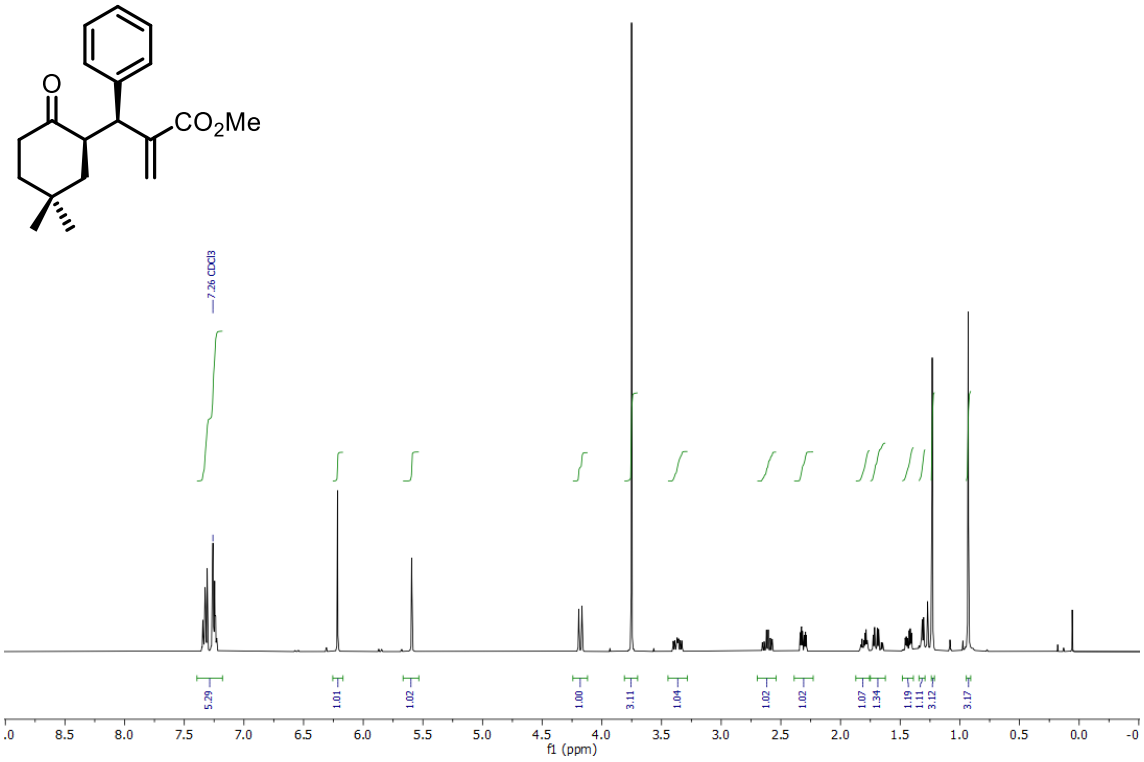

^{1}H NMR spectra of **3b**.

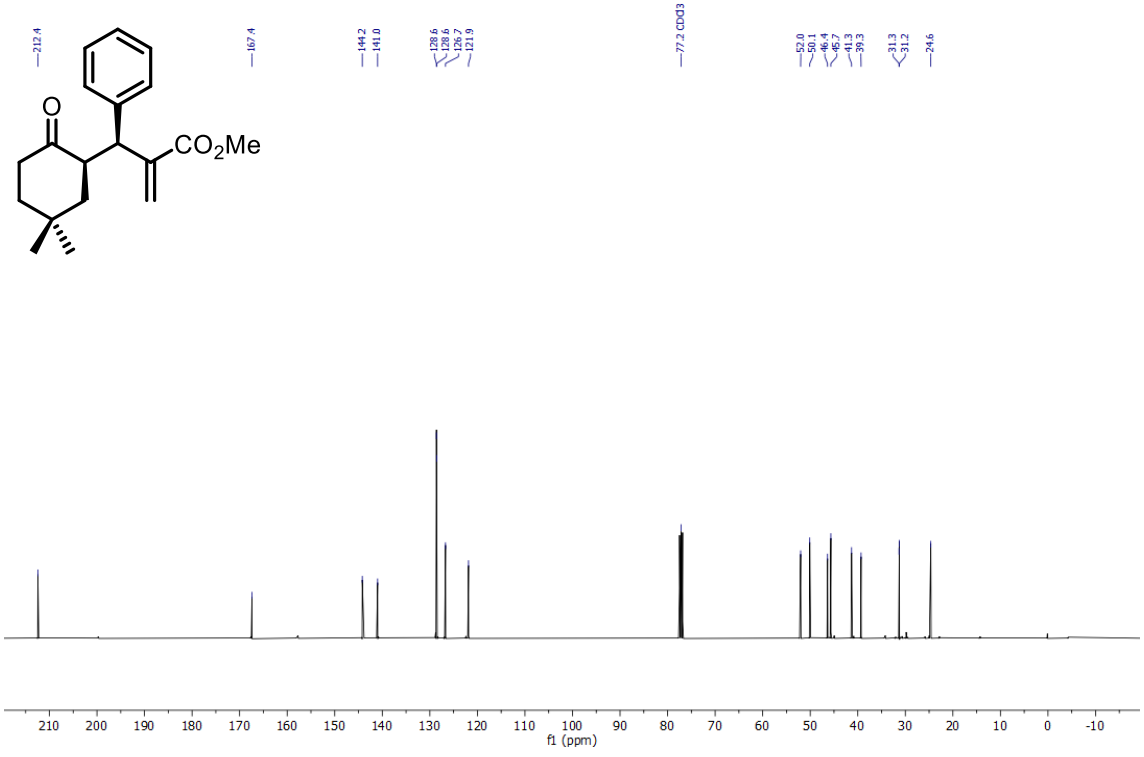

^{13}C NMR spectra of **3b**.

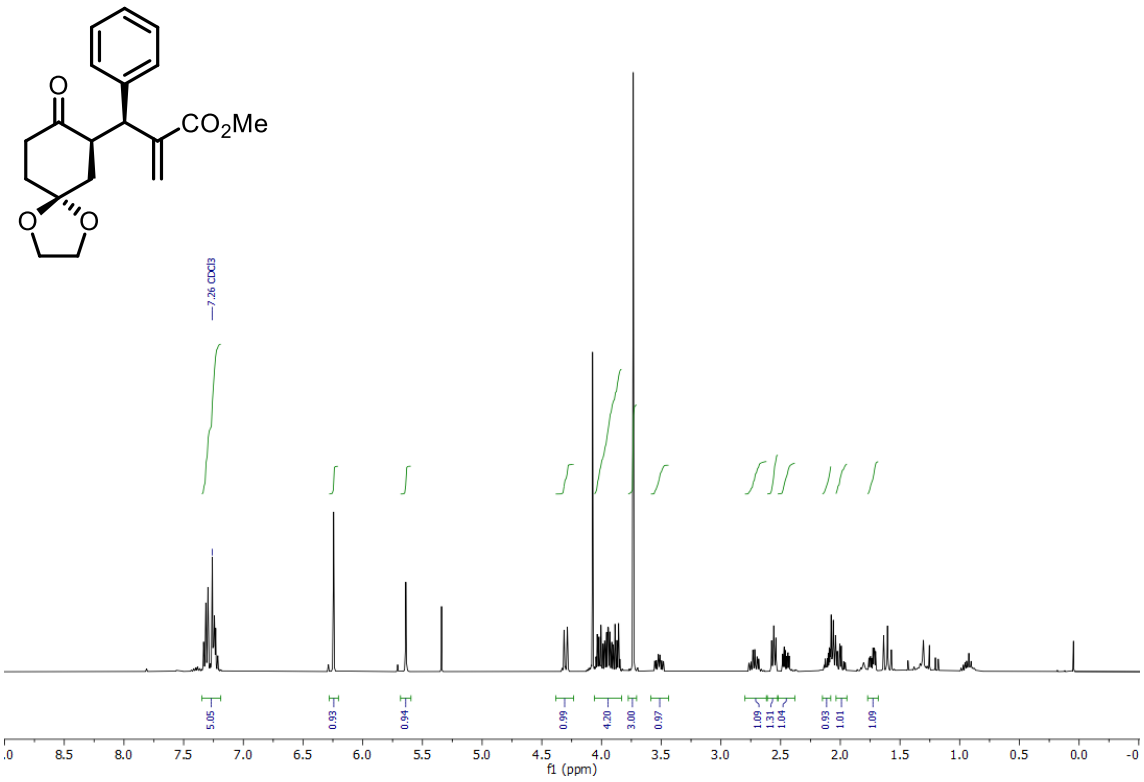

^{1}H NMR spectra of **3c**.

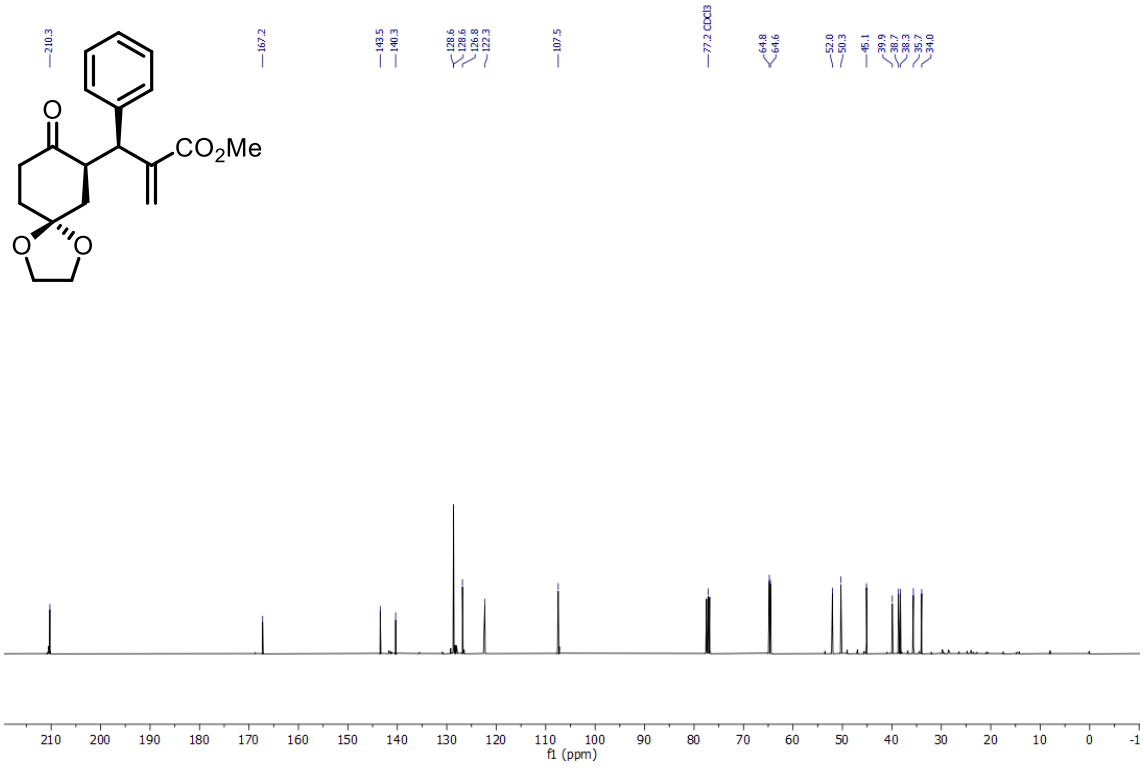

^{13}C NMR spectra of **3c**.

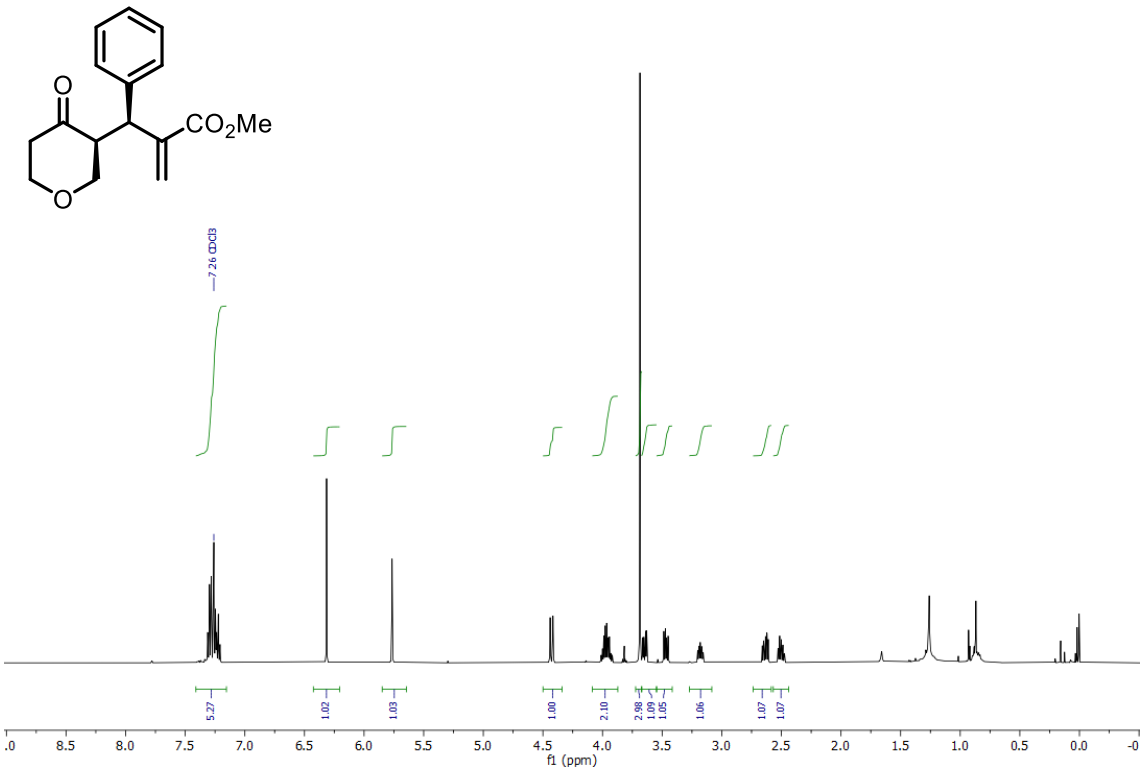

^{1}H NMR spectra of **3d**.

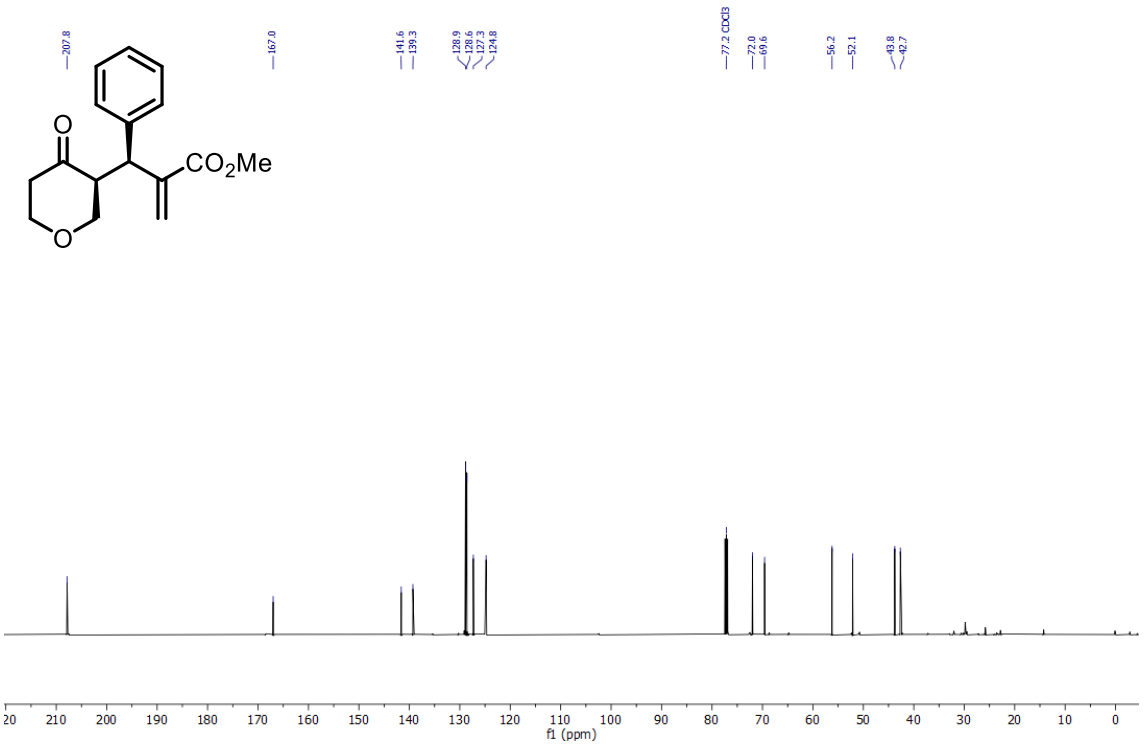

^{13}C NMR spectra of **3d**.

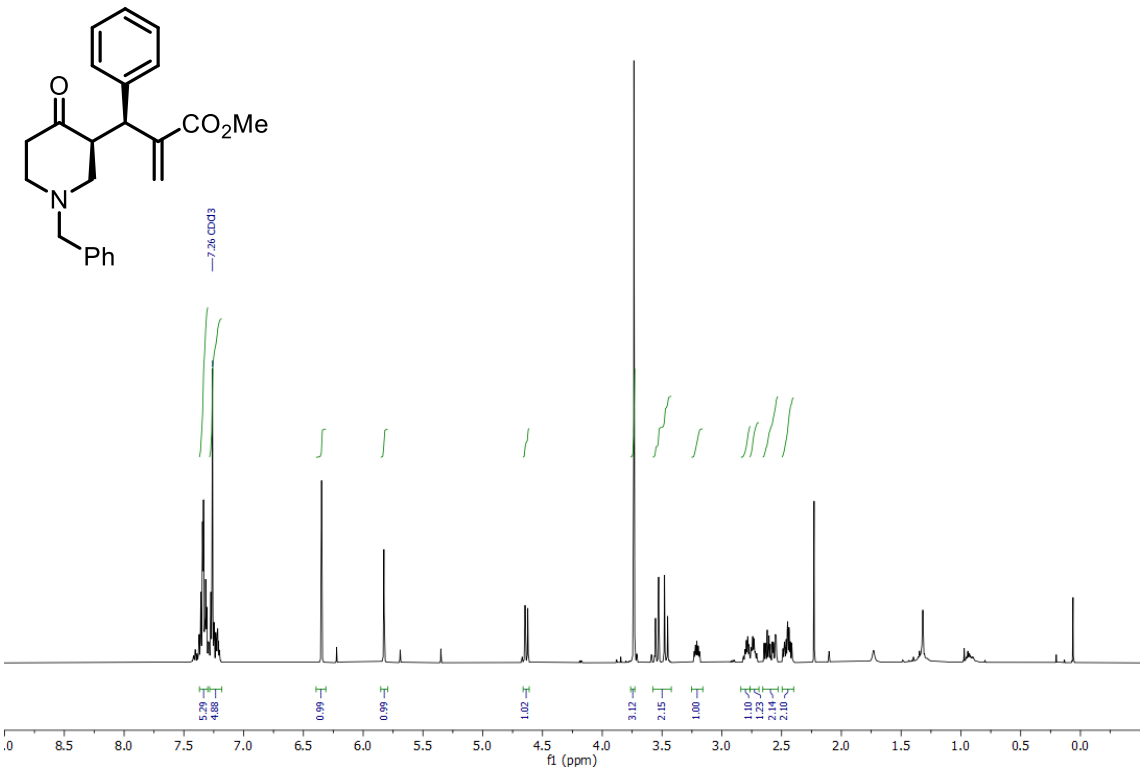

^{1}H NMR spectra of **3e**.

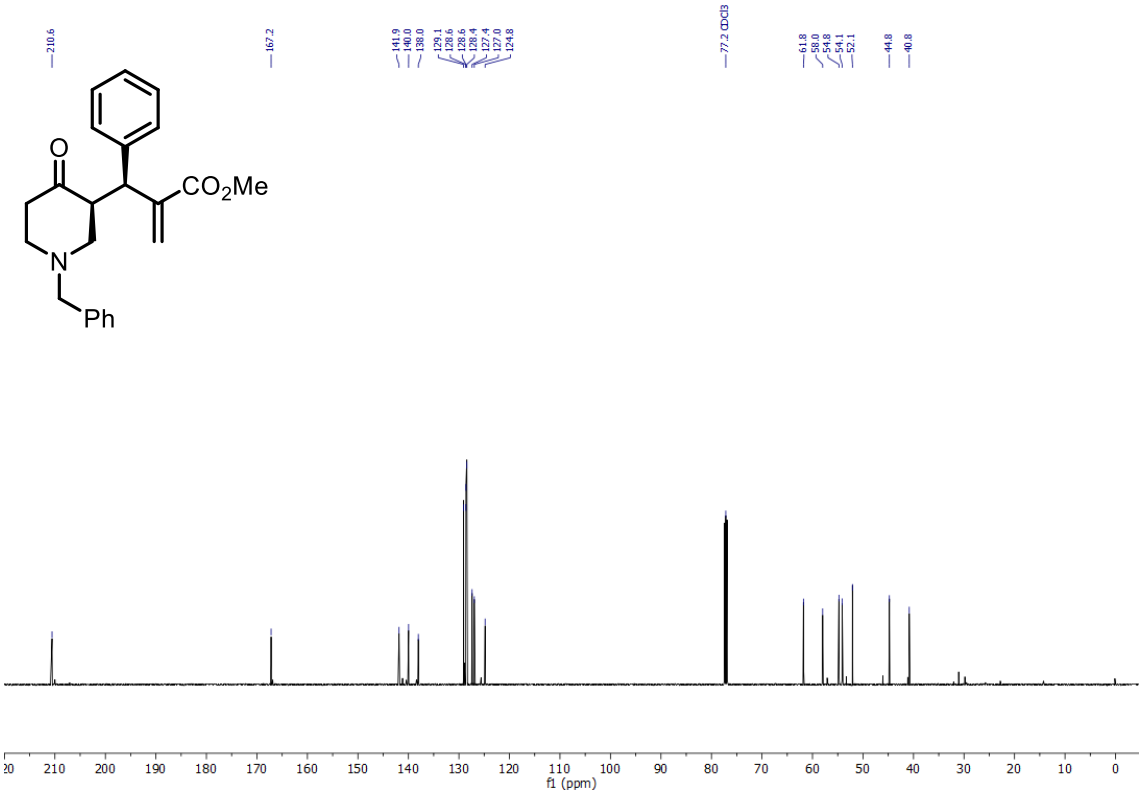

^{13}C NMR spectra of **3e**.

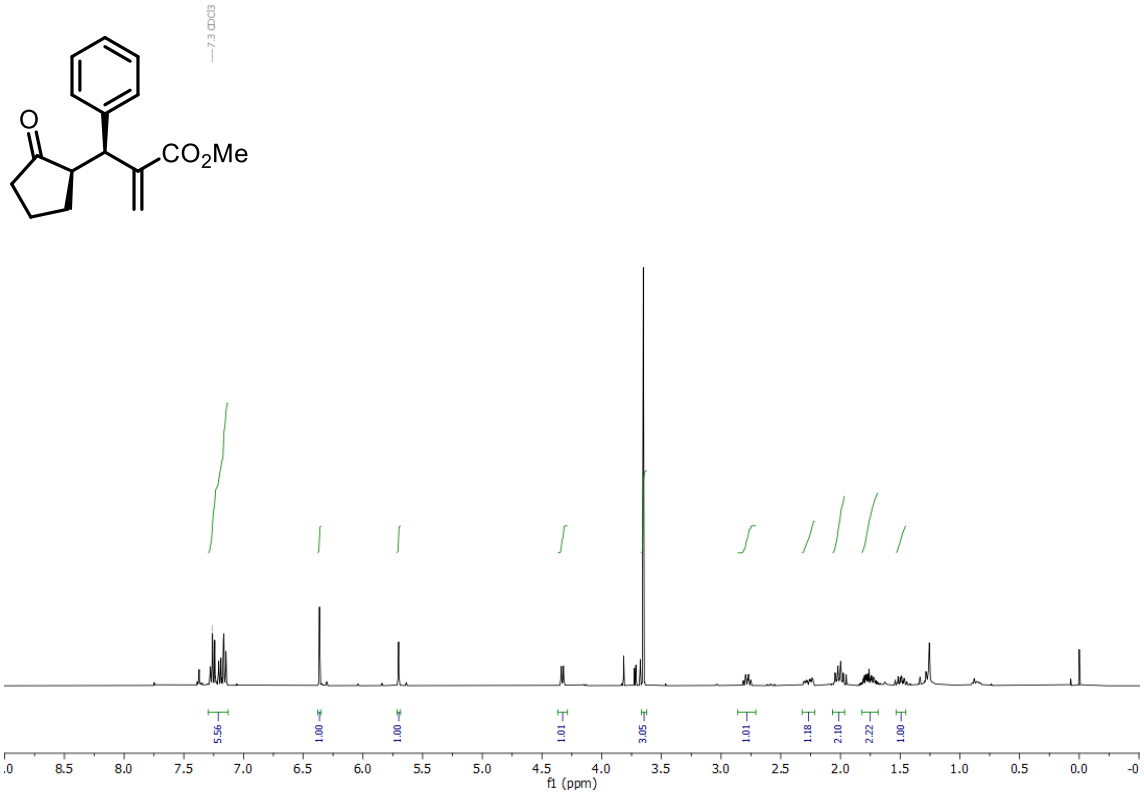

^{1}H NMR spectra of **3f**.

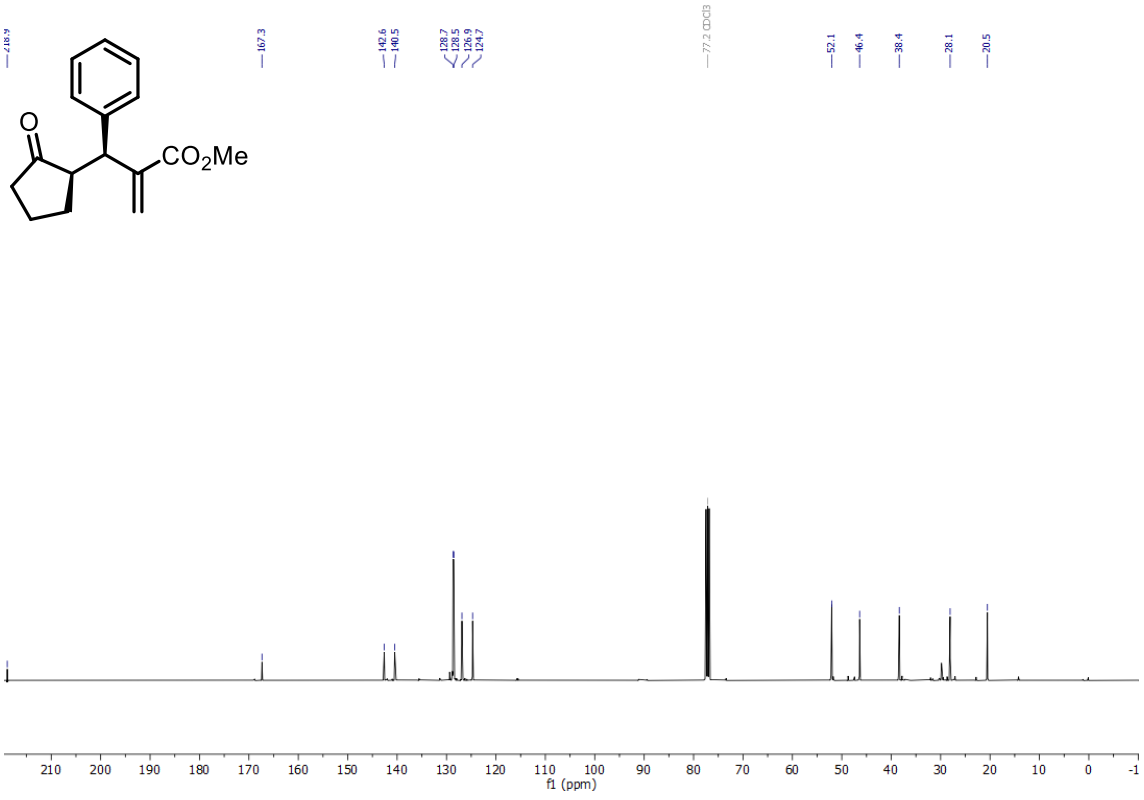

^{13}C NMR spectra of **3f.**

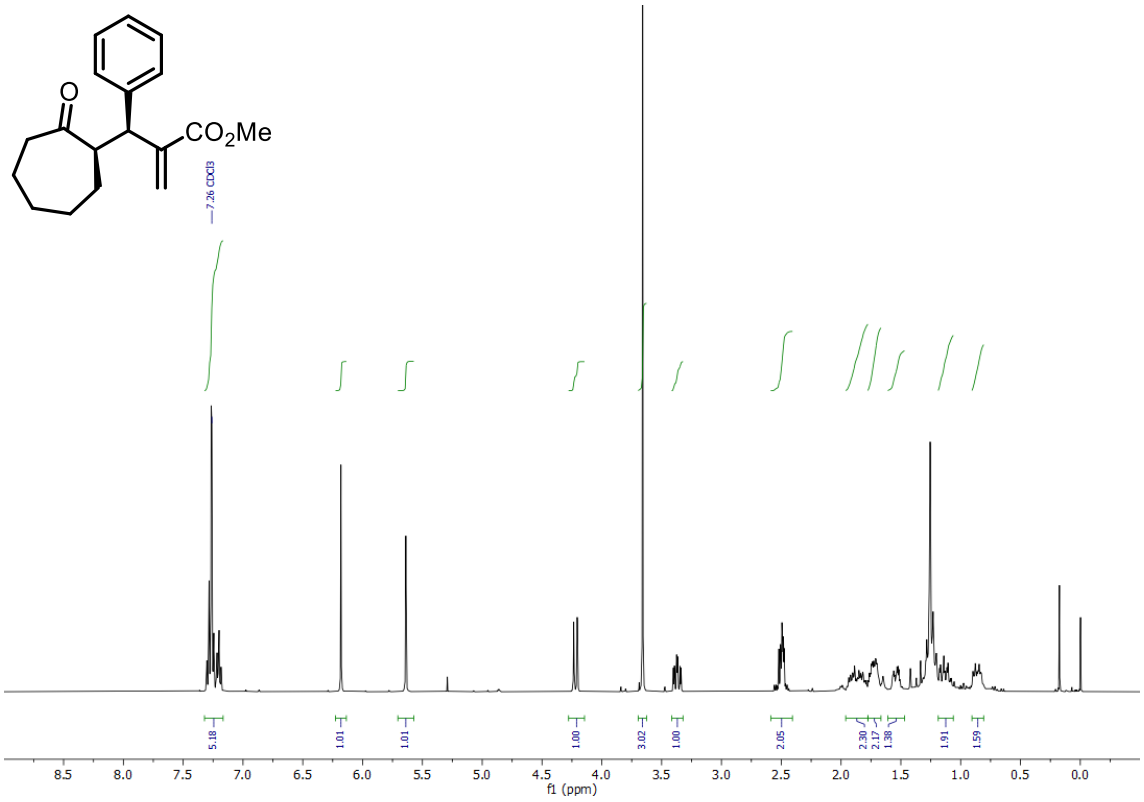

^{1}H NMR spectra of **3g**.

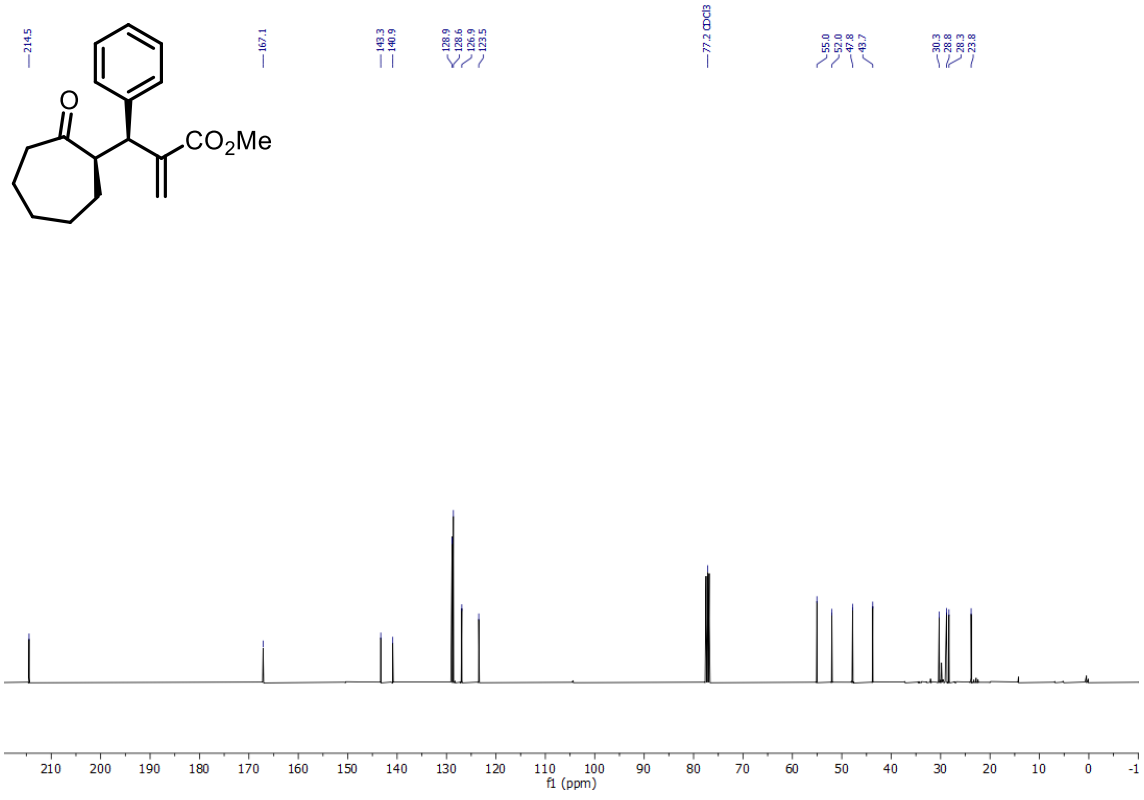

^{13}C NMR spectra of **3g**.

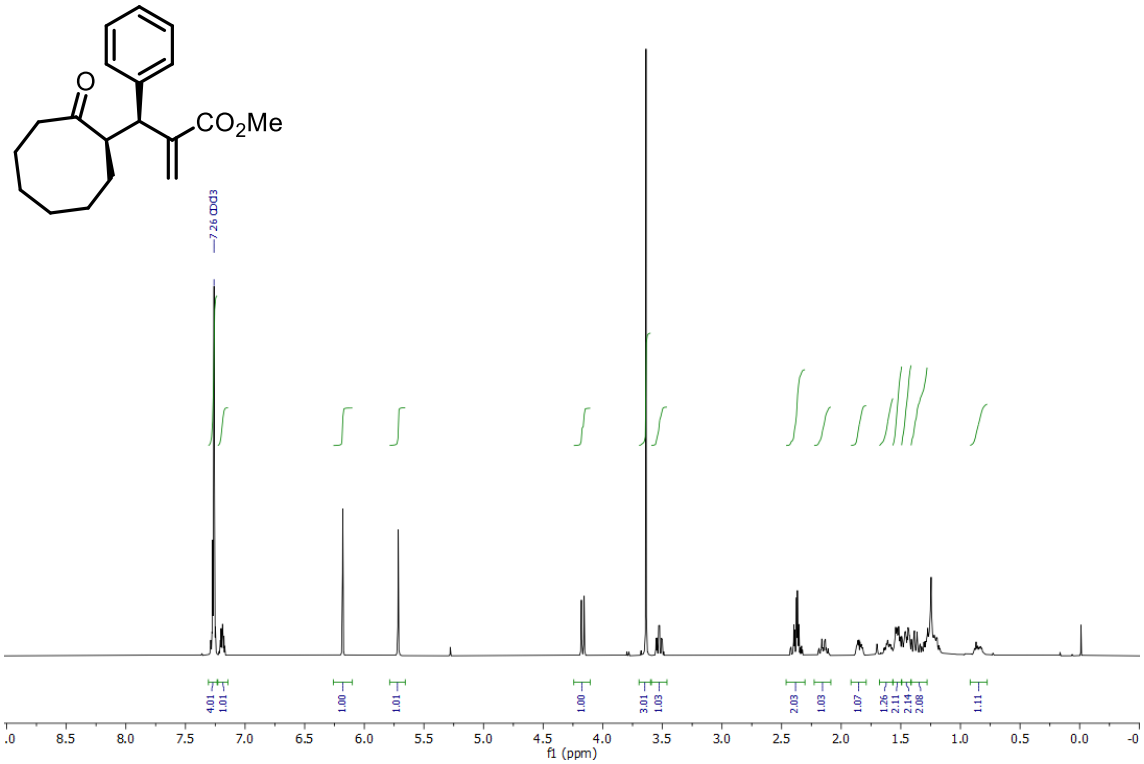

^{1}H NMR spectra of **3h**.

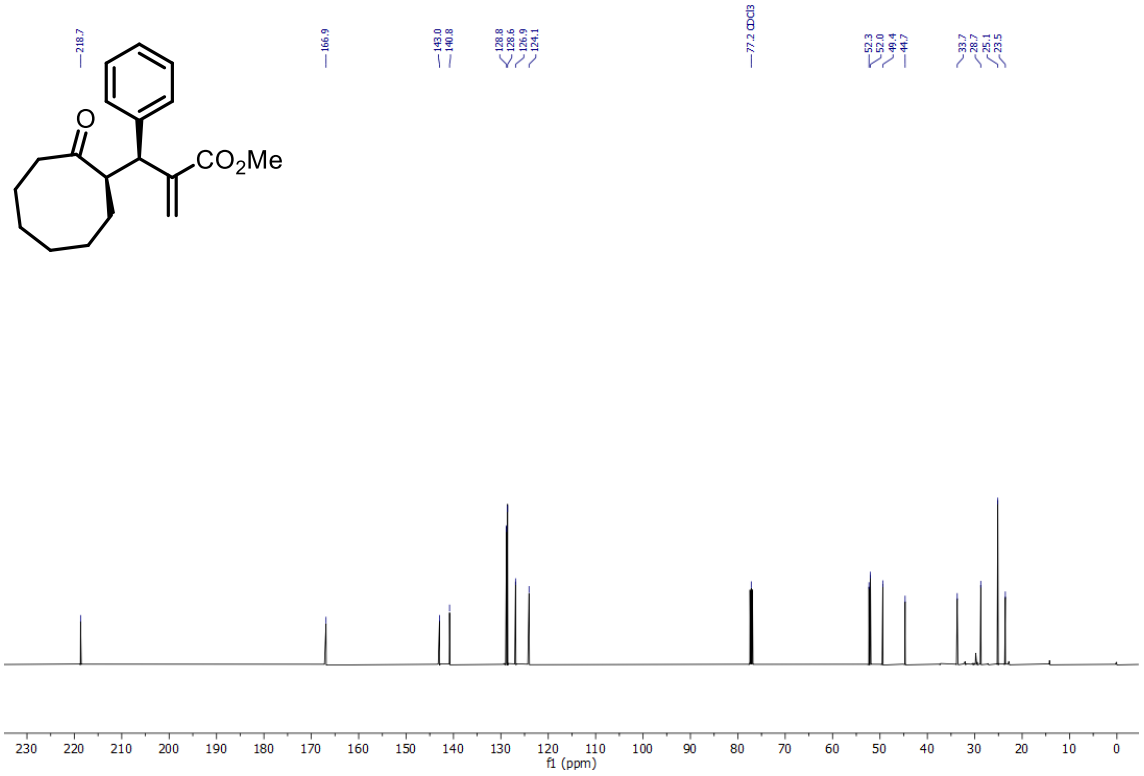

^{13}C NMR spectra of **3h**.

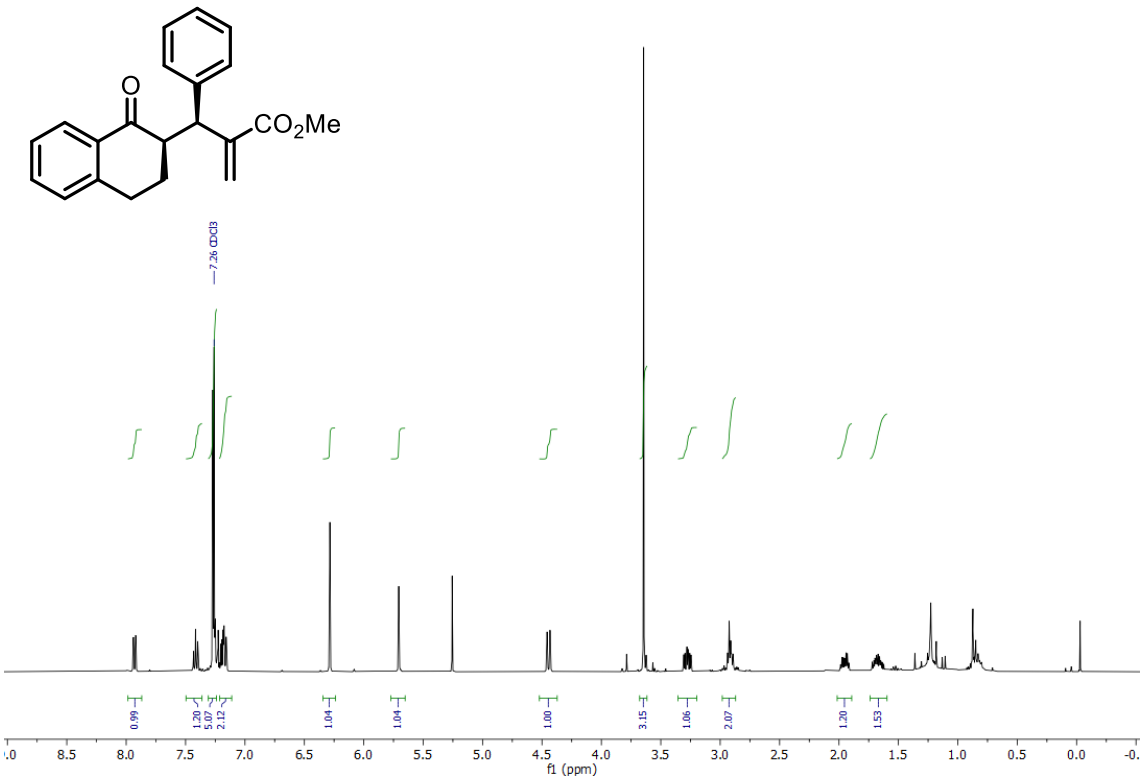

^{1}H NMR spectra of **3i**.

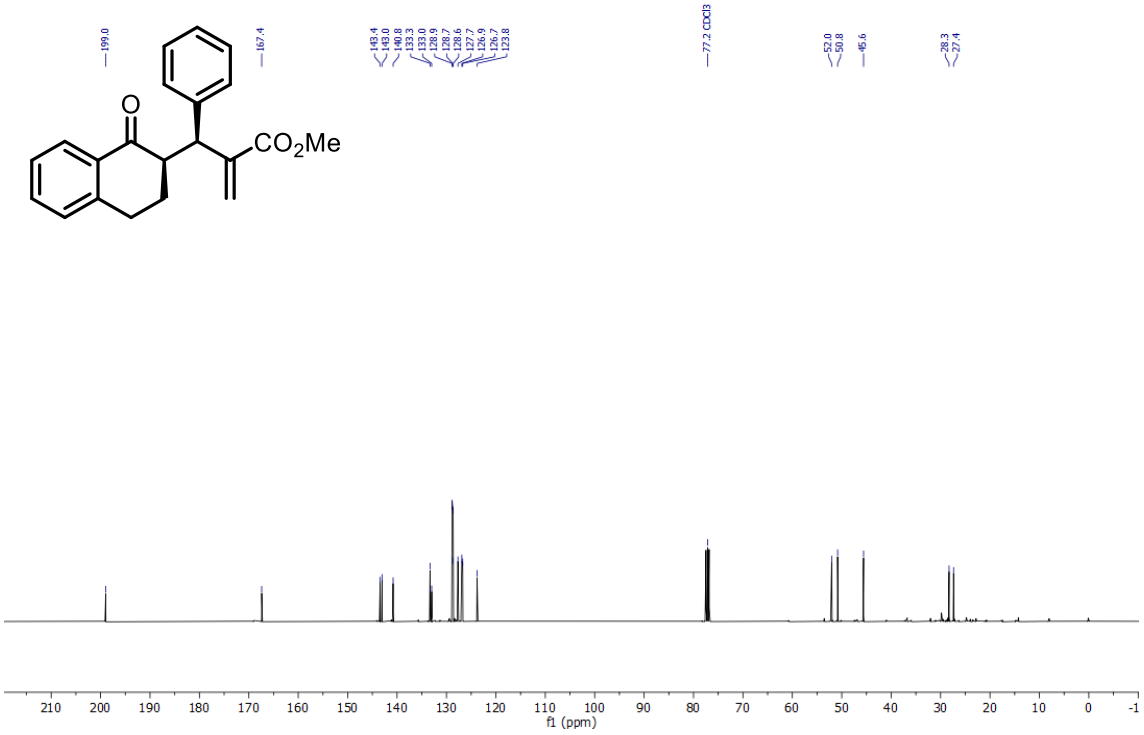

^{13}C NMR spectra of **3i**.

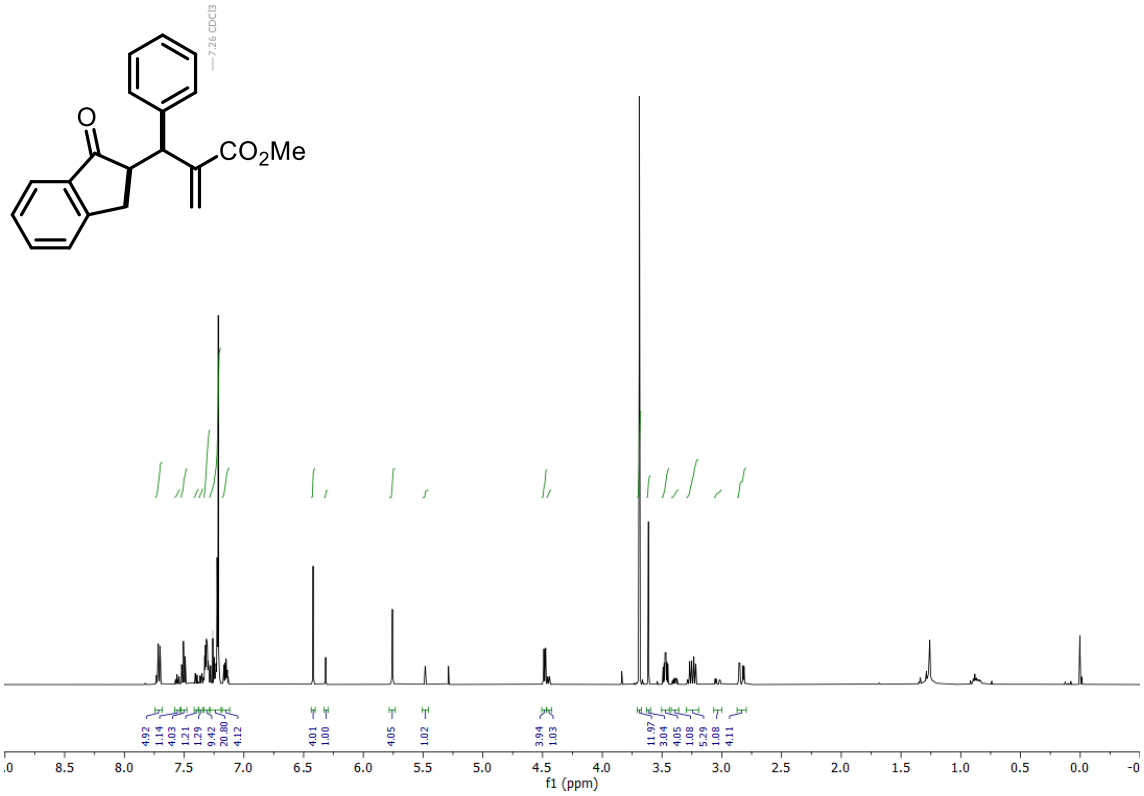

^{1}H NMR spectra of **3j** (mixture of diastereomers).

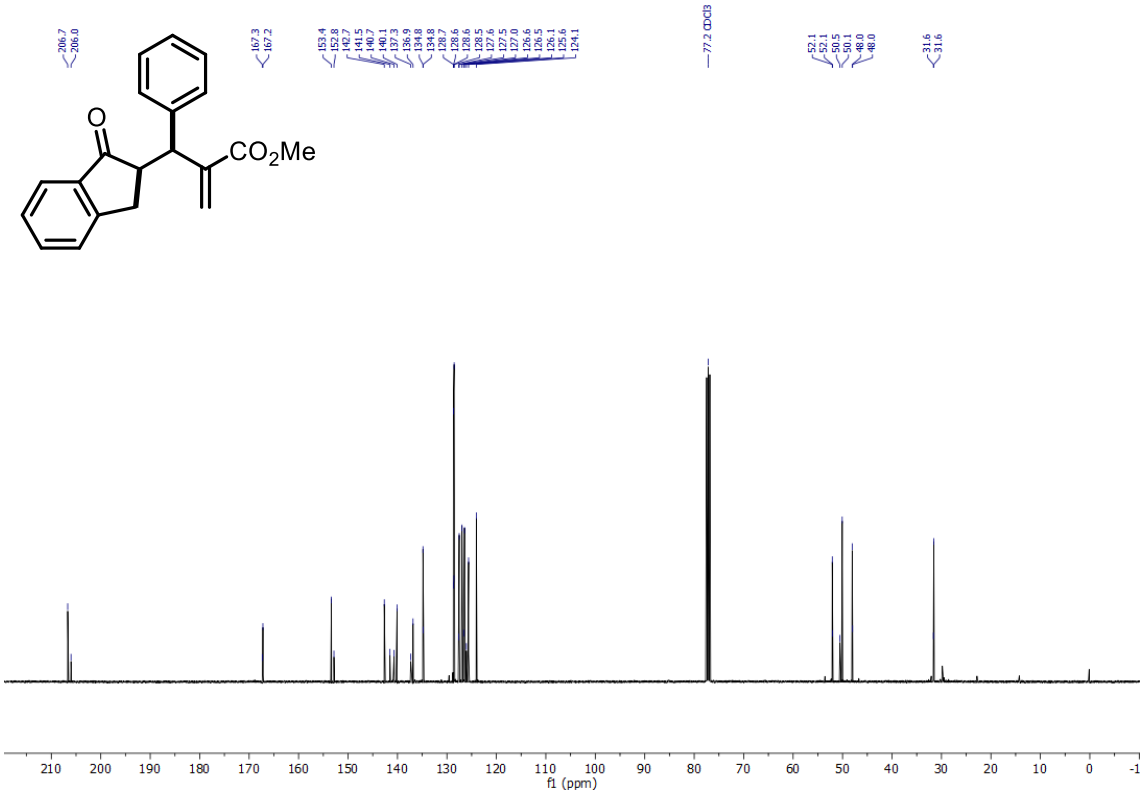

^{13}C NMR spectra of **3j** (mixture of diastereomers).

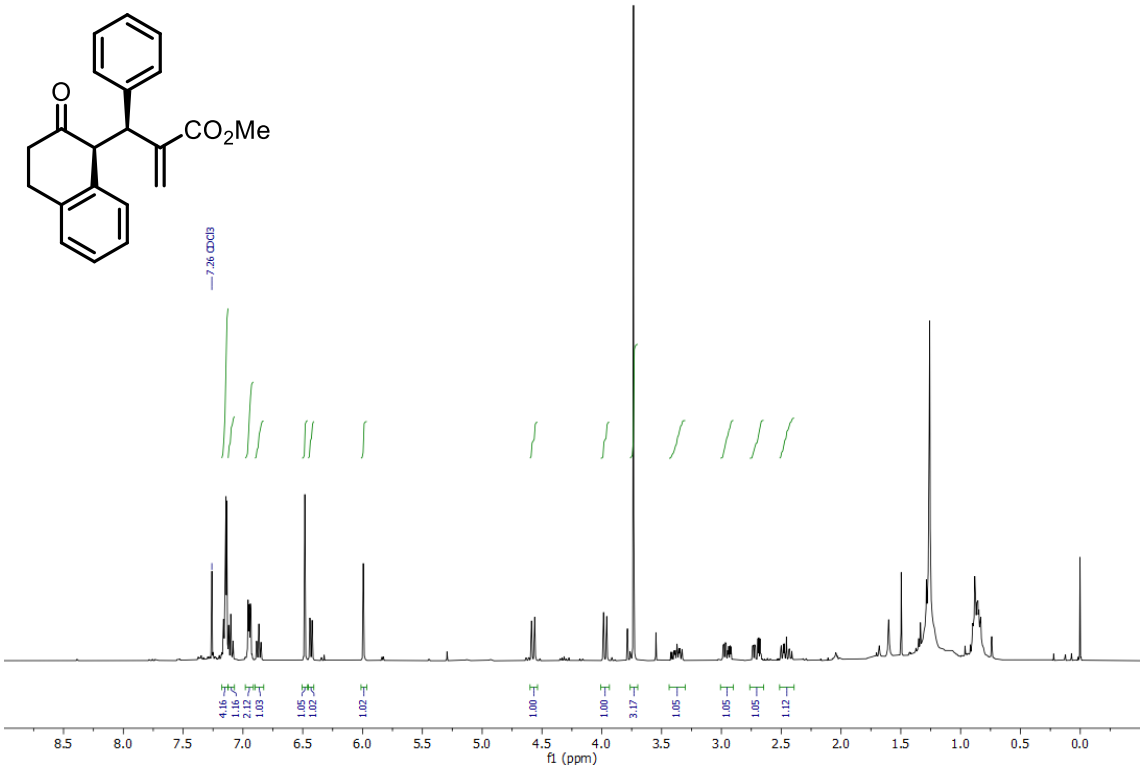

^{1}H NMR spectra of **3k**.

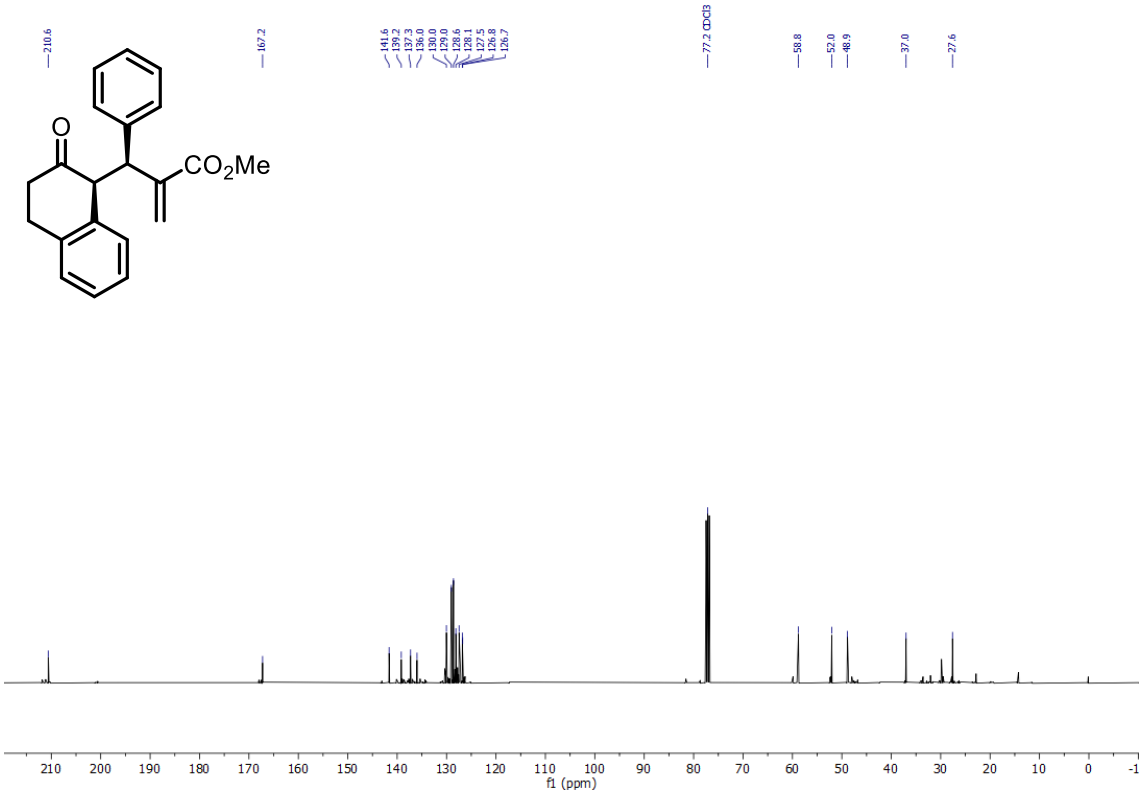

^{13}C NMR spectra of **3k**.

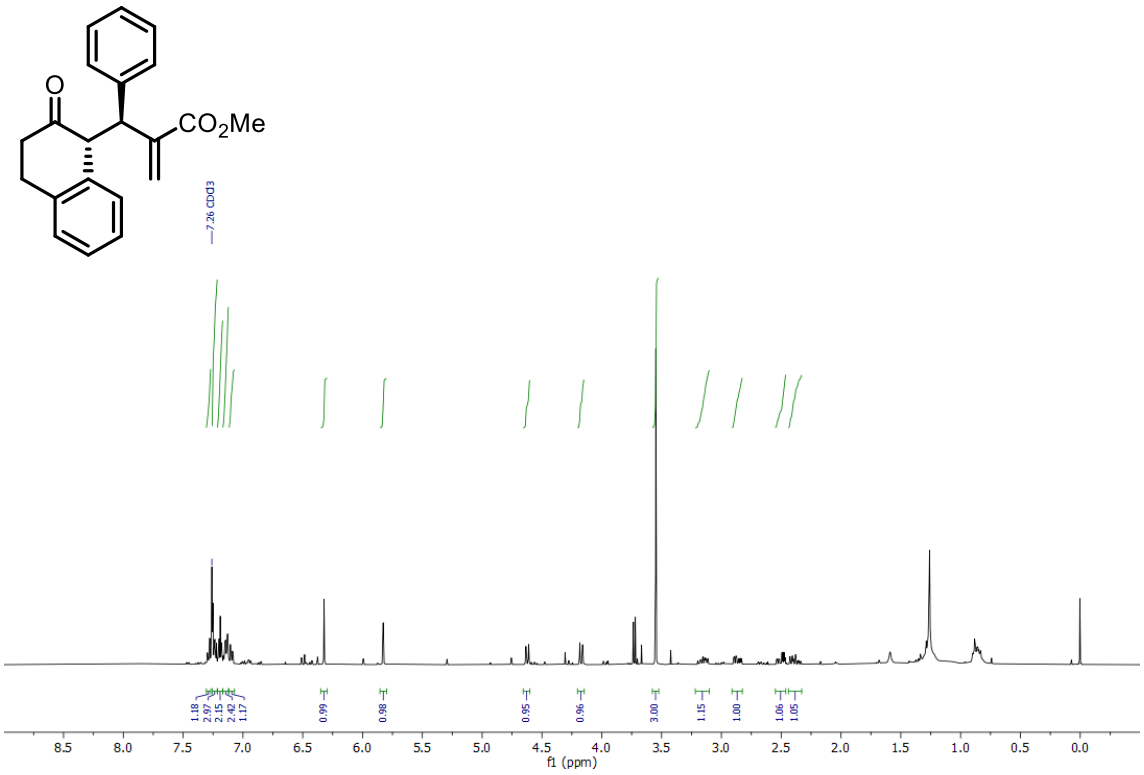

^{1}H NMR spectra of **3k'**.

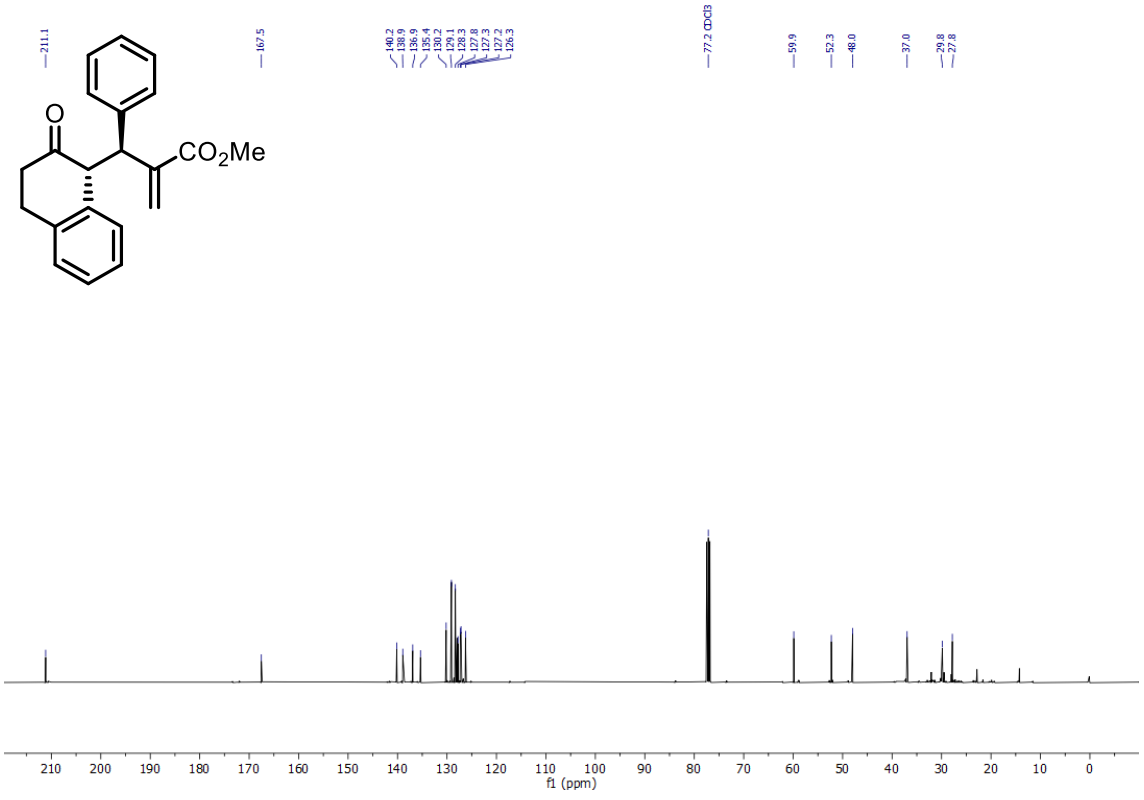

^{13}C NMR spectra of **3k'**.

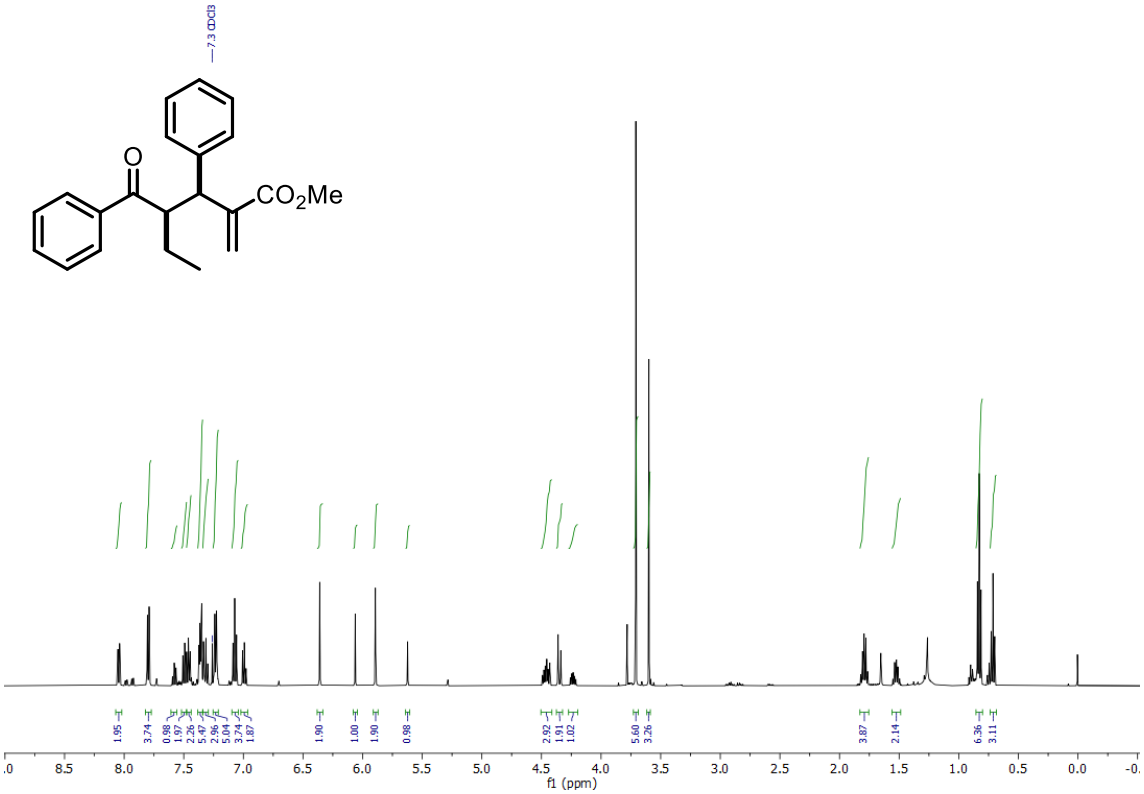

^{1}H NMR spectra of **3l** (mixture of diastereomers).

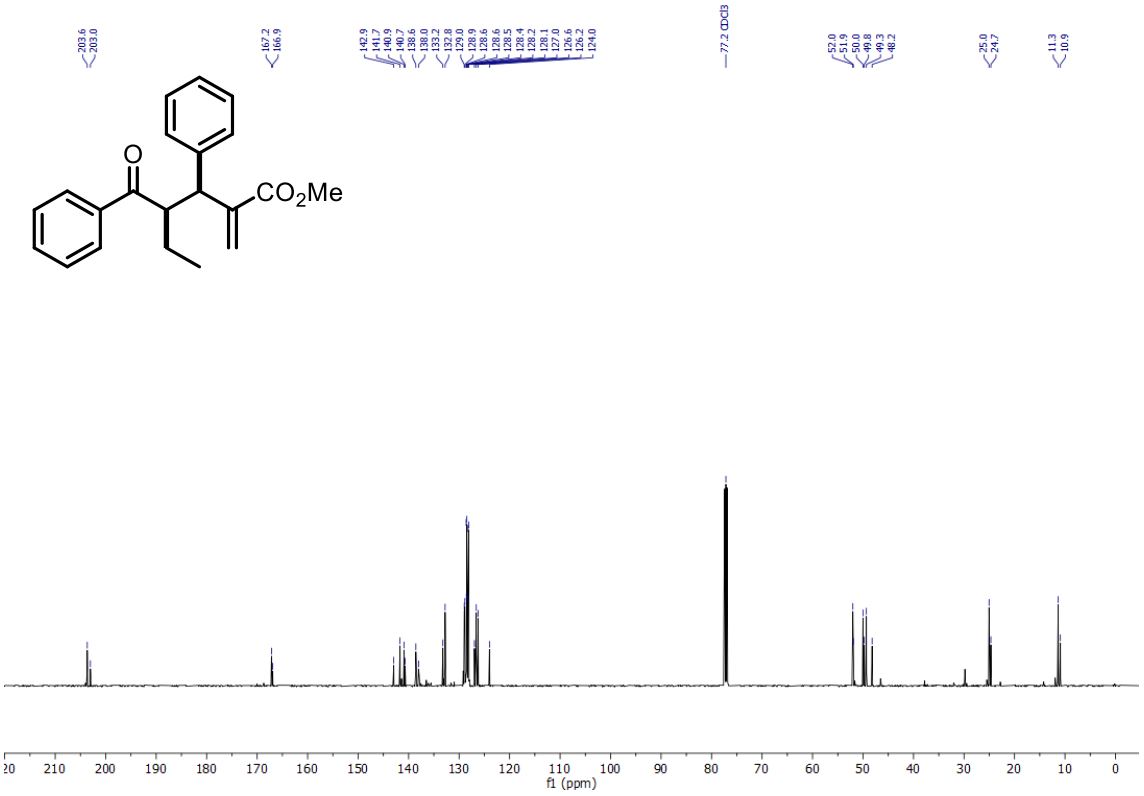

^{13}C NMR spectra of **3l** (mixture of diastereomers).

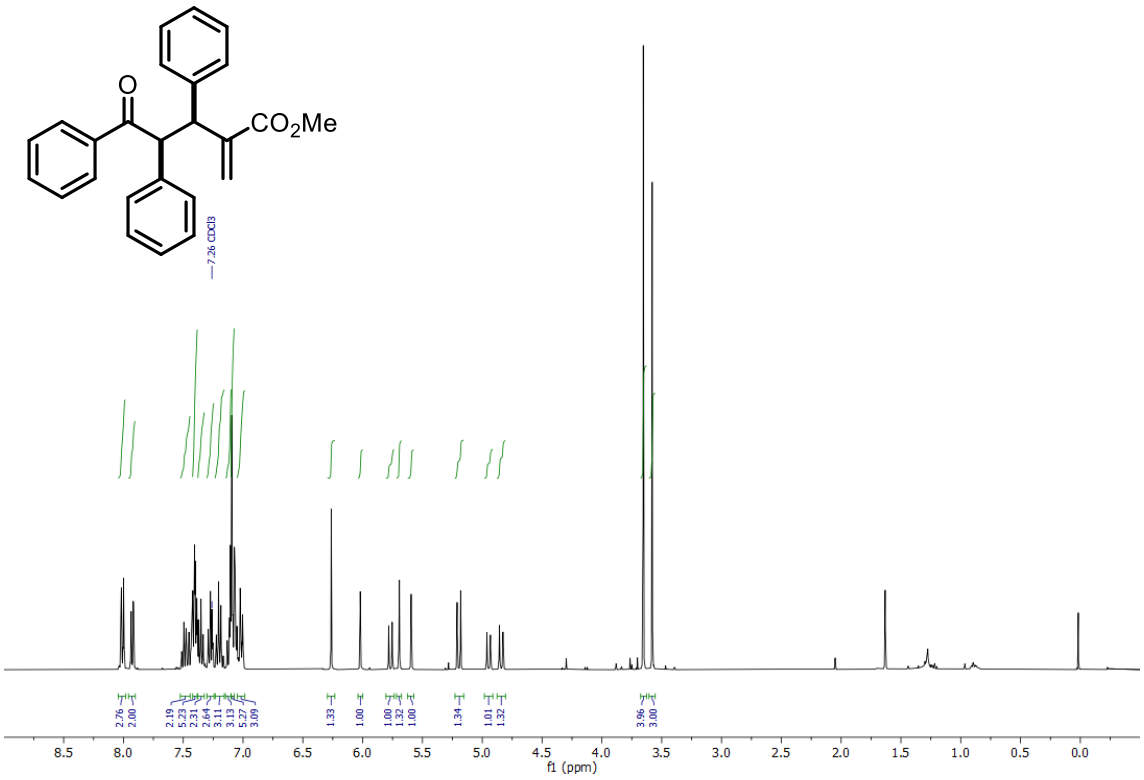

^{1}H NMR spectra of **3m** (mixture of diastereomers).

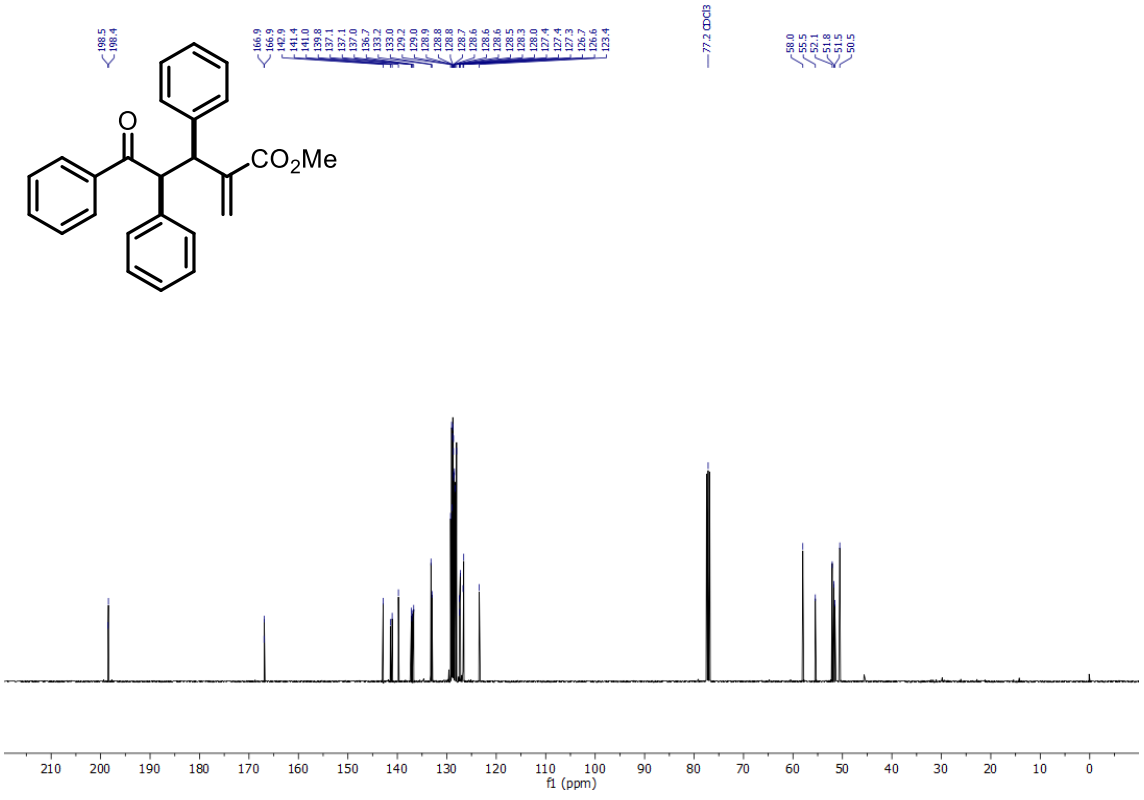

^{13}C NMR spectra of **3m** (mixture of diastereomers).

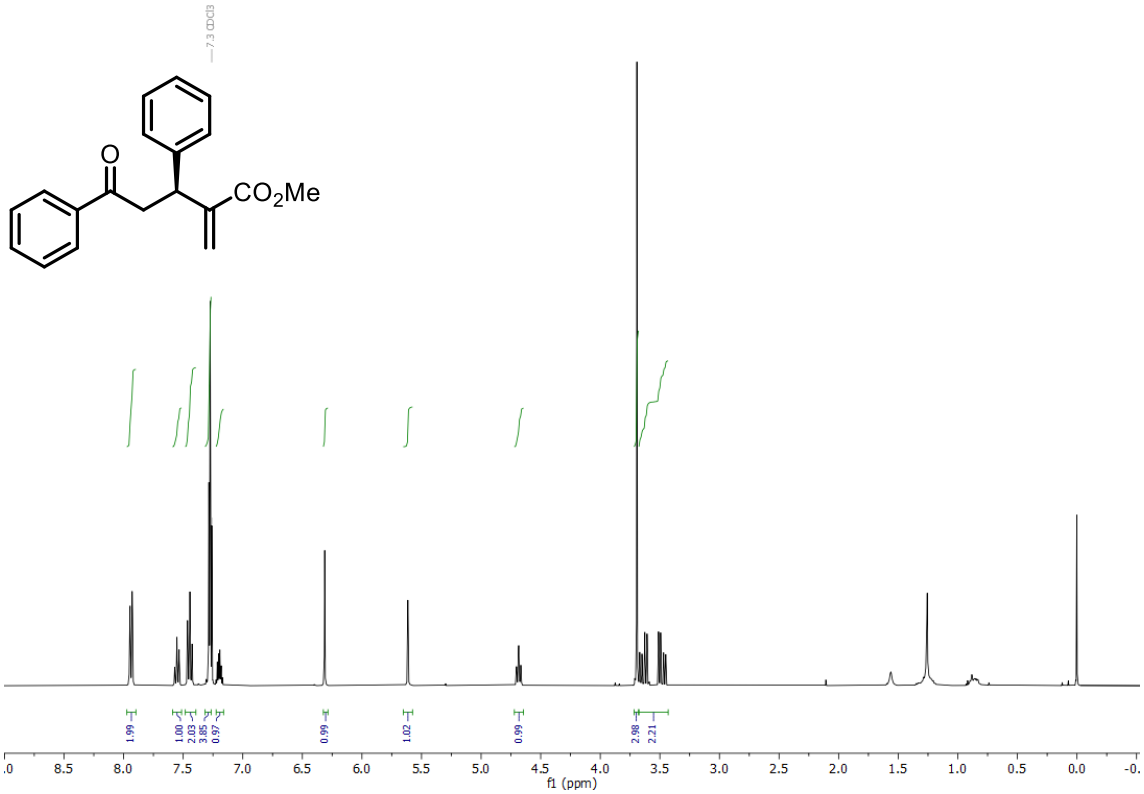

^{1}H NMR spectra of **3n**.

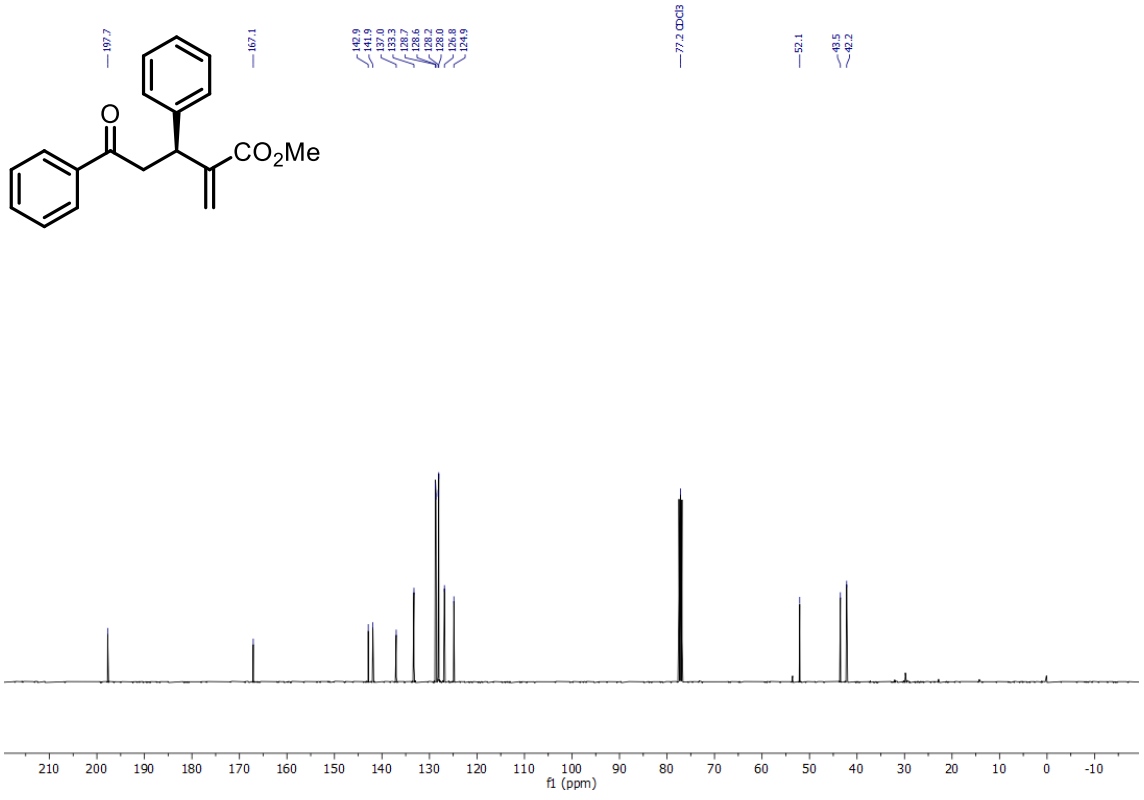

^{13}C NMR spectra of **3n**.

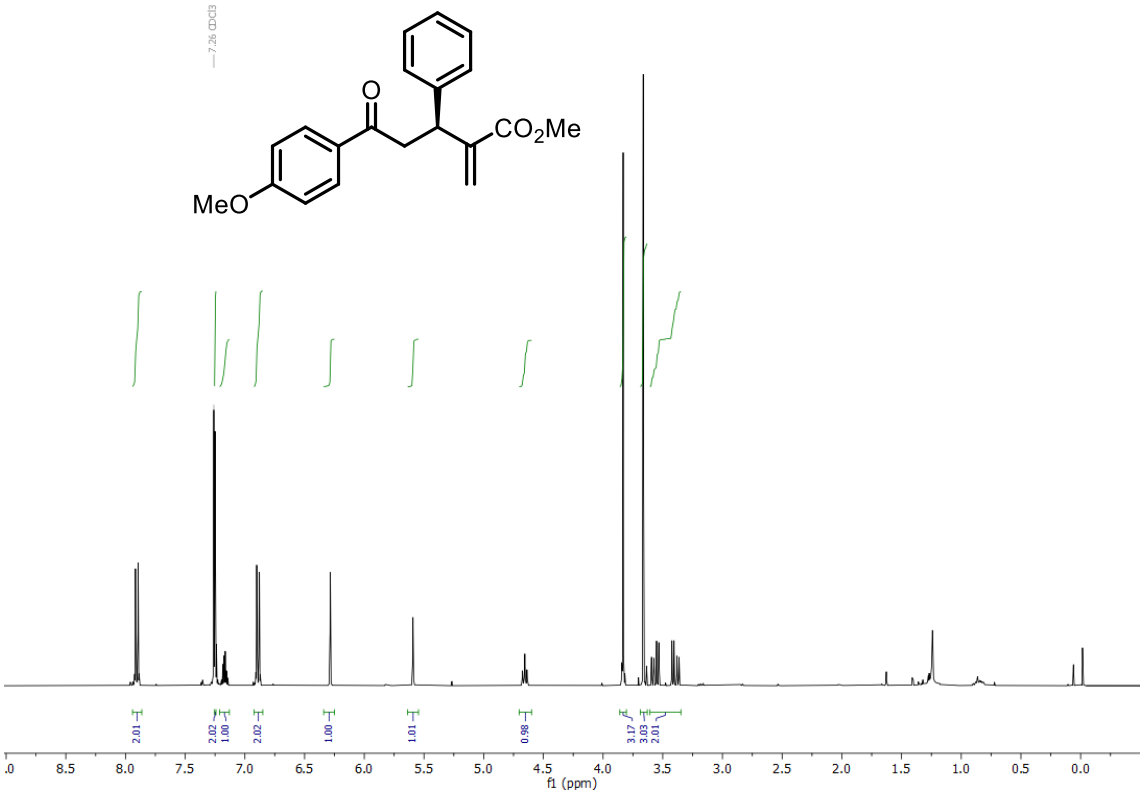

^{1}H NMR spectra of **3o**.

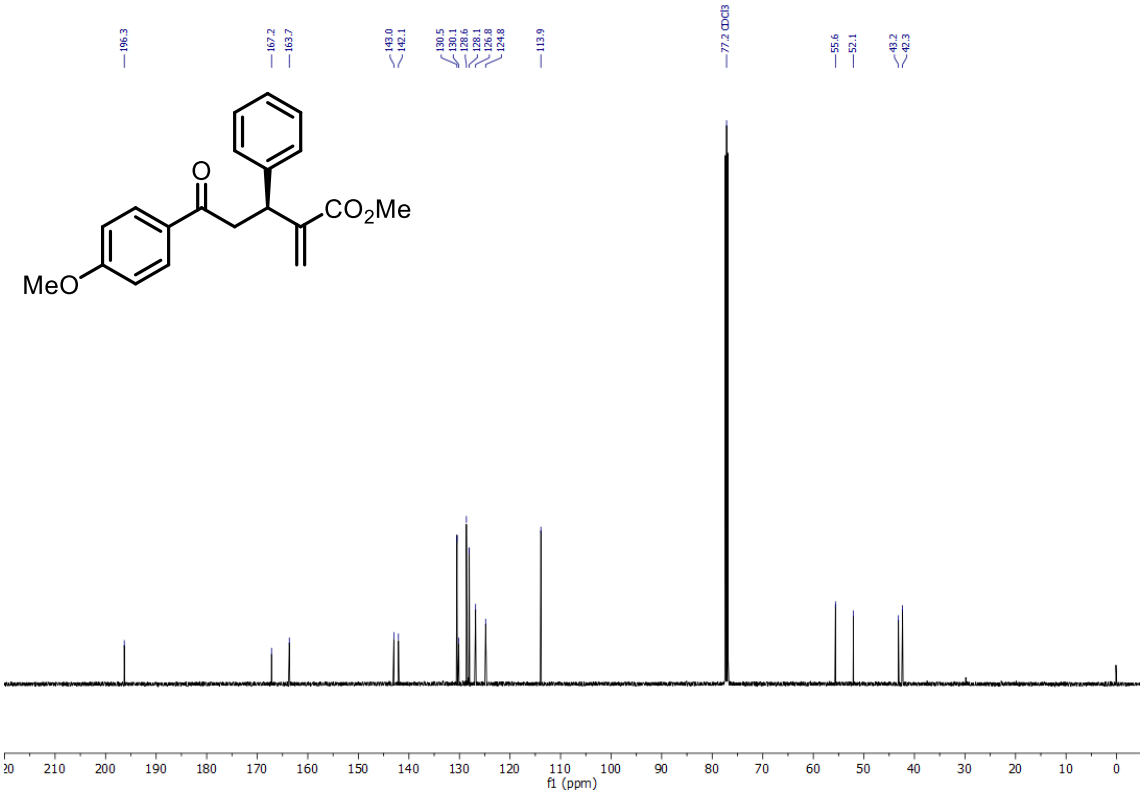

^{13}C NMR spectra of **3o**.

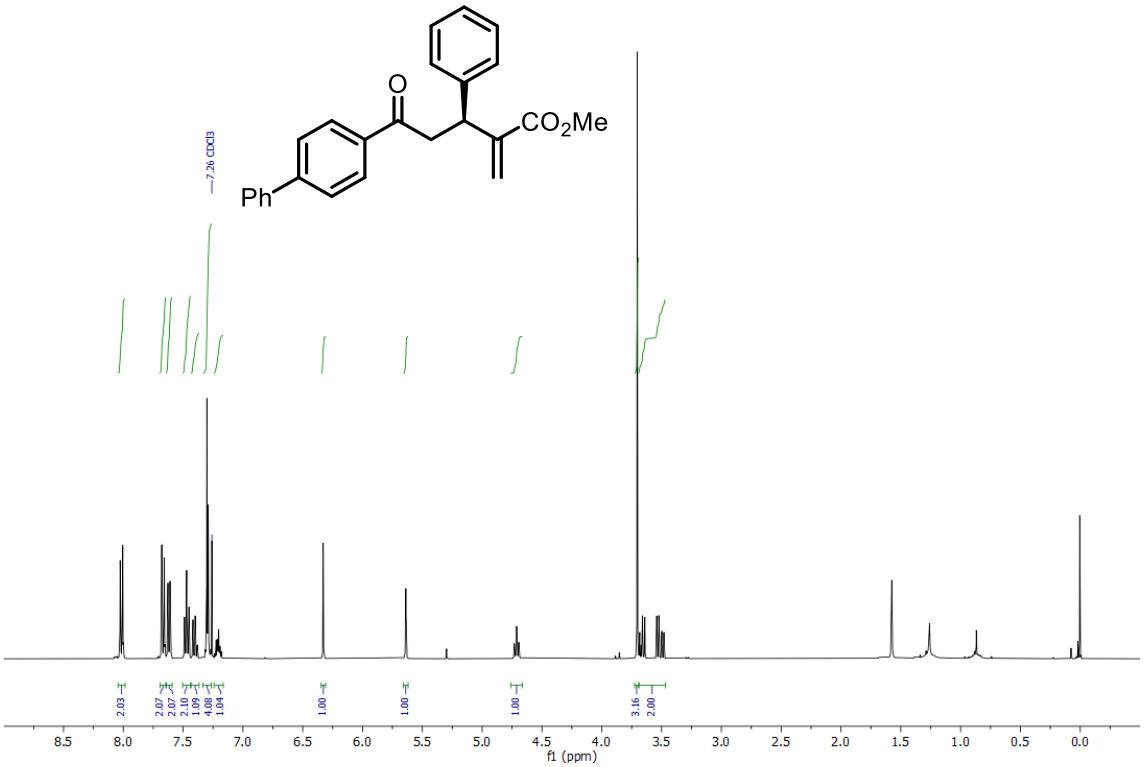

^{1}H NMR spectra of **3p**.

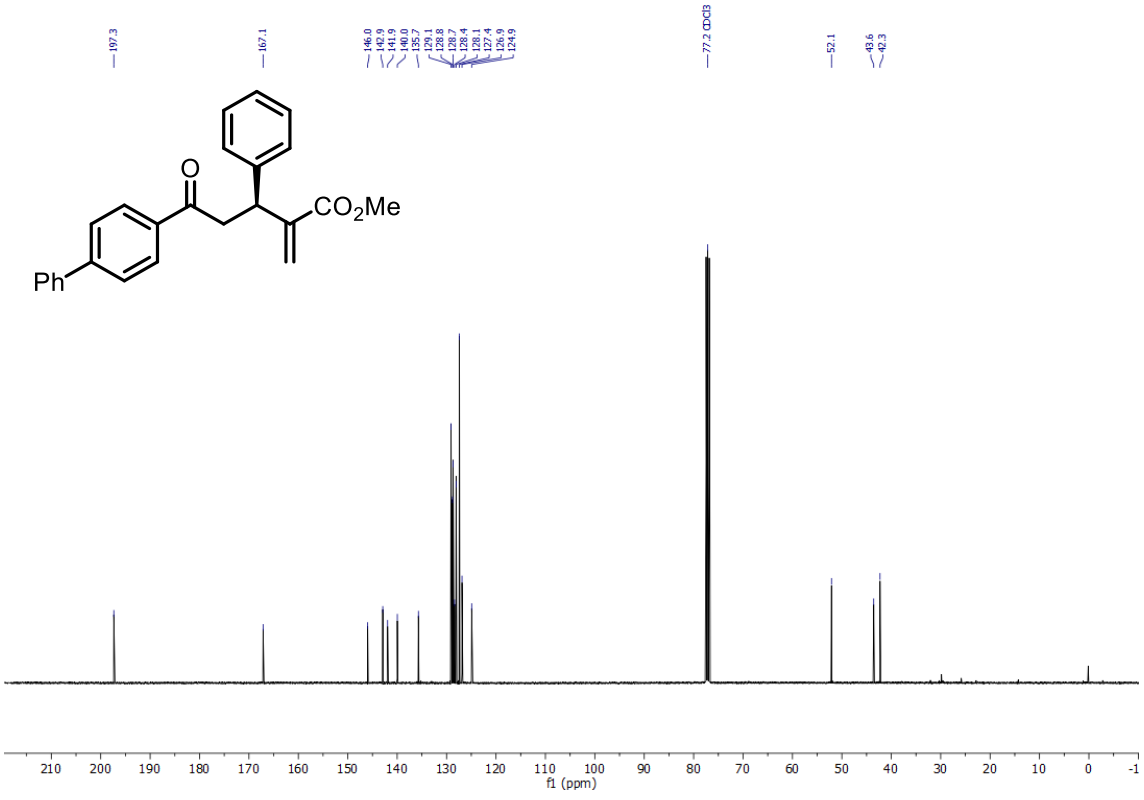

^{13}C NMR spectra of **3p**.

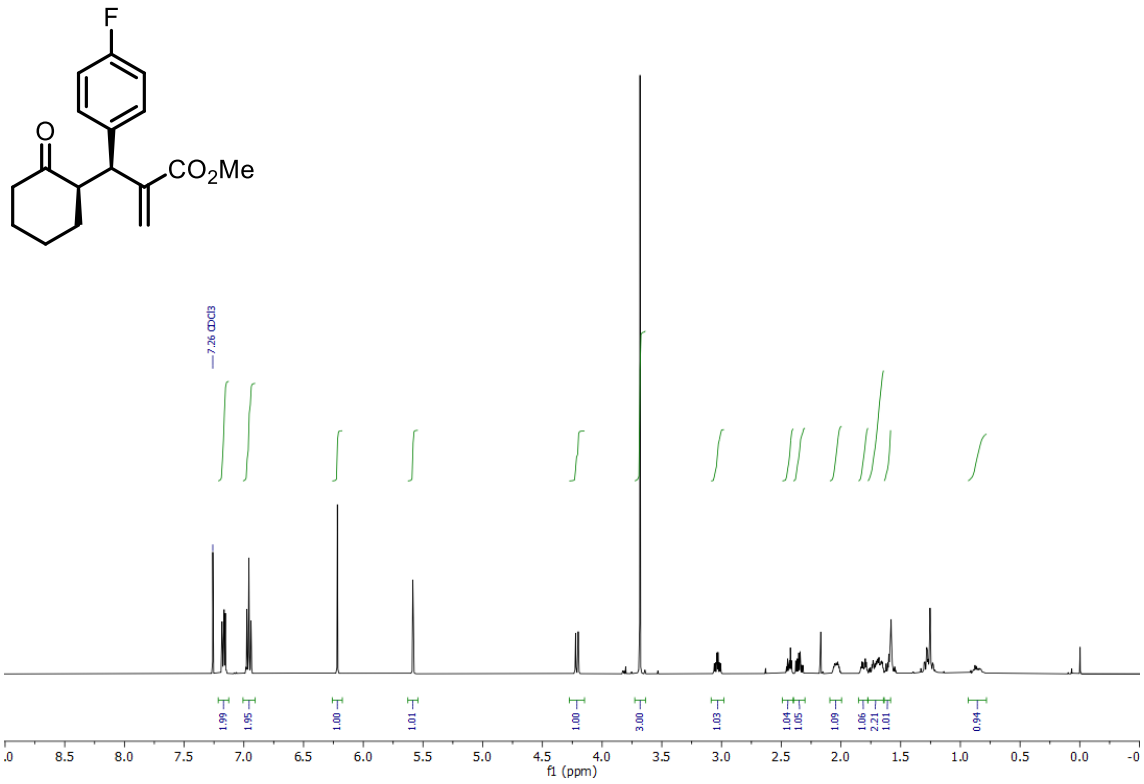

^{1}H NMR spectra of **3q**.

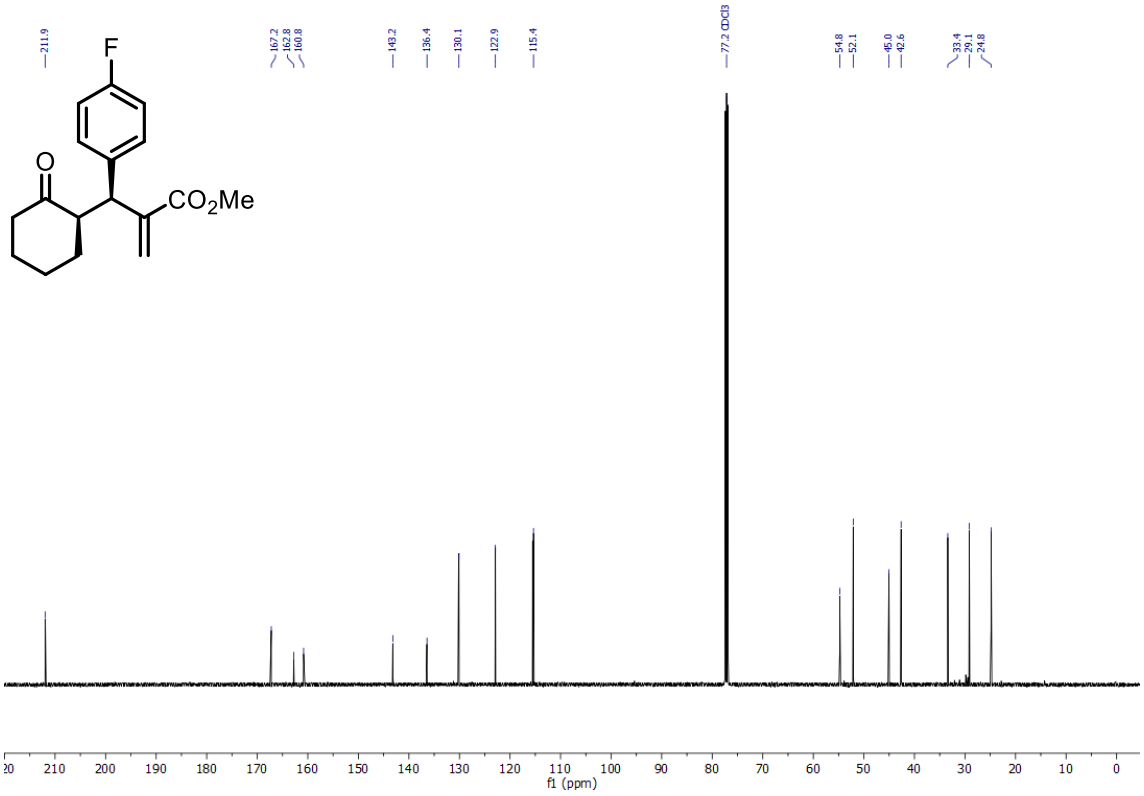

^{13}C NMR spectra of **3q**.

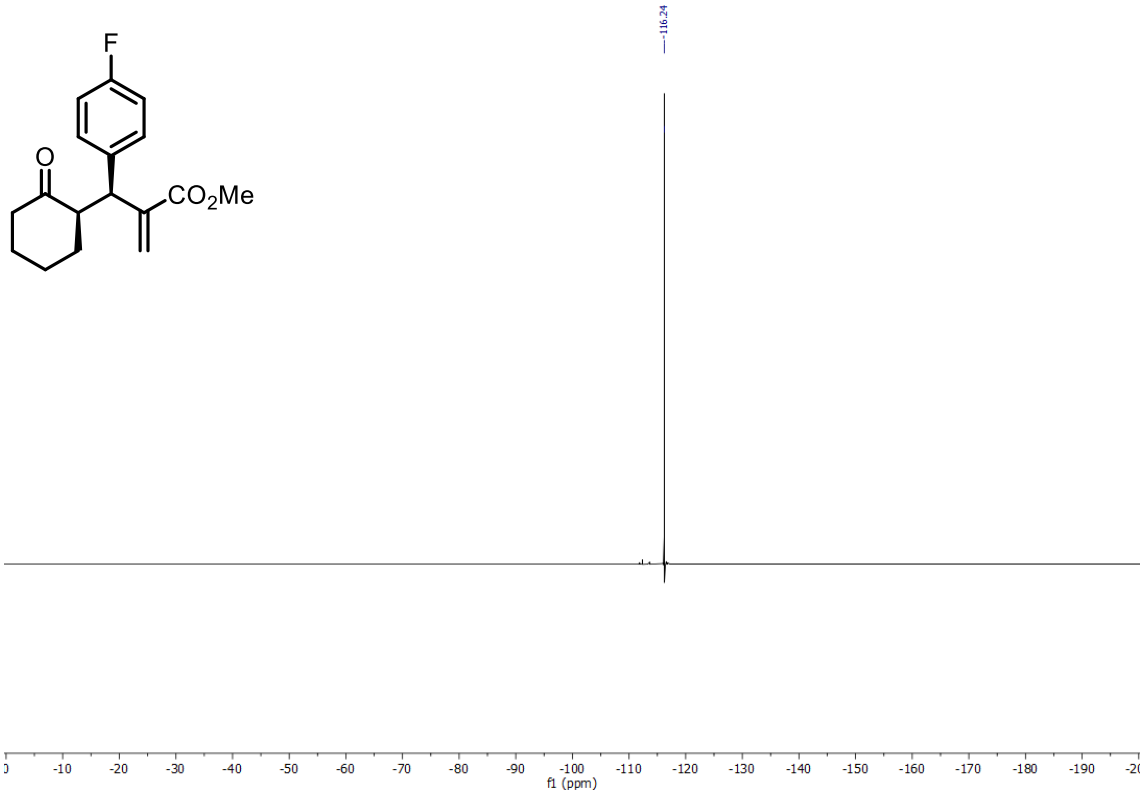

^{19}F NMR spectra of **3q**.

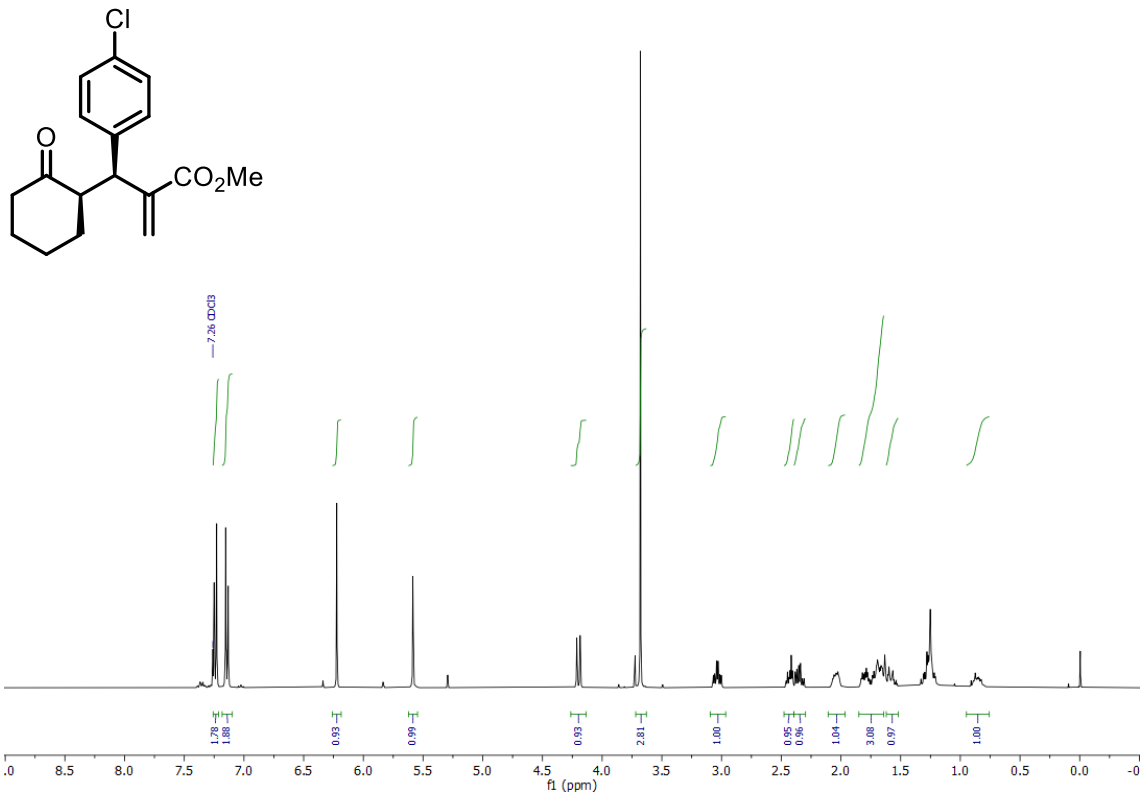

^{1}H NMR spectra of **3r**.

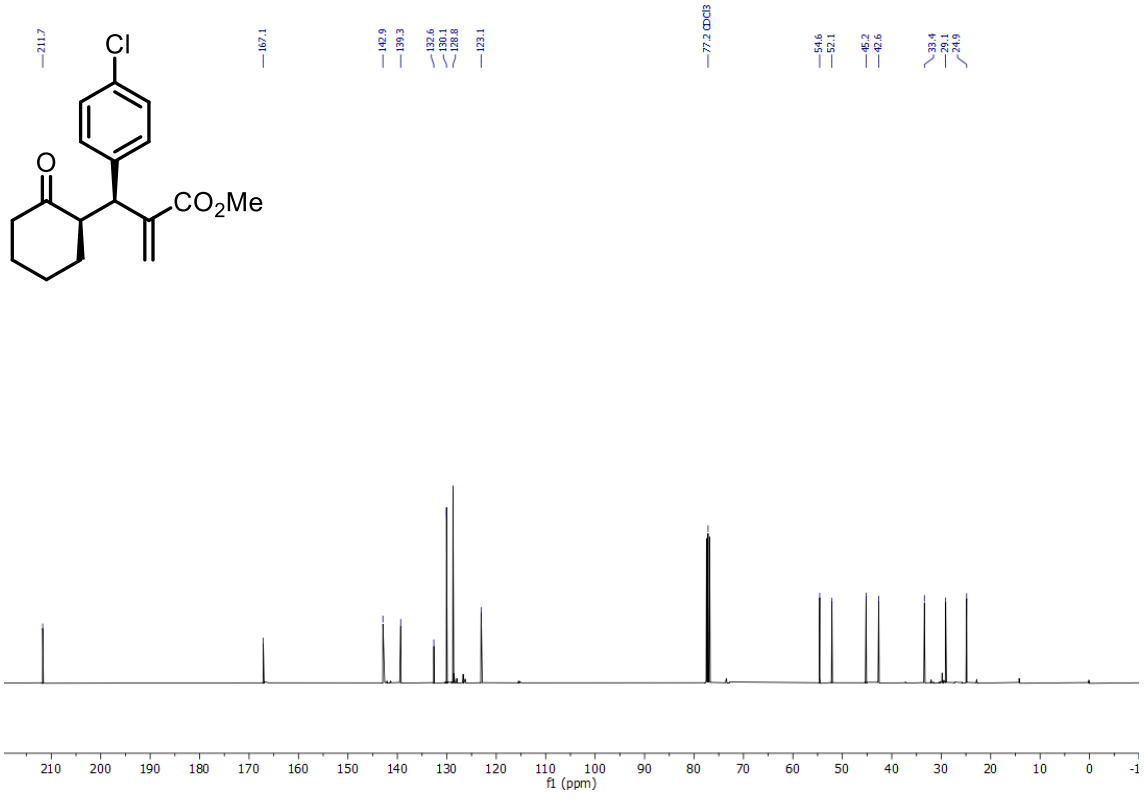

^{13}C NMR spectra of **3r**.

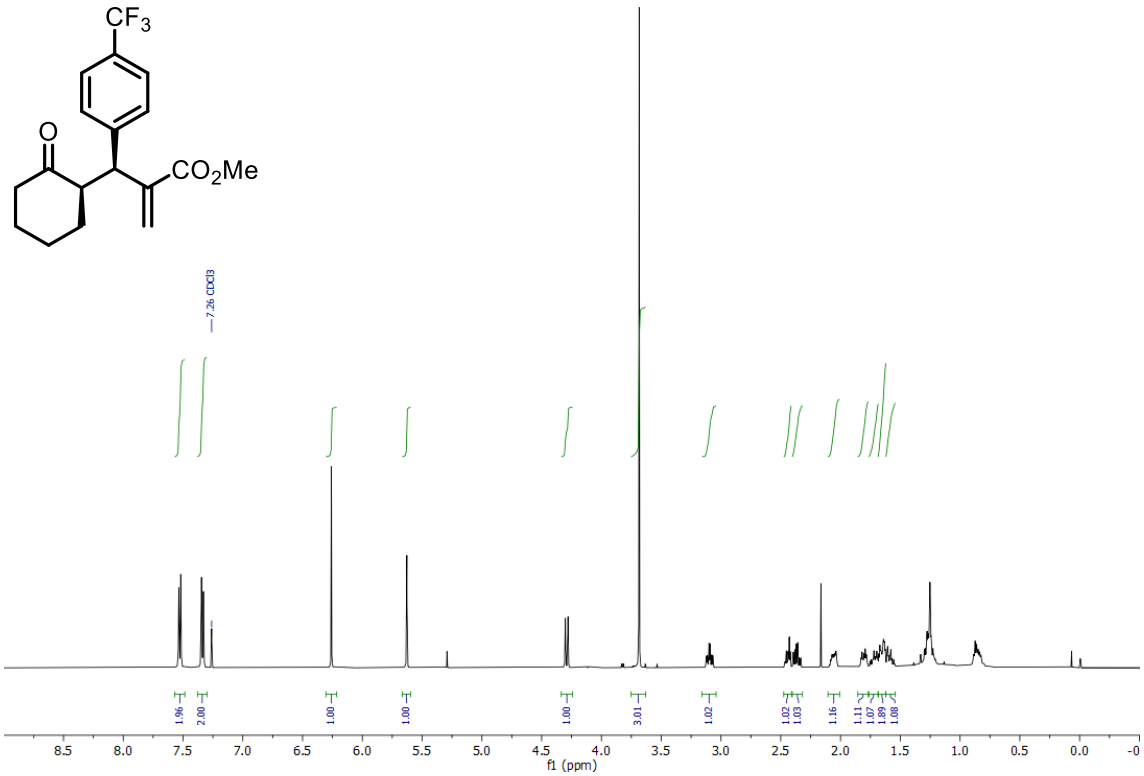

^{1}H NMR spectra of **3s**.

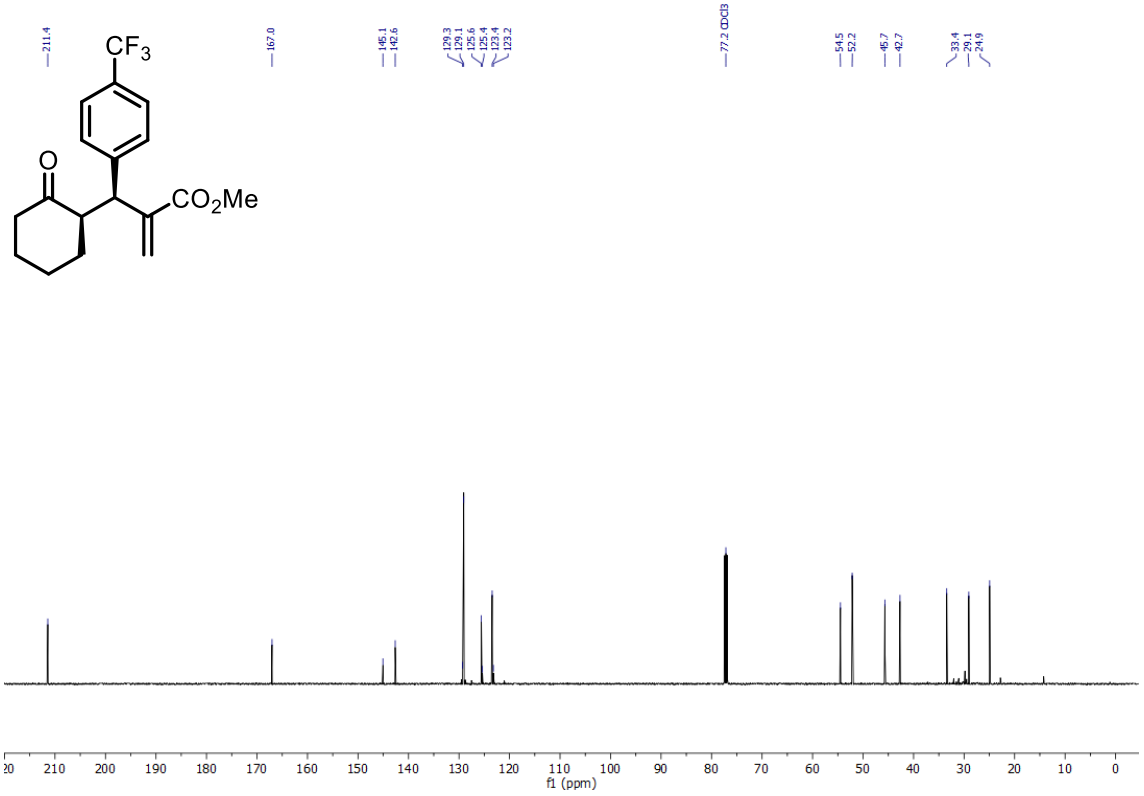

^{13}C NMR spectra of **3s**.

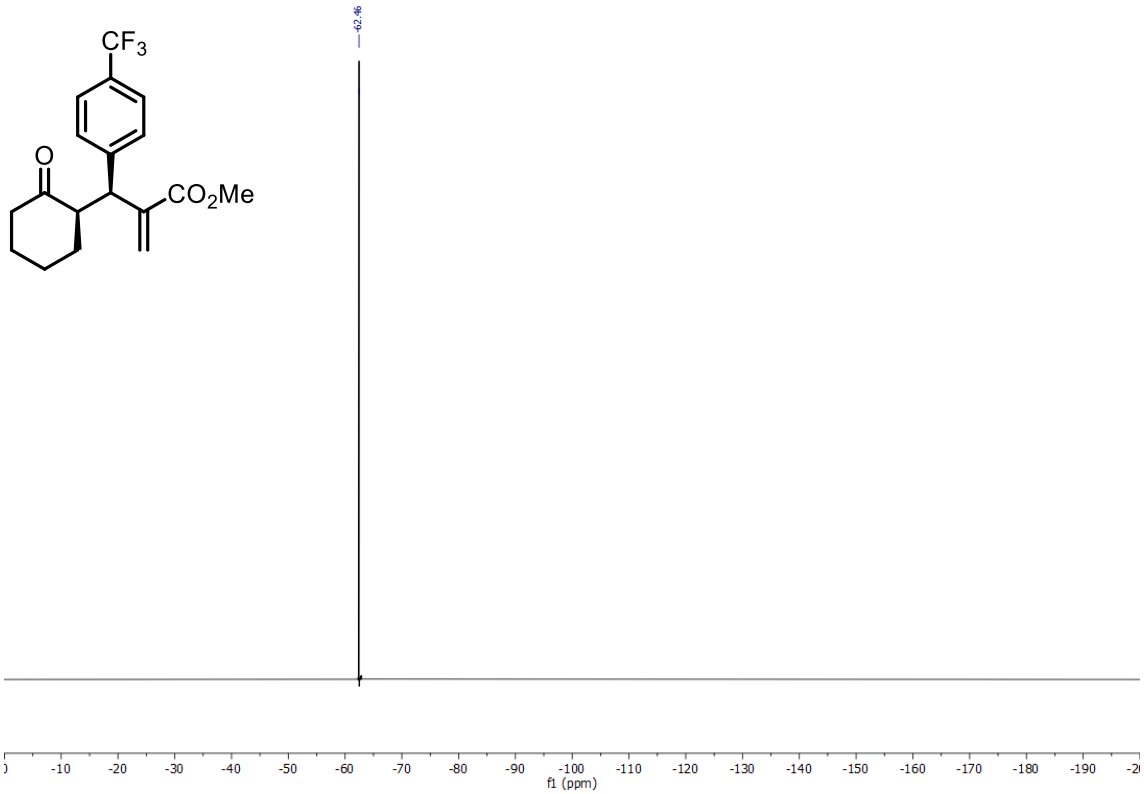

^{19}F NMR spectra of **3s**.

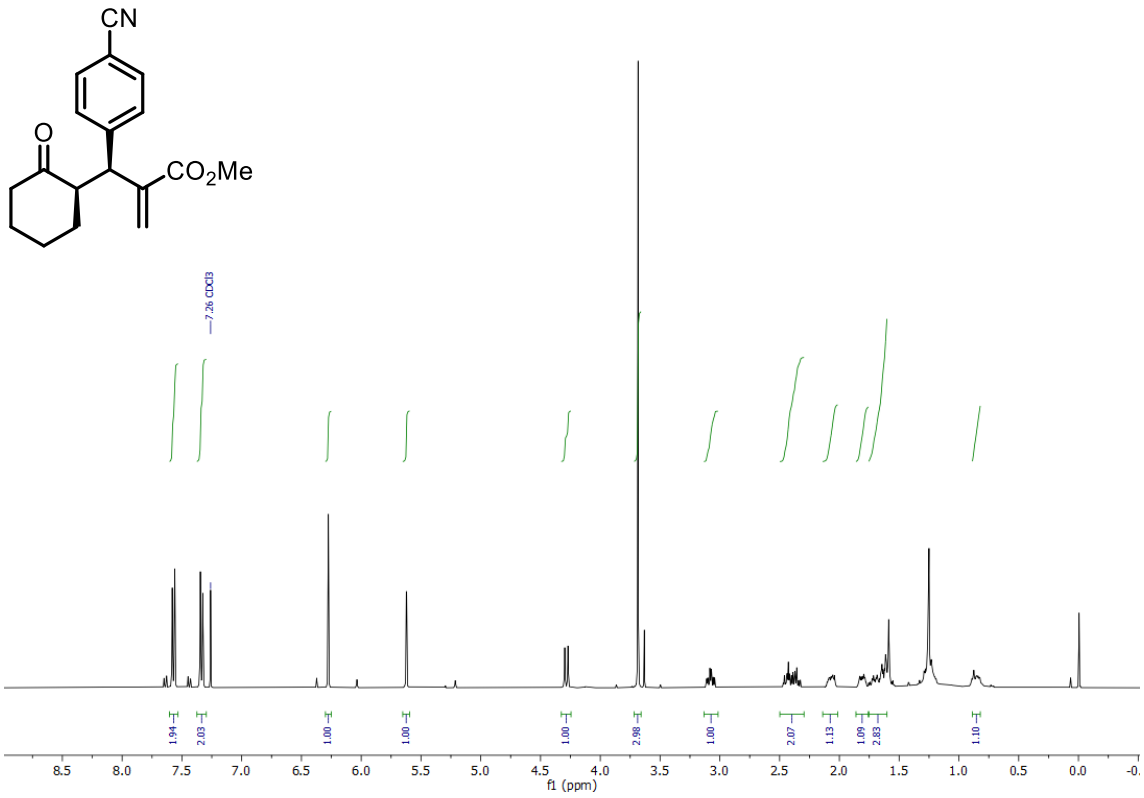

^{1}H NMR spectra of **3t**.

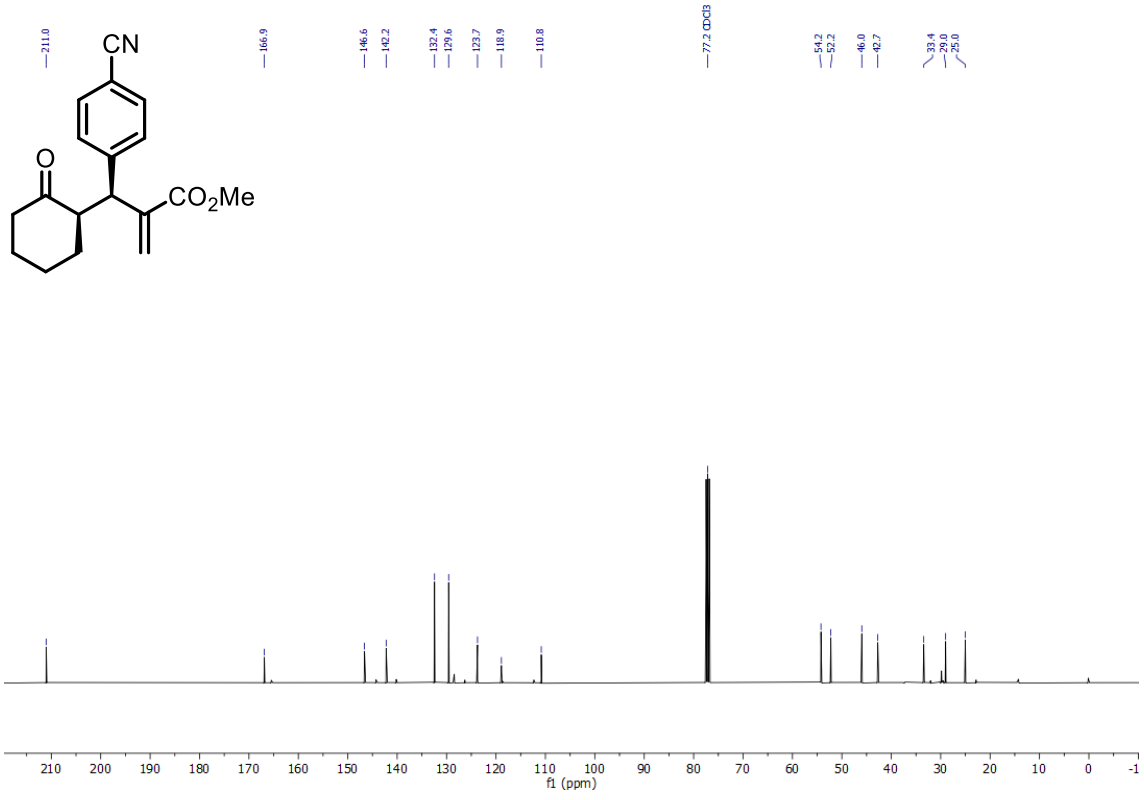

^{13}C NMR spectra of **3t**.

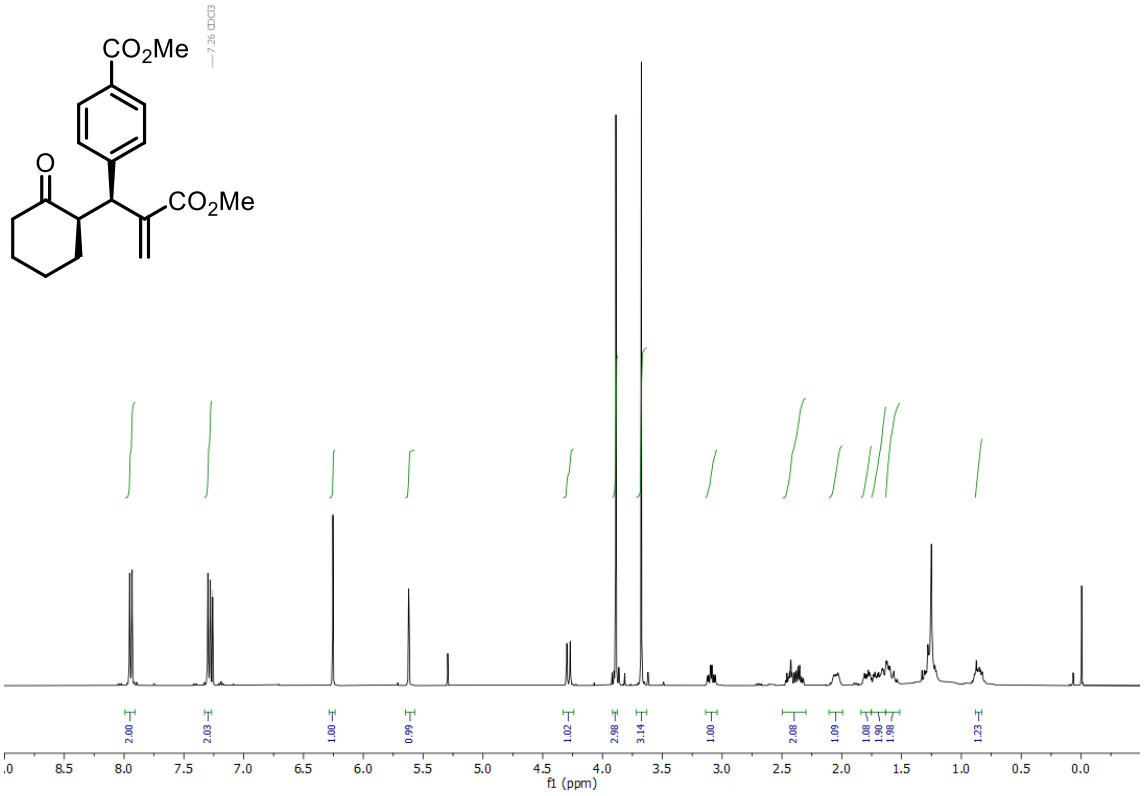

^{1}H NMR spectra of **3u**.

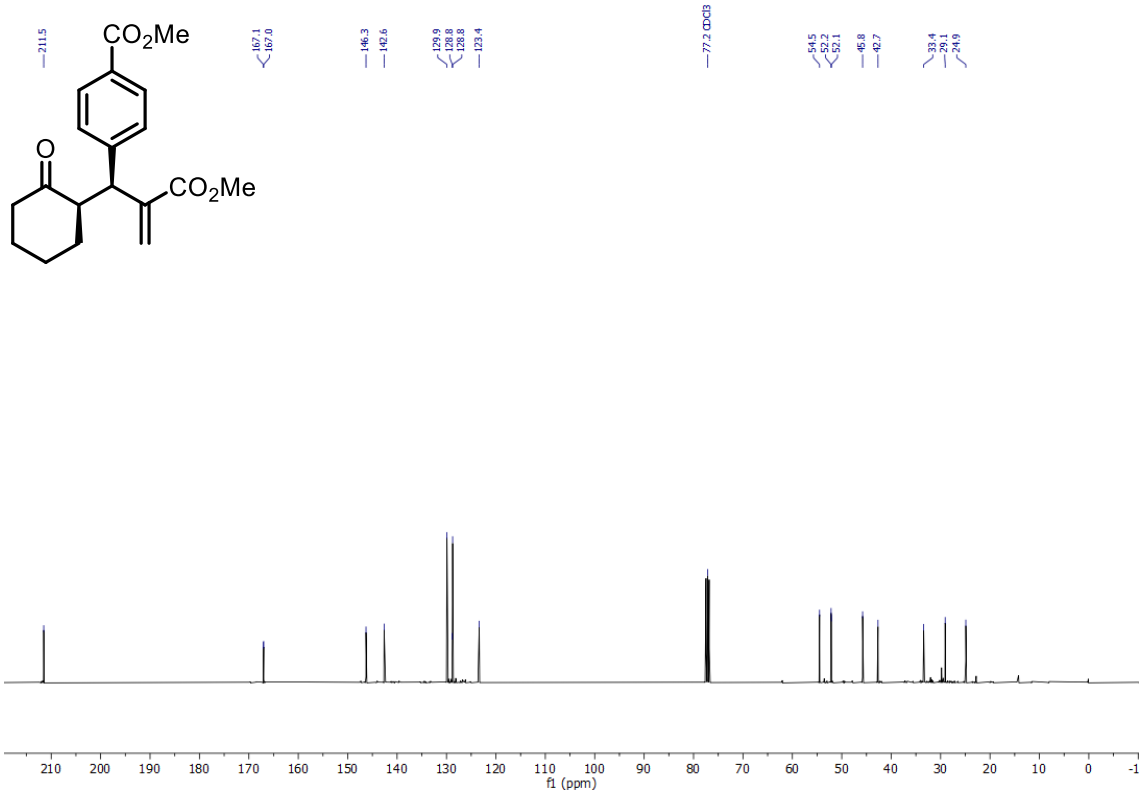

^{13}C NMR spectra of **3u**.

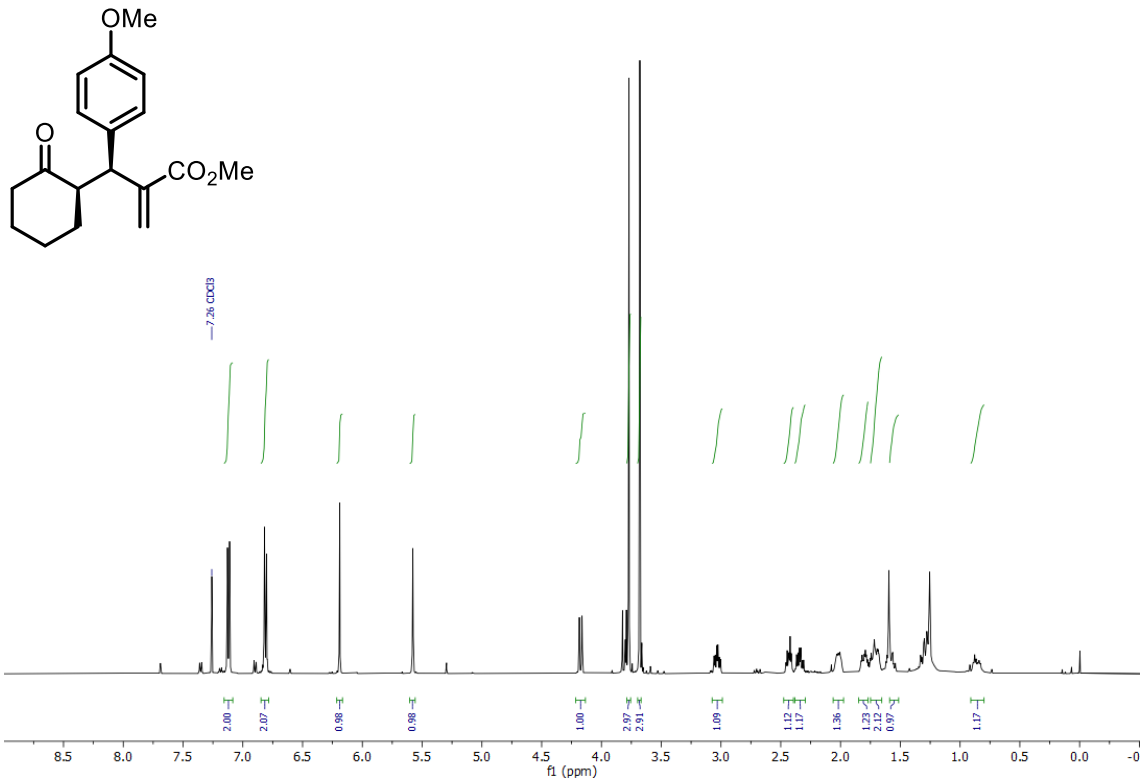

^{1}H NMR spectra of **3v**.

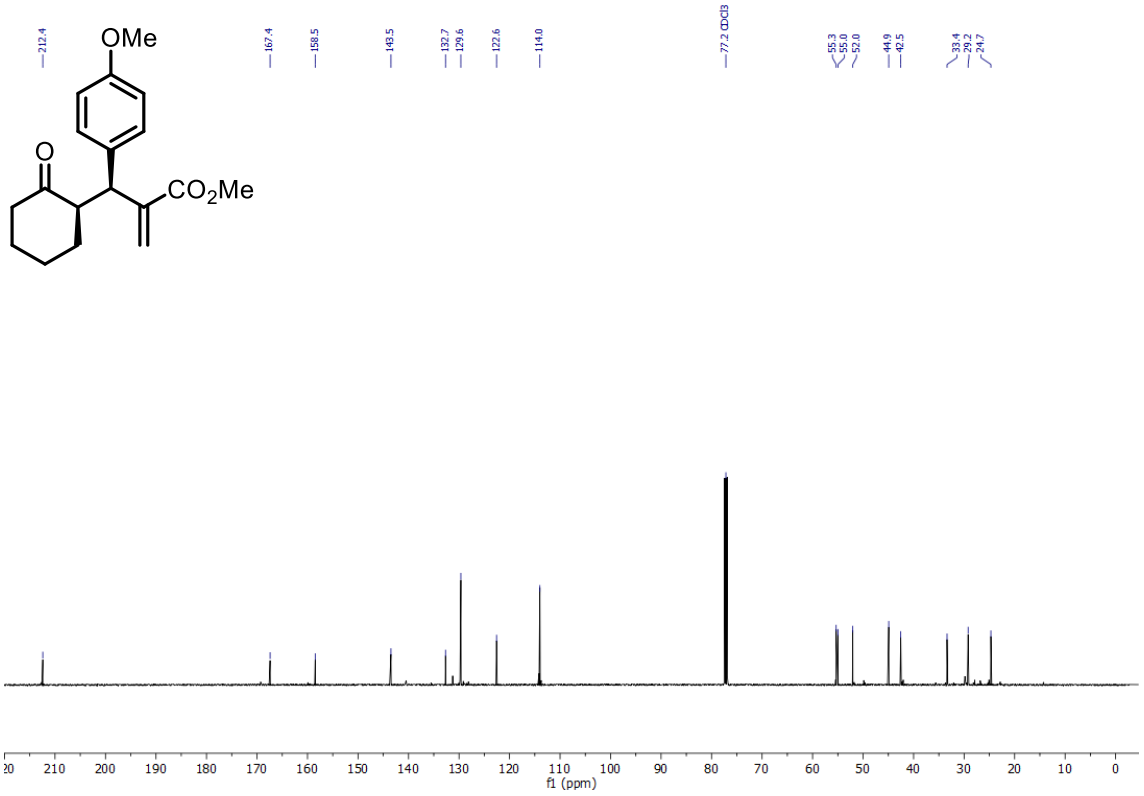

^{13}C NMR spectra of **3v**.

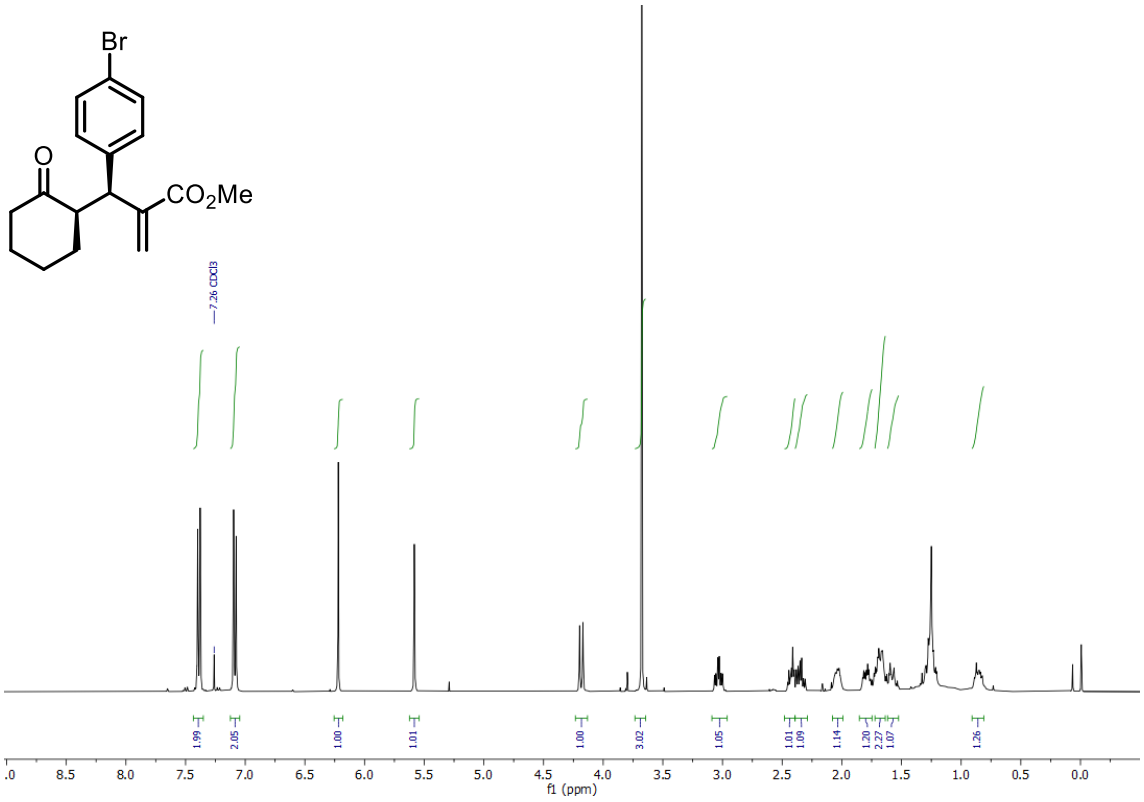

^{1}H NMR spectra of **3w**.

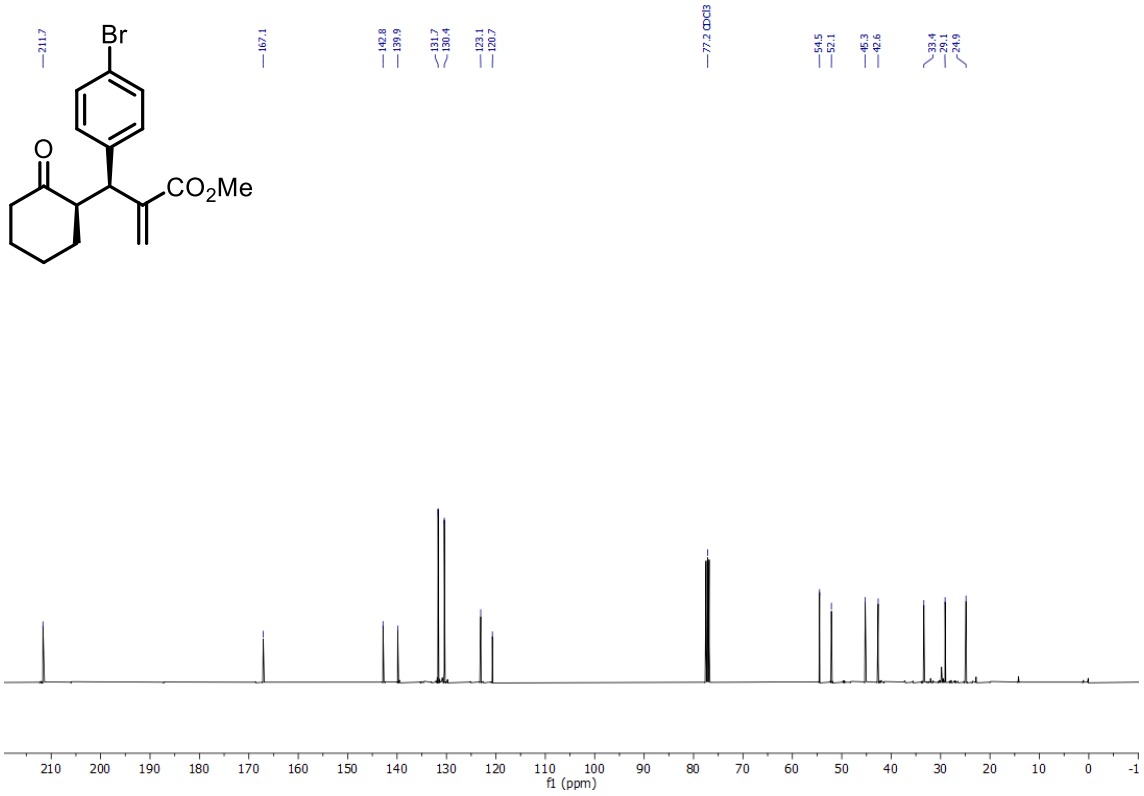

^{13}C NMR spectra of **3w**.

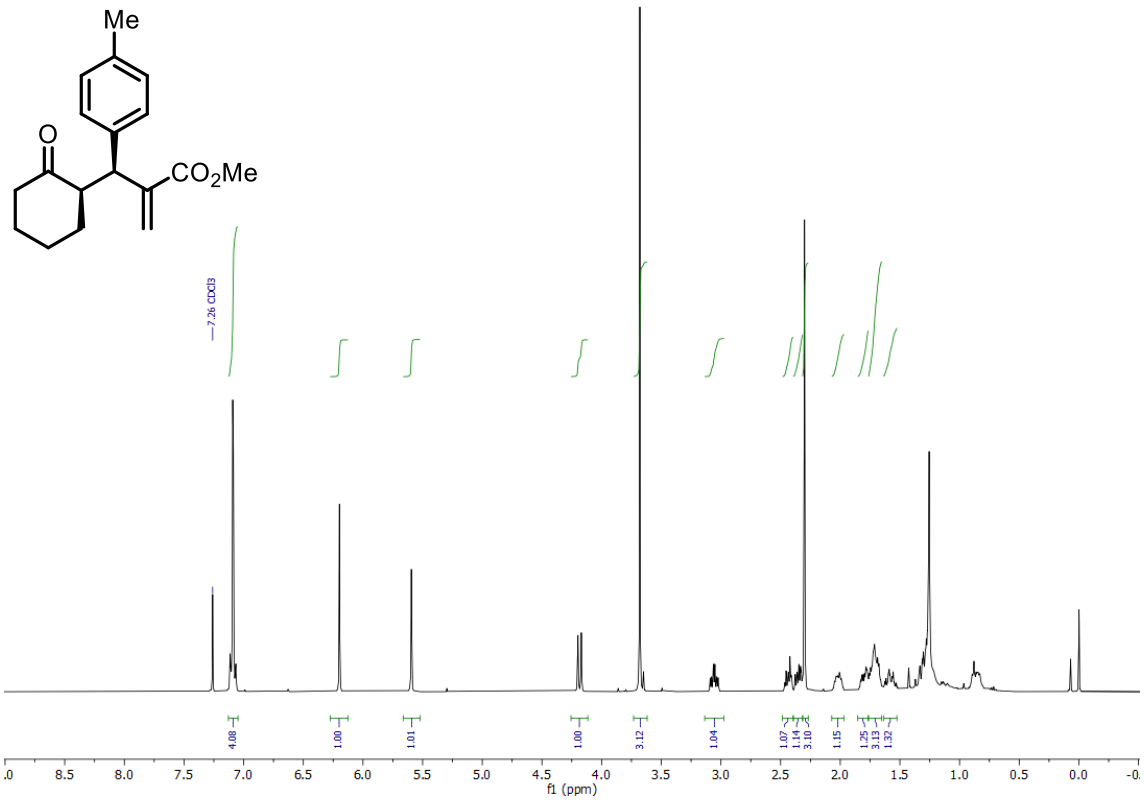

^{1}H NMR spectra of **3x**.

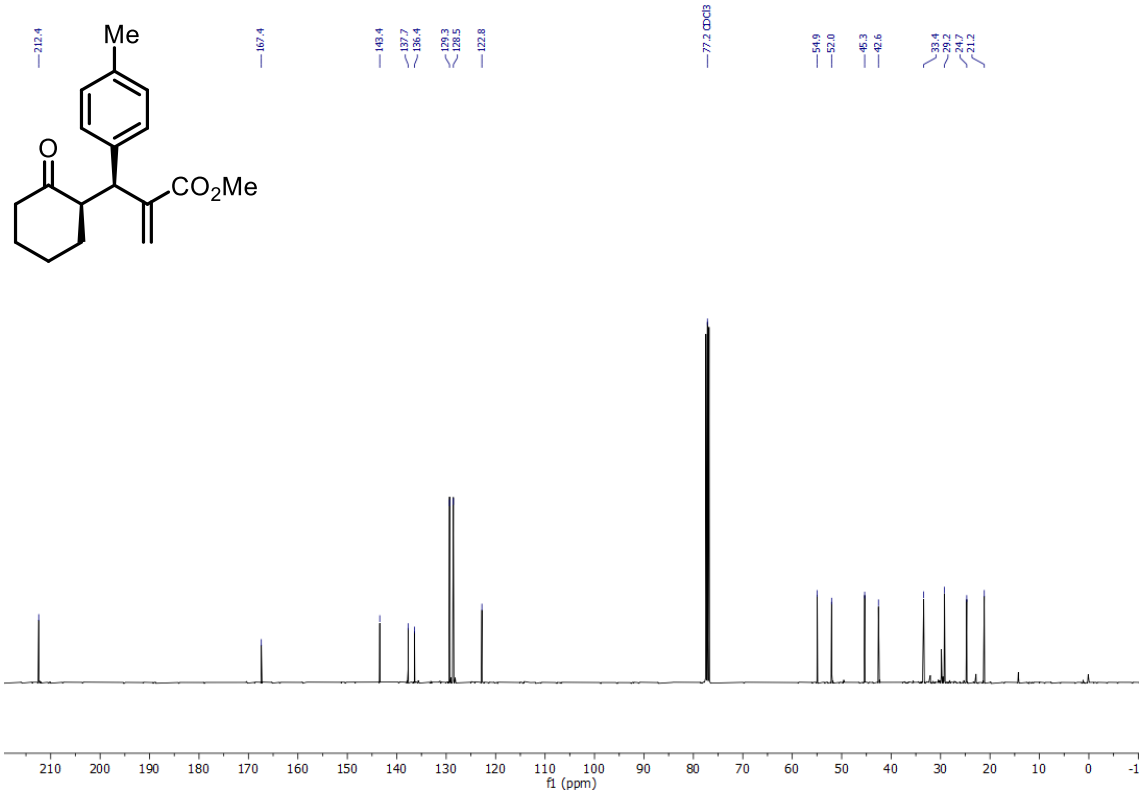

^{13}C NMR spectra of **3x**.

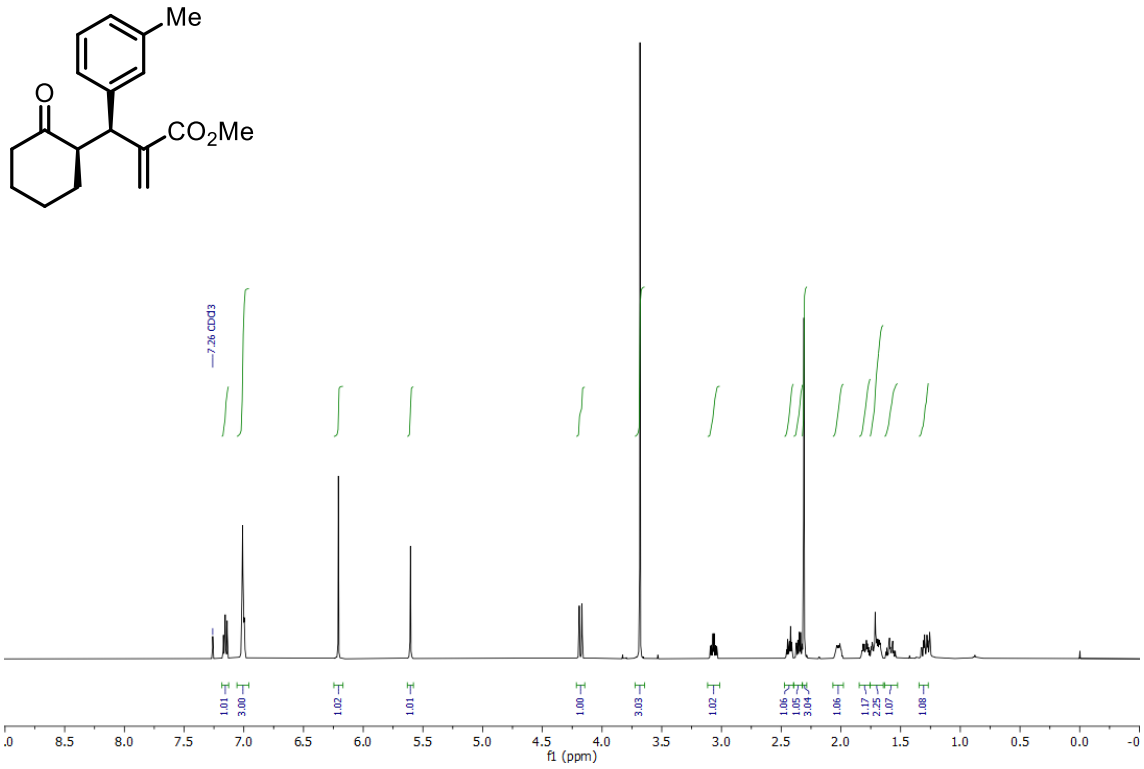

^{1}H NMR spectra of **3y**.

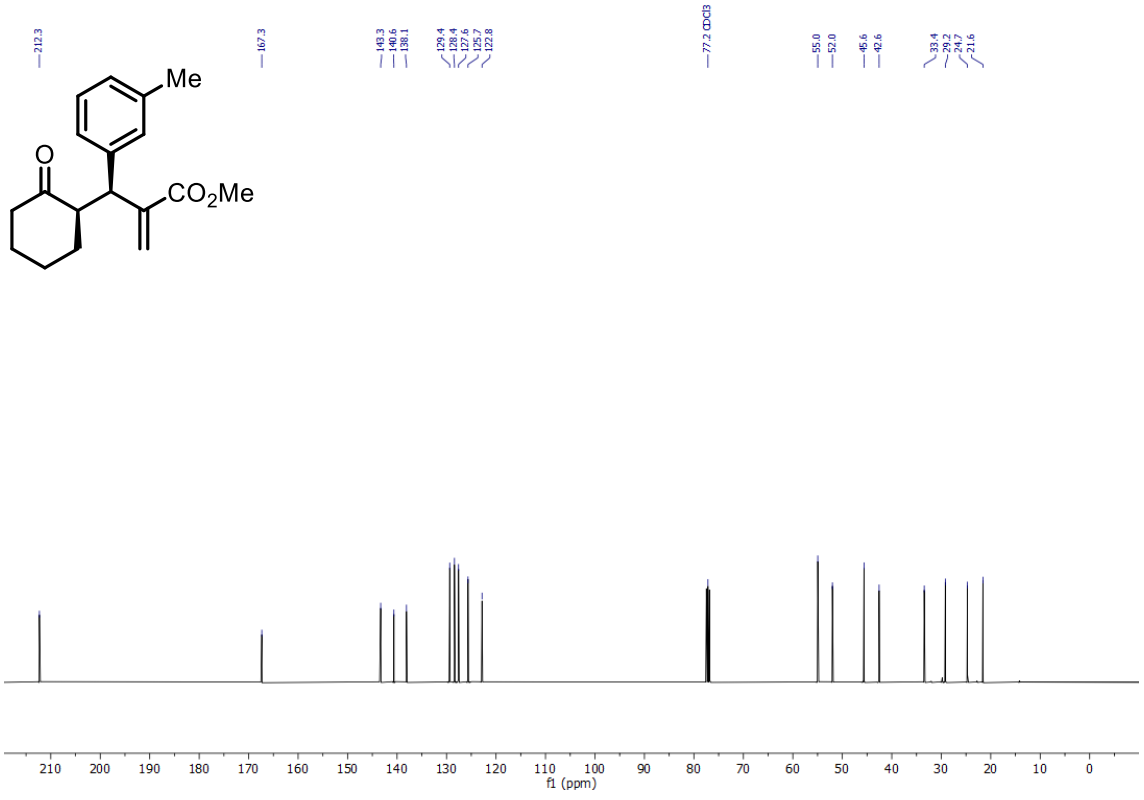

^{13}C NMR spectra of **3y**.

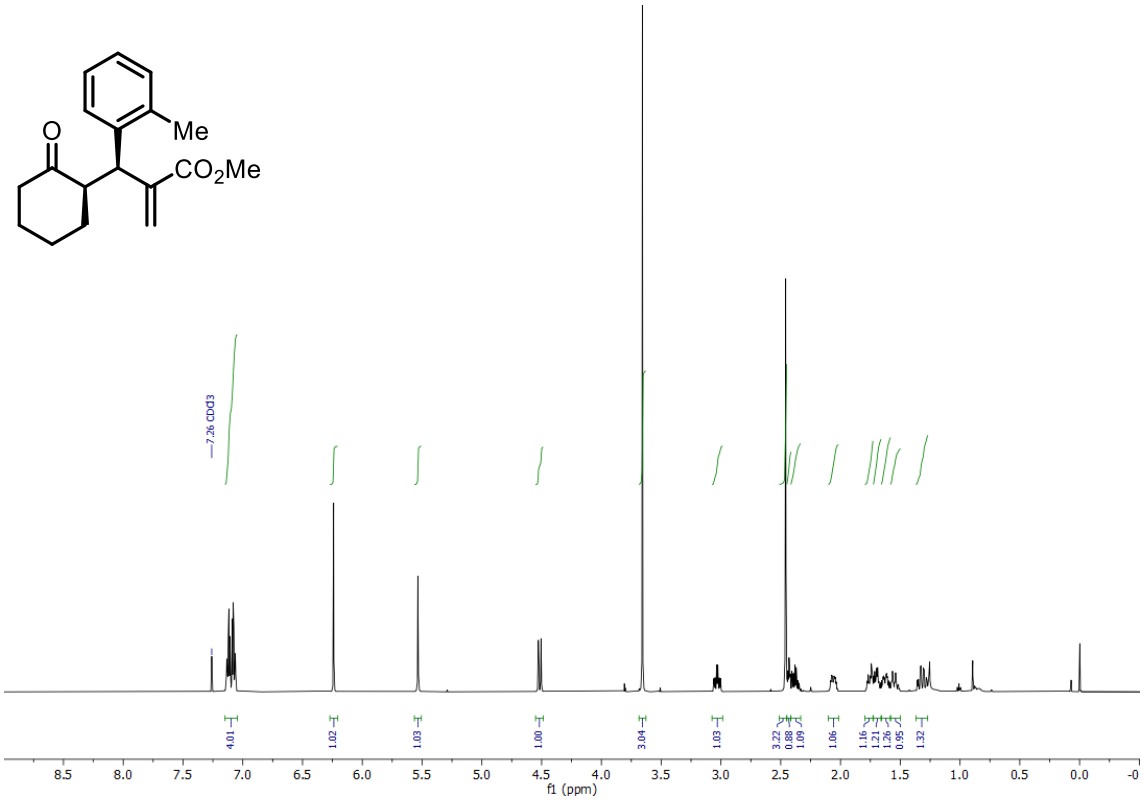

^{1}H NMR spectra of **3z**.

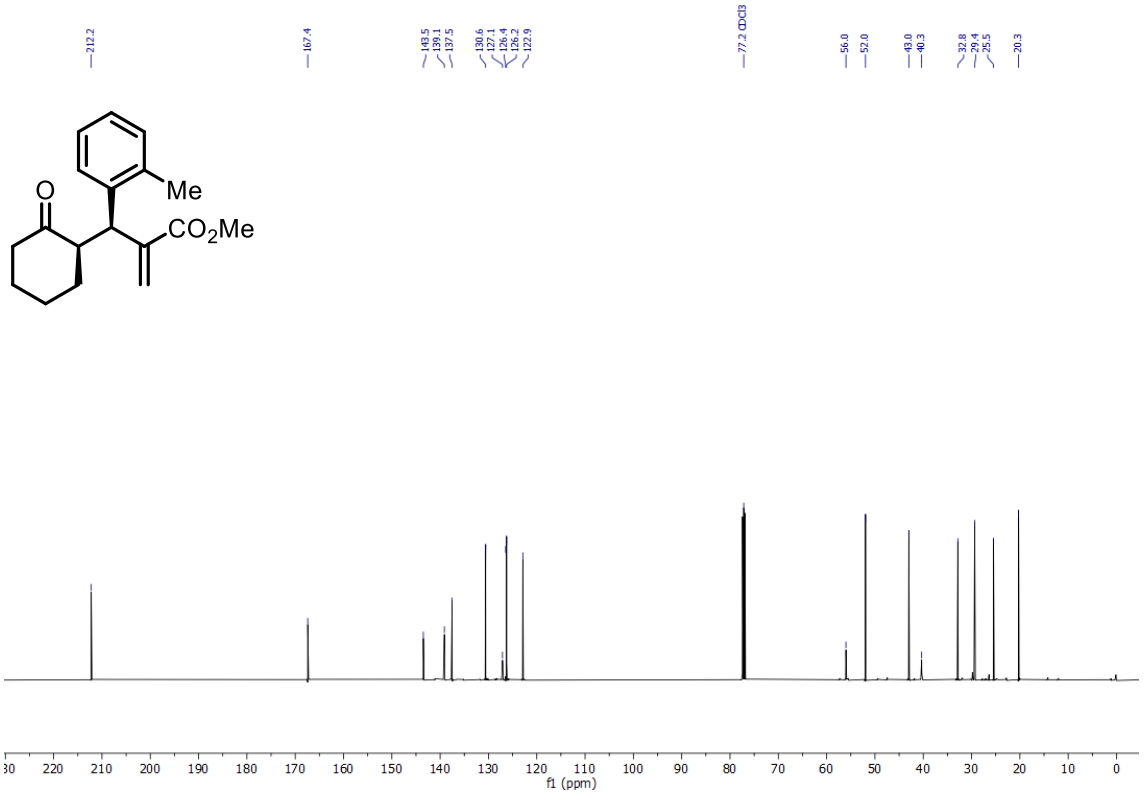

^{13}C NMR spectra of **3z**.

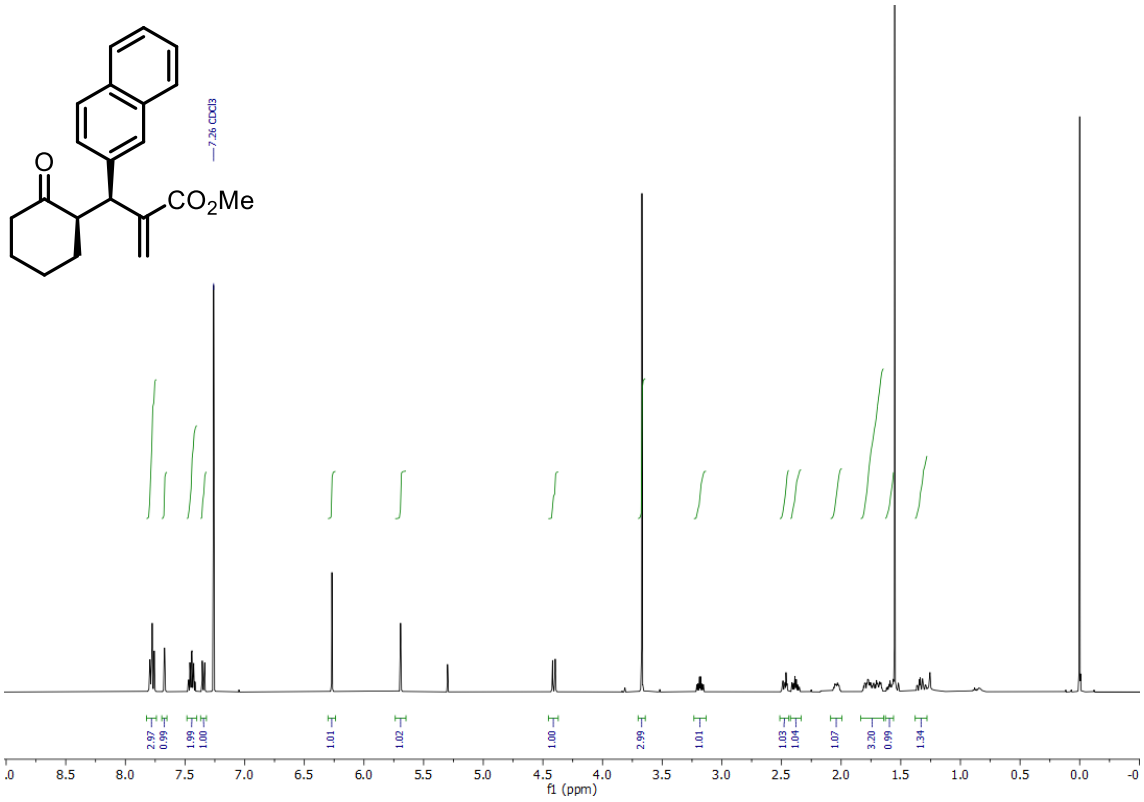

^{1}H NMR spectra of **3aa**.

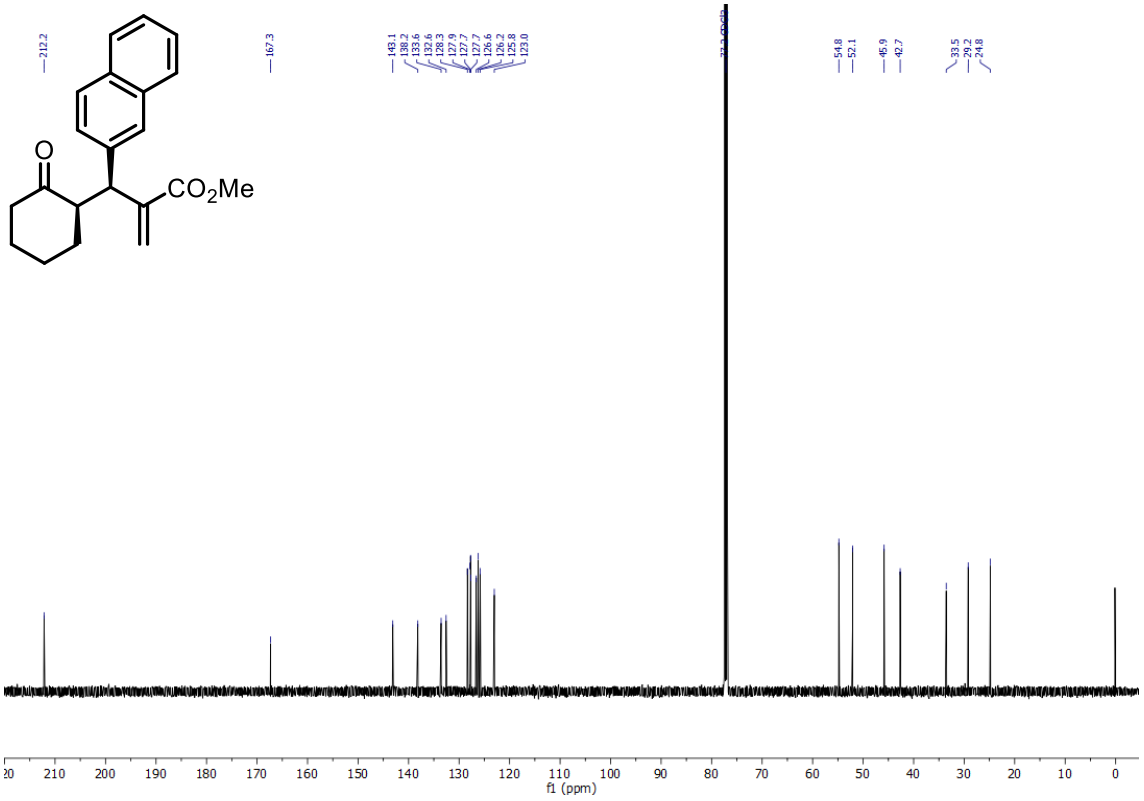

^{13}C NMR spectra of **3aa**.

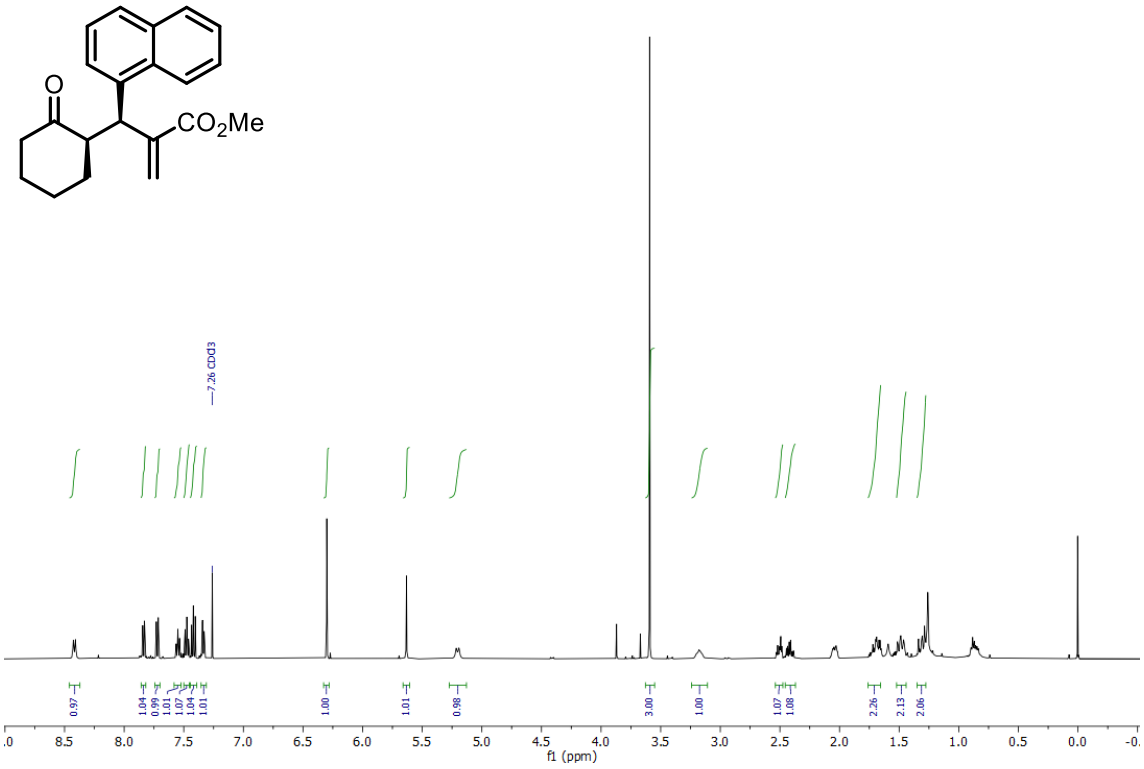

^{1}H NMR spectra of **3ab**.

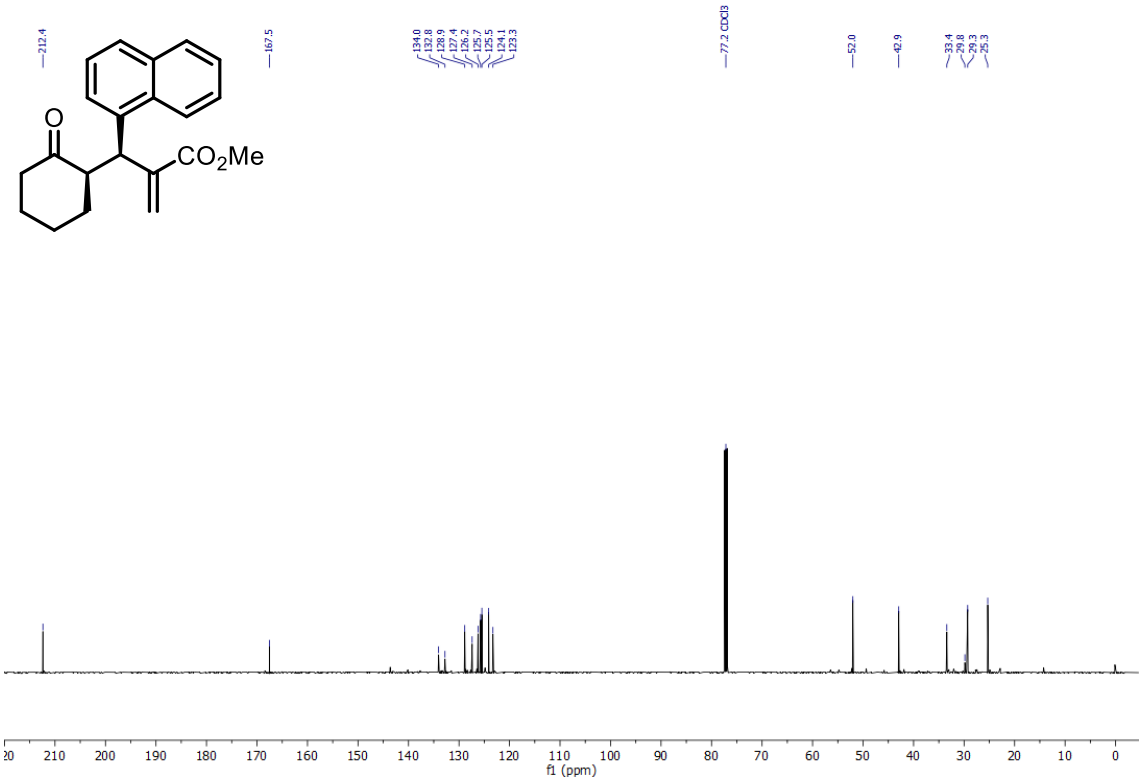

^{13}C NMR spectra of **3ab**.

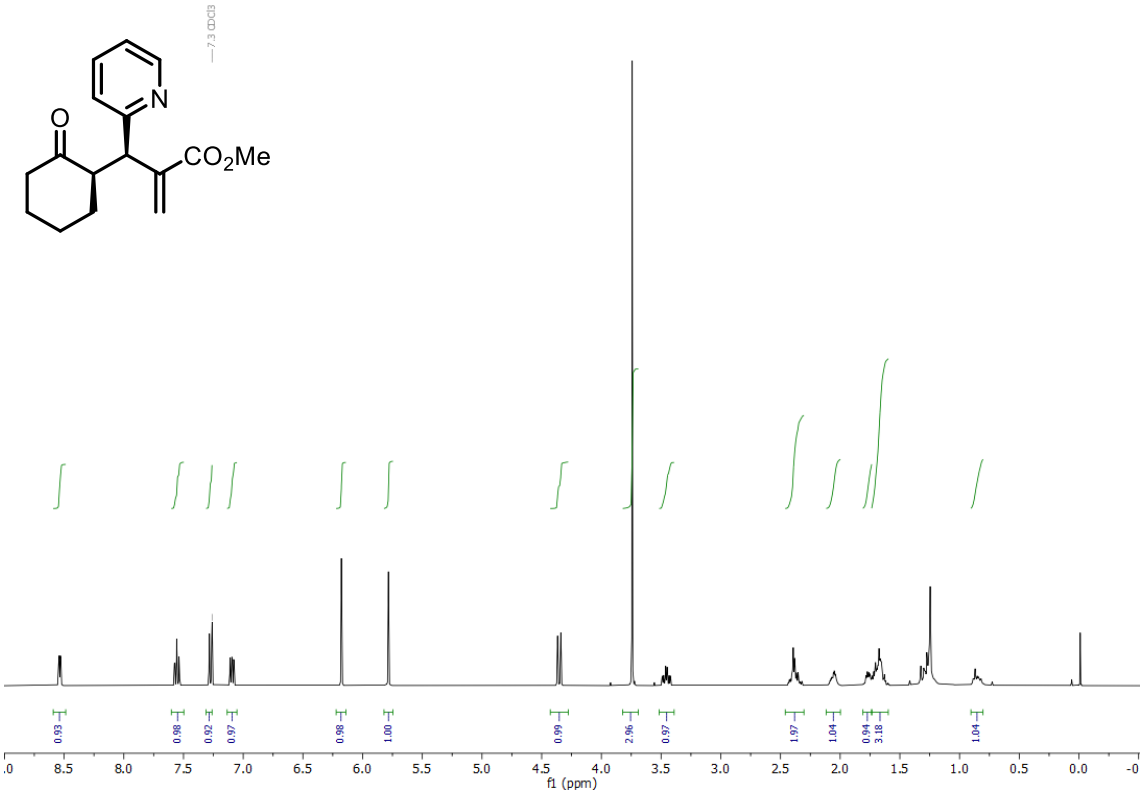

^{1}H NMR spectra of **3ac**.

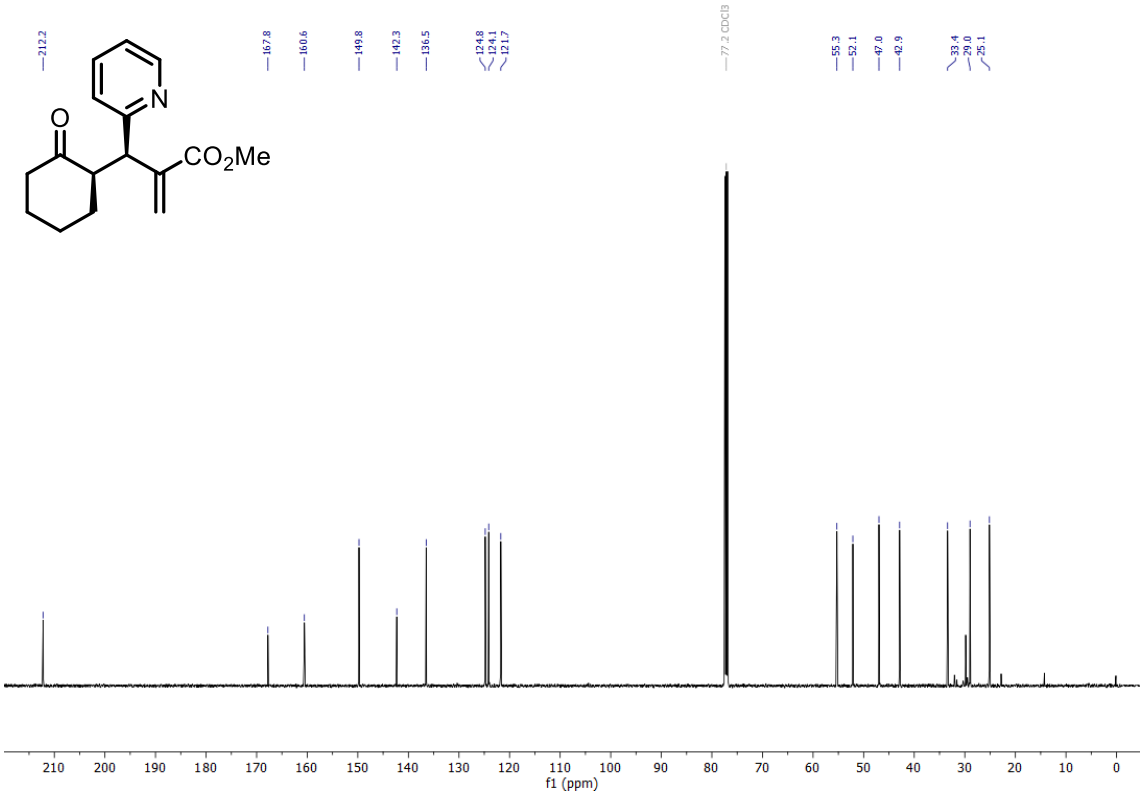

^{13}C NMR spectra of **3ac**.

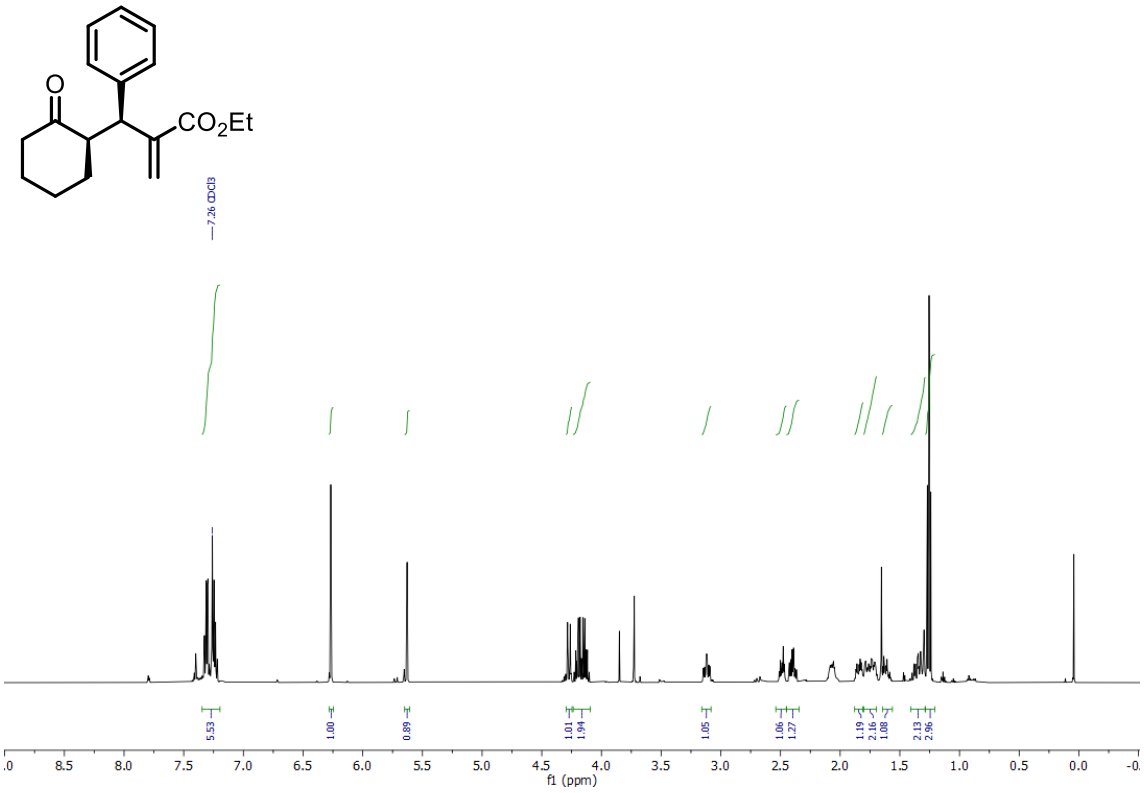

^{1}H NMR spectra of **3ad**.

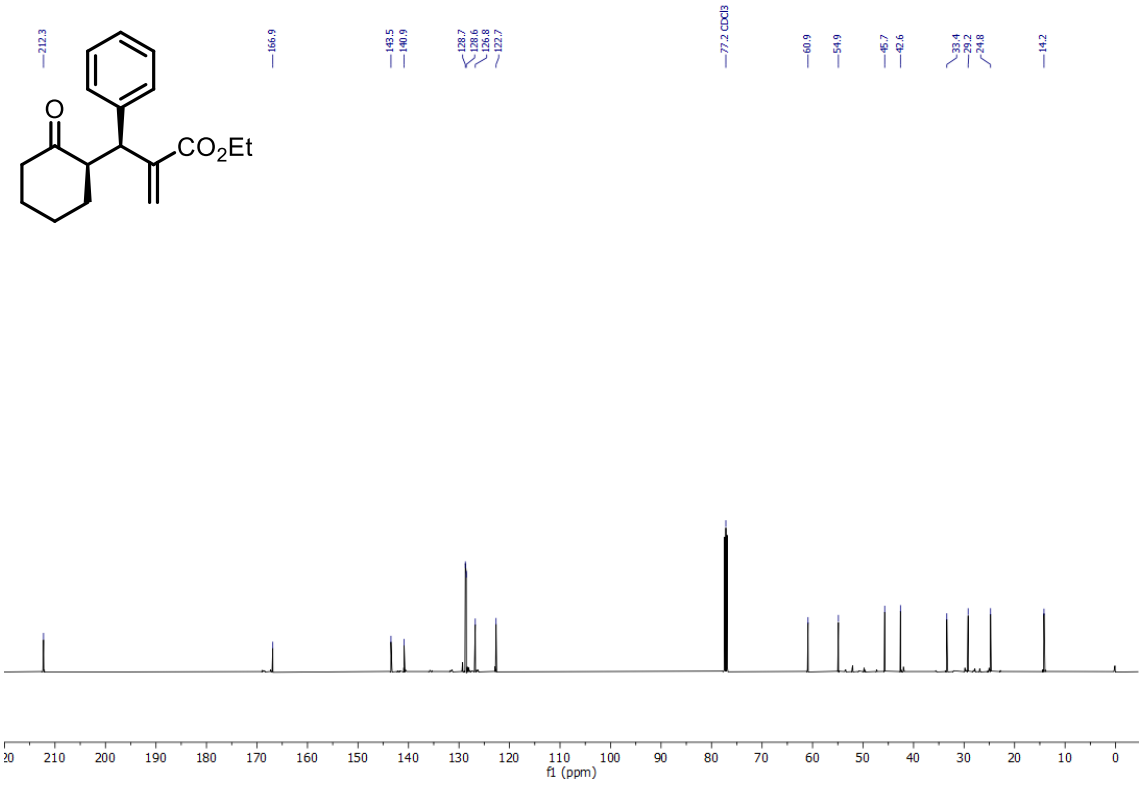

^{13}C NMR spectra of **3ad**.

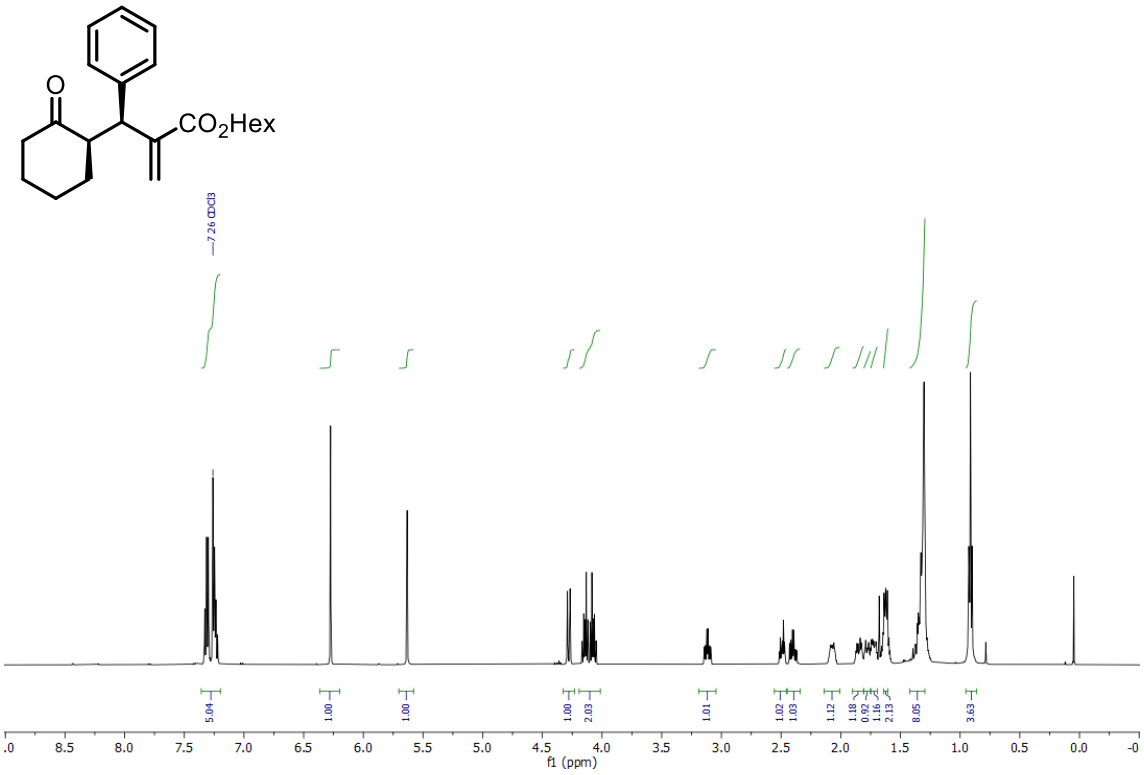

^{1}H NMR spectra of **3ae**.

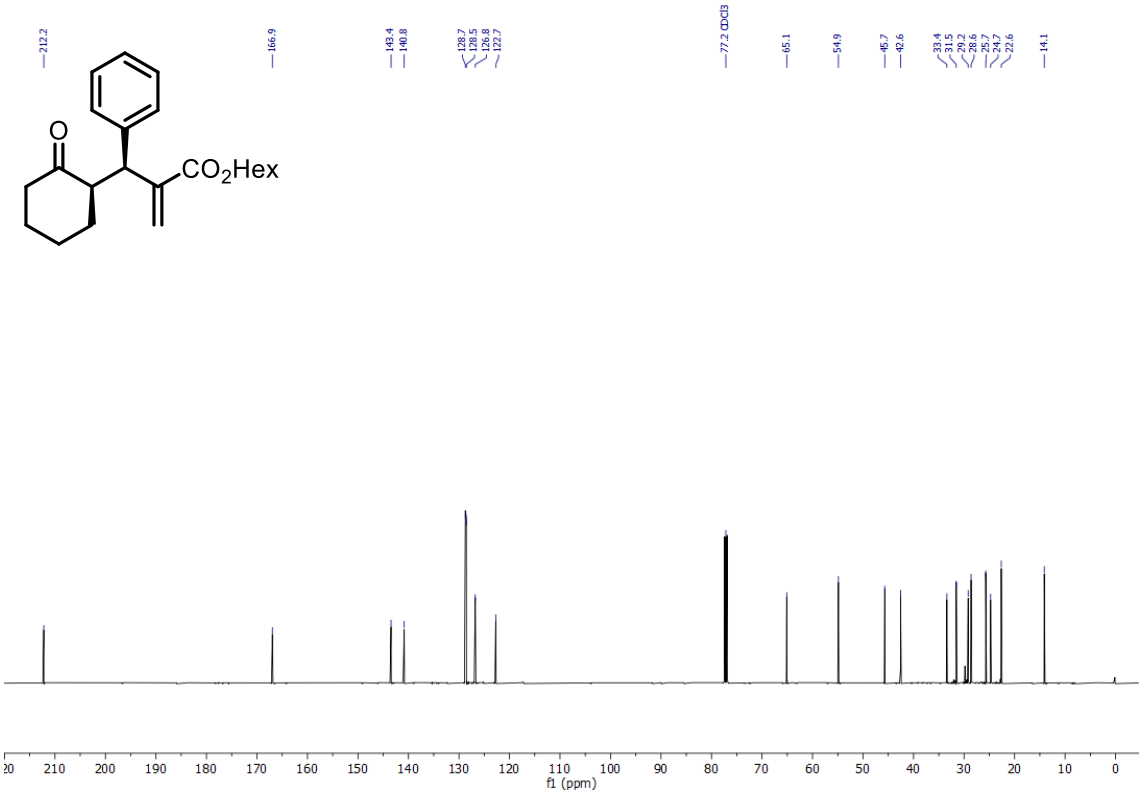

^{13}C NMR spectra of **3ae**.

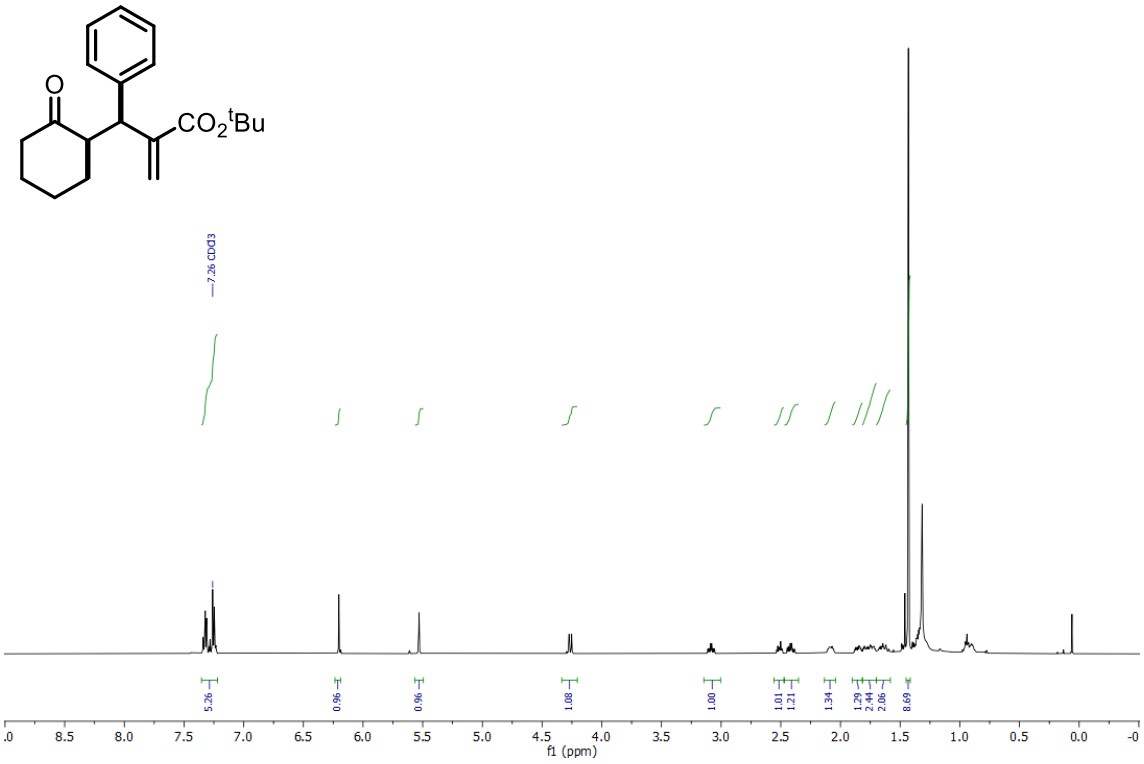

^{1}H NMR spectra of **3af**.

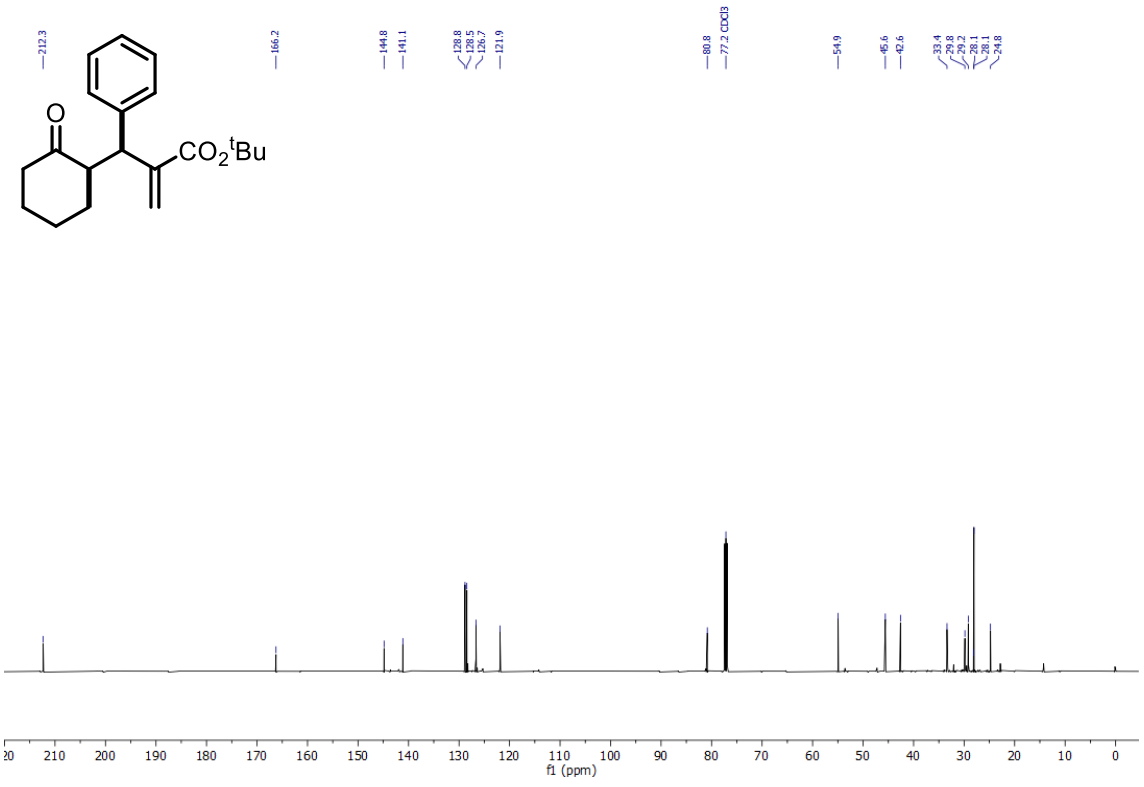

^{13}C NMR spectra of **3af**.

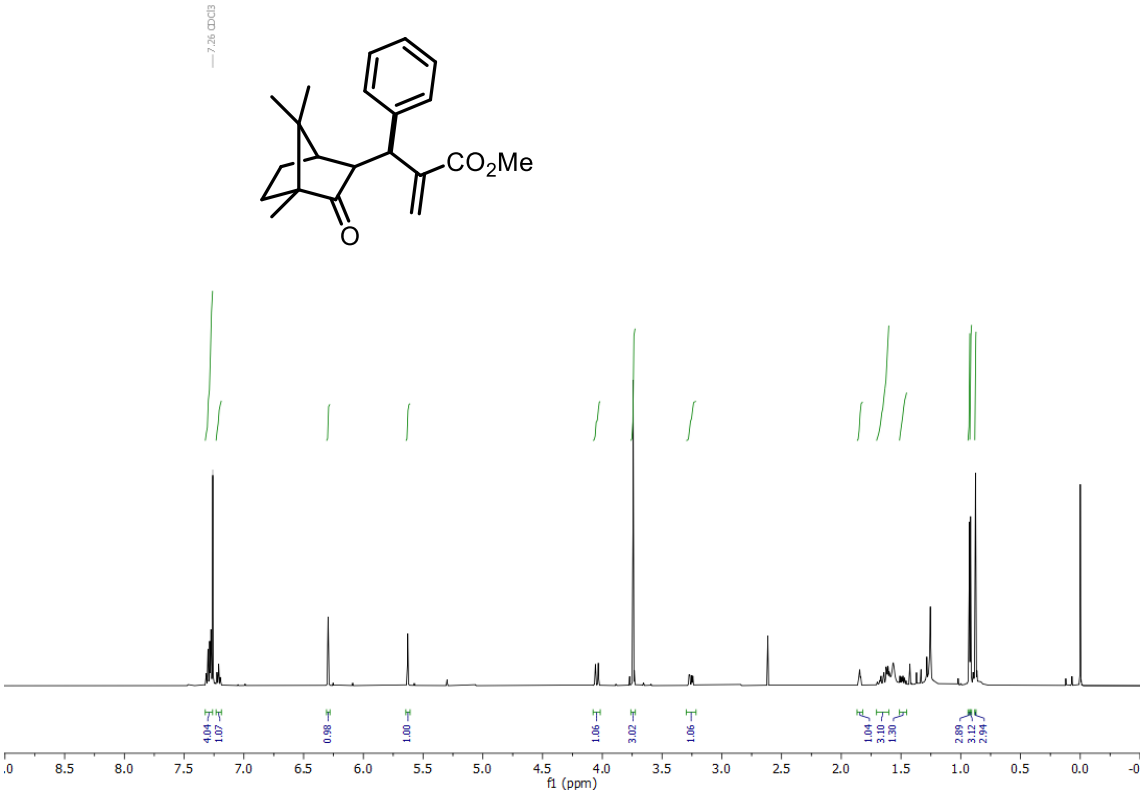

^{1}H NMR spectra of **3ag**.

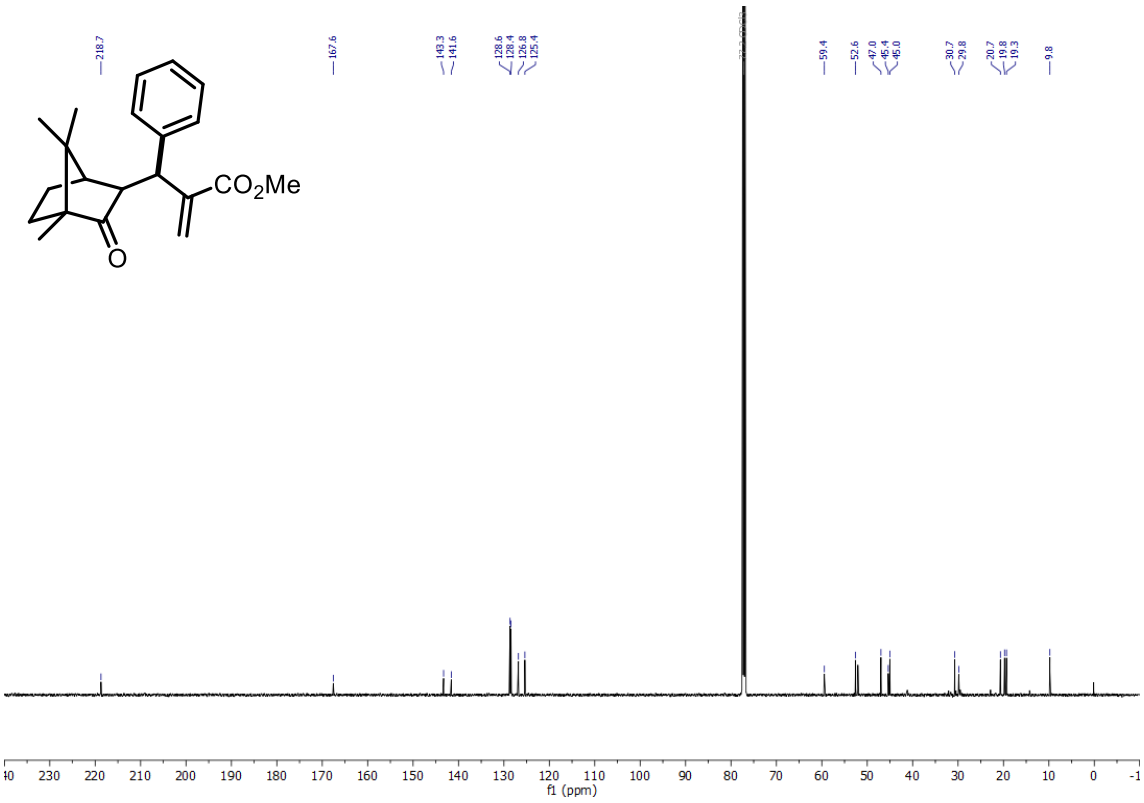

^{13}C NMR spectra of **3ag**.

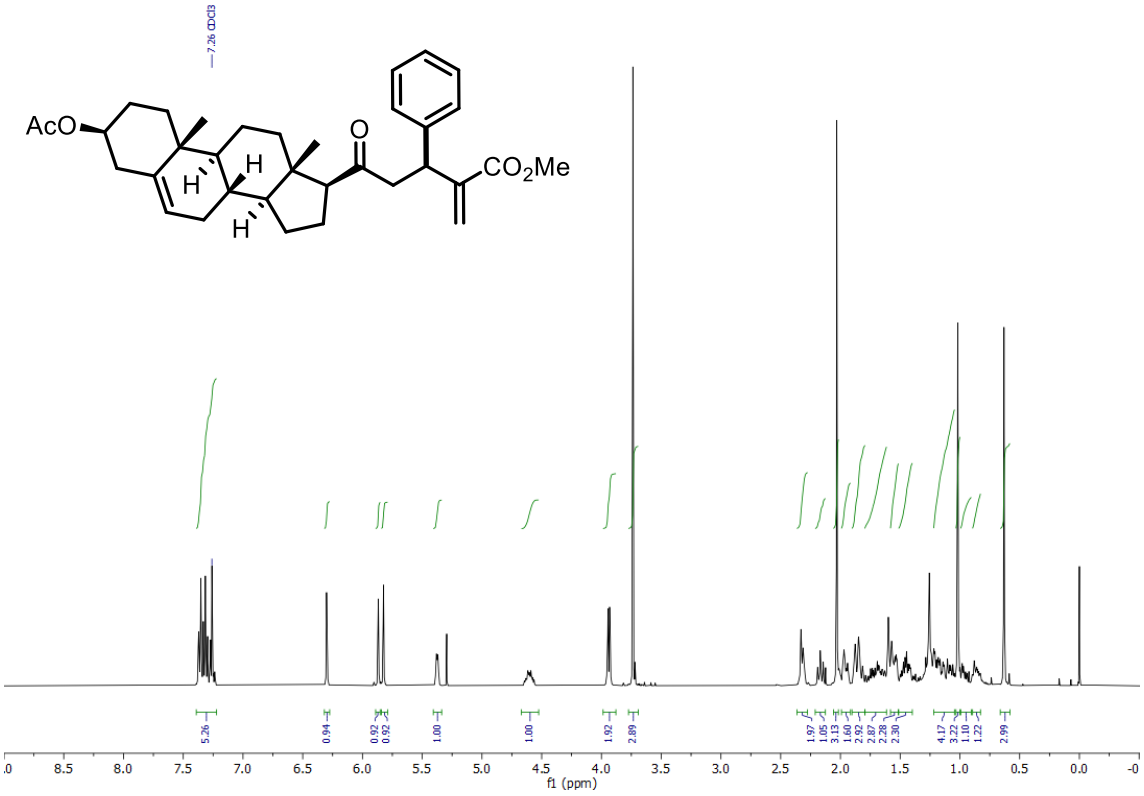

^{1}H NMR spectra of **3ah**.

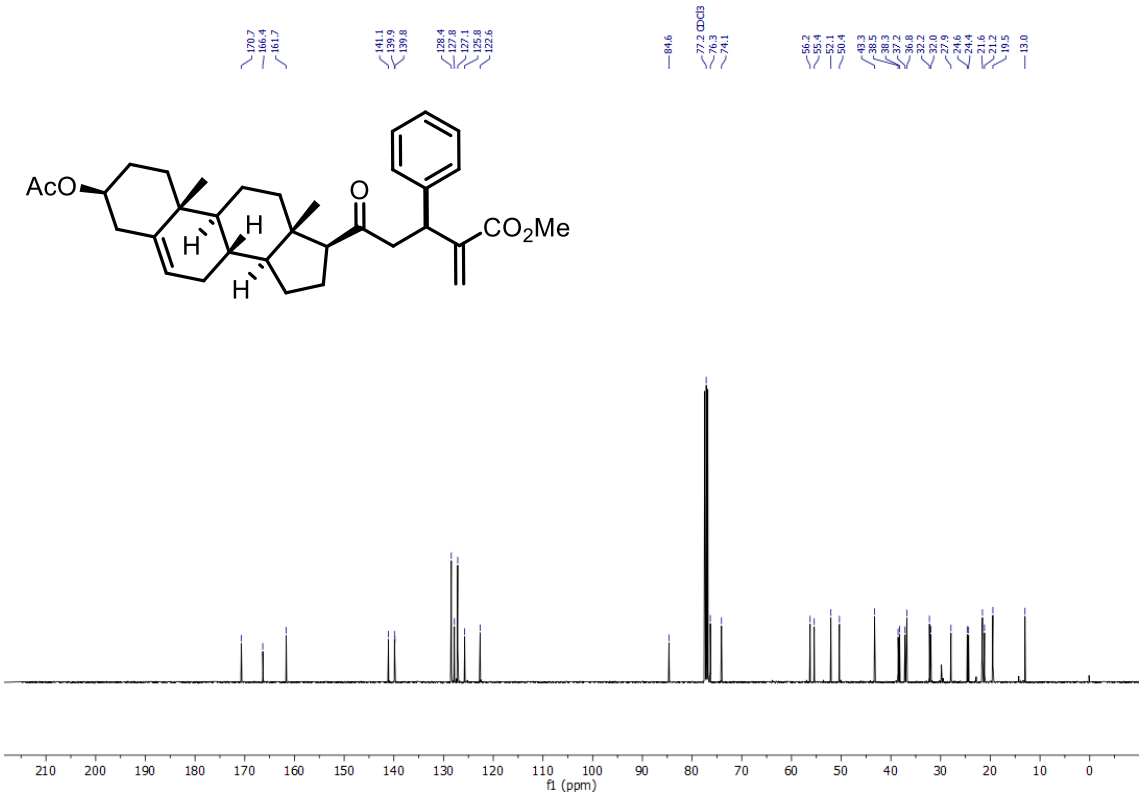

^{13}C NMR spectra of **3ah**.

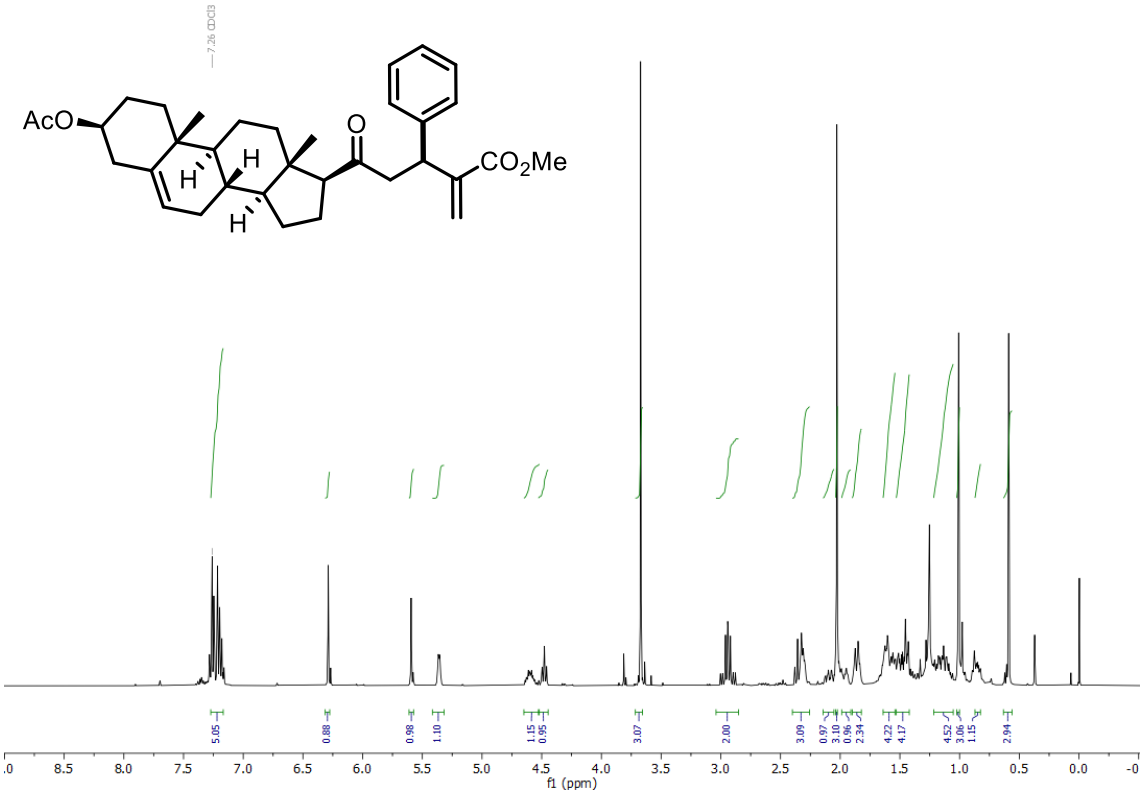

^{1}H NMR spectra of **3ah'**.

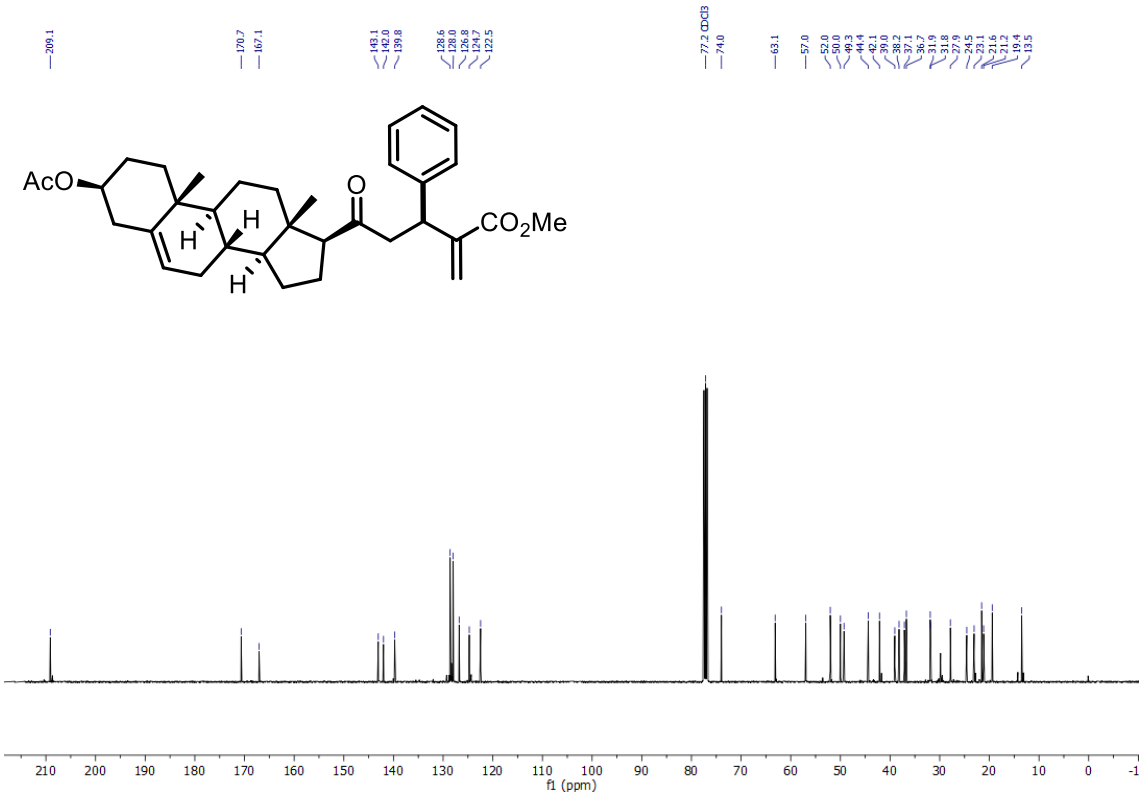

^{13}C NMR spectra of **3ah'**.

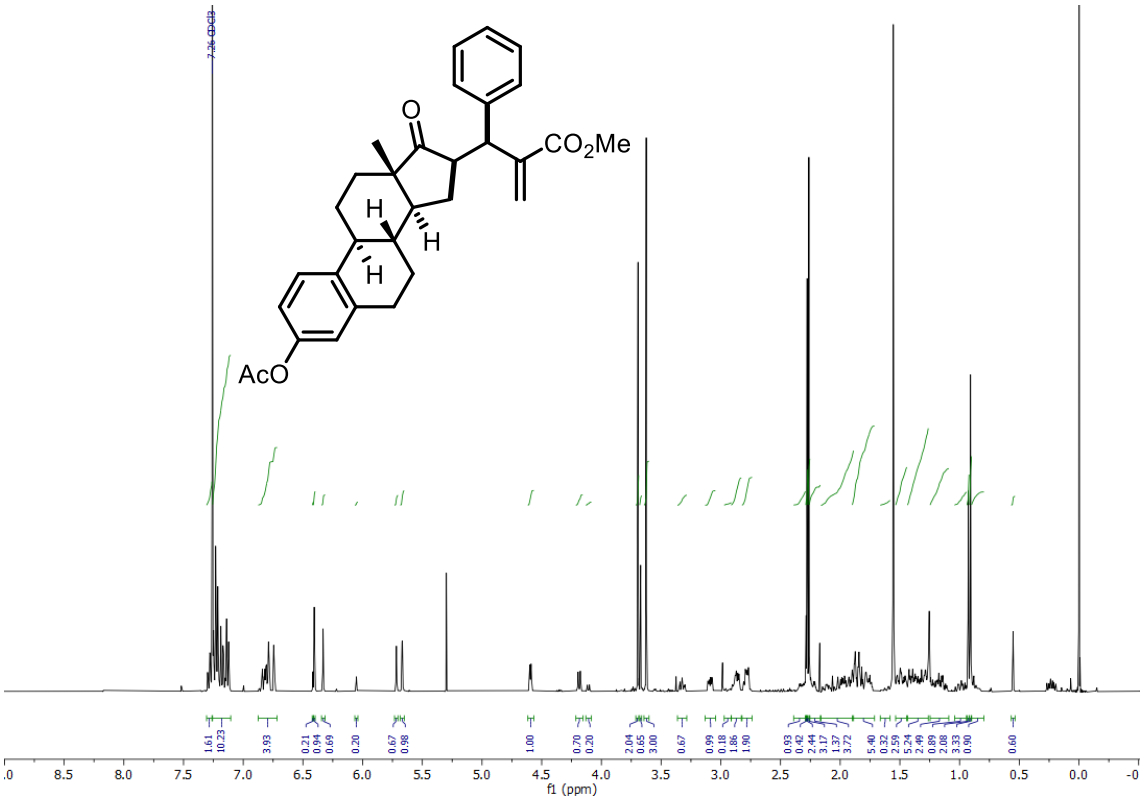

^{1}H NMR spectra of **3ai**.

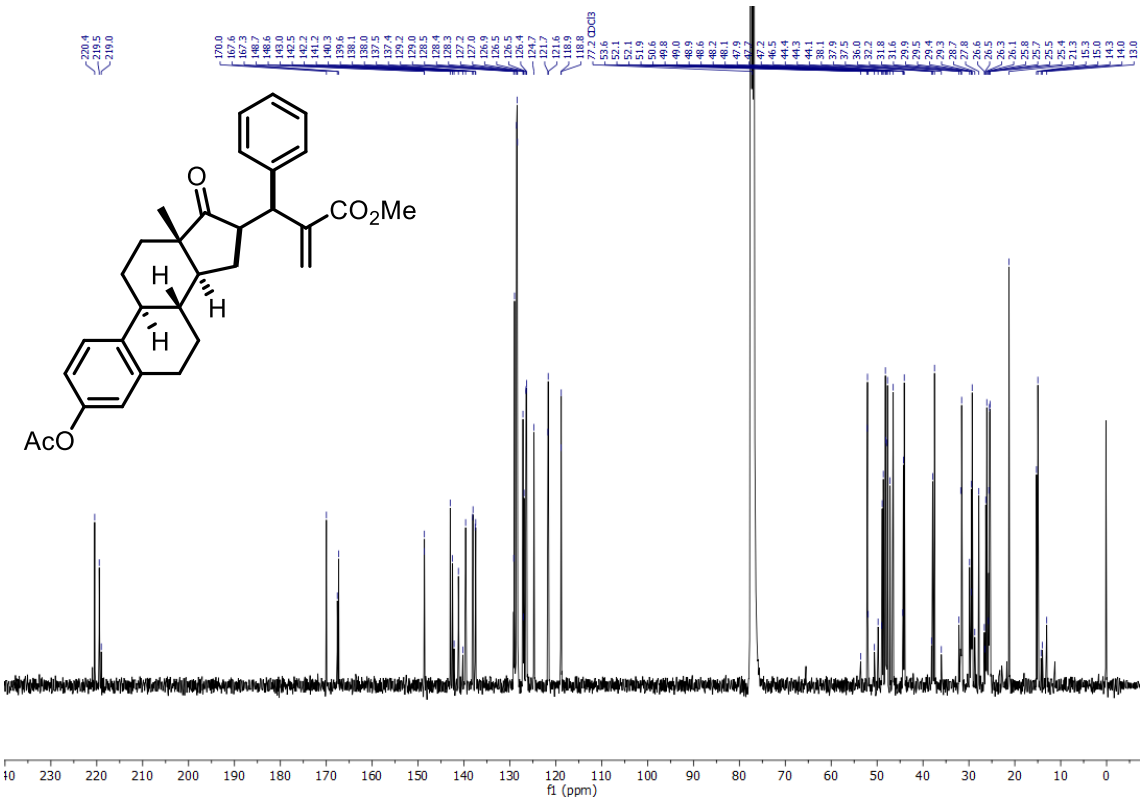

^{13}C NMR spectra of **3ai**.

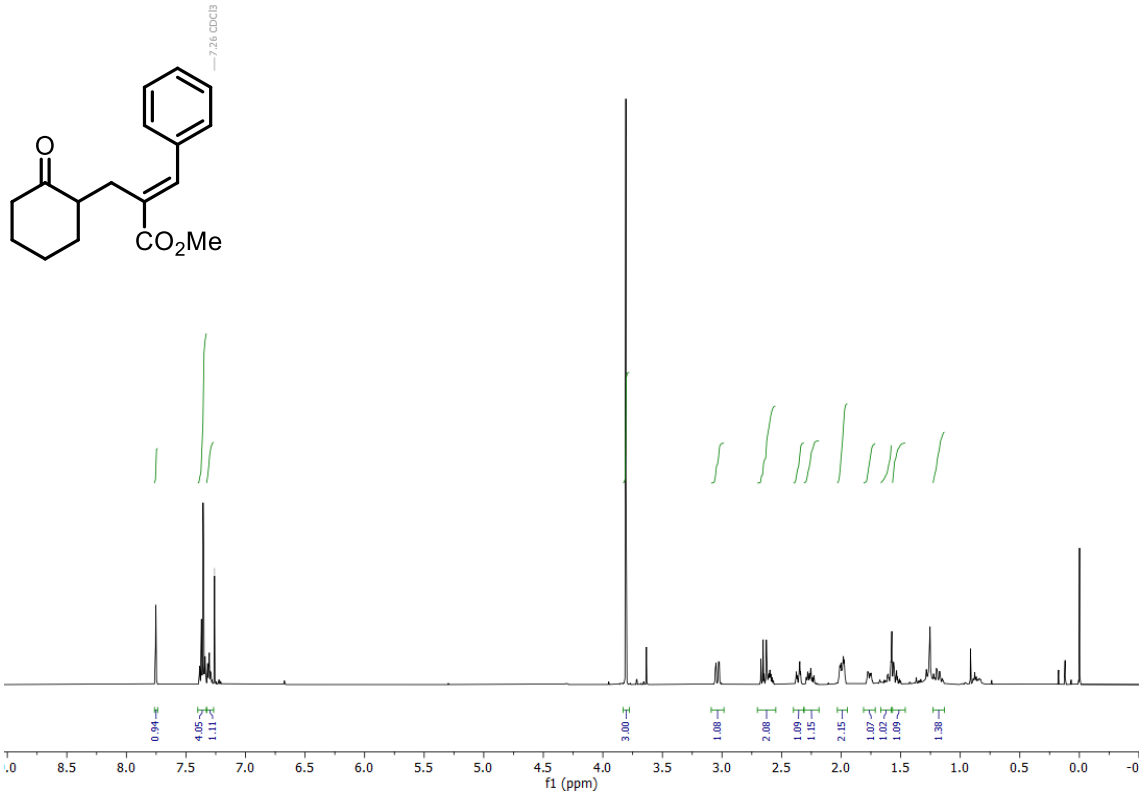

^{1}H NMR spectra of **4a**.

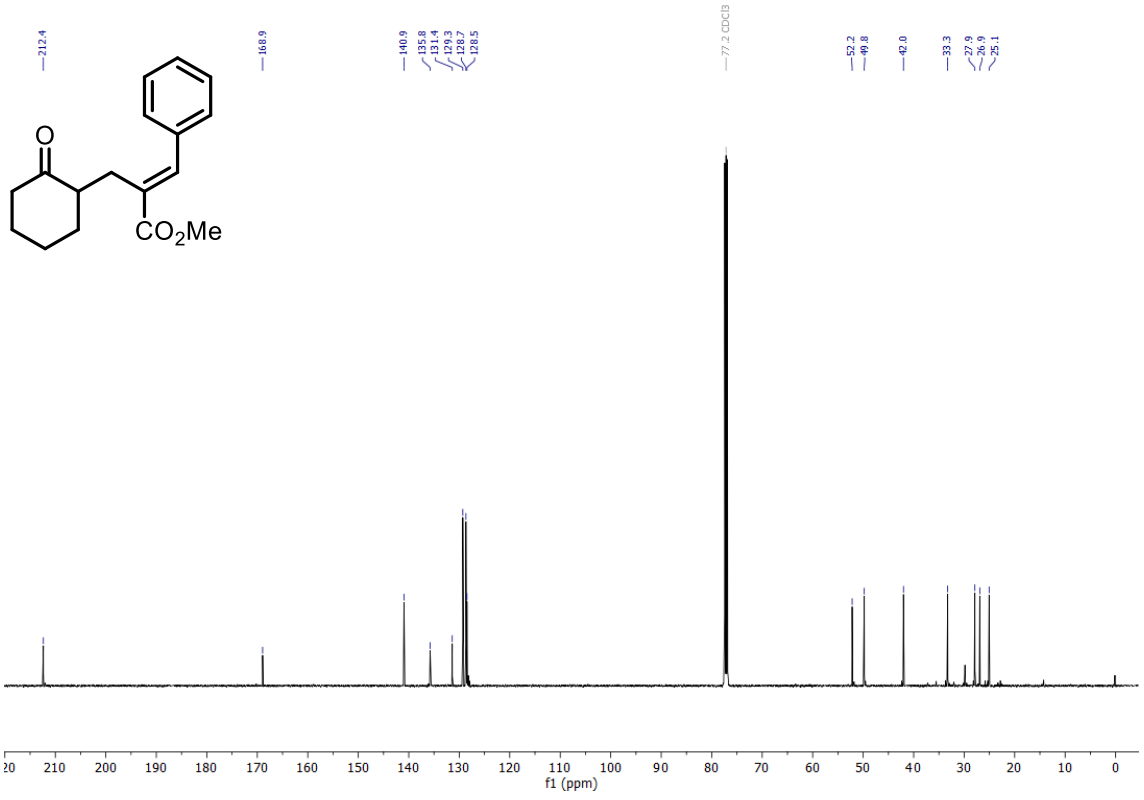

^{13}C NMR spectra of **4a**.

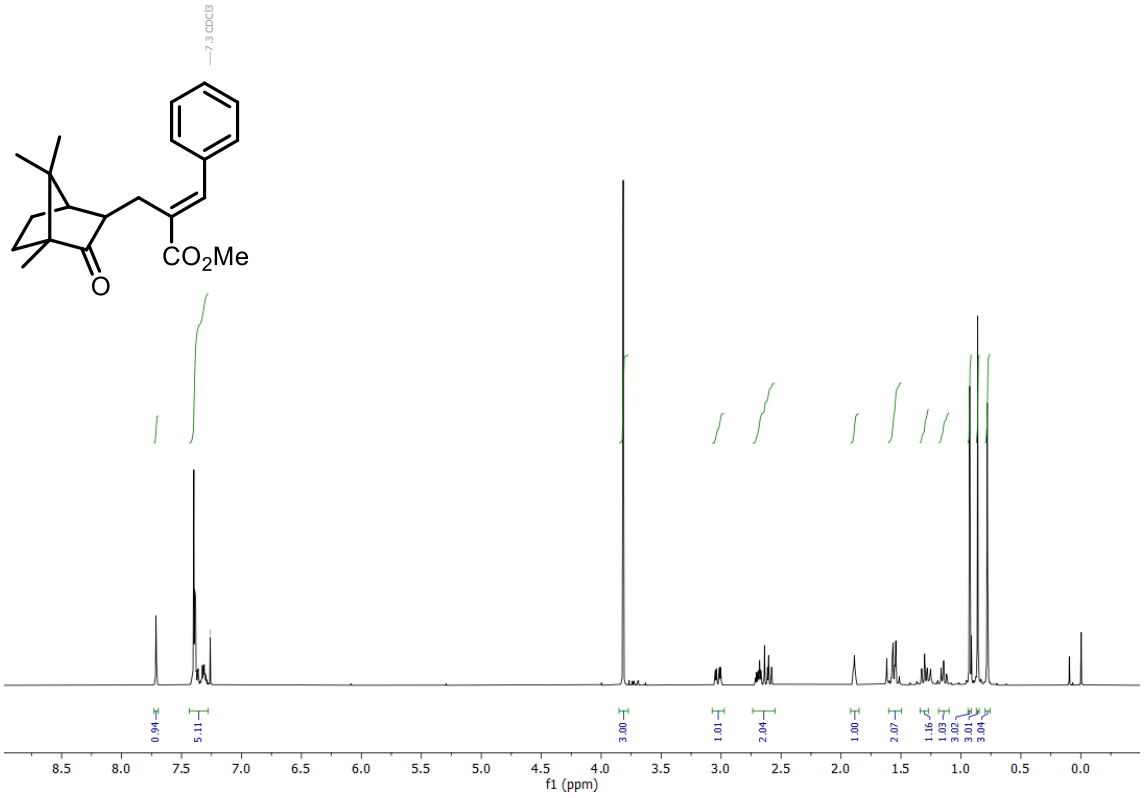

^{1}H NMR spectra of **4b**.

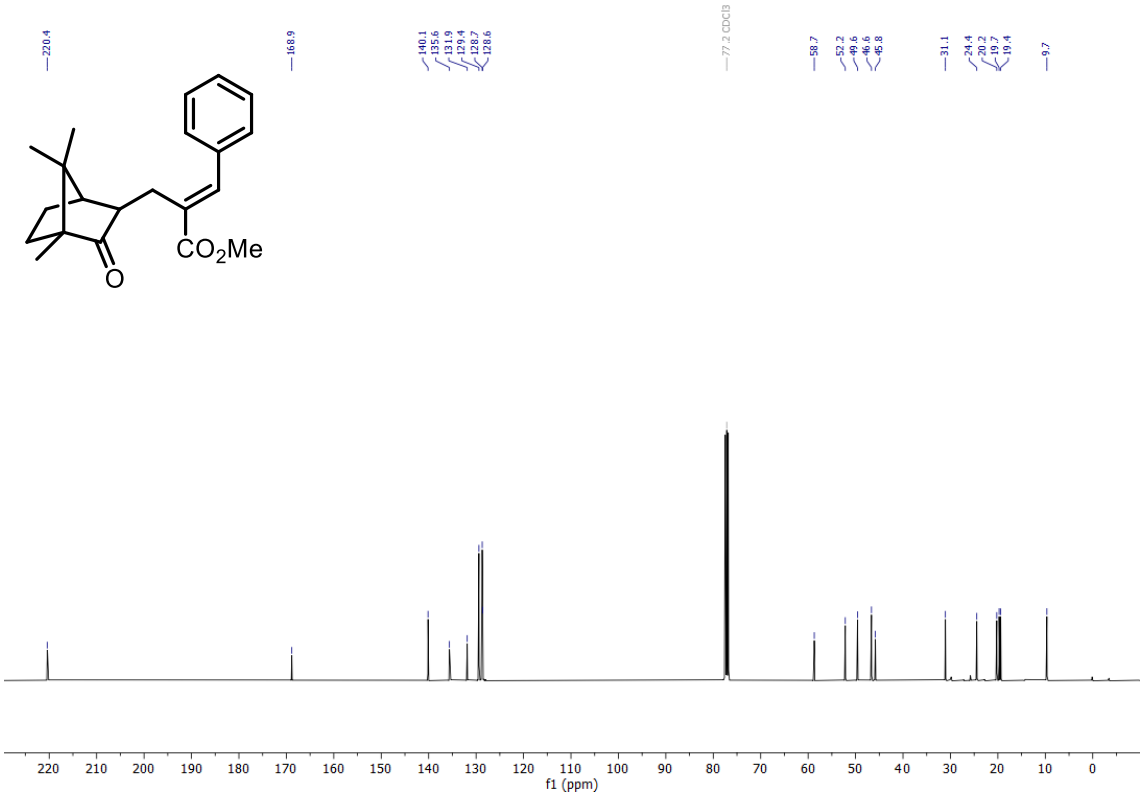

^{13}C NMR spectra of **4b**.

N.5. NMR spectra of derivatization products

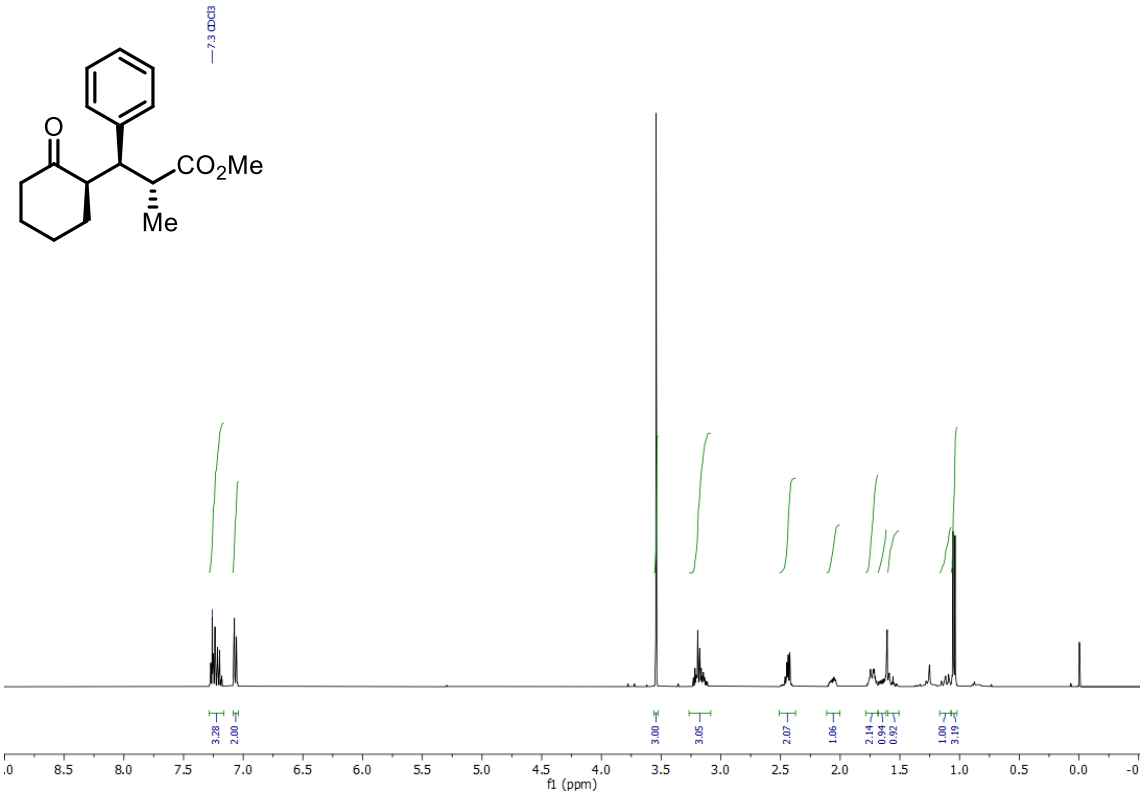

^{1}H NMR spectra of **6a**.

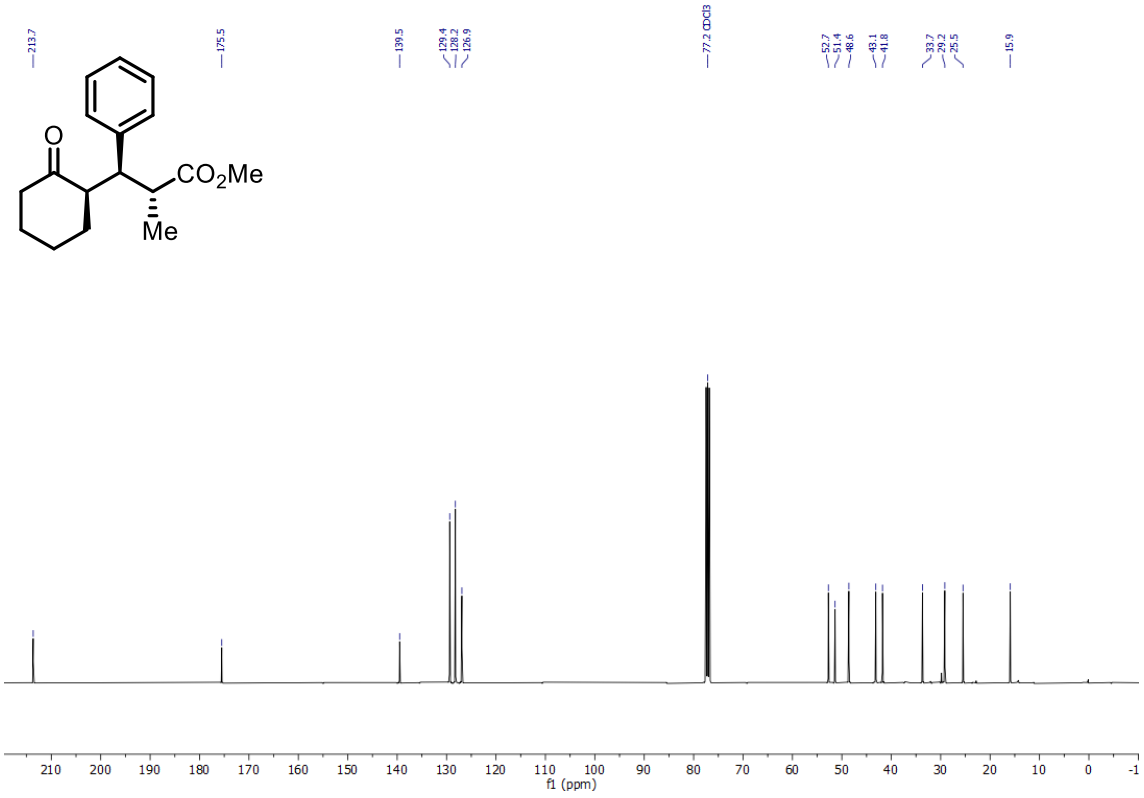

^{13}C NMR spectra of **6a**.

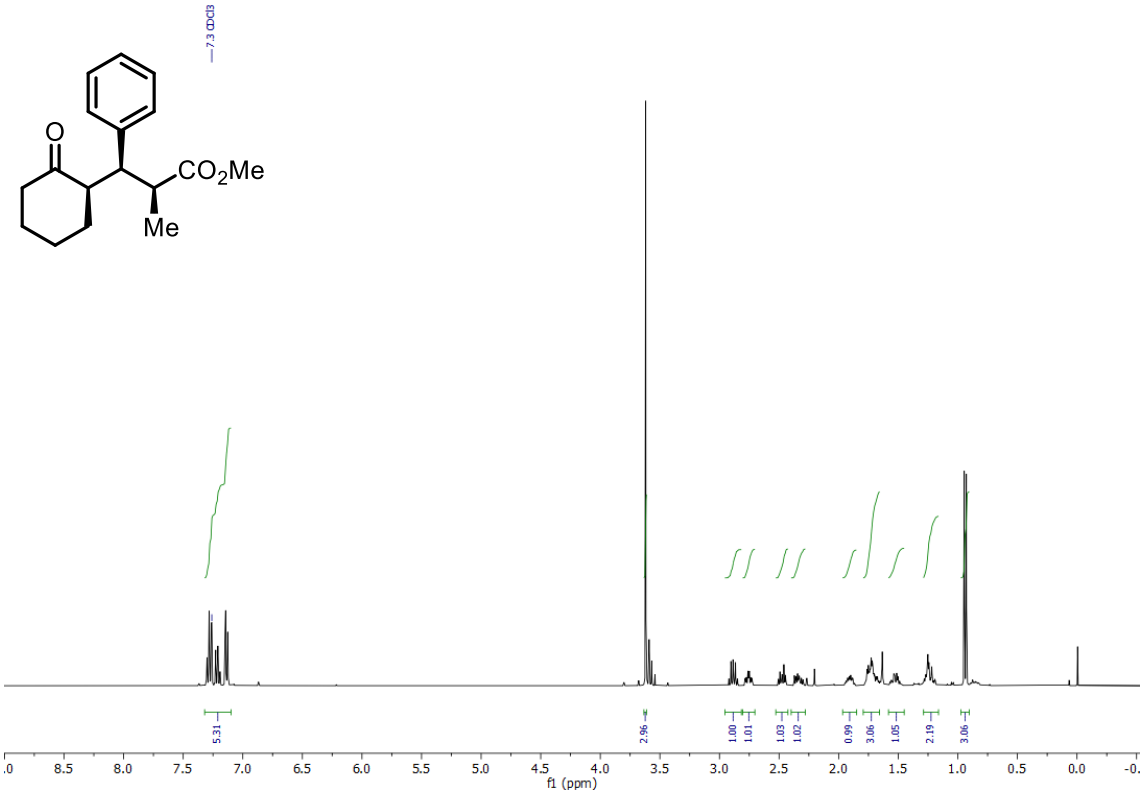

^{1}H NMR spectra of **6b**.

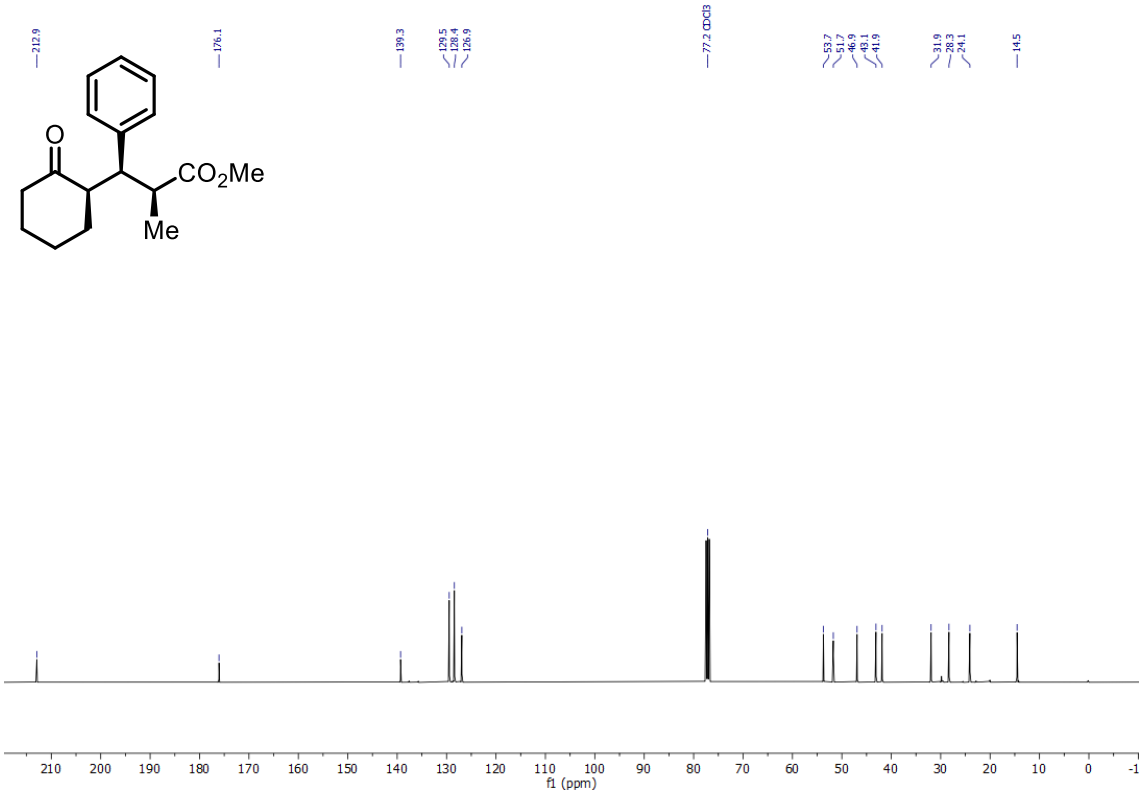

^{13}C NMR spectra of **6b.**

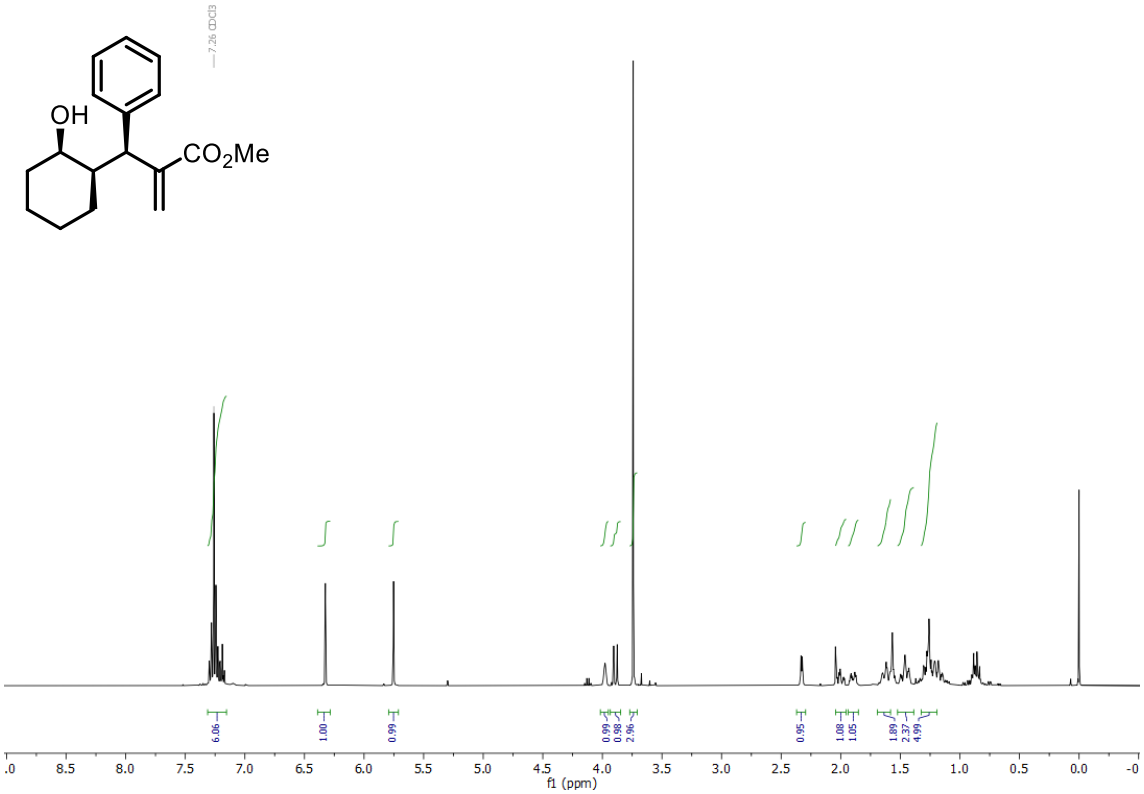

^{1}H NMR spectra of **8.**

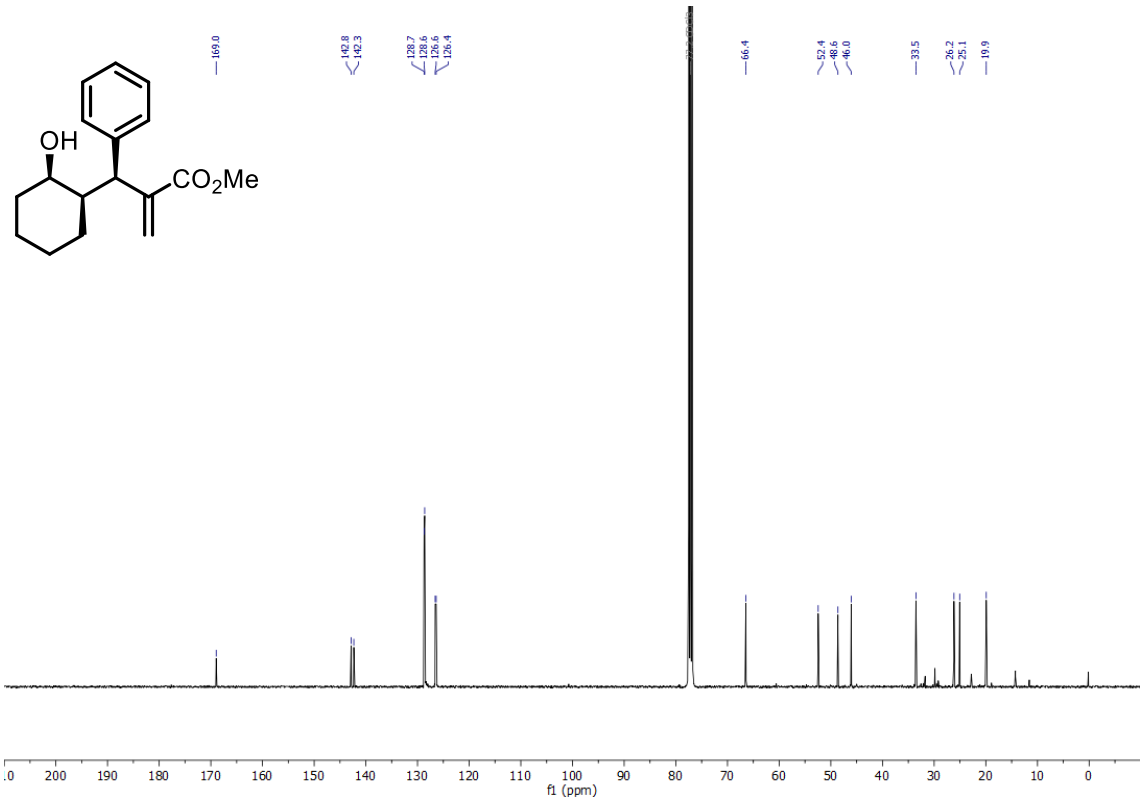

^{13}C NMR spectra of **8.**

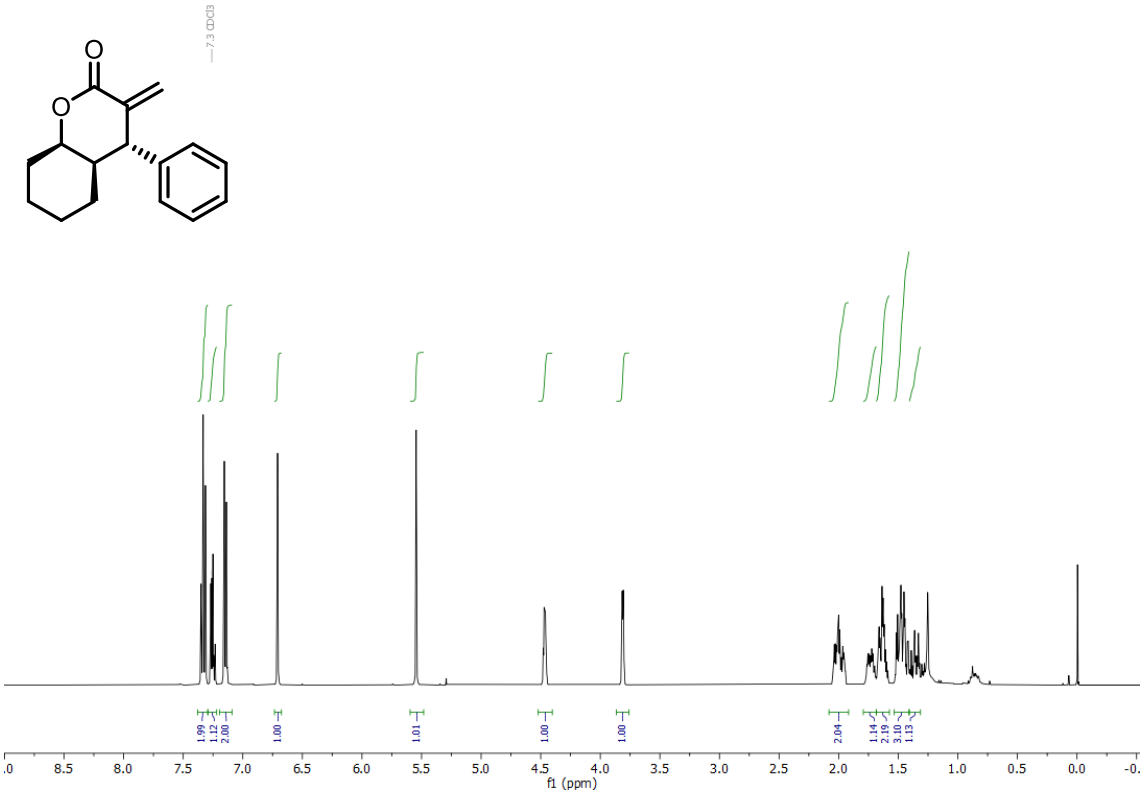

^{1}H NMR spectra of **7.**

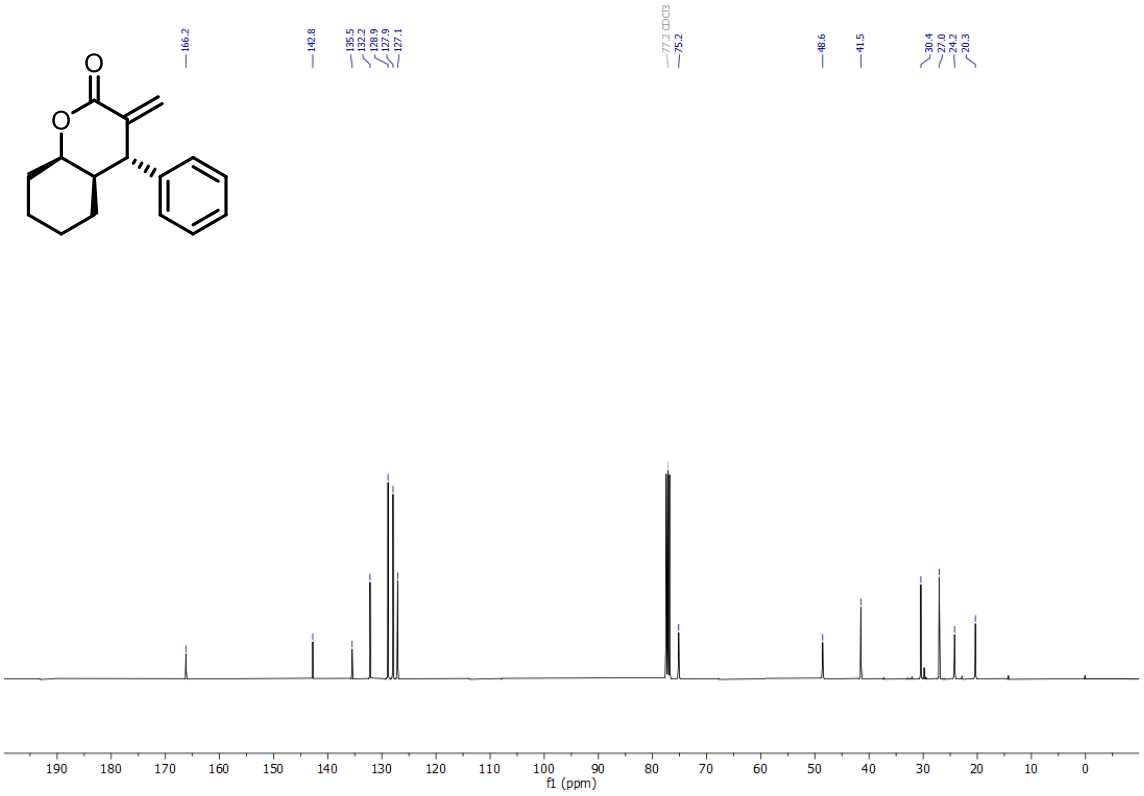

^{13}C NMR spectra of **7**.

.

O. Chiral HPLC Chromatograms

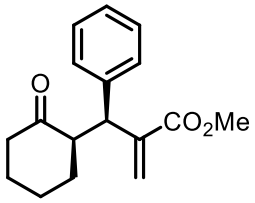

3a

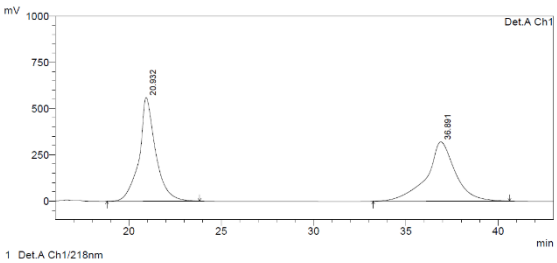

PeakTable

Detector A Ch1 218nm

Peak#	Ret. Time	Area	Height	Area %	Height %
1	20.932	34856538	560780	50.264	63.623
2	36.891	34490601	320637	49.736	36.377
Total		69347139	881418	100.000	100.000

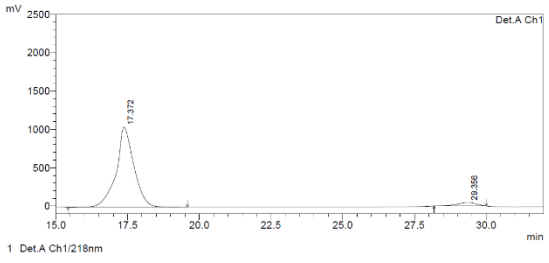

PeakTable

Detector A Ch1 218nm

Peak#	Ret. Time	Area	Height	Area %	Height %
1	17.372	44704191	1042631	95.349	95.726
2	29.356	2180645	46546	4.651	4.274
Total		46884837	1089177	100.000	100.000

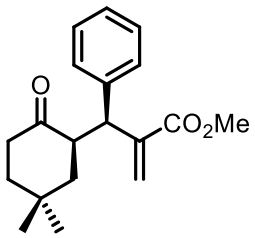

3b

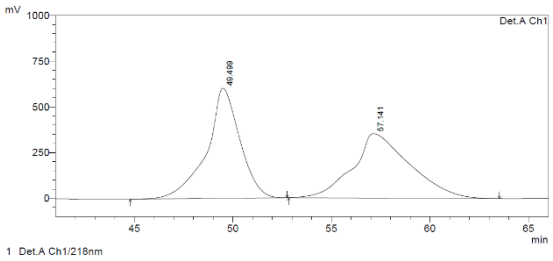

PeakTable

Detector A Ch1 218nm

Peak#	Ret. Time	Area	Height	Area %	Height %
1	49.499	70428479	601238	49.940	63.075
2	57.141	70598493	351970	50.060	36.925
Total		141026972	953208	100.000	100.000

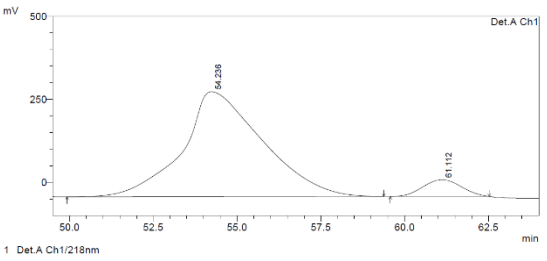

PeakTable

Detector A Ch1 218nm

Peak#	Ret. Time	Area	Height	Area %	Height %
1	54.236	52629791	316182	92.898	86.239
2	61.112	4023512	50453	7.102	13.761
Total		56653304	366634	100.000	100.000

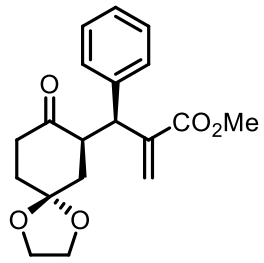

3c

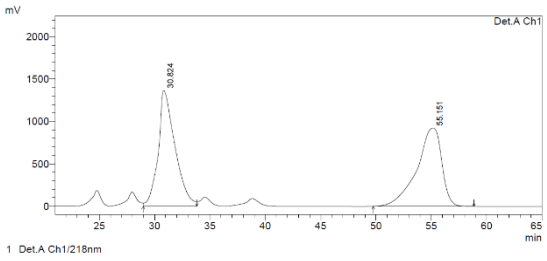

PeakTable

Detector A Ch1 218nm

Peak#	Ret. Time	Area	Height	Area %	Height %
1	30.824	145068468	1367574	50.042	59.628
2	55.151	144823195	925927	49.958	40.372
Total		289891663	2293502	100.000	100.000

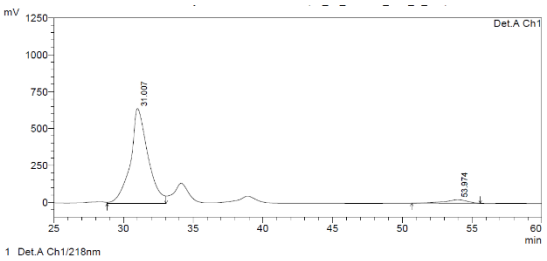

PeakTable

Detector A Ch1 218nm

Peak#	Ret. Time	Area	Height	Area %	Height %
1	31.007	56488913	643978	95.317	96.406
2	53.974	2775122	24007	4.683	3.594
Total		59264035	667985	100.000	100.000

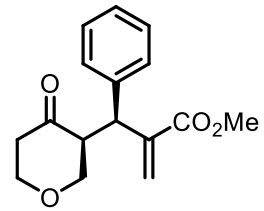

3d

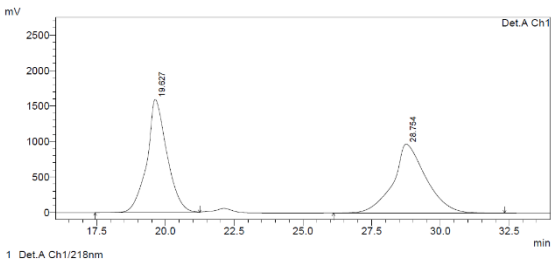

PeakTable

Detector A Ch1 218nm

Peak#	Ret. Time	Area	Height	Area %	Height %
1	19.627	81725372	1597822	50.246	62.180
2	28.754	80926117	971843	49.754	37.820
Total		162651489	2569665	100.000	100.000

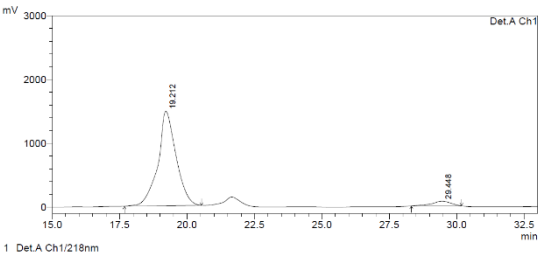

PeakTable

Detector A Ch1 218nm

Peak#	Ret. Time	Area	Height	Area %	Height %
1	19.212	69347139	1480247	94.983	95.174
2	29.448	3663102	75066	5.017	4.826
Total		73010241	1555313	100.000	100.000

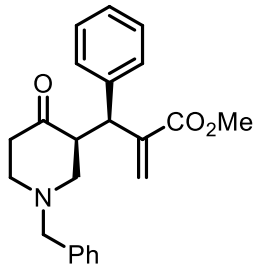

3e

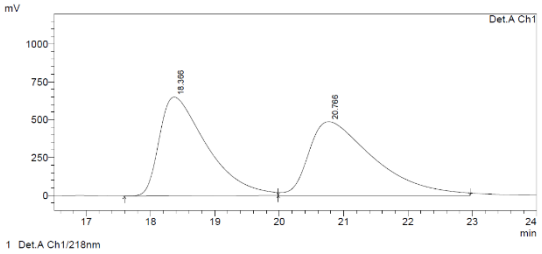

PeakTable

Detector A Ch1 218nm

Peak#	Ret. Time	Area	Height	Area %	Height %
1	18.366	33499262	652701	49.492	57.301
2	20.766	34187486	486380	50.508	42.699
Total		67686747	1139082	100.000	100.000

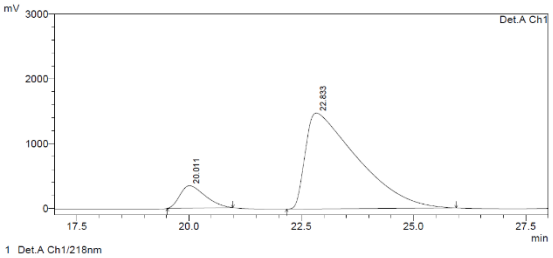

PeakTable

Detector A Ch1 218nm

Peak#	Ret. Time	Area	Height	Area %	Height %
1	20.011	13481377	345566	10.132	18.953
2	22.833	119574460	1477708	89.868	81.047
Total		133055838	1823274	100.000	100.000

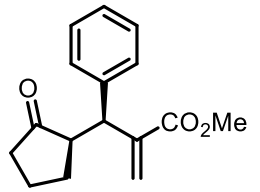

3f

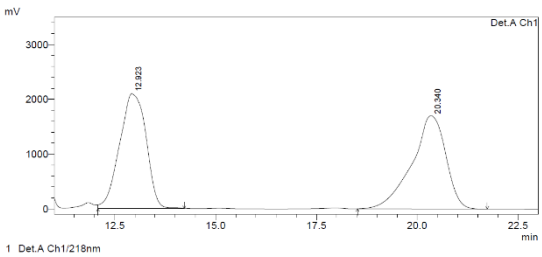

PeakTable

Detector A Ch1 218nm

Peak#	Ret. Time	Area	Height	Area %	Height %
1	12.923	96718522	2102978	49.309	55.289
2	20.340	99428258	1700641	50.691	44.711
Total		196146780	3803619	100.000	100.000

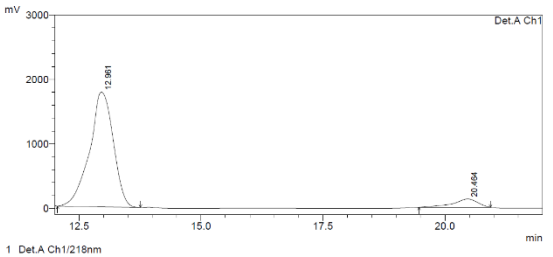

PeakTable

Detector A Ch1 218nm

Peak#	Ret. Time	Area	Height	Area %	Height %
1	12.961	60334301	1779612	93.094	93.327
2	20.464	4476002	127247	6.906	6.673
Total		64810303	1906859	100.000	100.000

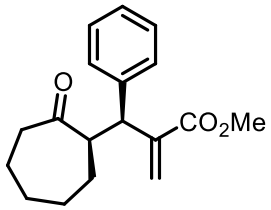

3g

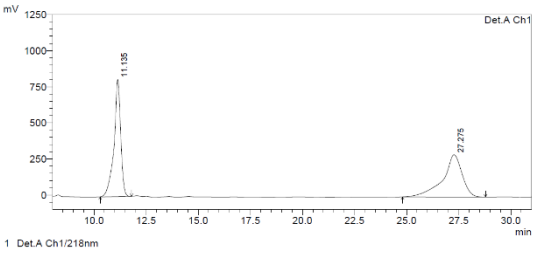

PeakTable

Detector A Ch1 218nm

Peak#	Ret. Time	Area	Height	Area %	Height %
1	11.135	18200178	811139	49.121	73.481
2	27.275	18851527	292744	50.879	26.519
Total		37051704	1103883	100.000	100.000

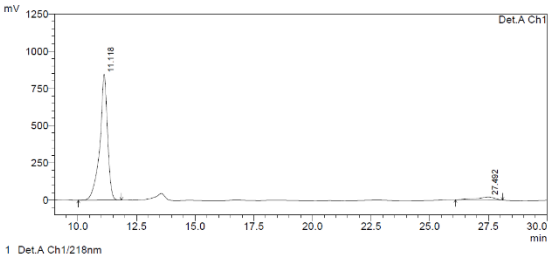

PeakTable

Detector A Ch1 218nm

Peak#	Ret. Time	Area	Height	Area %	Height %
1	11.118	19343836	844417	94.941	97.751
2	27.492	1030683	19426	5.059	2.249
Total		20374519	863843	100.000	100.000

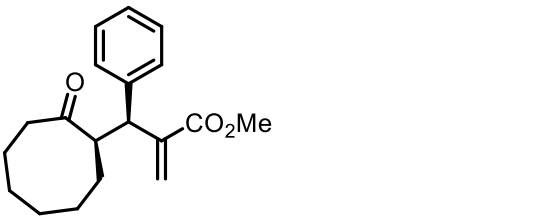

3h

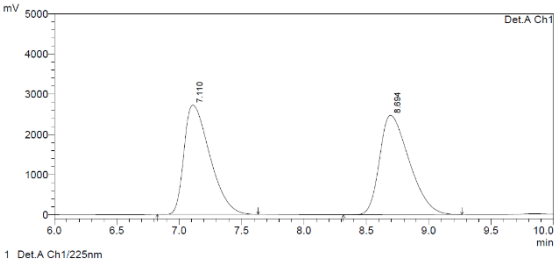

PeakTable

Detector A Ch1 225nm

Peak#	Ret. Time	Area	Height	Area %	Height %
1	7.110	39156233	2717064	48.955	52.393
2	8.694	40828321	2468861	51.045	47.607
Total		79984555	5185925	100.000	100.000

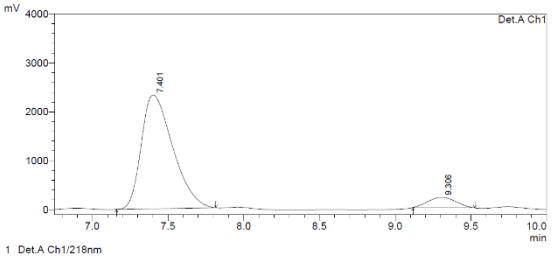

PeakTable

Detector A Ch1 218nm

Peak#	Ret. Time	Area	Height	Area %	Height %
1	7.401	33617791	2320862	92.509	91.635
2	9.306	2722171	211851	7.491	8.365
Total		36339962	2532713	100.000	100.000

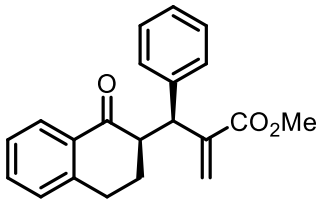

3i

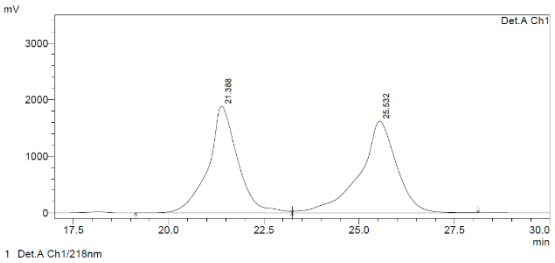

PeakTable

Detector A Ch1 218nm

Peak#	Ret. Time	Area	Height	Area %	Height %
1	21.388	101242940	1887961	48.026	53.808
2	25.532	109566001	1620752	51.974	46.192
Total		210808941	3508713	100.000	100.000

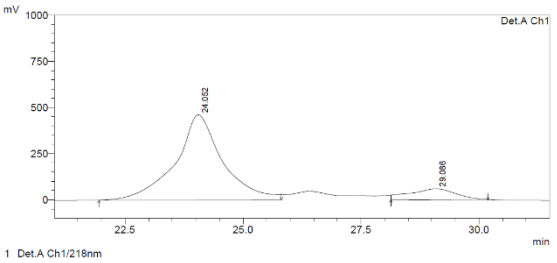

PeakTable

Detector A Ch1 218nm

Peak#	Ret. Time	Area	Height	Area %	Height %
1	24.052	32135473	461625	88.602	88.533
2	29.086	4134111	59789	11.398	11.467
Total		36269583	521414	100.000	100.000

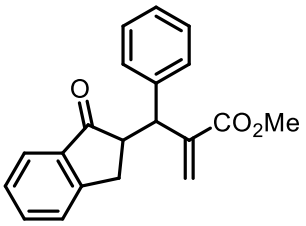

3j

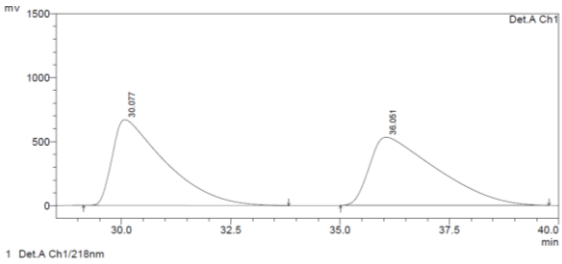

PeakTable

Detector A Ch1 218nm

Peak#	Ret. Time	Area	Height	Area %	Height %
1	30.077	56532152	669852	49.774	55.657
2	36.051	57046162	533673	50.226	44.343
Total		113578314	1203525	100.000	100.000

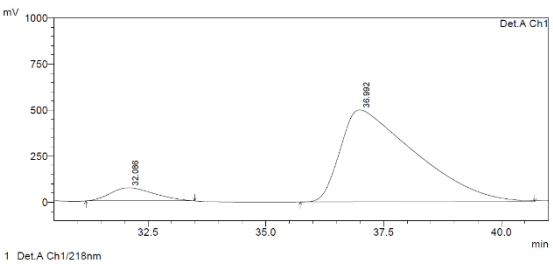

PeakTable

Detector A Ch1 218nm

Peak#	Ret. Time	Area	Height	Area %	Height %
1	32.086	4605768	71249	7.735	12.513
2	36.992	54941793	498134	92.265	87.487
Total		59547561	569383	100.000	100.000

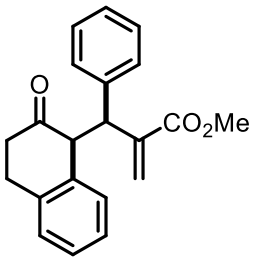

3k (mixture of diastereomers)

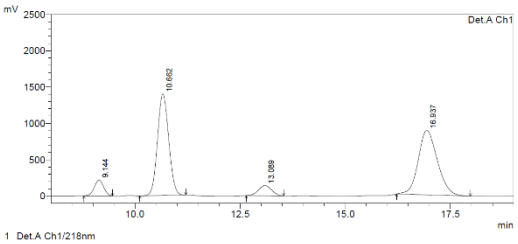

PeakTable

Detector A Ch1 218nm

Peak#	Ret. Time	Area	Height	Area %	Height %
1	9.144	3335926	217509	5.533	8.229
2	10.662	25848428	1397976	42.869	52.887
3	13.089	3057250	140194	5.070	5.304
4	16.937	28055197	887625	46.528	33.580
Total		60296800	2643304	100.000	100.000

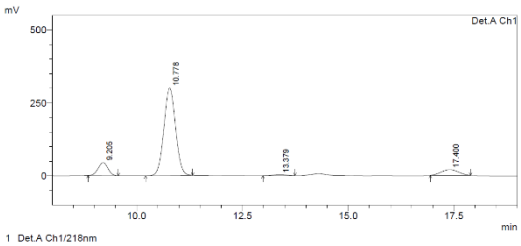

PeakTable

Detector A Ch1 218nm

Peak#	Ret. Time	Area	Height	Area %	Height %
1	9.205	710255	44477	10.051	12.121
2	10.778	5738352	300008	81.207	81.758
3	13.379	58415	2712	0.827	0.739
4	17.400	559339	19751	7.916	5.383
Total		7066361	366948	100.000	100.000

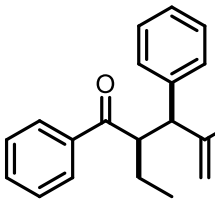

3l (mixture of diastereomers)

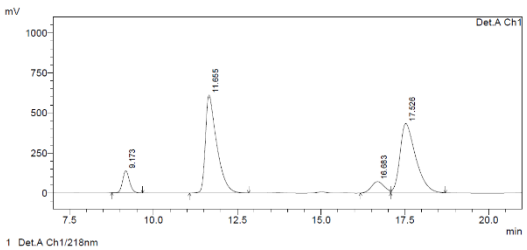

PeakTable

Detector A Ch1 218nm

Peak#	Ret. Time	Area	Height	Area %	Height %
1	9.173	1965933	137513	6.047	10.958
2	11.655	14458823	611872	44.469	48.760
3	16.683	1902858	71298	5.853	5.682
4	17.526	14281046	434174	43.930	34.599
Total		32508659	1254857	100.000	100.000

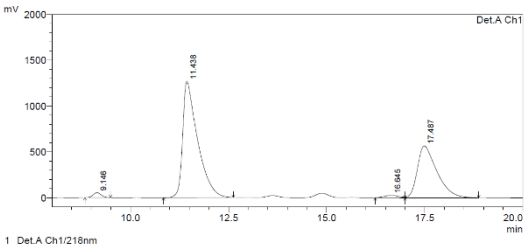

PeakTable

Detector A Ch1 218nm

Peak#	Ret. Time	Area	Height	Area %	Height %
1	9.146	778545	53774	1.430	2.806
2	11.438	33472435	1270334	61.500	66.290
3	16.645	717916	26771	1.319	1.397
4	17.487	19457882	565441	35.751	29.507
Total		54426779	1916320	100.000	100.000

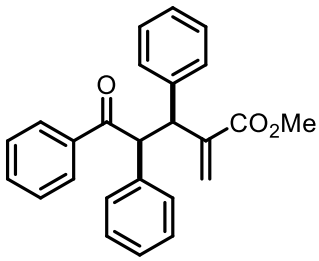

3m (mixture of diastereomers)

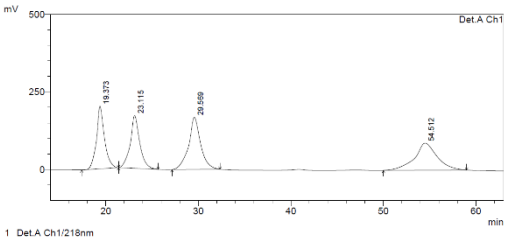

PeakTable

Detector A Ch1 218nm

Peak#	Ret. Time	Area	Height	Area %	Height %
1	19.373	12167328	201663	22.363	32.180
2	23.115	12216900	169963	22.454	27.122
3	29.569	15204267	167994	27.944	26.807
4	54.512	14820584	87053	27.239	13.891
Total		54409080	626673	100.000	100.000

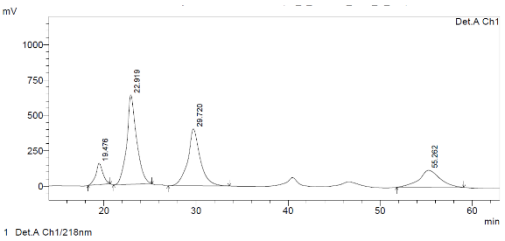

PeakTable

Detector A Ch1 218nm

Peak#	Ret. Time	Area	Height	Area %	Height %
1	19.476	8138966	150785	7.219	11.549
2	22.919	47392887	632110	42.038	48.414
3	29.720	37950619	402533	33.662	30.831
4	55.262	19256999	120198	17.081	9.206
Total		112739471	1305626	100.000	100.000

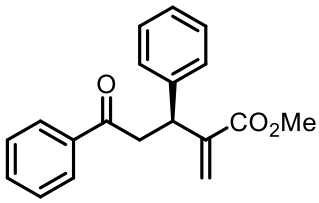

3n

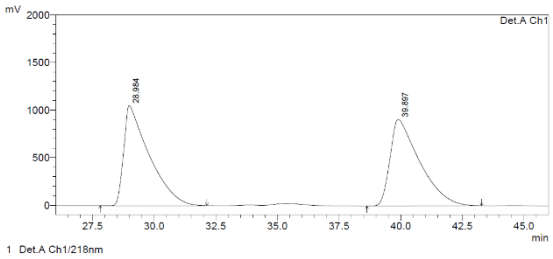

PeakTable

Detector A Ch1 218nm

Peak#	Ret. Time	Area	Height	Area %	Height %
1	28.984	75359391	1052337	49.850	53.639
2	39.897	75811525	909535	50.150	46.361
Total		151170916	1961872	100.000	100.000

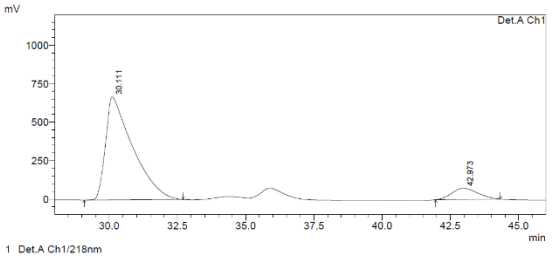

PeakTable

Detector A Ch1 218nm

Peak#	Ret. Time	Area	Height	Area %	Height %
1	30.111	46292986	669562	90.580	90.194
2	42.973	4814573	72794	9.420	9.806
Total		51107559	742356	100.000	100.000

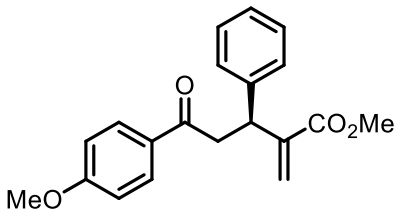

3o

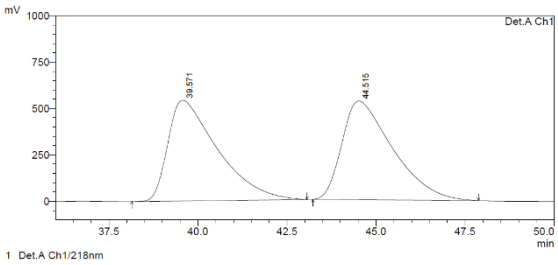

PeakTable

Detector A Ch1 218nm

Peak#	Ret. Time	Area	Height	Area %	Height %
1	39.571	52564380	542140	49.942	50.478
2	44.515	52685873	531880	50.058	49.522
Total		105250253	1074019	100.000	100.000

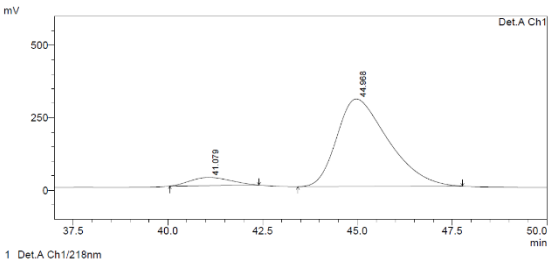

PeakTable

Detector A Ch1 218nm

Peak#	Ret. Time	Area	Height	Area %	Height %
1	41.079	2093667	28334	6.861	8.588
2	44.968	28420125	301587	93.139	91.412
Total		30513793	329921	100.000	100.000

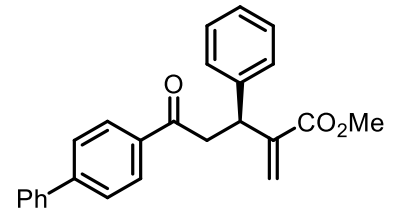

3p

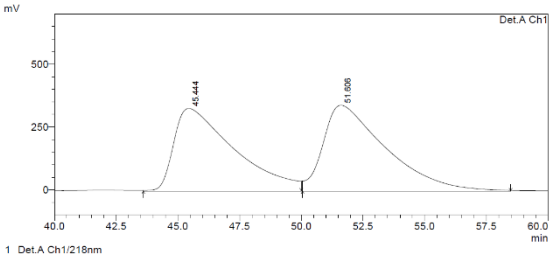

PeakTable

Detector A Ch1 218nm

Peak#	Ret. Time	Area	Height	Area %	Height %
1	45.444	55723232	328662	48.102	49.037
2	51.606	60120075	341566	51.898	50.963
Total		115843307	670228	100.000	100.000

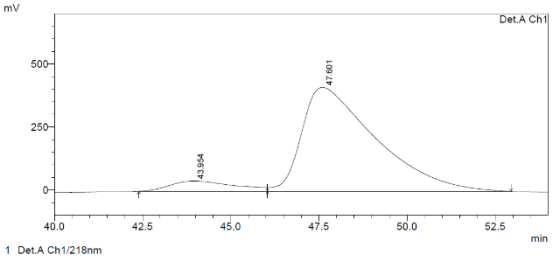

PeakTable

Detector A Ch1 218nm

Peak#	Ret. Time	Area	Height	Area %	Height %
1	43.954	5094760	40313	7.844	8.908
2	47.601	59852441	412211	92.156	91.092
Total		64947201	452524	100.000	100.000

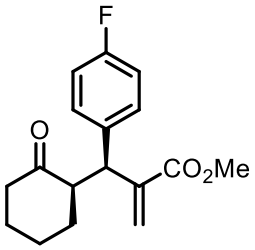

3q

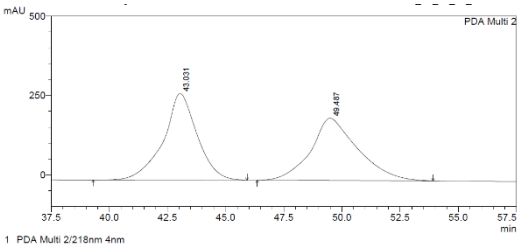

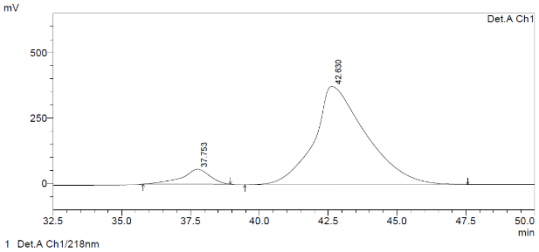

PeakTable

PDA Ch2 218nm 4nm

Peak#	Ret. Time	Area	Height	Area %	Height %
1	43.031	27572250	272662	50.072	58.132
2	49.487	27493236	196379	49.928	41.868
Total		55065487	469040	100.000	100.000

PeakTable

Detector A Ch1 218nm

Peak#	Ret. Time	Area	Height	Area %	Height %
1	37.753	4009312	56784	7.497	13.143
2	42.630	49471025	375276	92.503	86.857
Total		53480337	432060	100.000	100.000

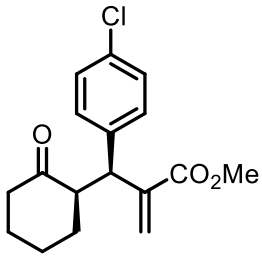

3r

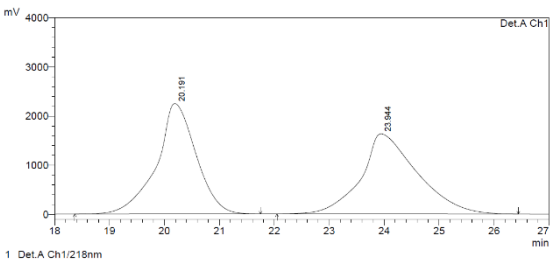

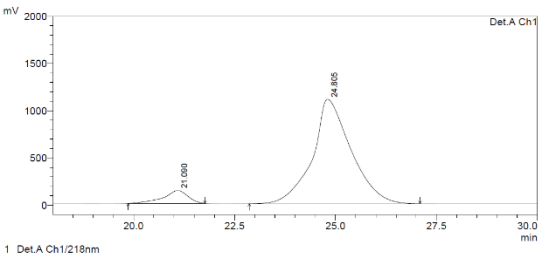

PeakTable

Detector A Ch1 218nm

Peak#	Ret. Time	Area	Height	Area %	Height %
1	20.191	112472070	2243072	49.296	57.953
2	23.944	115682472	1627441	50.704	42.047
Total		228154543	3870513	100.000	100.000

PeakTable

Detector A Ch1 218nm

Peak#	Ret. Time	Area	Height	Area %	Height %
1	21.090	5764799	136755	7.250	11.001
2	24.805	73752765	1106310	92.750	88.999
Total		79517564	1243066	100.000	100.000

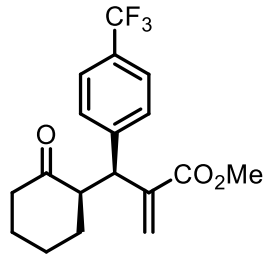

3s

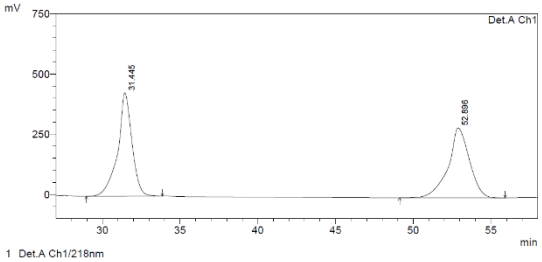

PeakTable

Detector A Ch1 218nm

Peak#	Ret. Time	Area	Height	Area %	Height %
1	31.445	27446106	429721	49.952	59.680
2	52.896	27498853	290324	50.048	40.320
Total		54944959	720045	100.000	100.000

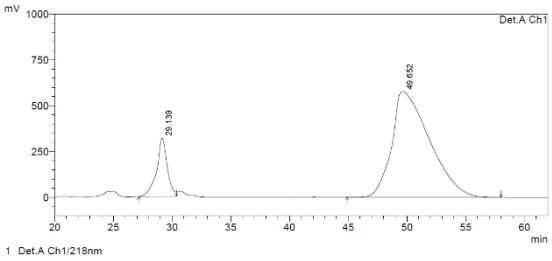

PeakTable

Detector A Ch1 218nm

Peak#	Ret. Time	Area	Height	Area %	Height %
1	29.139	20300927	319941	13.571	35.685
2	49.652	129292371	576641	86.429	64.315
Total		149593297	896582	100.000	100.000

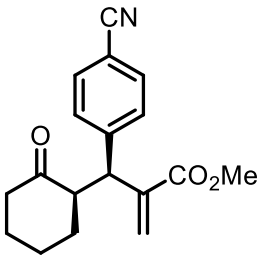

3t

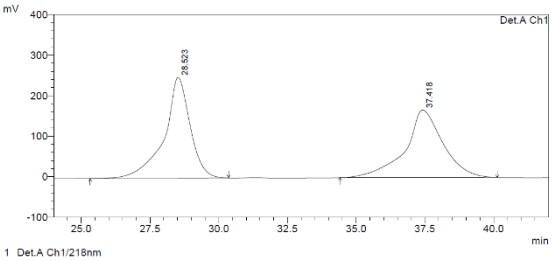

PeakTable

Detector A Ch1 218nm

Peak#	Ret. Time	Area	Height	Area %	Height %
1	28.523	16302636	248574	50.697	59.899
2	37.418	15854185	166416	49.303	40.101
Total		32156821	414991	100.000	100.000

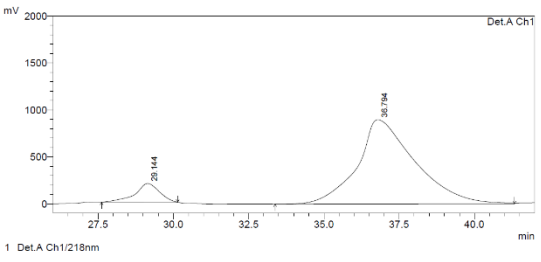

PeakTable

Detector A Ch1 218nm

Peak#	Ret. Time	Area	Height	Area %	Height %
1	29.144	11169938	199215	8.529	18.159
2	36.794	119789053	897838	91.471	81.841
Total		130958992	1097052	100.000	100.000

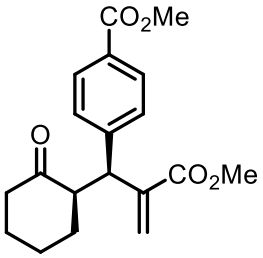

3u

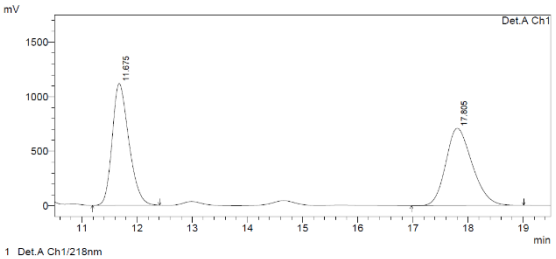

1 Det.A Ch1/218nm

PeakTable

Detector A Ch1 218nm

Peak#	Ret. Time	Area	Height	Area %	Height %
1	11.675	23440144	1115516	49.839	61.149
2	17.805	23591649	708610	50.161	38.851
Total		47031793	1823926	100.000	100.000

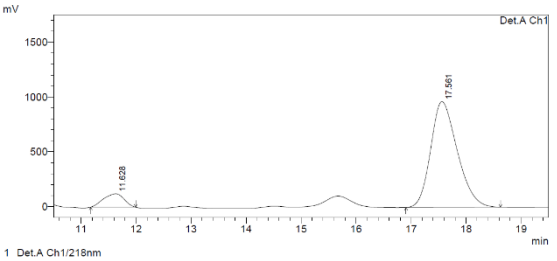

1 Det.A Ch1/218nm

PeakTable

Detector A Ch1 218nm

Peak#	Ret. Time	Area	Height	Area %	Height %
1	11.628	3163934	122377	8.887	11.255
2	17.561	32437148	964892	91.113	88.745
Total		35601081	1087269	100.000	100.000

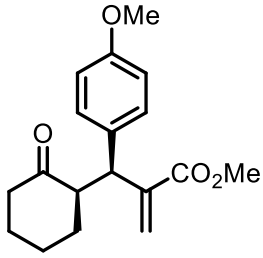

3v

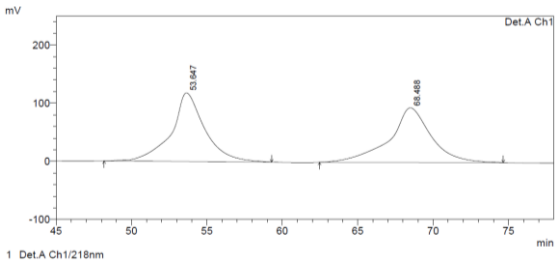

1 Det.A Ch1/218nm

PeakTable

Detector A Ch1 218nm

Peak#	Ret. Time	Area	Height	Area %	Height %
1	53.647	18239845	118075	50.224	55.676
2	68.488	18076798	94001	49.776	44.324
Total		36316643	212077	100.000	100.000

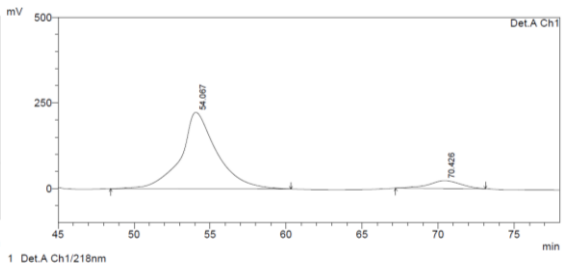

1 Det.A Ch1/218nm

PeakTable

Detector A Ch1 218nm

Peak#	Ret. Time	Area	Height	Area %	Height %
1	54.067	37064942	223495	91.667	90.701
2	70.426	3369441	22913	8.333	9.299
Total		40434383	246408	100.000	100.000

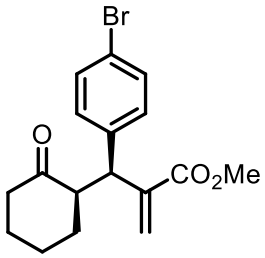

3w

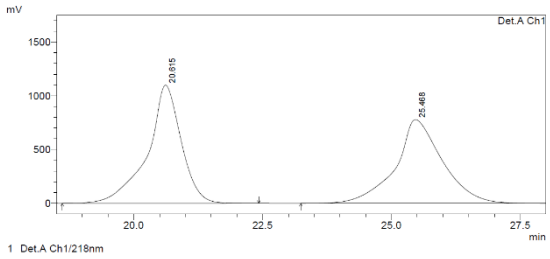

1 Det.A Ch1/218nm

PeakTable

Detector A Ch1 218nm

Peak#	Ret. Time	Area	Height	Area %	Height %
1	20.615	50253259	1099337	50.358	58.504
2	25.468	49539472	779737	49.642	41.496
Total		99792730	1879073	100.000	100.000

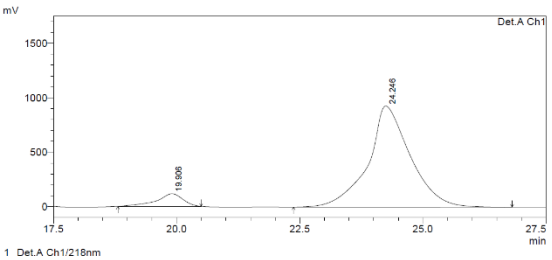

1 Det.A Ch1/218nm

PeakTable

Detector A Ch1 218nm

Peak#	Ret. Time	Area	Height	Area %	Height %
1	19.906	4343417	115769	7.285	11.091
2	24.246	55281293	928008	92.715	88.909
Total		59624711	1043777	100.000	100.000

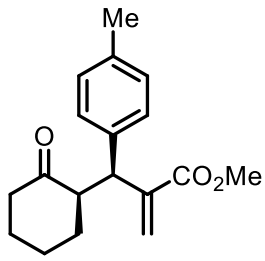

3x

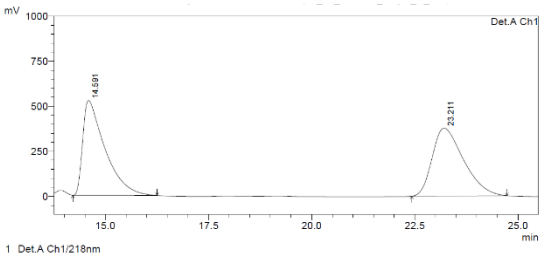

1 Det.A Ch1/218nm

PeakTable

Detector A Ch1 218nm

Peak#	Ret. Time	Area	Height	Area %	Height %
1	14.591	19756005	525937	49.831	58.274
2	23.211	19889866	376586	50.169	41.726
Total		39645871	902522	100.000	100.000

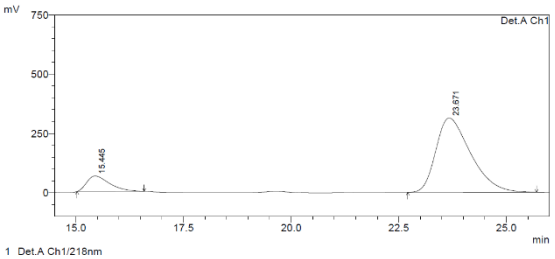

1 Det.A Ch1/218nm

PeakTable

Detector A Ch1 218nm

Peak#	Ret. Time	Area	Height	Area %	Height %
1	15.445	2411255	65531	12.065	17.306
2	23.671	17574134	313120	87.935	82.694
Total		19985389	378651	100.000	100.000

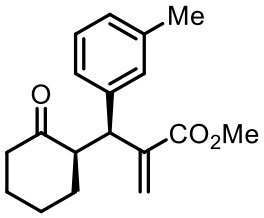

3y

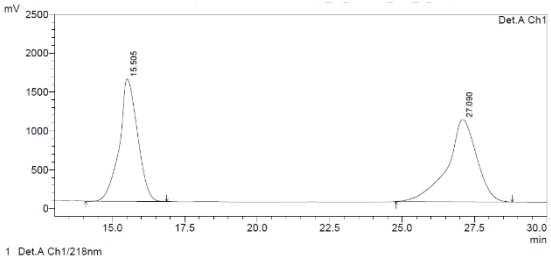

PeakTable

Detector A Ch1 218nm

Peak#	Ret. Time	Area	Height	Area %	Height %
1	15.505	68982049	1574998	47.975	59.782
2	27.090	74804447	1059593	52.025	40.218
Total		143786496	2634591	100.000	100.000

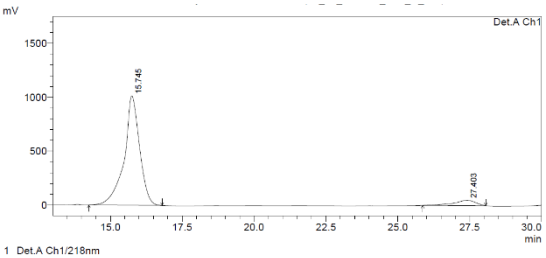

PeakTable

Detector A Ch1 218nm

Peak#	Ret. Time	Area	Height	Area %	Height %
1	15.745	37902151	1013906	93.641	95.363
2	27.403	2574008	49306	6.359	4.637
Total		40476159	1063212	100.000	100.000

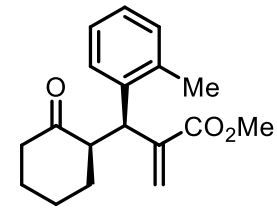

3z

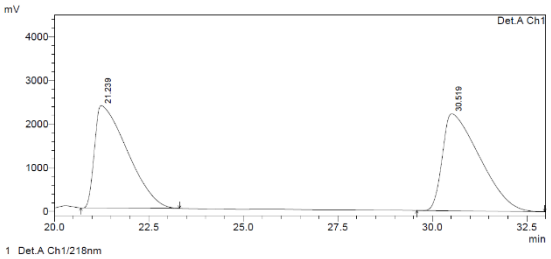

PeakTable

Detector A Ch1 218nm

Peak#	Ret. Time	Area	Height	Area %	Height %
1	21.239	141535076	2345222	48.122	51.352
2	30.519	152367398	2221702	51.878	48.648
Total		293702474	4566925	100.000	100.000

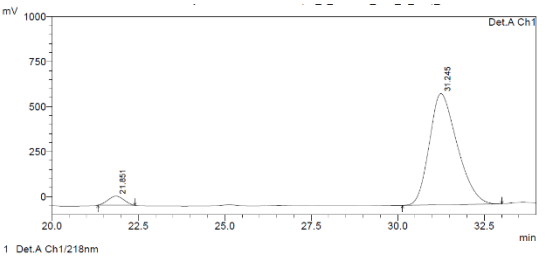

PeakTable

Detector A Ch1 218nm

Peak#	Ret. Time	Area	Height	Area %	Height %
1	21.851	1587047	49974	4.383	7.488
2	31.245	34625911	617419	95.617	92.512
Total		36212957	667393	100.000	100.000

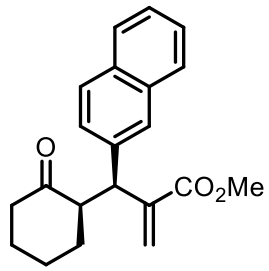

3aa

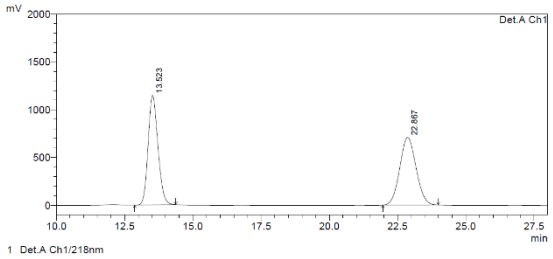

PeakTable

Detector A Ch1 218nm

Peak#	Ret. Time	Area	Height	Area %	Height %
1	13.523	28677198	1145328	49.337	61.802
2	22.867	29447768	707908	50.663	38.198
Total		58124967	1853236	100.000	100.000

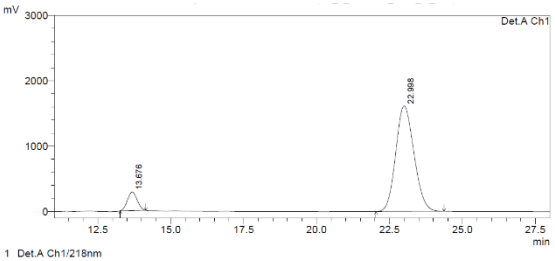

PeakTable

Detector A Ch1 218nm

Peak#	Ret. Time	Area	Height	Area %	Height %
1	13.676	6616131	284113	8.599	14.988
2	22.998	70322645	1611485	91.401	85.012
Total		76938776	1895598	100.000	100.000

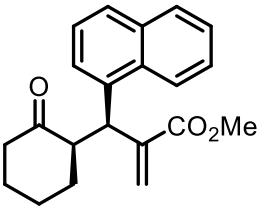

3ab

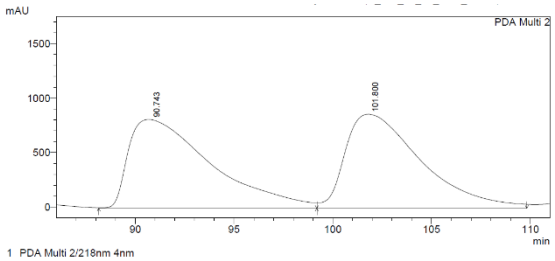

PeakTable

PDA Ch2 218nm 4nm

Peak#	Ret. Time	Area	Height	Area %	Height %
1	90.743	236665687	815649	50.644	48.538
2	101.800	230649323	864785	49.356	51.462
Total		467315010	1680434	100.000	100.000

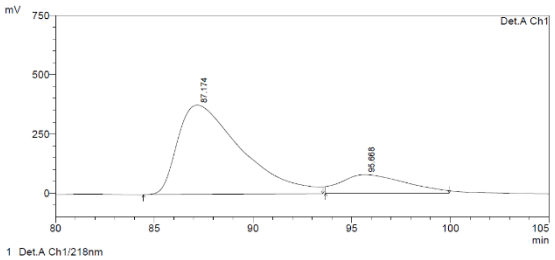

PeakTable

Detector A Ch1 218nm

Peak#	Ret. Time	Area	Height	Area %	Height %
1	87.174	84286130	376061	82.585	82.809
2	95.668	17773494	78069	17.415	17.191
Total		102059624	454130	100.000	100.000

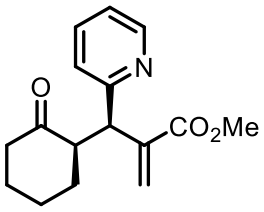

3ac

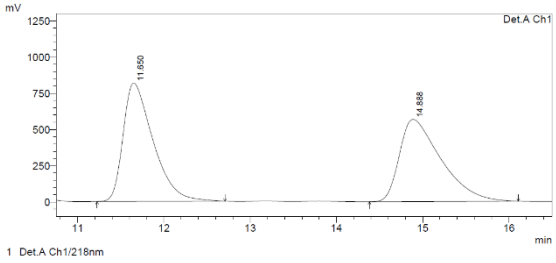

PeakTable

Detector A Ch1 218nm

Peak#	Ret. Time	Area	Height	Area %	Height %
1	11.650	19698740	814968	50.934	58.957
2	14.888	18976614	567350	49.066	41.043
Total		38675354	1382318	100.000	100.000

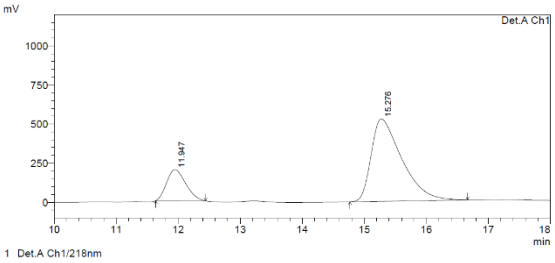

PeakTable

Detector A Ch1 218nm

Peak#	Ret. Time	Area	Height	Area %	Height %
1	11.947	4243494	198803	18.998	27.395
2	15.276	18093546	526880	81.002	72.605
Total		22337040	725683	100.000	100.000

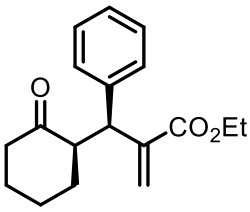

3ad

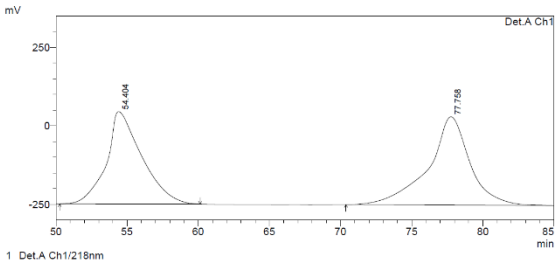

PeakTable

Detector A Ch1 218nm

Peak#	Ret. Time	Area	Height	Area %	Height %
1	54.404	50973950	294017	47.295	51.131
2	77.758	56804259	281012	52.705	48.869
Total		107778209	575030	100.000	100.000

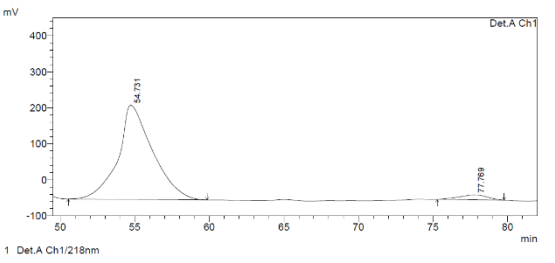

PeakTable

Detector A Ch1 218nm

Peak#	Ret. Time	Area	Height	Area %	Height %
1	54.731	42331880	261321	95.927	94.956
2	77.769	1797254	13881	4.073	5.044
Total		44129134	275201	100.000	100.000

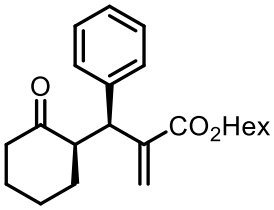

3ae

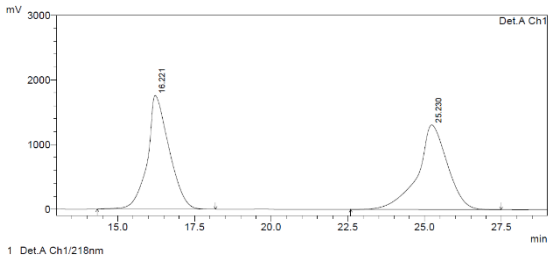

1 Det.A Ch1/218nm

PeakTable

Detector A Ch1 218nm

Peak#	Ret. Time	Area	Height	Area %	Height %
1	16.221	86661976	1758054	49.578	57.324
2	25.230	88138171	1308827	50.422	42.676
Total		174800147	3066881	100.000	100.000

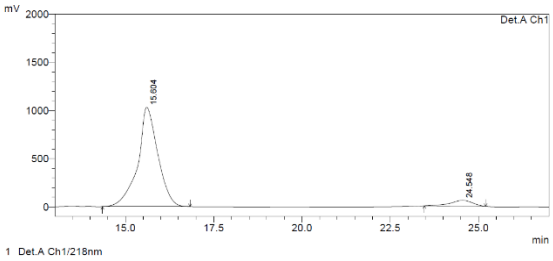

1 Det.A Ch1/218nm

PeakTable

Detector A Ch1 218nm

Peak#	Ret. Time	Area	Height	Area %	Height %
1	15.604	40935034	1030979	94.003	94.498
2	24.548	2611475	60029	5.997	5.502
Total		43546508	1091008	100.000	100.000

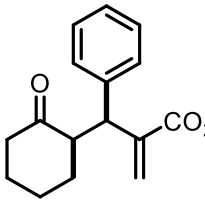

3af

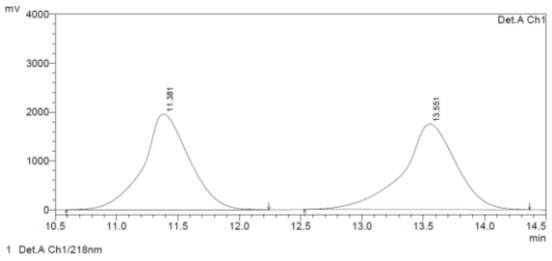

1 Det.A Ch1/218nm

PeakTable

Detector A Ch1 218nm

Peak#	Ret. Time	Area	Height	Area %	Height %
1	11.381	51072332	1952574	49.224	52.787
2	13.551	52682078	1746368	50.776	47.213
Total		103754410	3698942	100.000	100.000